Delft Aerospace Design Projects 2015

Challenging New Designs in Aeronautics, Astronautics and Wind Energy

Melkert, Joris

Publication date
2015

Document Version
Final published version

Citation (APA)
Melkert, J. (Ed.) (2015). *Delft Aerospace Design Projects 2015: Challenging New Designs in Aeronautics, Astronautics and Wind Energy*. B.V. Uitgeversbedrijf Het Goede Boek.

Delft Aerospace
Design Projects 2015

Delft Aerospace Design Projects 2015

Challenging New Designs in
Aeronautics, Astronautics and Wind Energy

Editor:
Joris Melkert

Coordinating committee:
Vincent Brügemann, Joris Melkert,
Erwin Mooij, Nando Timmer, Wim Verhagen

B.V. Uitgeversbedrijf Het Goede Boek / 2015

Published and distributed by

B.V. Uitgeversbedrijf Het Goede Boek
Surinamelaan 14
1213 VN HILVERSUM
The Netherlands

ISBN 978 90 240 6013 9
ISSN 1876-1569

Printed in the Netherlands

TABLE OF CONTENTS

PREFACE

The Design Synthesis Exercise forms the closing piece of the third year of the Bachelor degree course in aerospace engineering at TU Delft. Before the students move on to the first year of their Master degree course, in which they join one of the Faculty's disciplinary groups in preparation for their final year MSc thesis project, they learn to apply their acquired knowledge from all aerospace disciplines in the design synthesis exercise.

The objective of this exercise is to improve the students' design skills while working in teams with nine to ten of their fellow students for a continuous period of approximately ten weeks with a course load of 400 hours. They apply knowledge acquired in the first years of the course; improve communication skills and work methodically according to a plan.

Despite the fact that the final designs result from a design process executed by small groups of students with limited experience, it may be concluded that the designs are of good quality. Not only the members of the scientific staff of the Faculty of Aerospace Engineering have expressed their appreciation of the results, but also the external experts and industry, which have supported the design projects

This book presents an overview of the results of the Fall Design Synthesis Exercise 2014 and the Spring Design Synthesis Exercise of 2015, based on summaries of each of the projects. The Design Synthesis Exercise Coordination Committee, responsible for the organisation and execution of the exercise, has made this book with the aim to present an overview of the diverse nature of the various design topics, and of the aerospace engineering course itself. In addition, the book is intended as an incentive for further improvements to the exercise.

Finally the coordinating committee would like to thank the student-assistants, the academic counsellors, the educational office and all who have contributed to the success of this year's exercise.

The Design Synthesis Exercise Coordination Committee 2014:
ir. V.P. Brügemann, ir. J.A. Melkert, dr.ir. E. Mooij, ir. W.A. Timmer, dr.ir. W.J.C. Verhagen

1. THE DESIGN SYNTHESIS EXERCISE

1.1 Introduction

The design synthesis exercise forms a major part of the curriculum at the Faculty of Aerospace Engineering, Delft University of Engineering. The main purpose of the exercise is the synthesis of the curriculum themes presented in the first two years of the educational program at the faculty.

Since this design exercise is organized approximately half-way through the complete five-year program (three year Bachelor of Science in Aerospace Engineering + two year Master of Science in Aerospace Engineering), the design results are not expected to be of a professional quality. Nevertheless the students and their tutors strive to create the best design they can. This is accomplished in an iterative way. Such an iterative process is a typical element of building up design experience.

The way in which a project is carried out and reviewed is only partly focused on the design result. The design process itself is of greater importance. It is especially important for the students to work as a team, since this best reflects a design process in 'real life'. In this way, the students can take full advantage of their personal qualities.

1.2 Objective

The design synthesis exercise helps to meet the faculty's requirement to enlarge the design content of the aerospace engineering course. The goal of the exercise itself is to improve the design skills of the students, in particular project management, communication,

teamwork and the application of the knowledge gathered in the first three years of the course.

The student has the opportunity to increase his experience in designing. The whole process of designing is dealt with, from the list of requirements up to the presentation of the design. Typical aspects of such a process, such as decision making, optimization and conflicting requirements will be encountered. Acquiring experience often means going through iterative processes, so design decisions can be altered to make sure that the design requirements are met. The arguments supporting the decisions are reviewed, as well as the way the project is managed. Aspects of design methodology and design management are also taken into account.

During the project the student is expected to work in a team. This means that a student learns to cooperate, to schedule and meet targets, manage the workload, solve conflicts, et cetera. In this field, effective communication is of major importance. Apart from these capabilities the student is expected to be able to communicate ideas and concepts regarding the project subject with specialists and non-specialists. By means of integrated short courses in written reporting and oral presentation, the communicative skills of a student will be developed and assessed.

1.3 Characteristics of the exercise

The characteristics of the design synthesis exercise are:

- For all students, the design component of the study is reinforced by the design synthesis exercise.
- The design synthesis exercise consists of a design project integrated with workshops and courses on oral presentation, sustainable development, systems engineering and project management.
- The exercise has a fixed end date. This means that the third year ends with the design exercise.
- All discipline groups of the faculty provide the support needed during the exercise. This enhances the multi-disciplinary nature of the exercise in general and the design projects in particular.

- The design process is supplemented by lectures on design methodology and project management, as applied to the exercise.
- Aspects of sustainable development, such as noise emission, the use of raw materials, energy consumption and environmental impact are addressed explicitly during the exercise.
- Integrating short courses on oral presentations develops the communicative skills.

1.4 Organization and structure of the exercise

Students indicate their preferences after presentations by the staff introducing all project subjects. Students are divided into groups of approximately ten persons, as much as possible according to their preferences. The exercise takes place during a continuous period of eleven weeks, the last educational term of the third year of the Bachelor course. Technical aspects of the project take up 60 percent of the time; the remaining 40 percent is spent on general topics supporting the project work. General topics are spread over the full period of the exercise. The general topics are sustainable development, design methodology and project management and oral presentations.

1.5 Facilities

To complete the exercise design within the given period of time, the groups of students can make use of several facilities. Each group has its own room, with various facilities (tables, chairs, computers, flip-over charts et cetera). Commonly used software like CATIA, Matlab, MS Office, MS Project, Python, MSC Nastran and more project specific software are available. A special library is available, containing literature on typical project subjects. Finally each group has a budget for printing and copying.

1.6 Course load

The course load is measured in credit points according to the European Credit Transfer System, ECTS: 1 credit point equals 28 hours of work. The total course load is 15 ECTS credits.

1.7 Support and assistance

An essential part of designing is making choices and design decisions. During a technical design process, the choices made in the first stages are often based on qualitative considerations. When details of a design take shape, quantitative analysis becomes increasingly important.

The considerations accompanying these design choices need mentoring and tutoring, since students lack experience in this field. The execution of the project demands a fair amount of independent work of the design team. This means that the team itself is capable of executing the design process. The task of the team of mentors is mainly to observe and give feedback on the progress. The team of mentors consists of a principal project tutor and two additional coaches. Each has a different area of expertise. The method of working, the organization, the communication of the team and the collaboration within the team itself are also judged. Where necessary, the mentors will correct the work and work methods of the team. Warnings of pitfalls and modeling suggestions for certain problems during design will be given when needed, to ensure a satisfactory development of the design.

1.8 Design projects 2015

The Design Synthesis Exercise 2015 is divided into 28 different design assignments. In the table below an overview is given of these subjects. In the following chapters the results of the design teams are covered in detail. For each project, the important design characteristics are covered. These are: problem introduction, design specification or list of requirements, conceptual designs, the trade-off to find the “best” design, a detailed design and finally conclusions and recommenda tions.

Fall DSE

Nr.	Project Title	Principal Tutor
F1	Design of Next Generation Airlift Military Support Aircraft	Roelof Vos
F2	Solar Powered Paraglider to cross the Atlantic	Joris Melkert

F3	Durable and light weight wing for pumping kite power generation	Roland Schmehl
F4	A UAV capable of continuous flight by using external power sources	Roger Groves
F5	Lofarside: LOFAR on the far side of the Moon	Marc Naeije
F6	Electric paramotor	Bart Remes
F7	Low-cost wind-driven flight simulator	Rene van Paassen
F8	Stratos III: Mission Planning	Chris Verhoeven
F9	Unmanned POGO cargo delivery system	Ronald van Gent / Arvind Gangoli Rao

Spring DSE

Nr.	Project Title	Principal Tutor
S1	MUUDS – Martian Weather Data System	Kevin Cowan
S2	Design of a controllable inflatable aeroshell	Herman Damveld
S3	Disposal of a High Risk Space Debris Object	Eelco Doornbos
S4	Mountain High	Santiago Garcia
S5	A morphing aircraft: from research to reality	Antonio Grande
S6	Maritime Flyer	Erik-Jan van Kampen
S7	Plasma controlled UAV	Marios Kotsonis
S8	VLEO CubeSat designs for Earth Observation	Hans Kuiper
S9	The HUULC: Design of an Hydrogen-Powered Unmanned Ultra Large Cargo Aircraft	Gianfranco Larocca
S10	Next Stop: Europa	Erwin Mooij
S11	Electric helicopter	Marilena Pavel
S12	Medium range unmanned containerized cargo freighter	Paul Roling
S13	Internet via the satellite for everyone, everywhere, anytime.	Ernst Schrama
S14	Design of an Aerobatic Racing Aircraft of the future	Sonell Shroff
S15	Advanced Regional Aircraft	Jos Sinke
S16	The low-emission regional airliner	Wim Verhagen
S17	Distributed propulsion for conventional transport aircraft	Mark Voskuijl
S18	Inspection Pocket Drone	Christophe de Wagter
S19	A SIGINT/UHF smallsat constellation	Trevor Watts

1.9 The design exercise symposium

The one-day design exercise symposium forms the conclusion to the design project during which all student teams present their designs. The presentations cover the design process as well as the design result. The symposium is primarily intended for participating students, mentors and tutors. Other staff and students and external experts are invited as well.

A group of experts from within the faculty as well as from industry form the jury and assess the presentations in style and technical content. Three criteria determine the score of the group:

1. technical content (35%)
2. presentation (20%)
3. design content (35%)
4. sustainable development (10%)

The jury of experts this year consisted of:

Fall DSE

Hester Bijl	TU Delft
Avri Selig	SRON
Tineke Bakker - van der Veen	Airbus Defence and Space
Egbert Torenbeek	TU Delft
Henk van Leeuwen	Rijksdienst voor Ondernemend Nederland
Collin Beers	NLR
Huub Keizers	TNO
Ron van Manen	CleanSky
Sybren de Jong	Airbus Defence and Space
José Henrique Damiani	ITA Brasil
Paul Bogers	Shell

Spring DSE

Hans Roefs	NLR (retired)
Sven Grahn	KTH
Gianfranco Chiocchia	Politecnico di Torino
Rob Hamann	SEC^2

Pascal Bauer	ENSMA Poitiers
Jean-Luc Boiffier	ONERA/ ISAE Toulouse
Luis Campos	IST Lisboa
Martin Lemmen	Light Product Development
Pierpaolo Pergola	Alta Space Pisa
Vassili Toropov	Queen Mary University of London
Ton Maree	TNO
Jan Bos	TNO
Henk van Leeuwen	Rijksdienst voor Ondernemend Nederland
Richard Cooper	Queen's University Belfast
Tineke Bakker - van der Veen	Airbus Defence and Space
Sergio Hoyas	University of Valencia
Bernard Fortuyn	Siemens
Paolo Astori	Politecnico Milano
Rinze Benedictus	TU Delft
Avri Selig	SRON

2. NEXT GENERATION AIRLIFT MILITARY SUPPORT AIRCRAFT

Students: D.O. Berckmoes, J.-S. Fischer, M.W. Hayat, R.R.A. Hoefsloot, K.J.W. Kwakman, D.M.N. Milewski, N. van Oene, F.H.A. van Tilbog, S.J.J. Zuurendonk

Project tutor: dr.ir. R. Vos

Coaches: dr.ir. S. Hartjes, dr.ir. D. pool

2.1 Project objective

In the context of the ongoing modernization of the US armed forces, a new generation strategic transport aircraft needs to be developed. The anticipated Entry Into Service (EIS) is the year 2030. Therefore the American Institute of Aeronautics and Astronautics (AIAA) has set up an undergraduate team aircraft design competition.

The aircraft to be designed shall have a maximum payload of at least 136,000 kg and a minimum unrefuelled range of 11,670 km with a payload of 54,400 kg. This while flying at a Mach number of at least 0.6.

A minimum of 44 463L master pallets or one M104 Wolverine Heavy Assault Bridge shall fit inside the aircraft. Furthermore, the number of M1A Abrams tanks, Apache attack helicopters and M2 Bradleys carried by the aircraft should be optimized such that the versatility of the aircraft is increased.

The Mission statement is as follows:
"The design of an aircraft to enhance the modernization, to extend the life and augment the overall performance of the current fleet."

2.2 Design requirements and constraints

There are several important mission performance requirements that drive the design of the aircraft. These requirements can be found below:

- The aircraft shall have an 11,668 km unrefuelled range with a wartime planned load of 54,431 kg.
- The maximum war load shall be no less than 136,078 kg.
- The unrefuelled warload range shall be no less than 2,222 km.
- The cruise Mach number of the aircraft shall be no less than 0.6.
- The time to top of climb/climb to initial cruise altitude shall be no more than 20 minutes with a payload of 92,986 kg.
- The take-off field length and balanced field length with maximum payload as well as the landing field length with maximum landing weight shall be no longer than 2,743 m.
- The take-off, landing and climb requirements shall be met at sea level on an ISA +30 K day. Take-off and landing performance should also be shown at ISA +10 K at 3,048 m above MSL.
- The aircraft shall be able to loiter for 30 minutes at destination.
- The aircraft shall be able to perform a take-off, climb to pattern altitude, conduct pattern flight, and return to base with one or more engines out immediately after decision speed. Aircraft with an even number N engines shall meet this requirement with any N/2 engine inoperative; if N is odd then assume (N+1)/2 engines inoperative. This requirement has to be met in ISA +10 K, 3048 m conditions.
- The aircraft shall be able to perform a tactical approach for arrivals to bases embedded in combat environments.
- The internal cargo volume, and corresponding cargo weight capacity, shall be no less than 44 463L master pallets, or one M104 Wolverine Heavy Assault Bridge.

- The fuel reserves shall be enough for a change of airport in a 200 nm (370.4 km) radius from the original.
- The aircraft shall be able to climb at a speed no higher than 128.6 m/s below 3,048 m.

2.3 Concepts creation

The creation of concepts was done in two brainstorm sessions in groups of three students with changing team compositions. This way it was tried to generate concepts with different focus and approach. After these sessions each group presented its concept to the rest of the team. By discussing the concepts and asking critical questions the designs were altered until assumed feasible or, if that did not happen, the concept was rejected. In the end three concepts were left which were analysed in more detail with a class I analysis.

Concept 1: Canard blended wing body

The first concept to be discussed is a Canard Blended Wing-Body aircraft. The design is focused on a short turn-around time, efficiency and reliability. It features four turbofan engines mounted on top of the leading edge of the wing. The design has a front part that represents a conventional wide body fuselage which is pressurized. The pressurized part continues to the aft of the aircraft where a ramp-door can open.

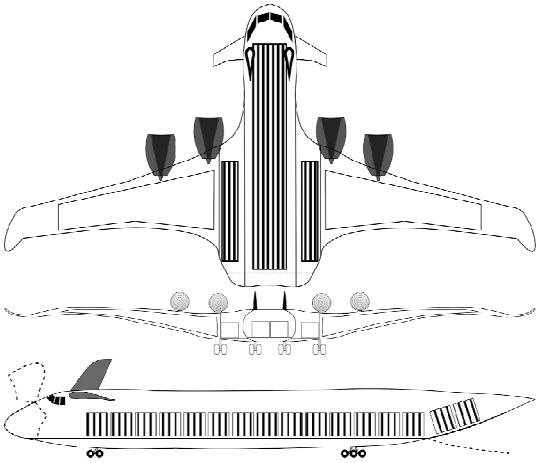

Figure 2.1: Canard blended wing body

It features a canard and double vertical fins which are located at the front of the aircraft. At approximately 45 percent of the fuselage length the wing start and blends with the tubular section. In the aft part, next to the tubular section, is an unpressurized cargo-hold in the wings on either side of the centre part that can fit a maximum of six 463L pallets each. These side-cargo areas each have a ramp door. The remaining volume of the wing can be used for fuel storage, accommodate control surfaces, flaps, slats and storage for the landing gear.

Concept 2: Modular integrated wing body

The second concept proposes a modular design. An integrated wing body carries a module that can be exchanged for different missions. This design focuses on a fast turn-around process, high aerodynamic efficiency and versatility. It features four counter-rotating open rotors and a V-tail configuration. On the sides of the module and the pressurized section pallets can be placed in unpressurized cargo areas with doors in the front of the aircraft.

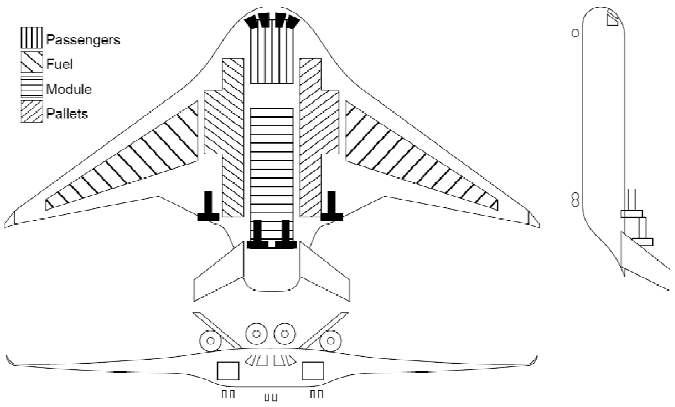

Figure 2.2: Modular integrated wing body

The choice of the integrating wing configuration results from the fact that this concept allows a module to be placed in the aircraft and still have a possibility to place the landing gears easily next to it, which is not possible for a conventional configuration. Additionally, the

promising prediction for aerodynamic efficiency by recent literature led to the selection of the integrated wing. The front area of the aircraft is pressurized and contains the cockpit and a passenger compartment.

Concept 3: Ultra wide body

The third concept that is proposed is an Ultra Wide Body aircraft. This aircraft will rely on a conventional tube and wing configuration similar to the C-5 with a high wing and a V-tail, which is propelled by four turbofan engines. Main design goals were lowering the turn-around time and increasing aerodynamic efficiency by focusing on a reduction of wetted area and increasing the aspect ratio of the wing. Main design aspects of the UWB are a wider cargo bay and door that help to reduce the turn-around time, a lifting nose surface and integration of the main landing gear in the fuselage body. The whole fuselage is pressurized, ensuring that any type of cargo and passengers can be carried. The use of struts to support the wings allows for a slender wing design with a large span without a high penalty in structural weight.

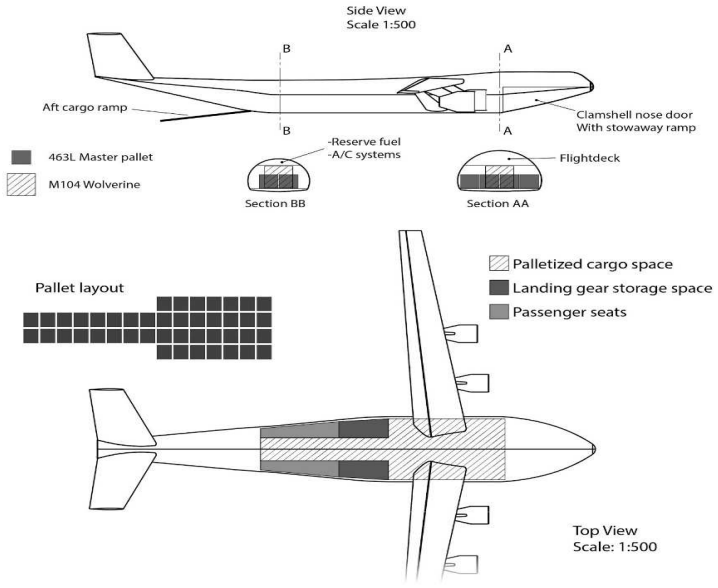

Figure 2.3: Ultra wide body

2.4 Concepts trade-off

As a first step, a method is set up which is used to select a concept to be taken into the class II design phase. The team decided to organize a down-selection workshop during which the students, together with their tutors, estimate the performance of all concepts with respect to predefined criteria. These criteria are given different weighting factors to take into account their relevance for the overall design feasibility.

Table 2.1: Assessment scale

-3	-1	0	+1	+3
very poor	poor	neutral	strong	very strong

Next to that a maturity assessment is part of the selection process. It assesses the likelihood of success (i.e. the feasibility of the proposed technologies) and the effort for realization of a concept (i.e. the effort to get the proposed technologies to the Technology Readiness Level (TRL) 9).

Table 2.2: Maturity assessment

Likelihood of success					
high	5	10	15	20	25
	4	8	12	16	20
	3	6	9	12	15
	2	4	6	8	10
low	1	2	3	4	5
	high		Effort		low

All the concepts were ranked on different criteria, firstly the mechanical and the design complexity should be low. Secondly the aerodynamic and propulsive efficiency should be high and the weight should be low. A military aircraft should have a high versatility such that is can be used for many missions. The cost should be as low as possible both in the production and operation phase. Lastly because the project was entered in the AIAA undergraduate competition the originality should be high. Table 2.3 shows how each concept scored.

Table 2.3: Trade-off matrix

Criteria	Weight	Concept 1	Concept 2	Concept 3
Complexity	0.15	-2.5	-1.5	0.25
Mechanical complexity	0.25	-1	-3	1
Design complexity	0.75	-3	-1	0
Efficiency	0.2	0	-0.05	0
Aerodynamic efficiency	0.35	-1	-1	1
Propulsion efficiency	0.3	0	1	0
Weight	0.35	1	0	-1
Mission performance/ Versatility	0.3	0.8	0	1.8
Ground operations	0.3	1	0	1
Cruise speed	0.1	0	0	-1
Harmonics range	0.1	0	0	1
Maximum cargo	0.25	1	0	3
Cargo versatility	0.25	1	0	3
Cost	0.15	0.5	0	0
Production cost	0.5	0	0	1
Operation cost	0.5	1	0	-1
Innovation/Originality	0.2	3	1	0
Aircraft novelties	1	3	1	0
Total score	1	0.54	-0.04	0.58
Maturity Assessment		2	9	16
Likelihood of success		2	3	4
Effort to get the technology ready		1	3	4

As it can be seen in table 2.3 concept 3 has the highest score and was worked out during a class II final design.

2.5 Final design

The selected concept, 'The W.H.A.L.E.', follows the design philosophy that the team used in many aspects. The turn-around time is minimized by implementing two large doors that allow for quick loading and unloading procedures. Additionally, the Ultra Wide Body (UWB) fuselage can be loaded from the front with four pallets at the

same time, offering space inside half of the fuselage to store four pallets next to each other.

In order to reduce the fuel consumption, highly efficient Counter Rotating Prop Fans (CRPF's) are attached to the wings. Furthermore, a high aspect ratio, strut braced wing with winglets maximizes the aerodynamic efficiency of the aircraft.

Versatility has many facets and the W.H.A.L.E. achieves high performance in many of them. The large, fully pressurized cargo bay can store many different cargo compositions, offers seats for 36 passengers and has a back ramp that is designed to allow air drops. Being a successor of the C-5 Galaxy, the W.H.A.L.E.'s performance is measured against the aircraft from Lockheed Martin. Hence, the team made sure that the new concept can compete with it in every imaginable way.

2.6 Layout

The aircraft features an ultra-wide body fuselage that offers a lot of space for the required cargo units. It has a lifting nose with a clamshell nose door, a rear door ramp and is fully pressurized. The wings are high-mounted in order to have enough ground clearance for the low landing gear and the large engine rotors. The high aspect ratio, nearly unsweep wings with winglets are designed for aerodynamic efficiency and are strut-braced to reduce the high weight of such slender wings. The wing span is maximized to 80 m, a longer span would not fulfill the span requirements. The six engines are mounted on the wings. They are CRPF's that are able to fly at a decent speed and altitude with improved efficiency compared to usual turbofan engines. An upper deck is located above the cargo bay and features a cockpit for a crew of 6 and accommodates 36 more passengers. A V-tail is attached to the tail of the fuselage. The V-tail is structurally a more efficient design than the conventional T-tail, resulting in a lightweight empennage.

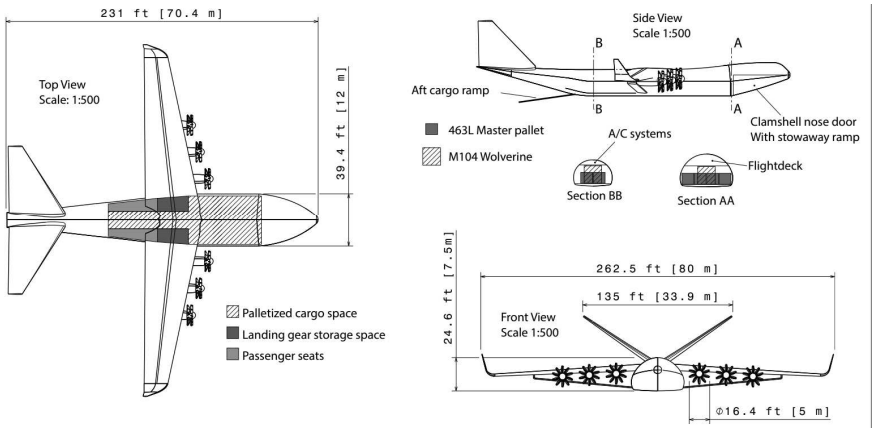

Figure 2.4: Dimensions of the W.H.A.L.E

Important characteristics of the W.H.A.L.E can be found below in the table 2.4. It consists of geometrical properties as well as other important parameters.

Table 2.4: Important characteristics of W.H.A.L.E

Parameter	Value	Units
Maximum take-off weight	480,000	[kg]
Operational empty weight	220,000	[kg]
Fuel weight	174,000	[kg]
Wing area	710	[m^2]
Wing span	80	[m^2]
Aspect ratio	9	[-]
Number of engines	6	[-]
Tail area	320	[m^2]

2.7 Conclusion

The objective of this competition was to design the next generation transport aircraft for the US Air Force. Inherently, this meant coming up with a successor for the C-5 Galaxy. This proved not an easy task. The design approach included a short turn-around time for efficient aircraft use. This was achieved by implementing two wide cargo doors for simultaneous loading and unloading of the cargo bay. Also a

relatively narrow turn radius improved ground handling. Increasing fuel efficiency was also one of the major design objectives.

Drag was reduced by choosing a slender, strut braced wing with winglets resulting in a relatively high aspect ratio, which helped reduce induced drag. The strut counteracted the weight penalty which typically comes with slender wings. Parasitic drag was lowered by implementing a V-tail design empennage and integrating the main landing gear in the fuselage, thus not requiring external pods.

A cradle-to-cradle design philosophy was adopted where possible for the manufacturing and operations of the aircraft, thus reducing environmental impact of the W.H.A.L.E. At 191 million USD, this aircraft will be very competitive in the market.

2.8 Recommendations

There are several recommendations that can be implemented for the design of W.H.A.L.E.

The wing and strut combination was sized by optimizing for total structural mass, but other considerations such as aerodynamics were not taken into account. The struts might require to be swept in order to increase the critical Mach number. Also, the strut is not load carrying when the wing is bending down, but should be carrying when the wing is lifting. The mechanism that is required to make this work was not designed and could prove to be a bottleneck for the strut design.

Detailed aerodynamic analysis should be performed to determine the exact performance of the dropped hinge flap. Also the prop wash effects on the aerofoil and high-lift devices should be looked into in more detail. Analysis of propeller slipstream effects on the downwash can be done for more exact downwash gradient that can have an effect on the sizing of the horizontal tail plane. For a more accurate vertical tail area estimation an extensive analysis of the side wash due to the

interactions between the engine prop wash, fuselage and tail needs to be done.

The space the landing gear takes could be designed into more detail, as the landing gear retraction kinematics require a more thorough design as well. Also, the bending introduced when loading the aircraft should be investigated, even though they are not critical for thickness when compared to the bending moments due to braking.

3. SOLAR POWERED PARAGLIDER TO CROSS THE ATLANTIC

Students: T. Buchenau, F. Fortman, M.P. Huijts, H. Hussain, L. Koomen, R.C. Kuipers, T.L. Mulders, L.M.C. Sijbers, D.L. da Silva Rosa, A.J. Vrasdonk

Project tutor: ir. J.A. Melkert

Coaches: D. Mehta Msc., dr. J. Khaliq

3.1 Introduction

Ever since the discovery of North America, pioneers have been trying and succeeded to cross the Atlantic with sailing ships, airplanes, balloons and even rowing boats. This design team was confronted with a new challenge. An external client approached the faculty with a new pioneering idea. Crossing the Atlantic in a solar powered paraglider, in continuous flight. The longest distance ever covered in a continuous flight by a powered paraglider was about 1,100 km, the distance between Newfoundland (Canada) and Ireland is more than 3,000 km, almost three times as far. As a starting point, a foundation the design can be based on, an objective statement, requirements and, the mission itself have to be established.

Project Objective Statement

"Investigate the feasibility of designing a solar powered paraglider that can perform continuous, safe, manned flight across the Atlantic, with 10 students in 10 weeks time."

Requirements

The following top level requirements where derived from the requirements given in the project description.

REQ-MIS-A1	The optimal time frame to cross the Atlantic must be determined, i.e. maximise the availability of solar radiation and favourable wind conditions.
REQ-MIS-B1	The transatlantic flight must be continuous or, if proven infeasible, intermediate stops are an option.
REQ-MIS-B2	The crossing must at least cover the Atlantic. However, the client has indicated that in addition to the Atlantic, crossing the North Sea is considered highly favourable.
REQ-MIS-C1	The paraglider must be manned, this means taking into account human factors such as fatigue, immobility and diet of the pilot.
REQ-MIS-C11	The pilot must have food and drinks for the mission.
REQ-MIS-D1	The maximum flight altitude must be such that the fuselage does not have to be pressurised.
REQ-SAF-A2	In case of landing on water the fuselage must offer survivability long enough to be rescued.
REQ-SAF-B1	The safety of the pilot must be guaranteed all throughout the flight.
REQ-SAF-B12	The PPG must be able to perform a safe emergency landing.
REQ-TECH-A1	The paraglider design must be within the stretched definition of a paraglider, i.e. the canopy is allowed to have semi-rigid parts.
REQ-TECH-B1	The paraglider must be completely solar powered; batteries charged with solar energy are okay.

Mission

Based on the requirements and project objective statement, a mission profile has been defined. The mission starts in Saint John´s, Newfoundland, crossing the north Atlantic to end in Portmagee, Ireland, after covering a distance of 3,040 km. The mission itself has a total duration of 38 hours, during which two night phases and two days phases are encountered.

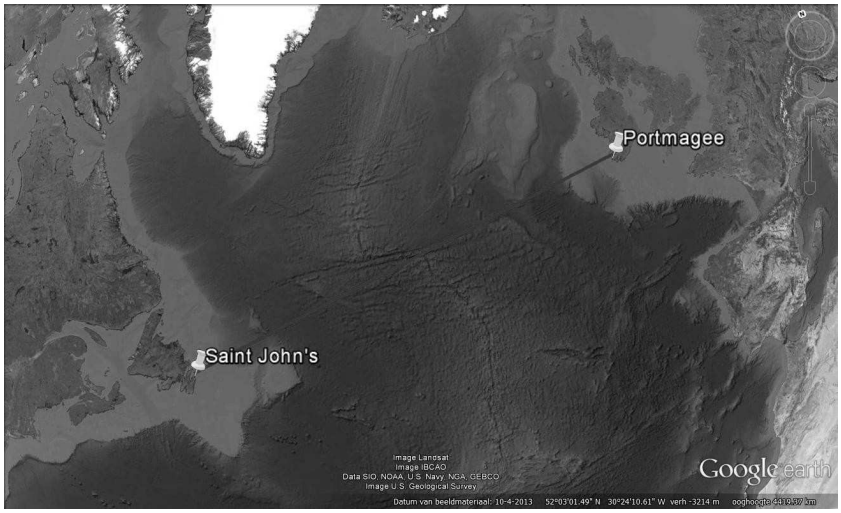

Figure 3.1: Route from Saint John´s to Portmagee

The paraglider is designed for being battery-assisted during take-off and cruise at night. After take-off, the first 8 hours of the mission will take place during night. This is followed by the first daylight interval of 16 hours, where the power supply is accommodated by wing mounted PV´s. The PV's will at the same time as providing power, recharge the batteries before entering another 8-hour night phase. The mission finally reaches its end during daylight.

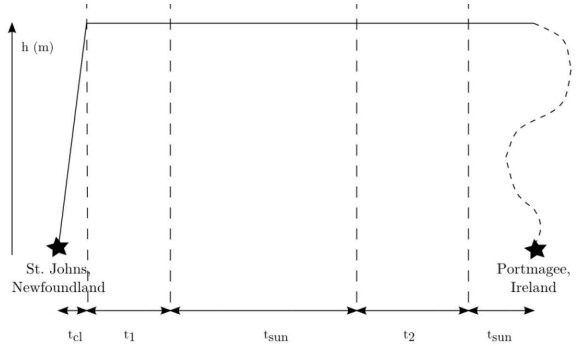

Figure 3.2: Mission profile

Since the paraglider is operated by a human pilot, as a limiting factor for the mission duration the maximum sleep deprivation a human being can handle while still being able to operate the system safely. This maximum sleep deprivation is approximately 42 hours.

Functional breakdown

The Functional Breakdown Structure (FBS) gives an overview of the different functions each subsystem has to provide. These are derived from the top level requirements and mission specifications.

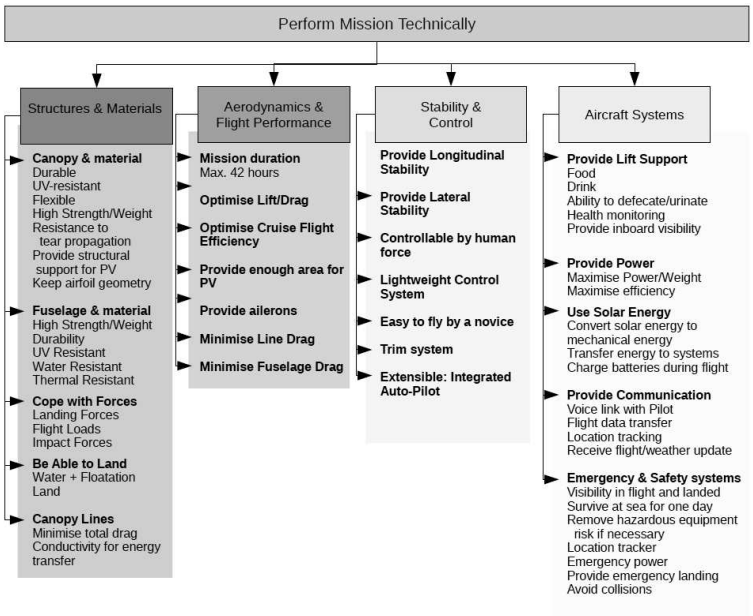

Figure 3.3: Functional breakdown structure

3.2 Concepts

Initially it was intended to find a design solution using commercially-off-the-shelf (COTS) components to guarantee pilot safety by using proven technologies and minimize the time frame from project kick-off until the actual execution of the mission, since this was a wish of the client. After it was found not to be realistic, the decision to come up with a new design, based on a combination of existing and new technologies with availability within 5 years. Due to the poor gliding performance of a conventional paraglider, it was necessary to stretch its definition. This paraglider definition implies that a paraglider does not have rigid structural elements. The fuselage was designed for minimum drag and weight while providing sufficient volume to fit all subsystems and assure pilot safety for mission loads and in case of emergencies.

3.3 Design

The major components of the powered paraglider (PPG) design are the wing-, fuselage-, control-, and power systems. In addition a number of subsystems for mission control, health monitoring and safety. The main systems are explained below.

Wing system

Starting off with the paraglider concept in mind, it was decided to have the canopy aerofoil pressurised with helium. Even though this gas has smaller molecules than air and can therefore escape easier through the pores of the material, it has been chosen because it also provides a lifting force of about 1 kg/m^3. Given a final canopy design which can provide about 32 m^3 of volume to store the gas, this additional lifting force counteracts the weight. Many different inflated canopy configurations have been researched, among which the multi-bubble design.

A conventional paraglider has several inflated cells along the wing span, while the Multi-bubble concept distributes the cells along the chord length of the wing. The bubbles are designed such that the

contour of the cross-section approximates the aerofoil as good as possible. An optimal design of 9 bubbles was found. Next, the canopy had to be structurally reinforced with stiffening elements in order to carry the loads such as lift, drag, weight, thrust and disturbances. A quite new concept called Tensairity was implemented ◎ to function as spars and ribs of the canopy.

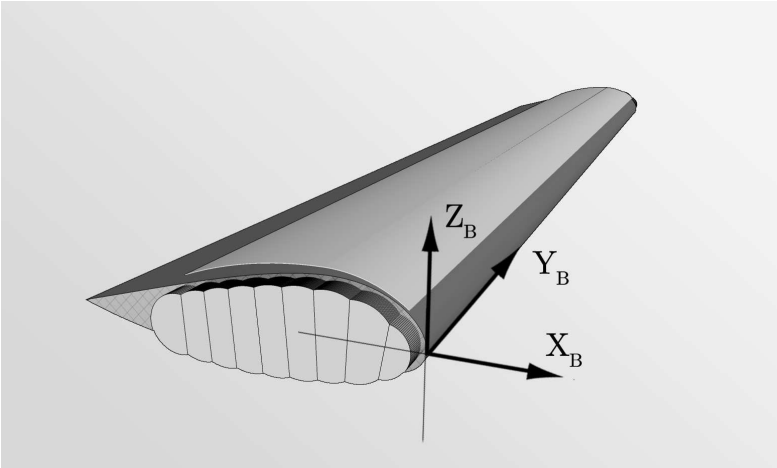

Figure 3.4: Wing structure

The idea is to increase the load bearing capacity of an inflated beam by spinning two tension cables around it, and adding a compression element. A total of two spars and six ribs were enough to provide structural rigidity for the 75 m^2 canopy. The whole canopy will be made out of different flexible materials. Furthermore, the canopy has a rectangular cross-section, such that the multi-bubble concept can be implemented without decreasing the aerodynamic performance drastically.

For stability, the canopy had to have anhedral, which means that the tips are deflected downwards. This divides the canopy in two different sections, the anhedral section at the tips with a span of 3.4 m, and the horizontal section of 19.2 m on which the solar cells are mounted. Finally, the canopy is equipped with jet flaps, which is newly developed technology from the paraglider company Skywalk, at 70 % of the chord length in order to provide controllability. The total weight of the canopy design is 6.75 kg.

Fuselage system

The fuselage shape is close to an ellipsoid with a length of 3 m, a width of 1 m and a height of 1.3 m. The internal frame structure, as shown in the figure below, consists of aluminium members to support the loads; It also serves as attachment points for the connection lines with the canopy and the motor. The total weight of the fuselage, including subsystems, is 228 kg. In case of emergency most likely an emergency landing on water will have to be performed. To increase safety, after releasing the canopy (including lines), the batteries and propeller are ejected and an emergency parachute opens. Integrated in the fuselage structure is a life raft, which self inflates when the fuselage nose hits the water.

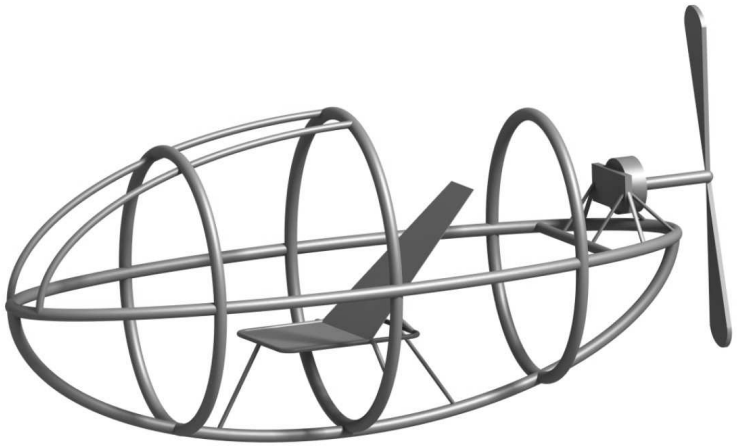

Figure 3.5: Internal fuselage structure

Power system

The PV cells, that have been integrated in the canopy design, are of space grade and are similar to the cells used in the Nuna. These PV cells have an efficiency of 29% and when they are combined into PV modules the module efficiency was estimated to be ~25%. Next to their high efficiency, other advantages are their low weight when comparing them to similar solar cells of only 1.234 kg/m^2 and their flexibility that allows the PV cells to be placed on the curvature of the canopy.

As the area of a single solar cell is only 26.6 cm^2 over 7,000 cells are required to meet the required 31 square meter of PV cells that are needed to generate enough power for sustained flight. Lithium-Sulphur batteries have been chosen for the aircraft as these batteries have a high energy density of 500 Wh/kg and are also quite reliable compared to their counterparts with similar energy densities. A total battery mass of 57.7 kg is required to store enough energy to power the aircraft during its cruise in darkness. A downside to using this kind of battery is that it is not yet available. It should be technically available within the next five years.

Control system
In the wing, jet flaps, which mainly function as control surfaces, are incorporated. These are connected to the steering system of the PPG by control lines which transfer the control forces applied by the pilot through the steering pedals. The control lines are integrated with electrical and structural support lines.

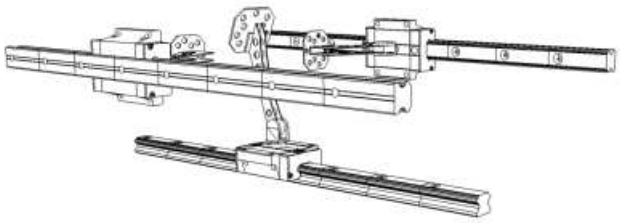

Figure 3.6: Pedal steering system

3.4 Conclusions

After 10 weeks of planning, exploring, analysing and designing, it was time to present the final outcome: it is feasible to cross the Atlantic with a manned solar powered paraglider in continuous flight.

In order to draw this conclusion many different angles of the mission have been explored. All possible difficulties and optimal design necessary to accomplish this mission has been researched. Not only the design of the vehicle was important but also the life and safety of

the pilot became a decisive factor. The main technical topics treated are stability and control, aerodynamics, structures of fuselage and canopy, flight performance and subsystems. In addition to all the technical work, group organisation, planning and communication are key ingredients for a design project to succeed. For stability and control it was concluded that it is unavoidable to have some form of instability due to the characteristics of the paraglider-fuselage system. The design Team has chosen to have lateral and longitudinal stability, but still allowing for some form of spiral instability. In the design there is enough time for the pilot to counteract this instability. Subsequently the control forces needed to achieve a normal turn are well within the range of human capabilities.

The canopy design started off with the definition of a paraglider. In terms of aerodynamics it became a challenge to find an aerofoil that could handle the low design speed for paragliders in combination with establishing wing parameters that provided the desired performance to achieve the Atlantic crossing. To get optimum performance and meet the aerodynamic requirements a thick aerofoil has been selected. It should be noted that the wing performance is sensitive to changes in profile drag. The wing became customized design in order achieve a gliding ratio of 13.1 which is higher than the average value of 10 for paragliders.

Research on inflatable structures led to an innovative canopy design that integrated a pressurised multi-bubble design, Tensairity® elements and jet flaps. By use of only high strength to weight ratio flexible materials, a semi-rigid canopy was designed that could support the flight loads and the heavy weight of the solar panels. Design parameters were also influenced by criteria set by aerodynamic, stability and control requirements.

Given the uniqueness of the mission, a fuselage had to be designed for this mission specifically. It was proven that it is possible to design a lightweight fuselage that can house all subsystems as well as providing sufficient room for the pilot to move during mission. In

addition the fuselage had to be structurally safe for the pilot to carry the high impact loads in case of emergency landing.

Throughout the whole design project, the power budget has been the driving factor behind the optimisation process. In order to achieve the lowest possible power required the weight and flight velocity had to be minimized, while trying to reach a large gliding ratio. This was a challenge since all factors are interrelated in all technical aspects of the design. Good communication and interaction of all subgroups was of high importance in order to build a tool that could take all factors into account. Validation and verification were needed to get a correct functioning tool. An optimal design was then accomplished through several iteration processes. Parameters had to be adjusted in order to satisfy all the criteria several times. Finally with a flight velocity of 10 m/s , a feasible design to cross the Atlantic was accomplished.

3.5 Recommendations

Many hurdles were encountered throughout the DSE project. Some were solved, other approached with estimates or assumptions. This leads to possible improvements and recommendations for further research within several design sectors.

First, for the mission profile it is recommended to investigate the possibility of taking-off in daytime. This way the PV system could be sized to power the climb phase instead of charging the battery as long as the mission duration stays under a maximum limit of 40 h. Secondly, for stability and control, a numerical analysis on the turn rates and magnitude of stability modes is recommended. Moreover for the aircraft subsystems, more accurate data on the motor performance could give more precise values of the power system efficiencies. Additionally it is also recommended to look into the possibility of starting emergency procedures remotely controlled.

When it comes to the structural analysis of the canopy system, it is recommended to perform further research and numerical analysis on torsion, deflection and wrinkling. Also the bridle of the suspension

lines and the geometry of the Tensairity® beam can be further optimised. Furthermore since the wing is a unique design, it is highly recommended to perform tests on a prototype wing in order to validate the numerical model. For the fuselage structure it is recommended to conduct further research on load damping and human factors with high g-loading to ensure a safe emergency landing. Also it is recommended to perform an FEM of the structure to find peak loads and stresses during impact, and assure that critical points such as the fuselage window are strong enough to impact the impact loads. Next, the canopy suspension lines have been designed according to the conventional paraglider certifications. More research has to be done to verify whether the new canopy design still has to comply with these conventional regulations.

For the aerodynamics, it is recommended to investigate whether the chosen aerofoil is suitable for the change in airspeed from 12.5 m/s to 10 m/s; also the climb performance of the aerofoil should be investigated in more detail. In addition, the validity of using the lifting line theory to go from 2D to 3D should be confirmed with CFD models of the wing. Another possible improvement could be altering the aspect ratio in order to achieve a higher gliding ratio.

Finally, the power budget tool has a central role in the design process. An error was found in the tool, which had clear consequences on the reliability of the design. Implementing the corrected power budget tool could therefore improve the design greatly.

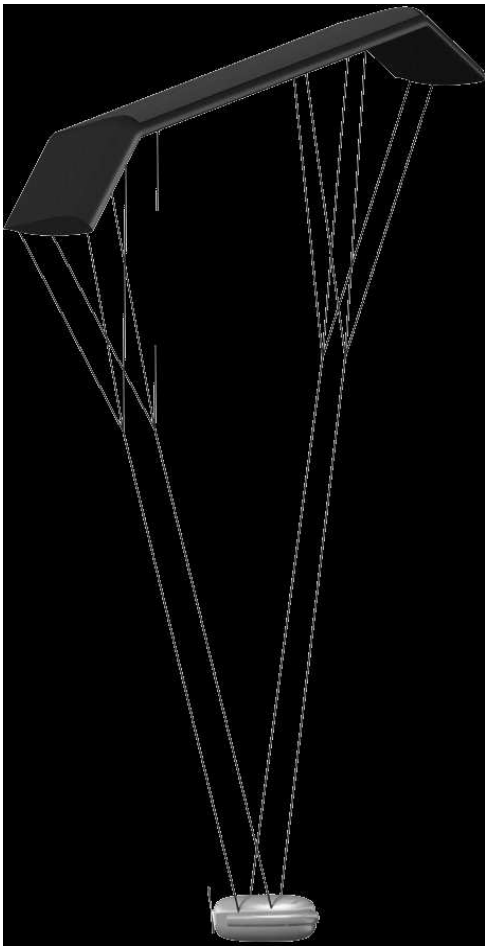

Figure 13.7: Final design

4. DURABLE AND LIGHT WEIGHT WING FOR PUMPING KITE POWER GENERATION

Students: R. Coenen, S. Drenth, M.D.T. Islam, R. Kruithof, K. Lindeborg, R. Meijer, F. Ndonga, T. Smits, M. Veraart

Project tutor: Dr.-Ing. R. Schmehl

Coaches: dr.ir. S.T. De Freitas, ir. J. Geul

4.1 Introduction

Kites have been in existence for a long period of time but only recently in the last two decades have they been explored as a means to generate power. Despite this short period of existence, this branch of Airborne Wind Energy (AWE) has proven to be technically feasible. At this moment in time, several players are working on making this economically feasible. Its advantage over the standard wind turbines is that it can easily reach higher altitudes with stable and higher wind velocities. At these altitudes there is increased potential power without requiring a large volume of material and foundation. This results in a mobile system, making it also a strong competitor to non-renewable energy sources such as diesel generators.

Following recent developments in airborne wind energy generation, a group of nine students of the TU Delft Design Synthesis Exercise have designed a durable and lightweight wing for pumping kite power generation. This prototype design will be an important step to reach widespread commercial usage of this AWE system, with scaling capabilities kept in mind for power generation up to and beyond 100 kW.

This chapter summarises the project by first illustrating the design requirements and their constraints in section 4.3. Section 4.4 discusses the concepts examined. The trade-off used to find the concept to be designed is highlighted in section 4.5. This concept is discussed in detail in section 4.6. The conclusions and recommendations are elaborated in sections 4.7 and 4.8 respectively.

4.2 Mission objective

The mission objective states:

"Design a durable and lightweight wing that can be used for cost-effective traction power generation in a pumping kite power system"

This objective ties in with the mission statement of this project which states:

"Develop a pumping kite power system that will generate electricity in a sustainable and cost effective manner while producing no environmentally harmful emissions."

4.3 Design requirements and constraints

To achieve these objectives, a list of requirements is provided by the tutors. Some of these requirements are modified by the group and additional ones included. The list of requirements and constraints reads as follows:

Requirements

- Sustain a maximum wind loading of 30 kN;
- Wing span ≤ 10 m;
- Maximum operating altitude of 1500 m ASL;
- Operational up to wind speeds of 25 m/s;
- Stall speed < 5 m/s;
- Reel in speed > 10 m/s with a traction force < 10 kN;
- Power output of 40 kW during traction phase at ground velocities of 5-12 m/s.

Contraints

- The wing shall perform a pumping cycle operation;
- The wing shall fly a figure eight trajectory;
- The wing shall be aerodynamically stable over the entire flight envelope;
- The system shall be fully automated over the entire flight envelope;
- The wing shall be controllable and well predictable over the entire flight envelope;
- The system shall have a safe mode;
- Operational life > 1000 hours;
- The life span of the AWE system shall be 20 years;
- Major components of the system shall be accessible and maintainable;
- Space for sensors shall be integrated;
- The wing shall be scalable;
- The system shall have an airborne power supply.

4.4 Concepts examined

Hybrid ram

The hybrid ram kite has the advantages of a ram kite i.e. lightweight, cheap materials and ease of manufacturing. To enhance the design, rigid ribs between air chambers are installed to reduce the stress concentrations in the fabric. This leads to a lower number of bridle attachments needed per rib as it can efficiently distribute loads. Two bridle lines per rib are needed thus reducing the effect of bridle drag on the system performance. The kite will have a bow shape, elliptical

planform and an airborne kite control unit with a power generating turbine.

Rigid hybrid

The rigid hybrid concept is akin to a conventional aircraft with a wing with a tail. The concept has two tail booms and an upside down U-shape tail. The main wing has an elliptical planform. Structurally, it consists of either one large wing box, or two smaller ones. Ribs are installed between the wing boxes to maintain the aerofoil shape as the skin is a pre-tensioned fabric. Kite control is achieved by using the V-shaped bridles for roll. The control unit is within the structure of the kite.

Rigid conventional

This concept looks similar to the rigid hybrid. The main difference is the planform and tail shape. The kite is controlled with conventional aerodynamic control surfaces.

Rigid flying wing

The flying wing concept does not have a tail therefore stability is achieved using wing sweep and/or a reflexed aerofoil. A dihedral on the wing enhances roll stability and winglets provide for yaw stability. In addition, the centre of gravity can be altered to achieve stability and controllability. The winglets have rudders installed on them while elevons are on the wings.

Prandtl plane

A very high aspect ratio wing with the wing folded on top of itself thus creating a boxlike front view. The fuselage is split and trimmed down, because it does not need to carry payload internally. Splitting the fuselage attachment points creates at least two bridle connections. The middle sections of both wings are non-swept because this is not needed for the low speeds the kite is set to operate at. The outer half of the bottom wing has a dihedral to provide roll stability - the other wing sections have no dihedral. For longitudinal stability to be effected, the bottom wing needs to generate 2% more lift whereas the

top wing should produce 2% less lift [1]. The kite is controlled with ailerons on the front wing, rudders on both vertical tail surfaces and an elevator on the non-swept part of the REAR wing.

4.5 Trade-off

A multi criteria analysis method, as invented by Thomas L. Saaty, is implemented to select the final concept. This method entails taking into consideration the importance of each criterion relative to the other criteria. The weights of each criterion are then normalised. The criteria considered are: Stall speed, durability, costs and reel-in energy. These criteria are deemed as most critical in the selection of a final design.

Each criterion is ranked from 1-10 with 1 being poor and 10 as excellent. These grades have the weight factored in and they are then added to find a clear overall winner. In this case, there is a tie between the rigid conventional and rigid flying wing concept. A sub trade-off is undergone. Risk of Design process, scalability, safety, maintainability and sustainability are used to rank these two concepts. The same process is undergone and the eventual winner is the rigid conventional concept.

4.6 The design

The chosen concept is a 'rigid conventional' kite. This concept is described in section 4.4 and is characterized by its conventional configuration. It consists of a wing with a tail connected by a tail boom. It is remarkable that there is no part of the 'fuselage' front of the main wing. The 'fuselage' is very small, because it only provides a structural connection between wing and tail. The tail boom is relatively small because of the low tail loads.

[1] John P Fielding Paul O Jamitola. Box Wing Aircraft Conceptual Design, 'Article'-Department of Aerospace Engineering, Cranfield University,2012.

The wing span was limited to ten meters to maximise the aspect ratio for aerodynamics optimisation. An elliptic lift distribution is desired and consequently a taper ratio of 0.4 for a single tapered wing is selected. All wing characteristic parameters are shown in table 4.1.

Table 4.1: Wing characteristic parameters

Parameter	Value
Surface Area [m^2]	12.7
Span [m]	10
Root chord [m]	1.8
Taper ratio [-]	0.4
Aspect ratio [-]	7.9
Dihedral [◦]	2.0

The aerofoil chosen for this concept is the Wortmann FX73-CL3-152. It is chosen because of its very high maximum lift coefficient, C_{Lmax}, and because of its high thickness. The latter argument is mainly for structural advantages. The aerofoil is shown in figure 4.1.

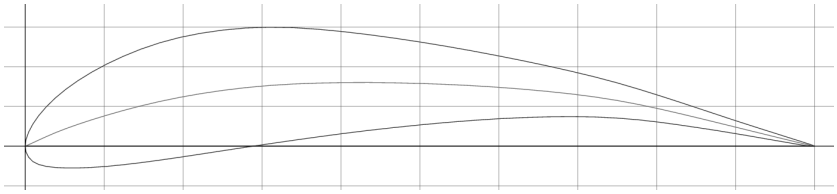

Figure 4.1: Wortmann FX73-CL3-152 aerofoil

The wing box for the main wing is from 0.1 to 0.5 chord and shown in figure 4.2. Part A is the front of the aerofoil for aerodynamics purpose. Part B is the main load bearing structure. Bottom part C and rear upper part D are then to finish the wing structure.

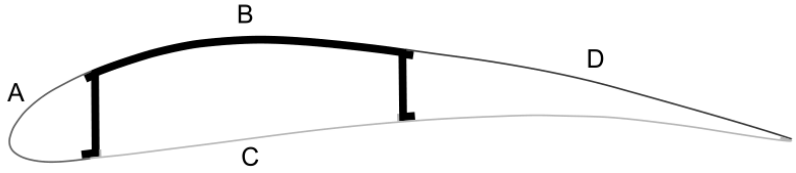

Figure 4.2: Panel division for the production of the main wing

This panel division is chosen for ease of assembly and minimization of mould size. First the boldly indicated structure is constructed; the ribs are then attached to this section. They are first inserted at the wingtip, then 2.95 m from the wing tip and finally 4.25 m from the wing tip. The section is completed by addition of C. D is mounted on this structure before A is glued onto it to complete the wing.

The tail boom connects the tail to the wing and starts at the wings' thickest part to the thickest part of the vertical wing. The boom has an elliptical cross section for a better airflow around the beam. The height over width ratio is two. The boom has an upward deflection with respect to the main wing, because the kite flies at high angles of attack at a large range of its operation. This results in the upward body being more tangent to the flow decreasing the drag. In order to have the horizontal tail at the same level as the main wing the boom connects to halfway the vertical tail with the horizontal tail at the bottom of the vertical tail. The vertical and horizontal tail both have a NACA 0010 aerofoil to not produce lift when no angle of attack on the tail surfaces is acting. The sizing of the tail is shown in table 4.2.

Table 4.2: Tail size characteristics

Parameter	Horizontal tail	Vertical tail
Span [m]	3.07	1.20
Chord [-]	0.62	0.62
Aspect ratio [-]	4.96	1.95
Surface area [m^2]	1.90	0.74

To control the kite, conventional control surfaces are used. These are the ailerons, elevators and rudder at the wing, horizontal tail and vertical tail respectively. The ailerons make the kite roll to a certain bank angle in a short time, because high manoeuvrability is preferred. Further the elevator is used to give the kite an angular pitch acceleration to pitch up or down when it finishes the traction or depowering phase. The rudder is used to perform the turns during traction phase. These turns are characterised by a small radius of ten meters at a maximum bank angle of 45°. This leads to the control surfaces shown in table 4.3. The aileron and elevator consist of two

parts, one on both sides of the wing or horizontal tail. The rudders consist of one part at the middle of the vertical tail.

Table 4.3: Control surfaces characteristics

Control surface	Aileron	Elevator	Rudder
(Half)Span [m]	2.50	0.31	0.60
Chord [m]	0.218	0.093	0.123
Inboard position [-]	0.41	0.40	0.00

The resulting side, top and front view of the kite design as described above can be found in figures 4.3, 4.4 and 4.5 respectively. These figures clearly show the taper ratio of the wing and the upward deflection of the tail boom. Also the control surfaces are shown in the wing, horizontal and vertical tail.

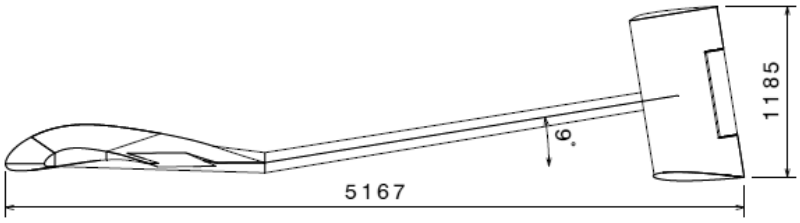

Figure 4.3: A side view of the kite

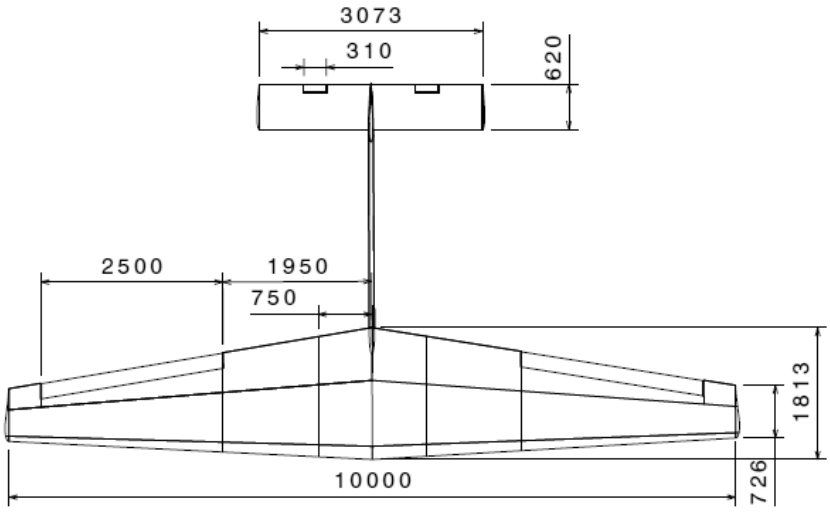

Figure 4.4: A top view of the kite

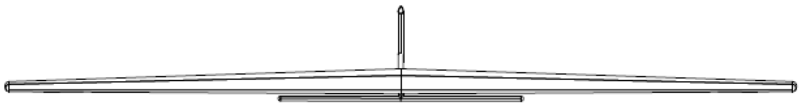

Figure 4.5: A front view of the kite

The resulting mass of the kite itself is 37.98 kg and the mass of the components are determined to be 7.2 kg. In order to control the kite a series of sensors are used. The electrical components used to aid in controlling the kite are found to consume 69.9 W of power. This power is provided by a battery which is charged by a turbine with a radius of 0.0645 m.

In order to get the best power performance the power output per height is taken into account. This is done with figure 4.6. As can be seen the best performance is around 150 m. That is because the higher the altitude not only the wind velocity increases, but also the tether length. The last one contributes a lot to the total drag of the system, reducing the power output. Therefore an operation altitude range is taken from 100 m to 350 m to achieve the required output of 40 kW.

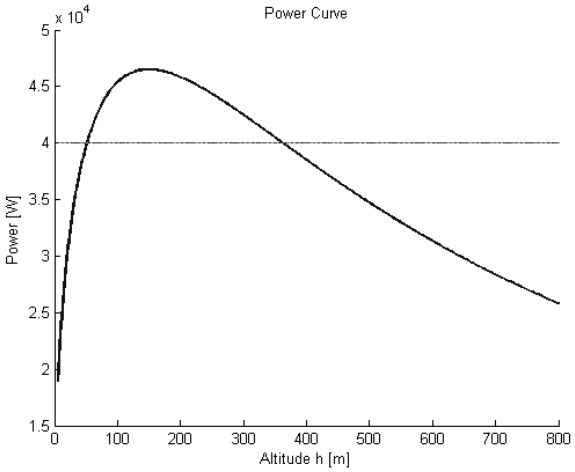

Figure 4.6: Power output versus altitude

4.7 Conclusion

After ten weeks of work it can be concluded that it is possible to design a durable and lightweight kite for pumping kite power generation. Furthermore, it is shown that the system can be sustainable and cost-effective. During this project several insights were gained. In the aerodynamic analysis, it became clear that the maximum lift coefficient, $C_{L_{max}}$, is the driving design parameter and not the expected C_L^3/C_D^2 ratio.

It was also concluded that flying at higher altitude is not beneficial in this case because of the large increase in drag due to the larger tether length. In the structural section, it became clear that a structure of prismatic tubes with ribs and cloth skin was not viable because of the high loads involved. Lastly, in the stability and controllability section it was shown that the kite is stable and, with the control surfaces, is controllable.

4.8 Recommendations

Completion of this project does not signify the completion of the design of such kite systems and therefore further recommendations are given for future developments.

In the case of aerodynamics further investigation can be done to improve validation and analysis. This has been done using the XFLR5 tool which is limited to Mach numbers of 0.1 and lower for validating the wing aerofoil. Full scale validation of the entire system with real data was not possible because of the extraordinary lift over weight ratio and also because of the slender boom, instead of a conventional fuselage. Therefore it is recommended in further development to do wind tunnel tests to get real data. In addition to this, investigation with CFD analysis is recommended to improve the aerodynamic investigation on, for instance, the use of high lift devices like flaps.

For the determination of the structure of the wing, an advanced method is used. However, more optimization and further investigation can be done. Weight optimization can be done, for instance, by using only sandwich panels locally in highly loaded areas or using strength compatibility for the stiffener calculation, where stiffeners taking only bending loads and the skin takes only shear loads. Also a further investigation of aero-elasticity, fatigue, compressive forces due to the bridle angle, shear buckling and buckling under its own weight is recommended. For the investigation of these effects the use of a FEA tool is recommended.

During this project the main focus was on the design of the kite itself. Therefore only a low level take-off and landing concept was developed. In future development a more detailed analysis should be executed to, for example, workout in detail the acceleration loads.

By the conclusion of this project, a kite-ground station interaction is assessed in low detail. Further analysis should be done in future developments. It is also recommended to investigate a system where the 'brain' of the kite is in the kite itself. In this case, the kite control is

not dependent on a data link between the kite and the ground and can fly autonomously thus increasing its safety.

The last section where improvement on the system can be made is the power production potential. There are two areas to improve: The low wind and the high wind cases. Investigation should be done on a resizing for lower wind speeds which improves the availability of the kite due to a lot of wind velocities below 5 m/s.

For the high wind speeds a decrease in reel-out speed is required to increase the power output. Decreasing the speed can be done in two ways: Using some speed breaker like a spoiler or by an increase in tether length without increasing the altitude of the kite. In both cases an increase in the drag of the kite is desired. This leads to much wider range of wind speeds at which the kite can operate and so a large increase in electricity yield per annum can be achieved. It should be investigated if this increase in yield justifies the increase of weight of the system.

5. AERIS

Students: F.J. Aendekerk, X.R.I. Mobertz, S. Rijal, A.G. Storteboom, N. van Dijk, J.R. Thuijs, B.B. Winters, T. Mkhoyan, G.J.H. Geurts, D.T.J. van Helvoort

Project tutor: dr. R.M. Groves

Coaches: S. Minghe, Msc., H.W. Ho, Msc

5.1 Introduction

In recent years, technological breakthroughs in lasers have widened their applications; they are no longer limited to cutting or welding, and may now be considered for wireless power transmission. Combined with other energy harvesting technologies, using lasers may increase an Unmanned Aerial Vehicle's (UAV) endurance, range and business potential.

As a final year Design Synthesis Project (DSE), a group of 10 students were assigned to design in 10 weeks a continuously flying Earth observation UAV that is partially powered by external laser. Soon after starting the project, the group named the concept "AERIS", standing for Aerial Research Inspection and Surveillance. The name also alludes to one of the ancient Greek goddesses, Iris, who served as a messenger for the other gods, and is the Latin word for air.

The mission statement of the project is to

"*provide a reliable, sustainable and accessible system capable of accurate and continuous monitoring urban areas, natural landscapes, coastlines and weather in the Netherlands from 2016 onwards,*"

which directly follows from the mission need statement:

"*Mankind needs longer range, more sustainable and more accessible UAV to provide accurate and continuous Earth observation*."

The scope of the project was partially set by the engineering skills learnt by the students prior to this project in their bachelor's degree in Aerospace Engineering, though some additional skills were learnt during the project. The project and additional assumed stakeholder requirements are summarized in table 5.1.

5.2 Project initiation

The project began with the proposal of a project plan. This designs the Human Resources (HR) management structure in which team members were assigned to certain roles and responsibilities within the team. The division of roles were made in such a way that each team member would have both technical and non-technical roles during the various design phases of the project. The Work Breakdown Structure (WBS) and Work Flow Diagram (WFD) were created to have a detailed overview of the required activities and the required order of their execution respectively. A detailed project schedule was produced in the form of a Gantt chart to identify the various project phases. The group's design philosophy – in particular its policy on sustainable design – and additional stakeholder requirements that the group expected to account for in a commercial environment were also given in the form of a Requirements Discovery Tree (RDT).

Table 5.1: Project requirements

Project Description Requirements		Assumed Stakeholder Requirements	
SUS-2	At least 20% of the energy used by the system shall come from renewable sources.	MG-1	Employees shall be employed for the whole mission.
GEN-2	The system shall be capable of monitoring every part of the Netherlands.	MG-2	Investments shall break even within 3 years of operation.
GEN-3	The operational lifetime shall be at least 5 years.	MG-3	Services shall be in the financial reach of micro-enterprises.
FPF-1	The UAV shall fly between 50 and 100 km/h.	SUS-1	Measures shall be taken to reduce the amount of energy that is used during life-cycle.
FPF-2	The UAV shall sustain continuous flight in normal operational and meteorological conditions.	SUS-3	The materials used shall be recyclable.
FPF-3	The operational altitude shall be between 100 m and 4000 m.	SUS-4	The materials used shall be non-toxic.
EQ-2	The UAV shall have a high-resolution spectral camera on-board.	EQ-1	There shall be a continuous stream of data available during the entire mission.
ENE-1	At least 50% of the energy used on-board shall be provided by remote power beaming.	GEN-1	In case of failure there shall always be a back-up system of stand-by.
ENE-2	At least 20% of the energy used on-board shall be provided by solar cells.	GEN-2	The system shall be capable of monitoring every part of the Netherlands.
SAF-3	The UAV shall have a fail-safe emergency landing mode in case of power loss.	MG-4	A manual shall be present, containing all information needed to operate the entire system.
ENE-3	Any remaining power shall come from COTS energy harvesting systems.	SAF-1	The system shall be capable of avoiding safety hazards such as bird strikes.
GST-1	The number of base stations required for remote power shall be minimized.	SAF-2	The position of the system shall be known at any moment during the mission.
SUS-6	Noise levels shall respect the norms set by environmental institutes.	SEC-1	The system shall be protected against theft and vandalism.
FIN-1	Road map and budget for introducing the technology to the market.	SEC-2	Measures shall be taken to reduce the risk of hacking the system.
		GOV-1	The system shall operate according to all relevant laws.
		GOV-2	The system shall respect each and everyone's privacy rights.
		SUS-5	The system shall not cause any harm to wildlife.
		GOV-3	Direct stakeholders' privacy shall be respected.
		EQ-3	The data link shall provide sufficient data transfer capacity to sustain a live-stream.
		SAF-4	The power available for the UAV shall not drop below a critical level, making landing on a safe location possible.
		SAF-5	The UAV shall have a collision avoidance system.
		SAF-6	The system shall be capable of recognizing weather hazardous to the UAV's operation.

The case study and the project requirements were then researched further, which substantially developed the scope of the project. Monitoring the waterways of the province of Zuid-Holland in the Netherlands would be priority and focus of the first years of the proposed business plan. The project's scalability is considered in the later stages of a five-year business plan where the objective would be to expand to every part of the Netherlands. These aspects and their associated risks are considered in a risk analysis, and following this certain measures to mitigate those risks are iterated.

A functional analysis was then performed, resulting in a Function Breakdown Structure (FBS) and a Functional Flow Diagram (FFD). The FFD ensured that all functions are addressed by the design to perform the mission. Meanwhile the FBS served to give a technical overview of the design problem.

5.3 Final concept selection

Initially, several design options existed to fulfil mission requirements and objectives. These options were given in the form of a Design Option Tree (DOT) in their respective categories. These categories included UAV types, take-off methods and propulsion types among others. Several options were rather innovative, which really allowed the team to consider the pros and cons of those possible solutions to the fullest extent of their ability. Solutions that were later seen not to comply with the project description and stakeholder requirements were eliminated immediately, and a few were directly traded off.

The design options that remained were then sized to give more concrete information to analyse. Some performance parameters relied on an 'engineering gut' sense, hence they were limited in their importance, as seen at the bottom of table 5.2.

Table 5.2: Trade-off

Parameter	***Importance***	***Glider***	***Flying wing***	***Prandtl wing***	***Zeppelin***
Endurance Vmax [hrs]	0.125	0.34	0.18	0.25	0.22
Endurance Vmin [hrs]	0.100	0.26	0.21	0.25	0.28
V_20 percent solar [km/h]	0.138	0.28	0.22	0.25	0.25
Noise Rating [W]	0.038	0.94	0.78	0.90	0.38
Battery Mass [kg]	0.125	0.94	0.78	0.90	0.37
Structural Mass [kg]	0.025	0.90	0.93	0.94	0.23
Engine Mass [kg]	0.063	0.94	0.78	0.90	0.38
Solar Panel Mass [kg]	0.075	0.94	0.85	0.91	0.30
Total mass [kg]	0.013	0.91	0.85	0.90	0.34
Thermals	0.025	0.03	0.09	0.05	0.83
Laser power [W]	0.088	0.94	0.78	0.90	0.37
Stability	0.038	0.32	0.08	0.28	0.32
Controlability	0.025	0.32	0.36	0.28	0.04
Reliability	0.038	0.43	0.29	0.19	0.10
Cost	0.013	0.37	0.30	0.22	0.11
Maintainability	0.025	0.31	0.35	0.27	0.08
Safety	0.050	0.40	0.28	0.28	0.04
OVERALL SCORES					
Standard weighted sum		0.575	0.468	0.525	0.282
Conservative design		0.281	0.215	0.252	0.249
Aggressive design		0.474	0.367	0.418	0.240

In this table, the team gave each design option overall scores that had different mathematical definitions. Simply put, the standard weighted sum was simply the sum of each score multiplied by its weight (importance), whilst the conservative and aggressive designs had worst-score and best-score biases respectively. This allows further

examination of discrepancies that may have gone unnoticed and re-iterate or revise the component scores, allowing implementing further learning about each design whilst double-checking one's work. The results of the trade-off in table 5.2 as well as the lower-level trade-offs are summarized in table 5.3.

Table 5.3: Lower level trade-offs

Functions	**Results**
UAV Types	High Aspect Ratio Glider
Take-Off Configuration	Catapult
Landing	Belly Landing
Power Transmission	Laser
On-board Power Storage	Battery
On-board Power Source	Solar Cells
Propulsion System	Electric Propeller

5.4 AERIS' characteristics

AERIS is a high aspect ratio glider with a high wing configuration, two fuselages, a vertically inverted V-tail connecting two fuselages and an electric propeller engine positioned behind the wing. The wing is the main load-bearing structures. The subsystems and their most important characteristics will now be described in the order of the N^2 chart from the payload to the stability and control system.

According to requirement EQ-2, AERIS has an on-board Hyperspectral Imager (HSI). It is able to capture a large portion of the electromagnetic spectrum reflecting from the Earth's surface. Not only is it able to make a high-definition map of the surface, it is also capable of detecting fires, oil leaks, chemical hazards, and natural disasters, not to mention various forms of pollution. The team added an infrared (IR) camera as an additional payload for night-time monitoring activities when the team realized that the HSI would be unable to function in low-light conditions. The IR camera would, for example, be able to detect fires as well as thermal leakages from homes and businesses on the ground. The IR camera is able to detect objects with temperatures between -25°C to 160°C. An additional IR

camera with the same specifications is used as a sensor for the autonomous detect-and-avoid system on-board the UAV.

Both payload cameras are mounted on a lightweight gimbal system, which has several integrated servos and gyroscopes to provide image stabilization about all three axes. The raw video stream produced by the HSI results in a data rate of 63 Mbps. The video stream processed by the payload and safety IR camera result in data rate of 5.2 and 35 Mbps respectively.

These data need to be analysed further at the ground station, requiring a communication system. The communication system of AERIS consists of a transceiver, an Automatic Dependent Surveillance-Broadcast (ADS-B), and a computer for compressing and uncompressing the data from the payload and from the ground respectively. The communication system uses ultra-high frequency band of 2.4 GHz to establish connection with the ground station. :The uplink commands are sent using a radio signal of frequency 480 MHz. The team found that the communications system easily functions over a radius of 60 km with a single ground station. The aforementioned computer has a compression ratio of 3:1 to compress the data gathered from the payload before it is transferred to the ground station; this compression is without losses.

The ground station consists of six different segments:

- The communication segment – consists of an antenna to establish connection with the UAV and a transceiver to send and receive data.
- The control room – consists of a flight control device to control and manage the movement of AERIS, as well as two pilots on stand-by.
- A data storage facility – consists of computers to analyse the retrieved data.
- The laser station – consists of a laser, the pointer and a cooling system to remove waste heat from the laser. This will be situated on top of the EWI building at the Delft University of Technology.
- A workshop for repairs.
- A launch site – consists of a catapult.

Table 5.4: Overview of functions

Functions	Results
Wavelength	1064 ±10 nm
Laser Output Power	2000 W
Beam Quality	5 ±3 mm·rad
Cooling Water Temperature	15 ±7.5 °C
Width	730 mm
Height	1375 mm
Depth	1120 mm

AERIS' payload and communication subsystems must, of course, be lifted into the air. The wing's sizing began with an aerofoil selection. Though there are thousands of aerofoils available, it is very difficult to select the best aerofoil most suited to AERIS' mission. Hence, a few seemingly appropriate aerofoils were chosen and their performance was simulated in XFLR5. These aerofoils were the:

- NACA 2410
- NACA 2210
- SA 7035
- HN 1023

The two-dimensional aerofoils' performances were plotted against each other to compare them. A trade-off was then performed; the NACA 2210 was found to be the most suitable aerofoil with a stall angle of 13°, a maximum lift coefficient of 1.35, and maximum glide ratio of 86.

The wing was then sized according to a reiterated total mass after it was assumed that an aspect of 30 would be most suitable – a figure that suggested itself as appropriate in the team's research. The wing was divided into a number of sections along its span. The contour of each section was divided into a number of segments, and the aerodynamic forces and moments were calculated for each section.

The propulsion system of AERIS is powered by an electric motor. An efficient propulsion system is most likely the key for AERIS' success as it uses the majority of the required power. The efficiency of the

engine largely depends on the Revolutions per Minute (RPM), and this in turn is affected by the propeller's angle of twist, chord distribution, radius of the propeller and its shape. The latter was determined by using a rather common Clark Y aerofoil, and the remaining parameters were optimized in an iterative multivariate optimization process.

To estimate the radius of the propeller blade, linear momentum theory was used. It was found that the radius of propeller increases with a decrease in exit velocity, which increases the propeller's efficiency. The iterative design of the propeller was terminated when enough thrust was finally produced by the propulsion system. The propeller has a theoretical efficiency of 0.95 with a propeller diameter of 1.00 m. The maximum power that the engine has to deliver was determined by its service ceiling, which is located at 4,000 m; AERIS' take off is made possible with the use of a catapult at the launch site. The thrust required during ascents changes with the change in air density and speed was computed to produce a 3-dimensional rate of climb performance graph.

The ability of AERIS to fly continuously depends largely on the on-board power sources and power storage. The power subsystem provides electrical current at the required voltage to the right location at the right time. AERIS' power subsystem consists of an on-board energy harvesting system, a laser energy collection system, batteries and cables. The solar array depends on the wing surface area, and was assumed to be able to cover 90% of the wing's top surface. The laser panel was attached to the winglets, and its size estimated to be 0.3x0.3 [m]. The battery system on-board AERIS consists of novel Lithium Sulfur (LiS) battery packs as well as a Lithium Polymer (LiPo) emergency pack. Each LiS battery pack has an 8-series 1-parallel configuration (8S1P) which resulted in 16.4 V and 10 Ah with an estimated mass of 584 g. Each of these packs have a capacity of 168 Wh at Beginning of Life (BOL) and 134.4 Wh at the End of Life (EOL). The battery degradation of 20 percent over 2,000 cycles was taken into account after which the battery would need to be replaced.

Charging the battery using solar cells is very achievable, whereas charging with the laser panel imposes a limit. LiS batteries possess very high charging efficiency. The maximum charge rate of LiS is 0.25C i.e. the maximum charging time is four hours when the battery is completely empty. During the course of charging, a fluctuation in voltages can occur that may potentially damage other systems, making laser charging relatively risky. The voltage fluctuations and proper voltage distribution to the various subsystems will be regulated with the use of Power Management System (PMS). The required cable sizes to connect each component in the UAV, was sized according to the amount of voltage and amperage used by that component.

Since AERIS will be flying autonomously, its stability and controllability plays a significant role in its mission performance. To make AERIS stable and controllable an inverted V tail was implemented. Two major advantages of this tail are that the tail is outside of the engine wake and that it provides the UAV with a closed structure. Since the design has two booms, the position of the subsystems may result in an asymmetric weight distribution. To minimize this the position of batteries was shifted until the desired plane of symmetry was attained.

The effects of margins on centre of gravity travel was analysed to define the effect of changing the mass and position of the batteries and payload. The effect provided a limit on the most aft and the most forward centre of gravity location the aircraft is allowed to have while the stability and controllability is ensured. The conventional tail sizing procedure involves an estimation of required horizontal tail and a vertical tail that was later combined to form an inverted V-tail. The V-tail requires less actuators compared to conventional configurations and also combines the function of rudder and elevator in a device called a ruddervator and makes the overall design lighter.

The sizing process of every system and subsystem of AERIS was done by making a MATLAB script. This script resulted in a numerical model. For verification, the analytical values of each module were

calculated using the corresponding governing equations. Those analytical values were compared with the numerical results. There exist several other methods to check the code. The checks performed were unit checks, common sense, and engineering intuition as to whether reasonable values were obtained by the code. The numerical model that was built during sizing process was verified for all modules. In every module the numerical results approximated the analytical solution very closely.

A numerical model cannot be fully approved unless it has been validated. One of the most common ways to validate a design is performing live tests. Since AERIS is still a concept these tests cannot be performed yet. Once AERIS had been sized it was modelled in X plane. The numerically sized AERIS successfully flew at different altitudes, flight speeds, weather conditions and angles of attack thereby validating the results obtained from the numerical model.

5.5 AERIS in bigger picture

Now that AERIS and its subsystems have been sized, the weight, dimensions and specifications can be obtained. The wingspan of AERIS is estimated to be 9 m with an aspect ratio of 30, a root chord length of 0.43 m, tip chord length of 0.17 m and a surface area of 2.73 m^2. To be able to charge up safely with the current pointing accuracy a winglet is applied to the wing with a slightly bigger length than the tip chord length. The propulsion system of AERIS consists of one propeller that can gear between two different engines, one for cruise and one for maximum speed. The propeller is foldable, has a diameter of 1 m, an angular velocity of 600 RPM and is positioned in between the two booms. To be able to deliver such low angular velocities a gear ratio of 10:1 is used.

The power system of AERIS consists of two systems on board to provide enough energy: Solar cells to harvest the energy from the sun and a laser panel to harvest energy from the laser. The 2500 solar cells are arranged in such a way that it covers 90% of the top wing surface. The maximum power that can be generated by these solar cells equals

535 W. This system weighs 1.28 kg. The size of the laser panel equals 0.3 x 0.3 m. The harvested energy is transferred into 7 batteries and these weigh 4.09 kg. The expected Beginning of Life and End of Life endurance for 2,000 cycles is estimated to be 7.46 h and 6.13 h respectively. The distribution of power among several system and subsystem in AERIS is managed by Power Management System (PMS). The width of the antenna cable and laser charging cable is estimated to be 0.1 and 4.1 mm.

The structure of AERIS consists of two materials: ABS and Titanium. ABS is Acrylonitrile Butadiene Styrene and is good for adding inertia, however it fails to cope with big stresses and with the thin-walled assumption used during the sizing process. Whereas Titanium holds a good property in terms of strength, but is very heavy. Hence, a combination of these two materials is used in both the fuselages and the wing. Resulting in a total structural mass of 3.35 kg.

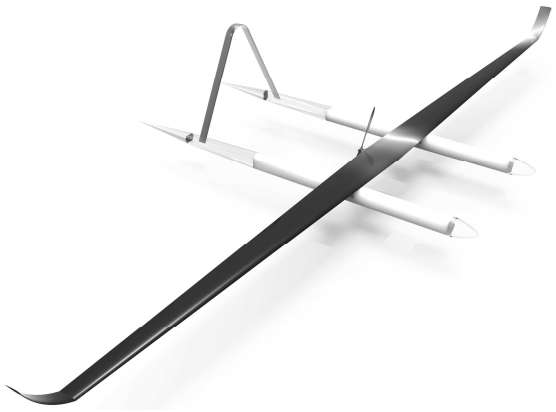

Figure 5.1. Overview of AERIS

Finally, the span of the inverted V-tail is estimated to be 1.5 m and has a surface of 0.157 $m^2$with an inverted tail angle of 57.97 degrees. The total mass of AERIS is calculated to be 12.5 kg.

5.6 Conclusion and recommendations

This executive summary marks the end of the design synthesis of AERIS: a UAV capable of continuous flight by using remote power. The project not only considered how to design a partially laser powered continuously flying UAV, it has also respected sustainable

development as a key value. It has fulfilled every client requirement with the exception of few requirements that were met partially due to current legislation towards autonomously flying and the lack of completely renewable materials.

AERIS started as a "prestige" project investigating the implementation of external laser power in UAV design. However, analysis of Western markets showed that there are enormous amounts of possibilities and there is a huge market potential, which can be targeted by AERIS to satisfy the needs of several different clients over a range of different industries.

Reflecting on AERIS' conceptual design, external laser power seemed to pose several performance limits to the design, as it is currently not well suited to long-ranged UAV designs. In addition to this, the latest market analysis showed that it would not be especially beneficial to a real design, as it might impose further unnecessary financial risk to potential investors with no outweighing advantage. The external laser power shows a lot of promise in future smaller-ranged UAV design. Not only does it have the potential to broaden the energy mix of future aircraft, it also has the ability to drastically reduce the size of those aircraft by eliminating the need of on-board power storage.

AERIS is not only ambitious because of its external power usage, it is also highly ambitious in its extreme endurance, as well as how it explores and attempts to exploit the advantages of additive manufacturing. The team not only moved away from the conventional wing-box and fuselage designs, it implemented a completely novel design technique to give the most efficient structure to bear loads whilst consuming as little material as possible and thereby keeping the weight down. Even though AERIS has been finalized within the scope of the DSE, several aspects of the design should be investigated in more detail to fine-tune and improve the design. The risk involved within the project should to be mitigated thereby increasing the reliability of the entire system which can be processed by detail analysis of the events identified as "high risk" and by testing the product physically. This will give insight to reassess the safety factors

and margins taken into account during sizing several systems and subsystems, which might eventually result in a lighter, higher performing design.

During the sizing process, it was assumed that the inflight vibrations on HSI are null and operates with perfect light reflection from the ground. However, this is not the case in real life missions as the weather influences the light reflection from the ground and inflight vibrations occur during the mission. Hence, an extensive research and additional integrated software needs to be included to compensate for the random spectral variations as well as the blur for the varying velocities and altitude settings.

To make AERIS able to communicate in every part of the Netherlands, research must be performed to determine the optimum number and location of additional communication stations. The actual effectiveness of the tail shape has to be investigated together with the double engine propulsion system. Apart from these, the possibility of implementing combination of titanium and ABS on the structure of AERIS needs to be investigated. Also real tests on the structure need to be performed to validate the model to ensure that it can sustain the expected loads during its life cycle.

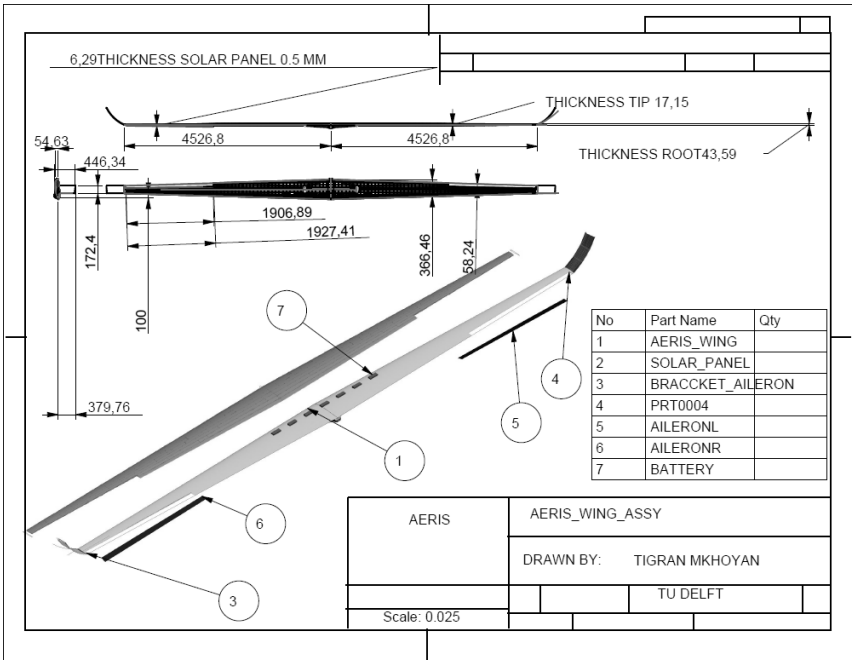

Figure 5.2. Technical Drawing of AERIS' Wing

6. LOFARSIDE

Students: K.A. Bossenbroek, A. Dorozsmai, N. Hadzisejdic, W.J. Bouma, F.C. Hogervorst, O. Mazouz, A. Gorbatenko, M. Ortega, T. Vergoossen

Project tutor: ir. M.C. Naeije

Coaches: dr. M. Gallo, ir. K.J. Cowan, ir. K.J. Sudmeijer

6.1 Mission objectives and constraints

Lofarside is a European, unmanned, scientific mission to the Shackleton crater at the South Pole of the Moon designed by 9 students of TU Delft. The main scientific objective is:
to deploy a 10 km long baseline ultra-long wavelength interferometer consisting of 21 crossed-dipole antennas and to detect signals with frequencies below 10 MHz.

This frequency band is yet unknown to humans and this mission would provide the first measurements ever. Results of the measurements would provide important information of the early phases of our Universe (Epoch of Re-ionization and Dark Ages) and they would help to create Extragalactic Surveys. The antenna array station would also act as a pathfinder mission for a larger lunar observatory (with 10^5 elements) and also as an extension of the Low Frequency Array (LOFAR) in The Netherlands. On Earth, it is

impossible to detect signals arriving from space below 10-30 MHz because the ionosphere reflects them. An eternally dark crater on the Moon (such as the Shackleton) would provide an ideal place for such measurements. It shields the system from man-made radio frequency, Sun and planetary interference. Moreover, it has a fairly constant temperature, which would make the calibration of the antennas easy. Furthermore, the Moon has a negligible ionosphere. In order to maximize the scientific output of the mission, a Langmuir probe and Multi-Purpose Sensors for Surface and Subsurface Science (MUPUS) will be brought to the lunar surface. The Langmuir probe will study the electrical properties of the regolith and its effects on electromagnetic waves. This will help to understand the severity of the effects on the astronomical measurements of the lunar dust.

The MUPUS will observe the thermal properties of the surface of the South Pole of the Moon. The top level requirements, which were stipulated by the client, Airbus Defence and Space include that:

- the VEGA or VEGA- C launcher shall be used,
- hardware and technology implemented shall have at least a Technology Readiness Level (TRL) of 5,
- the duration of the mission shall be six years (with not more than one year of transfer),
- the budget shall not exceed 500 million euros and
- the baseline of the interferometer shall be at least 10 km.

Furthermore, electric propulsion is preferred. Use of VEGA implies that payload (including the space vehicles) will be launched to Low Earth Orbit and it can weigh approximately maximum 2280 kg.

In the following text the design process of the LOFARside mission is summarized. First an overview of the design concepts and related trade-offs is provided, which is followed by a detailed description of the selected concept and the most important design parameters. Finally, conclusions and recommendations obtained from the feasibility study of the LOFARside mission are presented.

6.2 Concepts

During the Mid-term period the main focus was on generating concepts and choosing the optimal concept that can perform the mission. The mission was divided into three main phases: Moon transfer, landing and LOFAR system deployment/operation.

Transfer

For Moon transfer the main considerations were:

- What kind of propulsion will be used for the transfer, chemical or electric?
- What orbit configuration will be used to get to the Moon?

Electric propulsion electrically expels reaction mass at high speeds. This kind of propulsion is very efficient compared to chemical propulsion. The downside is that much less thrust can be generated, resulting in longer transfer times. Next to the shorter transfer time, chemical propulsion also had the advantage that during the transfer orbit and the lunar landing the same system could be used. The reason for this is that thrust levels of electric propulsion are simply too low to provide enough deceleration during a landing procedure. An electric propulsion system would have to be combined with a chemical system for landing. A trade-off was performed between these concepts. With electric propulsion, 1500 kg could be brought into low lunar orbit, with chemical propulsion only 500 kg. The electric propulsion system won this trade-off.

Using electric propulsion limited the choice for transfer orbits. Low-thrust propulsion results in an orbit with slowly increasing altitude, called a spiral transfer.

Landing

For the landing phase a landing location was considered. During discussions with experts, it came forth that the performance of the LOFAR system is greatly influenced by the interference of the Sun. A Lunar day is approximately four months with two weeks of darkness and two weeks of sunlight. This implied that a system should be designed that operates for two weeks and then generates power for two weeks. Realising that this would greatly increase system

complexity, landing sites were considered that would prevent these problems. The solution was found on the South Pole. The lunar South Pole has a lot of craters where regions could be found that are in permanent darkness. On the other hand, some peaks on the South Pole are in almost continuous sunlight during a lunar year. This kind of terrain is ideal for a lunar LOFAR system. A landing site had to combine these features, which set requirements on the landing procedure. The lander would have to target a relatively small area on the Moon. This meant that a soft and precise lunar landing was necessary.

System deployment/operation

The deployment/operations design team had three main questions:

- How large will the array baseline be and what will the configuration look like?
- How will the system be deployed?
- In what manner will the data be transferred to Earth?

The required baseline for the LOFAR system was discussed with Leonid Gurvits and Marc Klein-Wolt, leading experts in this field. It was determined that a 10 km baseline was sufficient to measure ultra-low frequencies. The antennas can be deployed in a straight line for simplicity. Because the system will be on the South Pole, the straight line will complete one rotation every month, hence creating a circular, virtual array.

For system deployment several options were considered, the most promising ones were:

- deployment during hovering;
- shooting the antennas from the landing site;
- deploying the antennas with a rover.

A trade-off was performed considering mass, power required and reliability amongst other criteria. The winner was the rover deployment. The rover will enter a crater carrying the antennas. It will be connected with a cable to the lander which will supply it with

power. The antennas are also connected to the cable to receive power, but they will also transfer their data to the lander through the cable.

Data will be collected in the lander to subsequently be sent to Earth. Three options were put through a trade-off for this:

- direct data transfer,
- data transfer via a relay satellite around the Moon and
- data transfer via a relay satellite in lunar Lagrange point 2.

A celestial, two-body system has 5 Lagrange points, a satellite in a Lagrange point remains in the same position relative to the two bodies as they orbit each other and move through space. The Moon has a very irregular gravity, which means that most lunar orbits are unstable and require a lot of station keeping. Lunar Lagrange point 2 is also unstable, fuel is needed to keep a satellite in this point. An advantage of having a relay satellite is that it provides longer connection with a Ground Station. Also the satellite could be used for additional science. A direct system does not need a relay satellite at all. The direct system was chosen after the trade-off.

6.3 Mission overview

The S/C will be launched using ESA's VEGA-C launcher. After launch the S/C will use an electric propulsion system to spiral out from its 300 km Low Earth Orbit (LEO) with inclination of 16.7 degrees. Solar panels will provide the system with enough power during the transfer to the Moon. During the transfer phase two helical antennas mounted on opposite sides of the body will provide continuous communications with Ground Control. Using a chemical thruster the satellite will be inserted into a lunar orbit, where it will spiral down with low thrust propulsion to a polar orbit at 100 km. The lander will decouple from the transfer orbiter Spílaio, which will be crashed in a controlled manner on the Moon. The Noor lander will land on the rim of the Shackleton crater at the South pole of the Moon with high accuracy of 100 by 100 m using chemical propulsion. This accuracy is achieved using terrain relative navigation in combination with multiple sensors. The lander, situated at a position with almost

continuous illumination, will deploy the tethered Colbí rover that will descend into the crater's eternal darkness. It will deploy 10 km of cable and 21 antennas over unequal distances powered by the Noor lander's solar panels of 6.9 m^2. Using a thermal knife the crossed dipole antennas will deploy and after calibration can start their surveys. The data will be sent via a direct communications link to Earth for processing and analysis.

6.4 Mission specifications

The transfer vehicle Spílaio will be propelled by two Snecma PPS-500 Xenon Hall thrusters delivering a constant thrust of 0.55 N. This will be powered by two 18 m^2 solar panels placed symmetrically with respect to the centroid axes and will provide a minimum power of 8.5 kW. Uplink transmission for commands will be received using a helical antenna with a 0.055 m diameter and 0.1 m length operating in S-band. During transfer, two boxes of Control Momentum Gyroscopes (CMGs) provided by Airbus Defence & Space will control the attitude of the spacecraft and will be placed on the transfer vehicle. Furthermore ten 22 N thrusters will be placed in the lander vehicle with two additional 200 N thrusters to provide further attitude control for transfer and landing.

Braking of the vehicles will be conducted with six 200 N thrusters as well as five 500 N thrusters from Airbus Defence & Space. Landing struts designed for a drop from 3 m will be deployed for landing.
The lander will house the Colbí rover, which will have the 21 antennas attached to the cable that is wound around the rover's axis. The rover's design is based on NASA's Axel rover design. Colbí is adapted to be able to carry 63.6 kg of cables and 11 kg of antennas. Adaptions to the design are amongst others a wider wheelbase and larger wheels, 84 cm in diameter. A high-gain parabolic antenna with a diameter of 0.7 m operating in X-band will be used for the downlink data transmission of 84 Mbits/s.

All temperatures throughout the mission will be controlled with a 5 layered Silver Teflon multi-insulator and with a heat pipe system

which will ensure an even distribution of the temperatures within the spacecraft. Further local heating will be provided by a heater system provided by MINCO.

As extra payload, the LOFAR system will carry up to 30 kg of extra scientific instruments, counting with a Langmuir probe and a MUPUS package.

6.5 Conclusions

The goal of the project is to show that it is possible to place a LOFAR system on the far side of the Moon with a budget of 500 M€, while using the VEGA or VEGA-C launcher, components with TRL 5 or higher, as well as within a transfer time of 1 year.

The required use of the VEGA launcher provided implications on the mass budget, the starting orbit and the project budget. It resulted in a limited mass budget and the restriction to a low LEO starting orbit. The use of an electric propulsion system, as was preferred by the client, means that the S/C will spiral out towards the Moon through the Van Allen belts. These are a cloud of ionizing radiation trapped by the Earth's magnetic field which causes a degradation of the solar panels of 20%. If the satellite is launched into a Geostationary Transfer Orbit a large part of the Van Allen belts can be skipped and less thrust is required to stay within the one year transfer time requirement. This would lead to a reduction in size of the solar panels and so save mass and volume. A shared Ariane V (or Ariane VI depending on launch time) launch into GTO is therefore recommended.

Cost analysis has indicated that the project can be completed within this budget, the current cost estimate is 401 M€. A market analysis has shown that up to 60 M€ can be obtained from taking additional instruments to the Moon. A performance analysis has proved the system's compliance with almost all requirements. The mass of the design at this point exceeds the limit of the VEGA launcher. However, further design iterations can reduce the mass, for example the configuration of the S/C is oversized. Any mass savings will lead to

less required fuel mass, so additional mass is saved. In the case the mass does not decrease sufficiently, the VEGA-C launcher can be used, which provides a 15% better performance.

6.6 Recommendations

For the design of the orbit, more sophisticated models, which include better simulations of gravity, disturbances and propagators should be used. This might conclude that the high-thrust lunar orbit insertion is not necessary. Furthermore, newer engines might have a higher specific impulse and therefore less power would be needed.

The power at the beginning of life of the Spílaio transfer orbiter is 4 kW higher than necessary. Implementing this extra power in the transfer orbit analysis will lead to a shorter transfer time.

The landing procedure needs to be integrated and tested with the for the terrain relative navigation (TRN) and hazard and detection and avoidance. Algorithms like crater pattern matching could be tested in Unmanned Aerial Vehicles (UAVs) and end-to-end simulations.

The illumination periods and peaks surrounding the landing terrain should be analysed in more detail to size the solar panels and batteries of the Noor lander more accurately.

How the antennas are connected to the cable and the tether spool is rolled up has not been designed in detail and needs to be tested to establish its reliability. Alternatively, a film antenna might be easier to deploy and should be considered as well. Furthermore, a more detailed analysis of the Shackleton crater terrain should be conducted.

A bottom-to-top approach for cost modelling is recommended for more detailed design phases. Also the identification of critical cost drivers and their sensitivity should be assessed.

It is recommended to gauge industry interest to find companies and educational institutions willing to contribute additional instruments

in return for funding. Extension of the European LOFAR system demonstrated a great increase in performance, therefore, an extendable array should be considered.

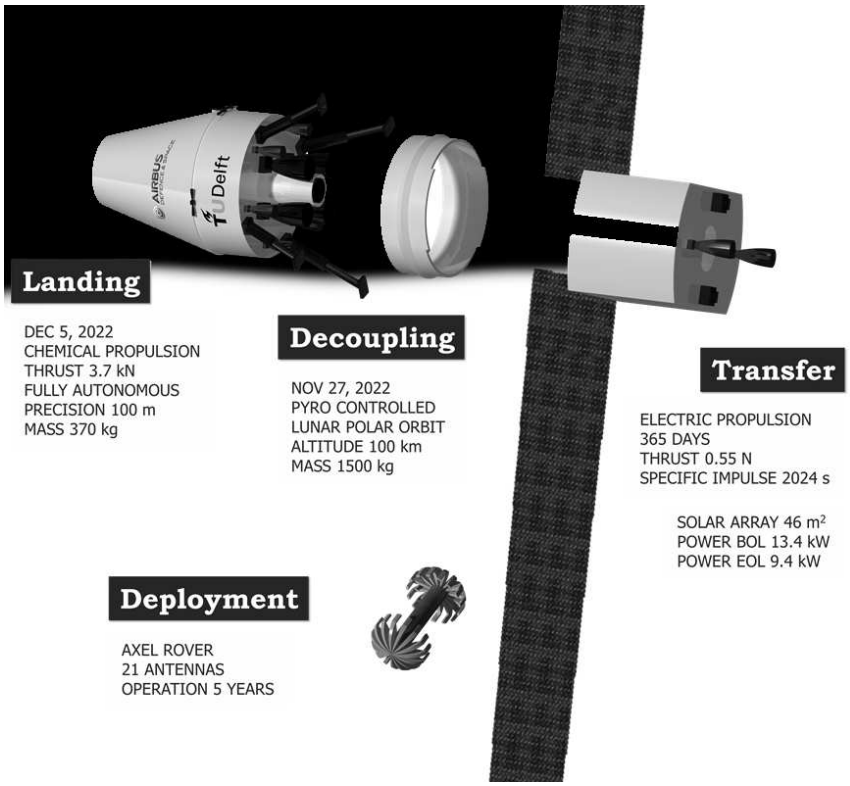

Figure 6.1: Main mission components

7. PZERO ELECTRIC PARAMOTOR

Students: A.D.J. Beets, J.L. Dorscheidt, M.P.J. Eversdijk, S.J. Folmer, M.N. Hirsch, A.J. de Leeuw, R.C. Nijman, B.W. Ossenkoppele, J.K. Sothmann

Project tutor: ir. B.D.W. Remes

Coaches: ir. S. Vitale, ir. J. Schneiders

7.1 Introduction

Paramotoring is the most lightweight form of powered flight, but unfortunately it has the image of being a noisy, smelly endeavour. Using electric propulsion could solve this problem.

Electrically powered paramotors that can fly for half an hour already exist, but to push the limits, a mission goal of flying 300 km through the Netherlands was adopted. This was eventually accomplished in theory by the use of high specific energy batteries and a natural source of energy: the dynamic updrafts at the dunes.

Additional requirements include the ability to take off within 20 m, and for the whole paramotor system to weigh less than 22 kg. This last requirement was dropped, however, when switching to a larger battery pack in order to complete the mission without any landings.

The most stringent requirement is the total budget of €5000, which was adhered to. Other, less limiting factors are airspace restrictions

and the bird breeding season, the former rendering the original route from the most southern to the most northern point of the Netherlands unfeasible, the latter requiring careful planning of the time of year in which to fly the coastal route.

7.2 Design

To extend the range as much as possible, efficiency must be maximized. Of big influence is the drag caused by the pilot's body. A body adhering to average dimensions was modelled, and multiple CFD simulations were done to gain quantitative and qualitative insight into the pilot drag at different body positions. It was found that reclining the pilot makes a big difference both in drag and in size of the wake, the latter of which is important for propeller efficiency.

As large decreases in drag were observed merely by adjusting the pilot's posture, many hours of thought on this problem were accumulated, which resulted in the idea of a low-drag fairing similar to those on recumbent bikes and zeppelins. This idea was further developed, and resulted in a significant decrease in drag, although the decrease was less than anticipated due to the poor aerodynamic shape of the pilot's head and arms.

Another great influence on efficiency is the paraglider itself: for minimum drag at a certain weight, the lift over drag ratio needs to be maximal. A wing only destined for the most experienced of pilots was chosen, the Ozone Mantra R11, a 2-riser high-aspect-ratio design that has a lift-over-drag ratio of 11.

Multiple concepts regarding the electric motor were explored, including AC/DC waveforms, and permanent magnet or induction rotor configuration. The brushless DC permanent magnet type of motor was chosen for its high specific power. It is widely used in low-power applications, from radio controlled aircraft to electric cars.

An important trade-off is whether to use a motor suitable for directly driving the propeller, or to use a reduction drive. As the power

required is very low, the lighter option was to go with a smaller motor that turns at a higher rotational speed, losing some efficiency in gearing but winning on mass, mass that can be used for bigger batteries.

To match the high efficiency of the rest of the system, a high-performance propeller was designed. Its design process relied on an optimization algorithm called particle swarm optimization to find airfoils with the highest lift-over-drag ratio at a given Reynolds number, using XFOIL for analysis. Then, XROTOR was used to optimize the blade twist for minimum induced loss, resulting in a propeller that operates at 78.5% efficiency at cruise speed.

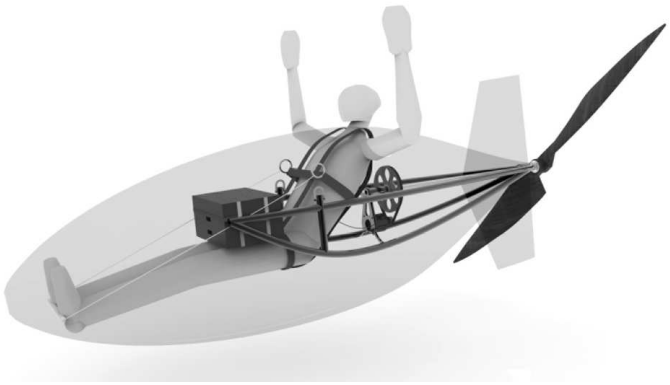

Figure 7.1: Complete system with translucent fairing

7.3 Details of selected concept

The complete system is shown in figure 7.1, with a translucent fairing to show its insides. Its technical details are:

- Take-off weight including pilot: 118 kg
- Time to fly mission (simulated, ideal day): 7 hours
- Wing: Ozone Mantra R11
- Motor: Hacker A80-10 (continuous power 3.3kW, max. 5kW)
- Reduction drive: 1:5.5
- Propeller: diameter 2m, cruise efficiency 79%, cruise RPM 600
- Battery: 22.5 kg Fanso primary batteries.

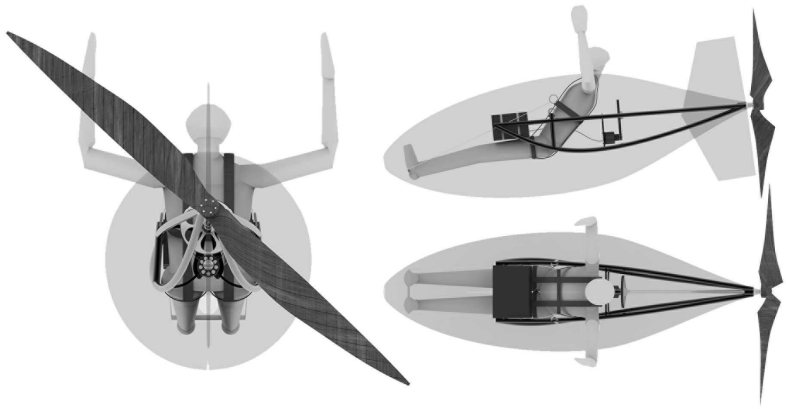

Figure 7.2: 3-view of system

7.4 Conclusion

The goal of this project was to design a machine capable of crossing the Netherlands in one single day, whilst giving the pilot the sense of pure flying, by taking away the noise, smell and strong vibrations that combustion motors induce.

This goal was achieved by designing a light-weight and highly efficient paramotor and by setting a route that made use of the natural possibility to soar along the Dutch coast to increase the machine's range even further. Efficiency was achieved by designing a propeller dedicated for the paramotor's flight envelope, reaching a propeller efficiency of 79%. Placing this propeller far enough back so it is out of range of the pilot's arms allowed for losing the heavy and drag-causing safety cage. The mission was designed to be flown at a low power setting, at the motor's most efficient RPM. In addition, a fairing was designed to reduce pilot drag and to allow a clean airflow into the propeller.

The low weight was achieved by setting weight budgets for the different subsystems in a very strict manner. Every system was critically analysed to see where weight could be lost. The fairing for example consists of a light-weight aluminium frame and a light cloth

that pressurizes in-flight due to a pressure port at the stagnation point.

The light-weight construction also had to allow enough room in the weight budget to account for the battery to be taken along. A 22.5 kg primary battery pack consisting of high energy density Li/SOCl2 cells is taken along in order to accomplish the mission in one go.

The pilot's safety is assured by several measures, the most important one being the fact that the paramotor system and pilot are attached separately to the glider's hang-point. This is done to make sure the paramotor system balances itself independently of the pilot's position, but also such that in case of emergency, the pilot can cut the paramotor system loose.

The whole system will be transportable inside a protective casing by only detaching the propeller and batteries from the frame. The propeller blades are placed alongside the frame inside this casing, and the batteries and wing will also fit inside this container. This should allow a set-up time of 5 min.

The paramotor will be combined with the high performance Ozone Mantra R11 wing allowing for the highest possible glide ratio. This way, when using 22.5 kg of primary batteries with a specific energy of 415 Wh/kg , the 294 km route along the coast of the Netherlands can be flown without any stops in approximately seven hours. A total of 5.65 kWh of energy is consumed with a maximum power of 2.67 kW.

An important part of the design process was depicting the verification and validation procedures for every subsystem of the paramotor, to check whether the results generated were realistic enough and thus close to existing cases.

Customer requirements were also analysed in-depth by carrying out a market analysis and creating a subsequent business plan to allow for continuing developing the paramotor and its accompanying

development software after the DSE has officially finished. Over 200 responses were received on the questionnaire.

The process was concluded with the creation of an appealing design and name for the paramotor. With pride we present the PZero: a high-performance, low-cost, electrically powered paramotor capable of crossing the Netherlands without stops. Finished in striking green, showcasing its sustainable nature.

Figure 7.3: Ready to fly

7.5 Recommendations

In order to actually complete the set mission of crossing the Netherlands using the designed paramotor several steps will have to be taken.

Firstly, a team should be gathered which is willing to continue with the process of design and mission execution. All subsystems that have

been designed should of course be validated. After this, a completed prototype has to be produced, where each part has to be tested separately as well as combined into the final system. Improvements and updates will be made where needed.

In order to complete all these tasks, funding is required. Financial support could be sought in crowd funding, sponsors or TU Delft financing. Only then, completing the mission as stated is a viable option.

In addition, completion of the mission can serve as a stepping stone for launching an online platform, as it would serve as a proof-of-concept for the developed system. The platform could consist of setting up an online forum, starting the sales of paramotor subsystems, and a DIY electrical paramotor design kit.

Furthermore, the platform should be kept up to date by incorporating technological advances in all paramotor subparts. Batteries have been identified as the subpart showing the most promise for future development and improvement, so this especially applies to them.

Keeping in contact with the paramotor community as well as the manufacturers and suppliers is of vital importance in making this platform a success.

8. AEOLUSIM

Students: A.B. Mahabir, T.R.J.W. Follender-Grossfeld, S.T. Spronk, S.C.F. Vrouwenvelder, E.J.P. Riegman, I.J. Welschen, O.W.M. Thijssens, G.M. ter Horst, C.H.P. Ramakers

Project tutor: dr.ir. M.M. van Paassen

Coaches: M. Alharbi MSc, ir. D. Baldacchino

8.1 Introduction

In 1910, Eardly Billing obtained a patent on a flight simulator. The simulator used wind energy for its operation and had controls much like airplanes of today. The Billing flight simulator was suspended on a pivot point and relied on wind to create aerodynamic forces on its wings and control surfaces, thus generating the motions of the simulator. This type of simulator has been abandoned however and current motion based simulators rely on hydraulic or electric power for generation of the simulator motion. On the other hand, there are a number of advantages to a wind-driven simulator:

The feel of the control surfaces can be tuned to accurately resemble the aircraft's feel. For aircraft where the pilot is exposed to the surrounding air, the feel of the wind enhances the simulation realism.

The motion can be generated by a low-cost mechanism instead of by a 4 to 6 degree of freedom high-precision mechanical, electric or hydraulic drive.

Because of these reasons, interest has been sparked to take a new look at this type of simulator. For this, the following mission need statement can be defined: Provide the user with the experience of flying a lightweight aircraft by combining virtual reality with a mechanic wind driven simulator. To accomplish this, a project objective statement has been determined:

"The team has to design an affordable and accessible wind driven flight simulator for entertainment and initial training purposes with at least 3 degrees of freedom, within a budget of € 35,000, by 9 students in 10 weeks time."

Some of the design requirements and constraints are already mentioned in the project objective. The following key requirements were defined for the Aeolusim project:

Cost

- Total cost of the simulator shall not exceed € 35,000. Running cost, excluding operator cost, should be lower than 50 €/hour, based on 1000 operational hours per year, and a five year operational life.

Performance

- The simulator can be used by a single pilot with a weight between 35 and 95 kg.
- The simulator displays responses to the control inputs that are typical for a light aircraft. Simulator movement is, of course, high-pass filtered by spring and damper mechanisms limiting the motion of the simulator. If needed, the shaping of the simulator motion is supported by computer- or mechanically controlled additional control surfaces.
- The simulator features at least a roll and pitch control interceptor, and optionally a rudder control interceptor. These are mechanically linked to control surfaces that are exposed to airflow,

and the control surfaces are balanced to provide realistic control surfaces.
- The control inputs are measured and provide input to a computer simulation of the aircraft.
- An outside visual system that is driven by the computer simulation is presented using a virtual reality head-mounted display.

Power budget
- Including power for the necessary computer and visual system, the total system's electrical power requirement should be lower than 30 kW during operations.

Other
- Preferably, the device has an attractive, aircraft-like shape.

8.2 Concepts and trade-off

Several designs have been proposed within the design space. The support structure with the spring-damper systems, and airframe are individually designed, as their design is to a certain extend not interdependent. The support structure determines the degrees of freedom and the dynamic behaviour of the Aeolusim. The latter is expected because of the small scale and low airspeed, making the spring-damper force contributions dominant over their aerodynamic counterparts.

Three concepts had been selected for further analysis. These concepts are presented in figure 8.1, 8.2 and 8.3, and were analysed individually. Concept I features four longitudinal spring-damper mechanisms and a slider. This combination results in three degrees of motion: roll, pitch and vertical movement. Concept II also features four spring-damper mechanisms, albeit they be inclined at an angle, and a torsional spring. This concept has three degrees of freedom: roll, pitch and yaw. Concept III supports the airframe by using a gimbal. These gimbals allow rotation about three orthogonal axes: roll, pitch and yaw. All gimbal joints have incorporated torsional spring-damper mechanisms to size for the concept's stability.

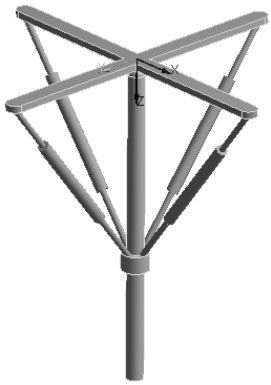

Figure **8.1**: Concept I

Figure 8.2: Concept II

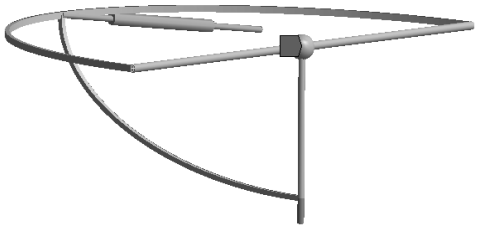

Figure 8.3: Concept III

The trade-off criteria need to be important points that make a good concept. These were chosen from the key and killer requirements and other requirements that the concepts differ on. Criteria that are important for the Aeolusim, but do not differ between the analysed

concepts, were not considered in the trade-off as they would not affect the result. The criteria that were used in this trade-off are as follows:

- Production Cost
- Quality
  - Roll & Pitch performance
  - Yaw performance
  - Vertical Movement
  - Realism
- Operability
  - Simplicity
  - Maintainability
  - Safety
- Sensitivity

The Roll & Pitch, Yaw and Vertical Movement terms entail how far and how fast a concept can move in this degree of freedom. If the concept scored a 0 in Roll & Pitch or in both Vertical Movement and Yaw the concept would get a no-go and was no longer considered in the trade-off, as the simulator should have at least three degrees of freedom. Realism represents how aircraft-like the concept would behave. Simplicity refers to the ease of operation for the users and operators.

The trade-off concluded Concept III to be superior due to the deciding factor of being far less sensitive than the other contenders. This concept was then adapted to a smaller size to avoid unnecessary production costs.

8.3 Details of the selected concept

The most important design parameters have been the power budget and the realistic aerodynamic simulator response to control inputs. The motion responses are closely related to the air velocity, which depends directly on the available power. Sustainability has been taken into account specifically in the material choices and by obtaining a high power efficiency.

The simulator is located in an open return wind tunnel, which is located in a larger enclosed room. The geometry of the wind tunnel is optimised to provide the maximum airflow velocity for the minimum power required. The simulation section is 1.9 m in height and 6 m in length. The complete wind tunnel is 15 m in length, to provide a steady and laminar flow.

The airflow is generated by 12 fans, with custom designed fan blades for high power efficiency. They are positioned behind the simulator vehicle in a four by three matrix to minimize disturbances in the flow. The airflow is guided back to the entrance of the wind tunnel through the room where the wind tunnel is located. An image of the fans and wind tunnel is provided in figure 8.4. For sake of clarity, only half of the wind tunnel wall is shown in this figure.

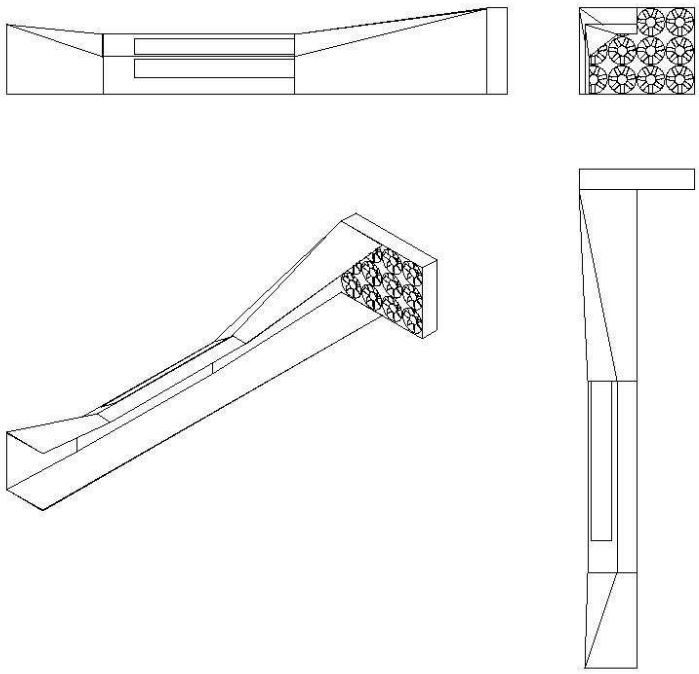

Figure 8.4: Three-view drawing of the fans and wind tunnel

Located aside the wind tunnel is the operator control booth. This room will provide the operator with a clear view of the simulation section. In addition, the Aeolusim can be entered via this room. A possible queue is to be positioned near the window, to provide the users with a clear view on the simulation section. The entrance to the wind tunnel itself is located near the nozzle of the wind tunnel. Locations near the test section do not allow for easy entrance due to the tilted shape of the simulation section ceiling.

Figure 8.5 shows the simulator vehicle. The simulator vehicle is positioned on a support structure, a universal joint allowing three degrees of freedom: pitch, roll and yaw motion. Integrated in this supporting structure are spring and damper subsystems which both limit and filter the simulator's motion response. To ensure a safe and stable vehicle upon entering, a locking mechanism is to be engaged when the simulator is not operational. This mechanism consists of four pistons, located near both wingtips and in front, and aft of the simulator.

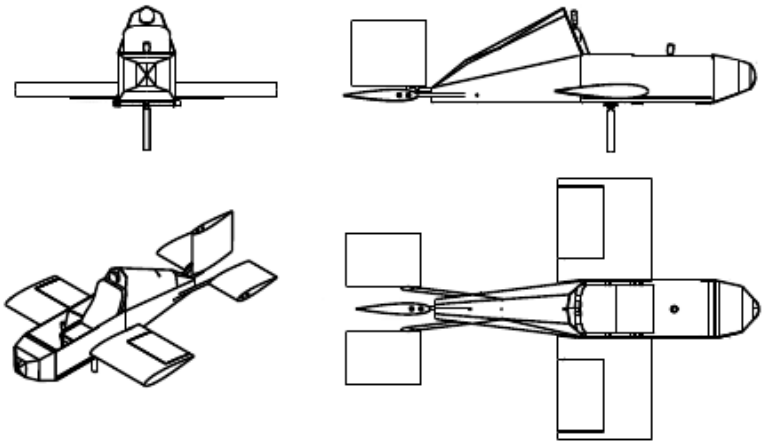

Figure 8.5: Three-view drawing of the simulator

The fuselage of the simulator itself is made of a load bearing beam structure with a canvas skin. The skin increases the aerodynamic performance and serves the aesthetics of the airframe whilst keeping

production costs relatively low. A fairing is positioned on the fuselage between the pilot and the vertical tail. This fairing reduces the turbulent airflow behind the pilot, therefore improving the airflow velocity about the vertical tail.

All aerodynamic surfaces have a NACA0015 aerofoil, and are positioned at a 0° incidence angle. Because of the small scale of the Aeolusim, the aerodynamic surfaces are quite large.

The ailerons are located between 22% and 92% of the effective wingspan of the main wing and start at 50% of the main wing chord. The tail surfaces are fully movable, so the two horizontal tail surfaces act as elevator, and the vertical tail plane serves as rudder. The point of rotation for the elevator and rudder are located inside the fuselage, 50 cm in front of the leading edge. This configuration, in combination with the fully movable tail surfaces, allowed for larger stick and pedal forces for the pilot, providing the desired feedback on the control input.

8.4 Results and conclusions

Conclusions

Following a preliminary conceptual design, system functions and relations were defined to guide the design process. Hereafter several aspects of the concept were analysed, either by creating and verifying new models, or by using existing software such as Xfoil, ANSYS Fluent and ANSYS Mechanical. These aspects include a custom fan design, an analysis of the aerodynamic performance, motion capabilities, control forces and structural integrity of the simulator. This resulted in a technically viable conceptual design for the Aeolusim.

The Aeolusim is a simulator located in an open return wind tunnel. Air is propelled through the wind tunnel by 12 ducted fans positioned in a 4 by 3 matrix, providing an airflow velocity of 12.4 m/s^2. These fans feature custom designed fan blades in order to boost the system's efficiency. All in all providing a volumetric flow rate of 5.3 m^3/s at a

nominal design efficiency of 51.2%. Incorporating the electrical motors yields a power consumption of 29.5 kW. The wind tunnel design consists of an open return wind tunnel with a diffusion angle of 7.3^0. It has an inlet of 3 meters length, a simulator section of 6 meters and a diffusion section of also 6 meters. Height of the tunnel in the simulator section is 1.9 meters, but due to the non-rectangular shape the area is only 5.14 m^2. The total area at the inlet and at the fans is 7.04 m^2 and 9.72 m^2 respectively, both being rectangular in shape.
The simulator itself has a span of 2.8 m and a fuselage length of 3.6 m and is suspended by a support structure. This support structure is a universal joint, allowing the simulator to pitch, roll, and yaw, respectively. Spring-damper systems are incorporated in this structure, in order to both limit and filter the simulator's motion response.

Analysing the aerodynamic performance highlighted several characteristics of the Aeolusim. Among them is the tip vortex, it results in an ineffective outboard region of 8% of the wing (half the span). Decreasing the distance between the wing and the wall decreased this tip vortex. However, this decrease turned out to be so small that it could be neglected.

In addition, the wake created by the pilot and structure causes a significant reduction in airflow velocity at the horizontal and vertical tail. Positioning an aerodynamic fairing behind the pilot increased the effective velocity with 57% and was therefore introduced in the design.

Since the simulator only has to rotate around its three axes, creating lift is not of great importance. On the other hand, creating a rolling moment is, and so a symmetric airfoil was chosen for its simplicity and to ensure that the ailerons are equally effective when deflecting up and down.

An initial assessment of the Aeolusim's motion response concluded that it is able to simulate aircraft-like behaviour, when compared to a Cessna Citation II. Large deflection angles are favourable for the

entertainment value of the Aeolusim, while aircraft-like behaviour is an amicable feature for any simulator. The latter case however urged an undesirable decrease in the maximum deflection and has therefore been disregarded in the design. This will lead to maximum deflection of 10, 20 and 9.4 degrees, reached after 2.3 seconds for pitch and roll, and 2.5 seconds for yaw.

An important conclusion that was drawn from the model, is that low powered suspended wind-driven simulators are inherently sensitive to a shift in the centre of gravity. It is very unlikely, if not impossible, to design a suspension where the rotation point coincides with the centre of gravity a 100% of the time for all kinds of users. A small offset in the x- or y-direction (body axis frame) leads to large and unwanted deflections. Increasing the stiffness of the springs will limit these deflections, though will not solve it and affect the simulator's motion response. Conventional solutions such as trim tabs are not effective for the design at hand due to the small scale and the low airflow velocity.

Maximum control forces were found to be 22.5 N, 21.4 N and 7.0 N for the ailerons, elevator and rudder, respectively. To ensure that such control forces could be obtained, the rotation point of the tail surfaces was placed inside the fuselage at 40 and 50 cm in front of the leading edge of the rudder and elevator, respectively. This increased the hinge moment, on which the control forces depend linearly. This, however, was insufficient for the rudder control force and was therefore mechanically increased to 12.75 N by introducing a spring between the stick and the rudder.

Structural characteristics have been analysed using ANSYS Mechanical APDL. The fuselage consists of a truss structure covered with a fabric, where the main wing is made of a combination of aluminium and wood; and the tail wings of wood covered with fabric. This configuration is chosen because a user is expected to lean/sit on the wing but is not expected to be in the vicinity of the tail wings. The latter would require the user to jump over the main wing, which has a main chord of one meter.

The structural integrity of the complete system was designed such that it is able to cope with all expected loads during its operational life. These include the aerodynamic forces and the loads caused by user interaction. The minimum safety factor found during stress analysis were 3.87, 2.56 and 1.97 for the wing, fuselage and support structure, respectively. Other load cases such as bumping in to the wing had safety factors reaching values in the 100s, indicating an over-designed structure. This however could not be overcome, since the design was limited by production and cost factors, rather than the applied load.

In the end, the Aeolusim is a technically viable product with the limitations being: its relatively low deflections and sensitivity regarding the centre of gravity. A market analysis proved that there are chances for the simulator to enter the entertainment market by using a launching customer, preferably a scientific museum. However the costs to operate the Aeolusim when compared to substitute products are expected to reduce the number of potential buyers.
This in combination with a high investment in research & development results in a dreary outlook on any quick return of investment. Several cases were analysed, only the best case scenario showed a small profit after six years. This makes the Aeolusim an economically unprofitable product: continuation of the development is therefore disadvised.

Recommendations
As previously stated, further development of the Aeolusim is not encouraged. If, however, development is continued some technical recommendations are to be made.

As mentioned earlier, this design phase focused on the Aeolusim's hardware. Software is integrated with, for instance, a flight dynamics engine yet to be designed.

The analysis of the fans required a pressure increase to be known. This pressure increase was in turn estimated using reference material, which introduces uncertainty. To analyse the actual pressure increase,

Computational Fluid Dynamics (CFD) analysis is to be performed. This CFD analysis is also to investigate the interaction between the fans. Each axial fan introduced an individual swirl to the airflow, in turn interacting with another swirl. This interaction is expected to affect the airflow upstream.

Regarding the simulator's aerodynamic performance, some improvements can be made. The flow around the simulator is currently influenced by vortices and wake structures. These arise along the wing and fuselage surfaces and behind the pilot. The flow around the fuselage can be smoothed by using bent beams instead of straight ones. Moreover, the flow at the rudder is quite ineffective. A possibility would be to investigate the use of an H-tail to remove the rudder from the wake of the pilot and increase its respective efficiency. The use of an H-tail does, however, imply difficulties in the design of the structure of the tail, since all control surfaces rotate about a point in front of their leading edge.

In addition, because the wing-tips are located relatively close to the wind tunnel, it is to be investigated what the effects are of the boundary layer of the wind tunnel. The propagation of the boundary layer from the nozzle to the simulation section might influence the lift generated by the ailerons.

In total, a secondary analysis is to be performed using more advanced viscous models. This will in turn increase the accuracy of the outcome. Current results did not allow for these advanced techniques due to the limited computational resources and the author's familiarity with these subjects.

Analogous to the analysis of the aerodynamic properties, the structural analysis could benefit from more computational resources. This will allow for a smaller mesh size in the Finite Element Analysis and yield more accurate results. For a complete analysis of the lifting surfaces it is advised to use Fluid Structure Interaction (FSI) analysis. FSI analysis uses CFD to compute the internal stresses due to the passing airflow. This will be of primary interest for the ailerons and

tail surfaces, since the aerodynamic loads are the only expected operating loads for these subsystems.

The main wing is in turn to be analysed when rivets are incorporated in the model. Analytical models sizing the rivet spacing could not be verified during the current design phase. In addition, proper references could not be found to determine optimum thicknesses for the chosen production methods and bend radii. Since the loads acting on the structure are relatively small, it will be the production limits that become dominant. Production costs can be optimised by investigating this optimum.

9. STRATOS III: MISSION PLANNING

Students: S.K. Appiah, J.R. Gahagan, P.J.M. Gilissen, B. Kim, J. Lee, L. Pepermans, M.D. Rozemeijer, B.A. Strack van Schijndel, L.A. Turmaine, S.E.C. van Buuren.

Project tutor: dr.ir. C.J.M. Verhoeven

Coaches: ir. G. Correale, H. Hu MSc

9.1 Project overview

Delft Aerospace Rocket Engineering (DARE) has carefully planned the launch of student-built Stratos II rocket in 2014. Due to some minor issues, the launch has been postponed to October 2015 with some modifications to be applied. Despite the bitter experience DARE has already taken step into yet another bold mission. To achieve the title of "the first student team in the world to launch a rocket into space", DARE initiated the mission called "Stratos III" with 10 aforementioned students. The objective of the mission is to

"launch a safe, reliable and sustainable rocket reaching at least 120 km carrying a 15 kg payload using COTS technology within TU Delft resources."

The DSE team has worked on the mission planning of Stratos III for 10 weeks.

9.2 Requirements

In order to achieve the mission objective successfully, requirements and constraints must be set before going further with the project. These are listed in table 9.1:

Table 9.1: System requirements for the Stratos III rocket

Identifier	Description
STR-SYS-01	The total cost of the Stratos III rocket shall be in the order of €100,000.
STR-SYS-02	The rocket shall be transportable from TUD to the launch site.
STR-SYS-03	The Stratos III program shall obey the law with respect to health, safety and legal regulations.
STR-SYS-04	The Stratos III rocket shall be safe to work with on a student level.
STR-SYS-05	The Stratos III rocket shall send flight information during the entire flight.
STR-SYS-06	The Stratos III rocket shall reach an altitude of 120 km.
STR-SYS-07	The Stratos III rocket shall carry a 15 kg payload.
STR-SYS-08	The Stratos III rocket shall prove that it has reached an altitude of 120 km.
STR-SYS-09	The Stratos III rocket shall be recovered with minimal damage.
STR-SYS-10	The Stratos III rocket shall have a method of terminating the flight.
STR-SYS-11	The Stratos III rocket shall remain within a predetermined flight path.
STR-SYS-12	The Stratos III rocket shall be launched from a ground-based launch site.

9.3 Design concepts and related trade-offs

To design the rocket efficiently, the Stratos III rocket system is divided into seven subsystems: Propulsion, Structure, Attitude Determination and Control (ADCS), Power, Communication, Flight Termination, and Recovery. Each subsystem contains components that are crucial for mission success. A subsystem was also created for the non-technical mission aspect. 32 initial design concepts from all the subsystems were generated and traded off according to the following criteria to select the best option for each subsystem: performance, cost, technological readiness, complexity, availability, environmental impact, probability

of failure, weight and safety. Each criterion is weighted with different scores on the basis of their importance. The trade-off is divided into two parts. The first part is to eliminate the unfeasible options that scored very poorly for each criterion. In the second trade off, the remaining design options are awarded scores relative to the performance of the best option. Scores are then normalized and multiplied by the weights assigned to that criterion. The total score of a design option is determined by summing up the products of the weight of the criterion and the score for that criterion option. The selected final design concepts are presented in table 9.2 below:

Table 9.2: List of selected design concepts for each subsystem

Subsystems	Selected design concepts
Propulsion	Single stage Nytrox-Aluminum-Paraffin hybrid engine
Structure	Aluminum tubes + glass fiber nosecone
ADCS	Fin stabilizers and active control canards
Power	Decentralized power distribution system with rechargeable batteries
Communications	800 MHz antenna located in radio transparent section of the nosecone
Flight termination	Antennas located at the bottom of the passive fins
Recovery	Ballute + cross-shaped parachute configuration

9.4 Final design

After 18 iterations the final design was reached. The major design characteristics are compacted and listed in Table 9.3. The final design of the rocket can be seen in figure 9.1.

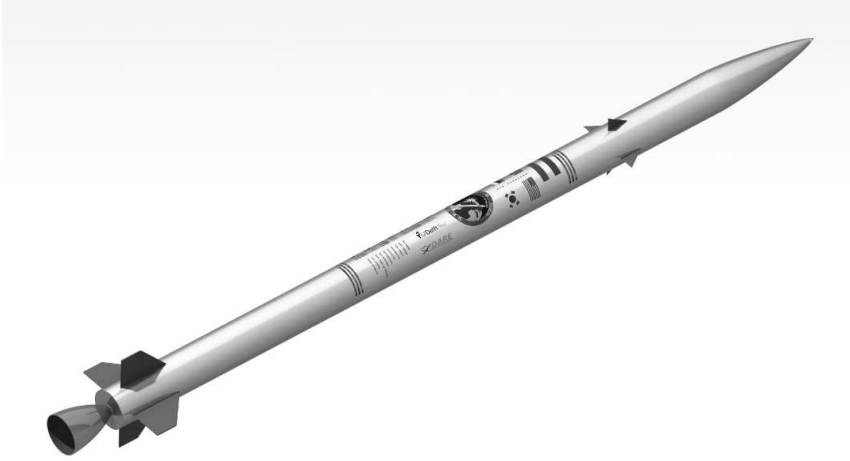

Figure 9.1 Isometric View of the Stratos III rocket

Table 9.3: Design parameters of Stratos III

Parameter	Result
Maximum Height [km]	134.39
Dry Mass [kg]	137.84
Wet Mass [kg]	309.55
Total Impulse [Ns]	427,760
Specific Impulse [s] (sea level)	232
Specific Impulse [s] (burnout)	282
Burn time [s]	29
Total Mission Time [s]	662.6
Total length [m]	5.65
Maximum Thrust [N]	16,454
Maximum Drag [N]	2580
Atmospheric Losses [%]	16.7
Maximum Acceleration [g]	11.15
Impact Velocity [m/s]	15

For the total system the mass breakdown is given in table 9.4, with the dry mass of 137.8 kg and the wet mass of 309.5 kg.

Table 9.4: Mass breakdown of the Stratos III rocket

Component	Mass [kg]	Percent of Dry Mass	Percent of Wet Mass
Payload	15	10.9	4.9
ADCS	10.2	7.4	3.3
Recovery	13	9.4	4.2
FTS	0.3	0.2	0.1
Power	2	1.5	0.7
Communication	1	0.7	0.3
Capsule Structure	19.4	14.1	6.4
Engine Nozzle/Plumbing	38.9	28.2	12.3
Tank Structure	37.1	27	12
Paint	0.9	0.6	0.3
Dry Mass	137.8	100	44.5
Nytrox	144	-	46.5
Paraffin-Al	27.7	-	9
Wet Mass	309.5	-	100

For the cost of the Stratos III rocket hardware the breakdown can be seen in table 9.5.

Table 9.5 Cost breakdown of the Stratos III rocket

Component	Cost [€]	Percentage
Propulsion	1520	16.62
Fuel (1 Tank)	3980	43.49
Structure	810	8.89
ADCS	1490	16.30
Power	120	1.31
Communication	110	1.2
FTS	180	1.97
Recovery	935	10.22
Total	9145	100

9.5 Subsystems

Propulsion

The key requirement of the Propulsion subsystem states that it has to provide a sufficient amount of total impulse to propel the rocket to the design altitude of 120 km. The propulsion subsystem uses a semi-cryogenic hybrid motor to propel the rocket to 134 km incorporating a safety factor of 10%. The motor is designed to utilize Nytrox as oxidizer and paraffin based solid fuel. By using Nytrox, a mixture of nitrous oxide and oxygen, the motor is able to provide higher specific impulse compared to that of the DHX-200 Aurora motor used in Stratos II.

In terms of total impulse, the new motor is estimated to produce 427,760 Ns while the DHX-200 motor produces 200,000 Ns, an increase of 114% to propel a heavier rocket to higher altitudes. However by designing a larger diameter rocket and utilizing propellants with higher specific impulse, the length of the propulsion subsystem was reduced to 3.86 m from 6.3 m while the absolute propellant mass has increased. The key design factor of the propulsion subsystem is the oxidizer temperature control which is crucial to ensure an adequate mass fraction of oxygen in the liquid phase of the oxidizer. The Stratos III propulsion subsystem oxidizer is kept at -60 °C where the mass fraction of oxygen in liquid phase would be approximately 15 %. The newly designed motor will have a burn time of 28.9 seconds reaching a maximum Mach number of 5.24.

ADCS

The ADCS for the rocket uses an active canard control system with passive tail fins to optimize and stabilize its flight path for maximum altitude. For the target altitude of 120 km, using only passive tail fin control is neither efficient nor sustainable as the rocket ‘weathercocks’ into the wind and loses altitude. Therefore, a trade-off was made between different types of active control (and spin stabilization) on the basis of complexity, performance, technological readiness and marketability. The system is controlled by the flight computer, which can calculate deviations from the flight path using sensor inputs from magnetometers, sun sensors, an unrestricted GPS and a 6-DOF IMU.

An increased accuracy filter called a Kalman filter is used to convert the sensor data into a state vector giving altitude, attitude, geographical location, velocities and rotation.

Figure 9.2 Internal Layout of the Stratos III rocket

Structures

The structure system is there to provide structural stability to the whole system. This means that it has to remain intact when it is sitting on the pad, during the powered flight, but also during re-entry. To make sure it fulfils this requirement two simulations were made. One simulates the stresses on the rocket while it experiences the maximum loading case during flight. The other simulates the thermal capabilities of the nosecone over the entire flight envelope which means it does the ascending as well as the re-entry part of the flight. The material for the main body is an aluminium 5 mm tube, due to Off-The-Shelf

technology. The nosecone consists of three material sections. One solid titanium tip of 3.5 cm and a glass fibre nosecone is used which has two different thicknesses of 1 and 3.5 mm.

Recovery

The key function of the recovery subsystem is to be able to recover the entire rocket with minimal damage in order to comply with sustainability, safety and the wish to put the rocket on display after flight. This requires a robust recovery subsystem as other similar sounding rockets are typically designed to only recover the payload section. A two-stage inflatable decelerator system is designed with a ballute, a combination of a balloon and parachute, as the first-stage decelerator and a cross-shaped parachute as the second decelerator. The stability and drag profile of a ballute is significantly better than traditional drogue parachutes during re-entry at velocities of larger than Mach 4. The main parachute's shape has been chosen because of its high drag coefficient, low opening force coefficient and DARE's heritage with cross-shaped parachutes. The ballute is deployed sideways using a mortar tube at an altitude range of 55 and 60 km. It is connected to the rear of the rocket via a riser and an explosive bolt. During ballute deployment stage, the rocket will flip into a nose-first attitude which is favourable in terms of stability and heat resistance. The ballute has a diameter of 0.9 m which is sufficient to decelerate the rocket to 75 m/s at an altitude of 3000 m. At this point a 14 m^2 main parachute will be deployed by the ballute and further decelerate the rocket to its final impact velocity of 15 m/s tail first. After splashdown, a sea dye marker will aid rocket discovery.

Communications

The rocket is required to provide communication with the ground station during most flight stages. This allows the ground station to keep track of the rocket's status and enables the world altitude record of 120 km to be verified. Communication is performed using radio due to its simplicity and high technological readiness. The monopole antenna consists of a 9.4 cm straight rod-shaped conductor which is mounted perpendicularly on a ground plane. The antenna is located in the radio transparent nosecone and is designed to work at a

frequency of 800 Mhz. Since the antenna only has a transmit efficiency in the order of 20%, a lot of heat is generated and thermal control is required so that the electronics do not suffer a loss in performance. The nosecone is pressurized because at an altitude of 30 km, air pressure is only about 1% of that at sea level and so, a cooling system based on air flow will be useless. The temperature in the nosecone is maintained using heat sinks combined with thermal grease and fans.

Power

The Power subsystem provides the necessary amount of electrical power to other subsystems except the Flight termination subsystem. The subsystem uses lithium-ion polymer (LiPo) rechargeable batteries to reduce the cost and hence to leave less environmental impact. It is configured in decentralized power distribution, with each component connected to a separate battery, which can reduce the complexity. The batteries are placed in two different locations: between the oxidizer tank and the combustion chamber, and in the nosecone. This offers a better maintenance capability.

Flight termination

The FTS is a vital requirement for launch safety but it is a risk in itself to the system as its responsibility of termination is potentially catastrophic. Therefore, great care needs to be taken during its design. The ground segment sends an IRIG standard monitor, arm or abort signal to the rocket. The FTS needs to receive a clear signal from the ground. If it loses this signal it is impossible to receive an abort signal from the ground so the FTS goes in fail-safe mode. Two quarter-wave monopole antennas of 17 cm at two opposite fins are estimated to be sufficient, but proper simulation and testing should be done in order to verify this. The fuselage of the rocket and the fins perpendicular to the monopoles will serve as a ground plane. The design of the flight termination logic is driven by the requirements from the launch site. The goal is to minimize the probability of a false positive, while still having an ‘fail-safe' option in case of a communications failure between the ground and flight segment. Stratos III uses a hybrid engine that can be relatively easy to shut down by closing the main valve, which will stop the oxidizer from entering the combustion

chamber. Being able to recover the rocket in case of a mission abort is desirable. Since an abort can happen during high dynamic pressure this has to be taken into consideration in the recovery system design.

Mission

After this DSE the project will be transferred to DARE with all the simulation and information as gathered by the team. DARE will first organize themselves and review the design in order to make sure DARE agrees with the design. After this the small scale tests can begin, these verify the assumptions made by the DSE and will prove design feasibility. If the design is considered to be feasible large scale tests can begin. These will develop the parts that will later take part in the record breaking space flight. After the large scale testing DARE will test the system integration, this ensures that no subsystems will interfere with each other. After the design has been fully validated and tested, the rocket can be build and launched. Per subsystem a detailed development and production plan will be handed to DARE. These plans show the major milestones, steps, and validation and verification that will have to be achieved in order to make this project a reality.

Resources

A lot of resources will be required in order to make the Stratos III mission reality. These resources come in several categories: finances, materials, knowledge, work and experience, and testing and launching. All finances and materials will be sponsored via DARE's sponsors and the university. Adding all the costs for the mission will total to about €100,000. The biggest part of this budget is the full scale propulsion testing. The knowledge will come from DARE internally, staff, and third party companies. Most of the work and testing is done on campus or near Delft; this ensures the lowest costs for these tests. If it is not possible to test in or near Delft, DARE will have to find a location that allows for the test. Launching is planned to be done on INTA's El Arenosillo test center, this is the same location from which the Stratos II mission will be launched.

Marketability

In order to get the sponsors required for the mission the rocket has to be sellable. This means that companies will need a reason to sponsor the rocket or fly their payload on the rocket. The primary reason why this rocket is interesting for companies is the fact that this rocket is a true record breaker. Besides being the first student team into space it will also break the European and world record for highest amateur rocket flight. The rocket will also a tested for new and revolutionary technologies for future sounding rockets. Stratos III will feature a new propulsion system, an active control system with four active canards, and an all new recovery system. Stratos III also differs itself from other sounding rockets in the sense that sustainability was taken into account from the very start of the project to the launch of the rocket. In order to properly sell the rocket extensive PR is required that makes the market aware of the existence of Stratos III and the reasons why Stratos III is better than any other sounding rocket on the market.

9.6 Recommendations

The design provided in The Final Report has a number of uncertainties that must be addressed in the following phases of the Stratos III mission. On an organizational level, it is highly recommended that DARE establish permanent positions for the highest leadership roles in the Stratos III project, as well as full-time positions for the board of DARE itself. As Stratos III should act as an important pillar program within DARE, it is vital that DARE develop a comprehensive knowledge management system to keep control over the flow of information within the Stratos III project as well as DARE as a whole.

It will be necessary that the rocket undergo a re-sizing to match the performance as seen from small-scale engine testing at some point. No construction of other subsystems should be started until the engine performance is more concrete, as a low specific impulse engine may require a change in the diameter of the rocket to accommodate additional fuel. Also, the nozzle skirt design in this conceptual design will likely require a re-design. It is recommended that DARE look into

a composite nozzle using a phenolic resin as it is believed that it may be better suited that the current steel skirt in the design.

It is important to carefully develop and test the active canard control system, since it is one of the largest uncertainties in the design. The current design assumed a perfect, parabolic flight as it was not known how effective the active control would be. For this reason, an appropriate penalty could not be applied to the flight path. It is best to design for overshooting 120 km in future iterations until the performance of this system can be better estimated.

The current design of the structure has minimal thermal and vibrational analysis, thus the small-scale supersonic nosecone test and vibrational tests are of paramount importance for the structural integrity of the rocket.

A single kilogram of dry mass can have an effect of about 2 km in maximum height using the same mass of propellant, so minimizing weight wherever possible can keep the rocket at a weight that the fully designed engine will be capable of launching into space.

10. ADVANCED HOVERING EMERGENCY AID DELIVERY (AHEAD)

Students: B. Alewijnse, J. Caron, E. Gelezinis, W.F. Holtslag, A. Kenger, D. J. Mansverlder, R. Reiff, S.J. de Roos, C. A. Schubert, C. Voogt

Project tutor: ir. R.N.H.W. van Gent

Coaches: ir. V.P. Brügemann, ir. S.F. Armanini

10.1 Introduction

Natural disasters and other catastrophes can be devastating, leaving behind numerous victims in need of aid. In general, vast amounts of aid are collected by helping parties to support these victims struck by disaster. The major problem is that in the wake of a disaster the regular transportation routes are often blocked or destroyed. Furthermore, airfields, which are still operational, are occupied to bring aid into the region. Getting the lifesaving aid to the victims, the so-called last mile transportation, can be very difficult. The design of a solution for this problem will help save countless lives.

The aim of this Design Synthesis Exercise (DSE) is to devise a method to provide the last mile transportation of aid. This needs to be done without relying on standard infrastructure and without hindering existing air traffic. The system should be broadly deployable and not interfere with the currently existing aid processes. The most

promising way to achieve this is to use a Vertical Take-Off and Landing (VTOL) capable aircraft. The aircraft will need to be semi-autonomous, as to leave aid workers free to help elsewhere. It will also make the system deployable in dangerous situations, without putting people at risk.

The project and its mission are embodied by the Project Objective Statement (POS) and Mission Need Statement (MNS).

Project Objective Statement:

''Impress our client with a design of a sustainable, unmanned, VTOL cargo delivery system, by 10 students in 10 weeks.''

Mission need statement:

"Deliver emergency aid over a distance of 500 km without the use of a runway."

The mission was defined further for Wings for Aid, which is a conglomerate with the main interest of helping people through technology, in collaboration with the Red Cross, the well-known disaster relief organisation and i+ solutions, which procures vast amounts of medicine for low and middle income countries.

10.2 Requirements

The mission need statement gives a rough outline, which the requirements fill in further, providing more detailed boundaries for the design. It is very important to formulate the requirements with care because the trade-off will be based on these requirements. The most important so called "killer requirements" are stated below.

- The system shall deliver its payload such that it will endure an acceleration of no more than 30 g
- The unit shall take off and land without the use of a runway
- The system shall have a delivery range of 500 km

- The system shall deliver the aid with an optimum price and time ratio from the warehouse to the end user
- The system shall provide a simple operation
- The system shall be mass producible

The killer requirements explain what the design has to be able to perform within its mission.

10.3 Concept selection

In order to come up with the best design for the mission, 34 concepts were generated and analysed. These concepts were then evaluated in a first elimination round. This round eliminates concepts by using a trade-off table which checks the compliance of the concepts with the killer requirements and eliminating concepts on engineering sense. A second elimination round has been used to reduce the amount of concepts to four. This has been done by use of a second trade-off table. This trade-off table consisted of an expansion of the cost estimation and the compliance of the concepts to more specified requirements. The four concepts are listed and explained below:

- Tail sitter
- Gyrocopter
- Flying Wing Catapult
- Aircraft Catapult

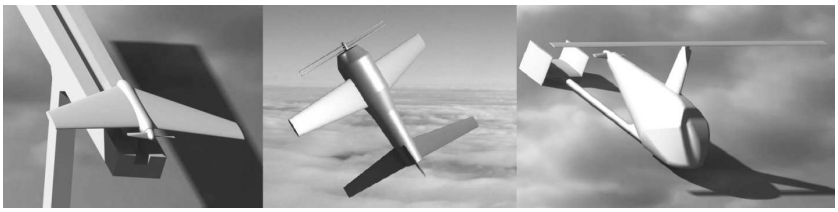

Figure 10.1: The final concepts

Flying wing catapult

The flying wing catapult can be seen at the left of figure 10.1. This concept has a propeller on the back and is launched with the use of a catapult. It is launched so it does not need the use of a runway and

flies very efficient. The flying wing lands by flying into a net and it can carry a payload up to 80 kg which is dropped by use of a parachute.

Aircraft catapult

The aircraft catapult concept is very similar to the flying wing catapult. This concept also uses a launch system to save fuel and is able to take-off without the use of a runway. It also lands by flying into a net. The aircraft catapult is less efficient then the flying wing, but the aircraft has a lower stall speed for the delivery. This concept also carries 80 kg of payload and drops the packages by use of a parachute.

Tail sitter

The tail sitter concept, see the middle of figure 10.1, is an airplane which can take-off and land vertically on its tail. The tail sitter is powered by contra rotating propellers and is also able to hover during delivery. This concept is able to carry a payload of 200 kg and drops the packages by cable, parachute or by landing.

Gyrocopter

At the right of figure 10.1 the gyrocopter is shown. It flies using the concept of autorotation. The forward momentum of the vehicle spins the rotor which creates the required lift. Although the gyrocopter is not capable of vertical take-off it will only need up to 70 m to take off. It is able to take off from a small field and not rely on a runway. The landing distance however is next to none. The delivery is therefore done either by dropping the cargo with a parachute or by landing the unit. The main advantage of a gyrocopter is that it is cheap.

Trade-off

For the final elimination round a third trade-off matrix is made. The trade-off matrix consists out of four criteria:

- Cost
- Effectiveness
- Reliability
- Versatility

A qualitative representation of the trade-off table can be seen in figure 10.2. A larger area is positive. As can be seen in the figure the tail sitter has high scores on the reliability and the versatility criteria combined with the other criteria it was selected as the final design, henceforth known as the AHEAD.

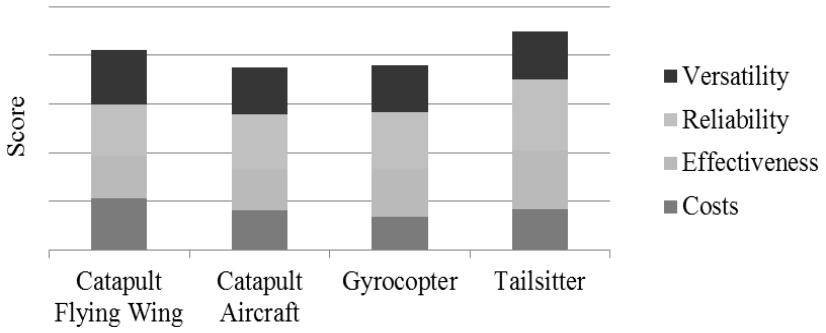

Figure 10.2: The final trade-off

10.4 Details of selected concept

Now a final design is selected with the use of the requirements the detailed design of the AHEAD was made. In this part the AHEAD was designed for the different components separately but it was taken into account that they influenced each other.

Weight estimation

For the detailed design the Class I and Class II weight estimations were used. The results gave weights for the different subsystems of the AHEAD and a design point. Eventually the design point based on the power loading and the wing loading gave results for the most suitable wing surface and power. From the weights of the components the operative empty weight (OEW) and the maximum take-off weight (MTOW) were computed. Table 10.1 shows the different weights determined for the AHEAD.

Table 10.1: Weights

Component	Weight [kg]
OEW	801
MTOW	1216
Payload Weight	200

Wing design

The wing design was done in several steps. First the aerofoil selection after that it was converted to a 3d wing design using the wing surface found with the use of the weight estimations. Next the control surfaces were selected for the manoeuvre of the AHEAD.

For the aerofoil selection Javafoil was used to find the airfoil which would fit the best into the performance of the AHEAD. The NACA 63-211 was selected which is an asymmetric aerofoil. A main issue in the selection of the aerofoil was the question to use a symmetric or an asymmetric aerofoil because of the vertical take-off and landing part. This is important to consider beacuse the propeller gives a downwash which generates an airflow over the aerofoil which then generates an asymmetric lift force.

When selecting a symmetric aerofoil it would generate no lift but it will be less efficient during cruise and therefore an asymmetric aerofoil was chosen. The choice was also based on calculations on the actual lift generated by the downwash and it was easily compensated by the tail and its control surfaces. Next a 3D lift distribution and design were made which further used during the calculations for the control surfaces. It was chosen to use ailerons to perform all the manoeuvres of the AHEAD. In table 10.2 the dimensions of the AHEAD can be found.

Table 10.2: Main dimensions

Dimension	Value
Wing span	8.64 m
Wing surface	9.96 m^2
Aileron Width	0.97 m

Tail design

The tail is used to stabilise and control aircraft by creating moments which counteract those created by the wings. Therefore the tail needs to be sized such that it can control the AHEAD during each of its flight phases; Hover, Transition and Cruise.

Preliminary analysis of the hover and transition showed that since the propeller creates wind speeds of approximately 100 km/h, the moments created by the tail are estimated to be large enough for small tail surfaces during each of these two phases.

Therefore, a conventional fast sizing method for cruise was used. This is mainly based on reference aircraft. Even though the AHEAD has an x-tail configuration, the size is determined by calculating a horizontal and vertical tail surface. The dihedral of 90° requires these to be equal and therefore the lager, vertical tail size defined the total surface area. The most important design parameters are shown in table 10.3

Table 10.3: Tail plane parameters

Parameter	Value
Tail surface	8 m^2
Aspect ratio	6.25
Taper ratio	0.6
Sweep angle	20°

Stability and control

A preliminary analysis of the stability of the AHEAD was performed during cruise. This analysis showed that during longitudinal motions the AHEAD shows a stable and similar behaviour as conventional aircraft such as the Cessna Citation II. Whereas during lateral motions the AHEAD showed a higher sensitivity to disturbances. This indicates the necessity for an artificial stabilising and control unit on board the flying unit.

Propulsion

The selection for the engine was done taken ordinary engines and automotive engines into account. In the end the automotive was the better choice for the AHEAD. Mainly because the power to weight

ratio is a lot better and the costs are less for automotive engines. Therefore an automotive engine was selected.

Next the propeller sizing was done. It was chosen to use a contra-rotating propeller because it would be moment neutral. Than the actual size of the propeller was calculated using the actuator disk theory. Main components in the sizing were the propeller wake generated by the blades, the noise and the thrust generation needed. After the use of the actuator disk theory and calculations on the noise and the wake it resulted in a diameter of 5.56 m with 2 blades on each rotor.

Flight performance

The AHEAD was designed for a range of 1,100 km which is a delivery at 500 km because it has to fly back and forth and needs to deliver at a low altitude. With the power available and power required determined for the engine the maximum velocity which can be used in case of emergency is 142.7 m/s but the cruise speed is 102.8 m/s. Also the limit load factors for the manoeuvres and gusts were calculated. The maximum load factor was 4 and this was used for the design of the structure of the wing box and the fuselage.

Structures and materials

The structural integrity of AHEAD is also an important aspect of the design, since it is absolutely essential that the aircraft is able to withstand all introduced loads during its mission. The material that was selected is aluminium, since it has a very good strength-to-weight ratio, it is not toxic and it is easy to manufacture and maintain.

The structural design of AHEAD mainly included the design of the fuselage and the wing box. Both of these were designed to be semi-monocoque structures, where the skin was designed to carry all shear stresses and the stringers were designed to carry all normal (compressive) stresses. Furthermore, the amount of stringers in the wing box was optimised by designing for three segments of each wing.

After numerous iterations and optimisation processes, it was found that the fuselage will have a skin thickness of 0.8 mm, enforced with 16 stringers (1820 mm^2) The wing box will have a sheet thickness of 1.1 mm, enforced with 11 stringers (100 mm^2) on the top panel and 7 stringers (100 mm^2) in the bottom panel.

Payload

The packages in the AHEAD can be dropped separately by two different dropping mechanisms. One is dropping it by parachute from a certain altitude and the other one is dropping it on a cable while hovering which will give the precise delivery. The size of the different packages can change depending on the size of the payload. The AHEAD payload was designed on 200 kg and the packages are round with a diameter of 50 cm and a height of 30 cm when 10 packages of 20 kg are used. Also the payload integrity is taken into account while designing the delivery system.

Market impact and analysis

A comparison was made to find out what the impact of the AHEAD would be on the market. Now aid is delivered using truck and helicopters so these were the ones comparing with. A truck is cheaper but it will take more time and it is not able to get to every delivery location and a helicopter is able to get to all locations but it is very expensive. The AHEAD is much cheaper than the helicopter and the AHEAD can reach every location which makes the reachability much better than the truck. Thus the AHEAD would be the best solution for Aid Delivery, with relatively cheap costs and a perfect reachability.

The humanitarian impact of the AHEAD within a disaster area is that it can help 1,600 people every day with 4 flights a day. Estimating that one person only needs 0.5 kg of food a day. Meaning that for a disaster like Haiti it would take 1000 AHEAD systems to help all the 1.5 million people that were in need.

10.5 Final design

Figure 10.3 shows the final design of the AHEAD during flight, loading and transportation. The loading of the payload is done via the cargo door at the side of the fuselage as can be seen in the image. The figure also shows two disassembled AHEAD units inside a standard shipping container, since these are used for transportation.

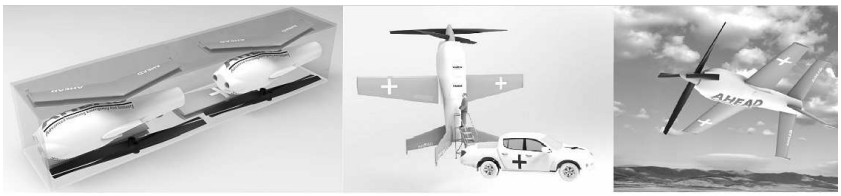

Figure 10.3: Final design

10.6 Conclusion

After 10 weeks of investigation, engineering and dedication, this group of 10 students is proud to present a viable preliminary design i.e. the AHEAD concept. Through extensive analyses on the market, the design of the subsystems, the total mission operations and the feasibility, the end result proves to be a both technically and financially credible concept. The market analysis shows that a lot of shortcomings exist in the current supply chain of disaster relief and in military logistics. The existing delivery systems are flawed in operation costs, risk to human life, effective supply distribution and response time. The main potential clients that may be interested in an improved delivery system are identified to be European and North American countries, having an expenditure of billions of US dollars in disaster relief operations and military logistics.

The unmanned AHEAD can offer great improvements for these clients, due to its impressive technical performance. It is able to ensure a fast, accurate and efficient distribution of supplies, without using a runway or infrastructure. The distribution is performed semi-autonomously, since the AHEAD performs the flight according to a flight plan autonomously, however the decision to drop a package is made by control personnel on the ground. The ground station will be

able to be set up and operational within 24 hours. Every control unit in the ground station base location will operate up to ten aerial vehicles and communicate mission data with the flying units and with Air Traffic Control. Sense and Avoid equipment has been incorporated in every AHEAD, making them swarming capable during their flights.

From the feasibility analysis it becomes clear that AHEAD is a financially feasible concept. The cost calculations show that AHEAD is the most financially attractive aerial aid delivery system, compared to helicopters and its direct UAV competitors in the aid delivery market. This is mainly due to a relatively low unit price of $325,000 and the very low operational costs of $0.0024 that are needed to transport 1 kilogram of aid over 1 kilometre.

This leads to the conclusion that AHEAD is a technically and financially feasible aerial delivery system that will impact the market by outperforming competing delivery systems on aspects like risk to human life, delivery time and effective distribution of supplies. However the design still has room for improvements, therefore the recommendations from the design team are presented in the next section.

10.7 Recommendations

The recommendations which should be focused on in further development of this design were identified to be concerning the following four subjects.

Propeller wash
The airflow of the propeller affects the airflow over the wing and tail. This may have a significant effect on the lift, stall angle and zero lift angle of attack. Further research in this field is important because full knowledge of the aerodynamic forces on a tail sitter during transition is imperative for a successful completion of the mission. Finally, almost all of the control of AHEAD during the vertical phase is achieved by the propeller wash over the control surfaces. In order to

successfully model a control system for AHEAD these forces must be fully known.

Tail sizing and planform

The current tail sizing is based on the stability during cruise and the consecutive vertical tail sizing. Although this method is validated using reference aircraft it does not take the stability during hover into account. In order to investigate this stability a six degree of freedom dynamic model should be made. The effect of the tail sizing and the sizing of the control surfaces should be investigated using this model to assure the stability and control of the AHEAD while hovering. A flight model could be used in wind tunnels in order to determine the effectiveness of the control surfaces.

Propeller sizing and selection

To obtain a more precise calculation for the propeller sizing, the blade element theory can be used which incorporates a simple model of the geometry of the propeller. However to account for the contra-rotating propeller more accurate results could be obtained by means of an advanced numerical model. This model should take into account horizontal and vertical flight and the sound production during the entire mission. The wake velocity is currently 102 km/h, this value could still cause slight damage to infrastructure. A model of jet engine exit stream and its interaction with ambient air can be used to obtain preliminary results in how much the wake velocity reduces with distance from the propeller.

Overall weight

From the weight budget breakdown it is concluded that the overall system weight has a critical impact on the efficiency of the total system. It is therefore recommended that methods to decrease the overall weight of the AHEAD are investigated and implemented. For example, the implementation of composites for certain wing box and fuselage parts could be considered. Furthermore, an in-depth evaluation on minimising the material costs could be performed during the material selection.

11. MUUDS - MARTIAN WEATHER DATA SYSTEM

Students: A. Broer, J. Claes, J. Jorissen, B. Leune, S. Martens, S. Onderdelinden, V. Van de Putte, M. Snijders, M. Voorn

Project tutor: ir. K.J. Cowan

Coaches: A.H. Giyanani, Y. Li

11.1 Introduction

Proposals to organise a manned mission to Mars are getting more serious by the day. In order to ensure a successful manned Mars mission in the future, more knowledge is required on the habitability of the Martian environment. The purpose of the Martian Weather Data System (MUUDS) project is to continuously map the Martian atmosphere and ground climate during two consecutive Martian years.

The mission consists of the following six phases. The first phase is the launch, for which the Falcon Heavy launch vehicle will be used. The next phase is the interplanetary trajectory, which is followed by the Martian orbit phase. The subsequent phase focuses on the release of ten modules from the space probe called the entry, descent and landing phase (EDL). The operations phase accommodates for both in-orbit and ground measurements, which will provide data on temperature, pressure, wind velocity, dust content, radiation and

atmospheric composition. The last phase is the end-of-life of the mission.

Mission statement and requirements

The mission statement of the MUUDS mission is as follows:

"the mission will collect data on the atmospheric and the radiation environment at the surface of Mars, as well as provide a vertical profile of the Martian atmospheric properties."

The mission was designed by a group of 9 people over a period of 11 weeks. The purpose of the mission is to provide enhanced, localised information on the climate on Mars, in order to prepare for future human exploration. The mission's goal is to deliver a minimum of two Martian years of atmospheric data before 2025. The top-level requirements of the mission are:

- Data must be collected, at least every hour, for: atmospheric properties (temperature, pressure, dust content, composition, wind velocity) and radiation.
- For measurements not taken at ground level, atmospheric data should be collected through the full height of the Martian atmosphere a minimum of once every 50 Earth days.
- At least 8 ground stations, at feasible human landing sites, should be positioned on the Martian surface. They should be equally divided over each hemisphere; three shall be located on the night-time side at any time, with maximal spread and diversity of local conditions.
- Data should be collected over the course of two Martian years, and should be available by 2025.
- Eventual data losses shall be less than one Martian day for each ground station, and a period of 100 days without orbiter data may not occur more than once per Martian year.
- The chemical composition of propellant required for launch should be minimally harmful to the Earth environment.
- Propellant mass required for the mission, space debris and impact on Mars should be minimized.

- The COSPAR regulations shall be adhered to.
- The cost of the mission may not exceed €2 billion including launch.

11.2 Concepts and trade-offs

Several concepts for the space probe, lander and ground station were made before a final design was selected. The three chosen concepts were combined into one vehicle and are thus influenced by each other.

First, the EDL module was selected using a trade-off as shown in table 11.1. The concepts considered for the landers were an airbag landing, a rocket landing and a penetration landing. Mass is very important in space missions, and the penetration concept has the lowest mass of the three considered concepts. The penetration concept also scores high on the other criteria, therefore the penetration concept was chosen as the EDL module.

Table 11.1: EDL lander concepts

Criterion	Airbags	Rocket landing	Penetration
Mass	✗	✗	✓
Complexity	✓	✗	✓
Altitude of maximum deceleration	✓	✓	✗

The concepts considered for the space probe are shown in figure 11.1. A trade-off of these concepts was performed as shown in table 11.2. The ball concept scored low due to the complexity of the design and the low reliability. Furthermore, the chosen EDL modules did not fit into the ball concept; therefore the ball concept was discarded. The stacked round pods concept scored lower than the ballistic pods concept on the criteria of mass and costs, but was still under consideration. The EDL modules fit better into the ballistic pods concept. Therefore, the ballistic pods concept was chosen for the space probe. The space probe will travel from Earth to Mars during the interplanetary phase of the mission.

The selection of the ballistic pods concept as a space probe and the penetration concept as an EDL module resulted in the selection of the

flower as a ground station. Furthermore, this concept scored high on all criteria in the trade-off for the ground stations, as can be seen in table 11.3.

Table 11.2: Space probe concepts

Criterion	The ball	Stacked round pods	Ballistic pods
Redundancy	✗	✓	✓
Mass	✓	✗	✓
Cost	✗	✗	✓
Reliability	✗	✗	✗
Complexity	✗	✗	✗
Sustainability	✓	✓	✓

Table 11.3: Ground station concepts

Criterion	The turtle	The saucer	The flower
Mass	✗	✓	✓
Complexity	✗	✓	✓
Altitude of maximum deceleration	✓	✗	✓

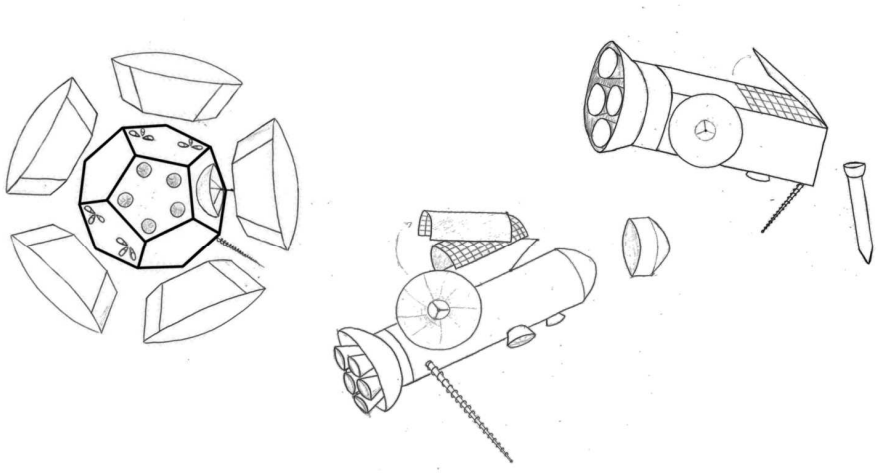

Figure 11.1: Concepts considered for the space probe, from left to right: the ball, stacked round pods, ballistic pods

11.3 Detailed design

Detailed designs were made for the interplanetary phase, the entry, descent and landing projectiles, the orbiter for the atmospheric measurements and the ground stations. The designs, and their main characteristics, will be elaborated upon in this section.

Launch and interplanetary trajectory

The MUUDS mission is scheduled to launch with SpaceX's Falcon Heavy on the 24th of August 2020 from the Boca Chica launch site, which will bring the spacecraft directly into a trans-Martian orbit. The journey to Mars will take 278 days using a Hohmann transfer orbit. During its journey, the spacecraft will be tracked using the Deep Space Network. After arriving at Mars, a ΔV of 1.89 km/s is delivered in order to bring the spacecraft into a circular orbit of 220 km altitude around Mars. The Mars orbit injection is done using a bipropellant rocket engine. After the Mars orbit injection, the stage containing the propellant tanks and engines will be jettisoned.

The space probe

The objective of the space probe is to bring the payload – the ground stations and the orbiter – to Mars for the operational phase. The space probe consists of a large propellant tank and thruster system, the orbiter with the in-orbit measurement instruments and two cylindrical containers encasing the ten EDL modules. These EDL modules will be released one-by-one into the Martian atmosphere. The space probe is depicted in figure 11.2.

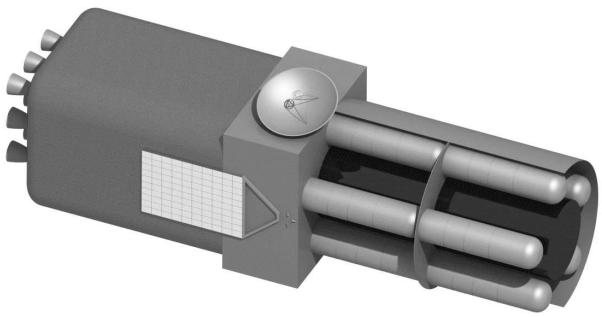

Figure 11.2: The space probe with cut-open view of the EDL modules

The EDL modules

The EDL modules, of which there are ten, each decelerate using the (thin) Martian atmosphere and their deceleration mechanisms. Ten modules are chosen instead of the required eight to provide redundancy. The deceleration mechanisms, and the velocity after each EDL phase, are described in table 11.4. An exploded view of the EDL module including the ground station is described in figure 11.3. The EDL is not actively controlled but is instead guided by the inflatable heat shield, parachute and the reversed thrusters. The remaining energy is absorbed by the impactors, which crush into the Martian surface.

Table 11.4: The EDL mechanisms and their release velocity

Mechanism	Velocity when part is released
Inflatable heat shield	400 m/s
Parachute	80 m/s
Thrusters	25 m/s
Impactor	-

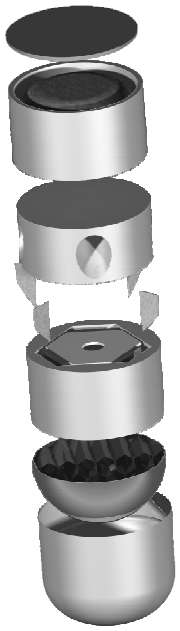

Figure 11.3: Exploded view of the EDL module

The orbiter

The orbiter remains in orbit after the release of the interplanetary propulsion system and the EDL modules. Its orbit around Mars is at an altitude of 220 km with an inclination of 35°.

Orbit maintenance is of importance: the orbiter descends to an altitude of 219 km in 14 days, where two ΔV's are given by the ADCS thrusters to transfer it back to the initial orbit.

Measurement instruments collect atmospheric data using stellar occultation, spectrometry and LIDAR technology. The collected data is processed by the command and data handling system and stored until the next communication link. In between the measurements, communication tasks are performed because the orbiter functions as a relay station between the ground stations and the Deep Space Network on Earth. An intelligent ADCS system positions the orbiter in the desired attitude for communication and measurements. In order to generate the required power, solar panels are constantly directed by gimbals towards the Sun whenever situated on the day side of Mars. Energy is stored in batteries to provide power while the orbiter is in eclipse. Large temperature differences occur between the day and night side of the orbiter, and the subsystems generate heat as well. To control the temperature of the entire system insulation coatings are used. The orbiter is shown in figure 11.4.

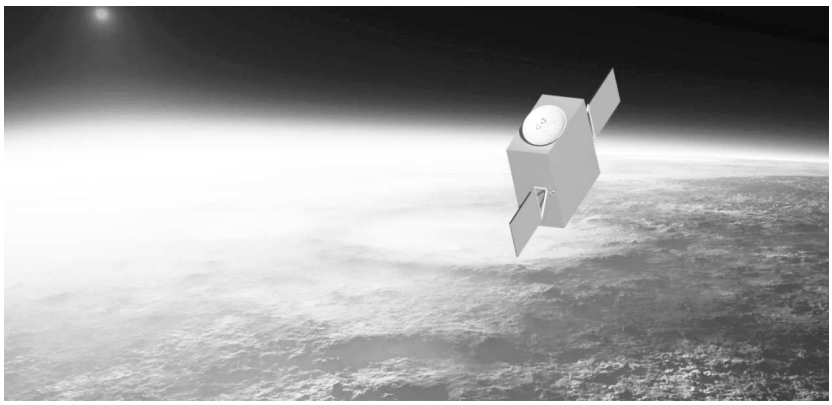

Figure 11.4: The orbiter in operation in orbit around Mars

The ground stations

After landing, the ground stations are deployed to their hexagonal form and measurements begin for hourly atmospheric data and radiation assessment. The stations are 50 cm tall and have an approximate diameter of 35 cm. The required power is collected with solar panels, movable over two axes. During the night, power is obtained from the batteries, which are charged during the day. To compensate for the temperature differences, a thermal control system is implemented. In figure 11.5, the ground station is shown in its deployed state on the Martian surface. Once a day, the ground stations communicate with the orbiter during its fly-over. The orbiter track during one Martian day is shown in figure 11.6, where the circles indicate the communication window. The ground station locations are shown as well in figure 11.6, and were selected based on their elevation, surface conditions, temperature, spread, diversity and feasibility for human habitation.

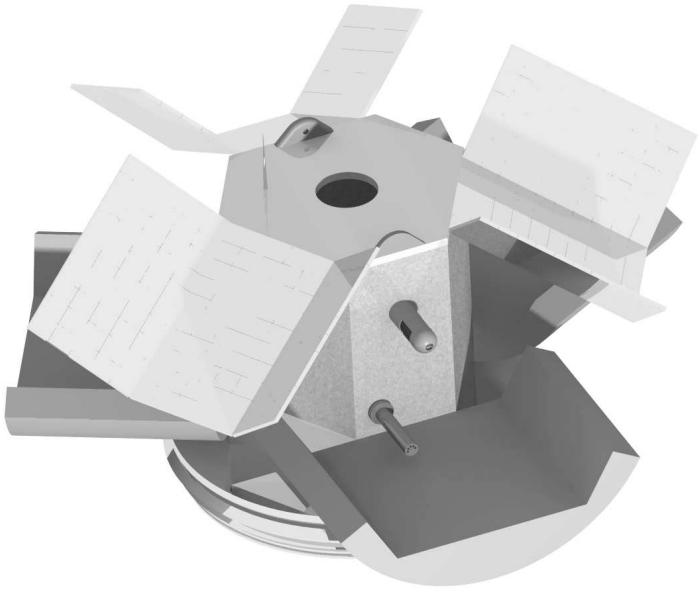

Figure 11.5: A deployed ground station

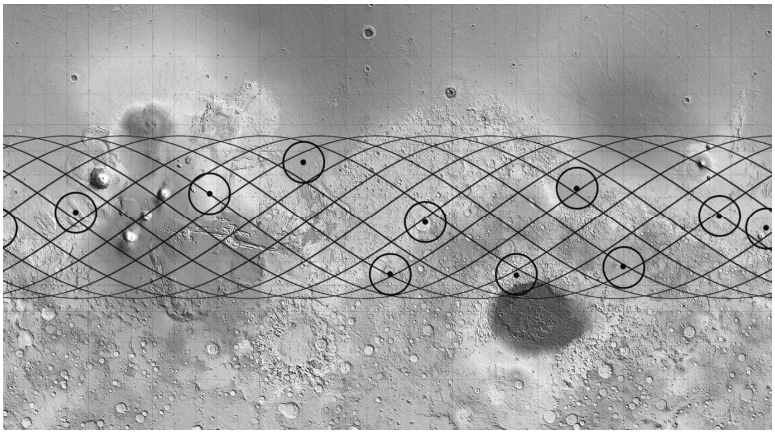

Figure 11.6: Map of Mars indicating the orbiter track and ground station locations (Figure adapted from MOLA, NASA)

End-of-life

The operation phase will last for at least two Martian years, but if enough propellant is left in the orbiter, the operational phase will last longer. When only one month of propellant is left, the orbiter sends a signal to Earth to let ground control know that the end-of-life phase is near. When all propellant is used, the orbiter will decelerate slowly and be passivated to a level where the remaining, internally stored energy is insufficient to cause breakup. The ground stations will also be shut down once the orbiter starts its end-of-life phase and will retract their instruments to prevent excessive debris on the surface of Mars.

Mass and power budget

Table 11.5 contains the total mass and power consumption of the components of the mission.

Table 11.5: Mass and power consumption per component of the final design

Component	Mass in kg	Power in W
Launch vehicle	5365	-
Orbiter	200	409
EDL module	90	-
Ground station	44	151

11.4 Conclusion and recommendations

Launching MUUDS will contribute to the next giant leap in manned space exploration by providing extensive data on the environmental conditions that will be encountered by humans landing on Mars. One orbiter will be placed in an orbit around Mars and ten ground stations will be placed on the Martian surface. Data will be gathered on the atmospheric and radiation environment, which can be used to make an enhanced profile of the climate on Mars.

The MUUDS has the following characteristics:

- One orbiter.
- Ten ground stations.
- Temperature, pressure, wind speed, dust content, air composition and radiation measurements.
- Measurements on both the Martian surface and through the full height of the Martian atmosphere .
- At least two Martian years of data measurements.
- Maximum launch dimension of 3 m by 3 m by 10.2 m.
- Maximum launch mass of 5,365 kg.
- Maximum orbiter power of 409 W.
- Maximum ground station power of 151 W.
- Total costs of €1.46 billion.

Further testing and simulation is required to make this MUUDS mission successful. The most important recommendations are stated below.

During the design of the trajectory, a simplified model of the heliocentric orbits of both Mars and Earth was developed. Using this simplified model leads to an increasing time offset vis-à-vis the correct value. Therefore, it is recommended that a 3D planetary ephemerides is used. Using a more sophisticated model will enable the selection of a more accurate launch window, which results in more efficient fuel usage.

Not all perturbations that influence the orbiter during its orbit around Mars have been taken into account. To make a more accurate

prediction of the orbiter, e.g. more J_n effects, as well as the effect of solar radiation and magnetic perturbations should be taken into account.

Extensive testing is required on the landers. The crushable parts have only been roughly sized, and these tests should evaluate impact performance and the effects of the impact on the payload. Furthermore, the analysis of the inclination with which the landers hit the ground should be further evaluated to decrease uncertainties.

More detailed research on the power usage and time of usage for each system should be conducted for more detailed sizing of the batteries and solar arrays. A power budget for the lander should be made to size the battery for the power supply during the EDL phase.

The structural loads on the space probe should be further analysed, with particular focus on the vibrations and shock loads experienced by the space probe. The effects of these shocks and vibrations on the different subsystems should also be analysed through testing of a prototype. Furthermore, the effects of bolts and material imperfections leading to higher stress concentration should be taken into account.

The MUUDS mission will provide virtually continuous global and local profiles of the Martian environment. These profiles will help prepare for human arrival at Mars. MUUDS will assist in making the next step in human space exploration possible!

12. DESIGN OF A CONTROLLABLE, INFLATABLE AEROSHELL

Students: S. Balasooriyan, B.R. van Dongen, D.D. Hage, T. Keijzer, G. van Koppenhagen, L.C.J.M. Mathijssen, J.F. Meulenbeld , A.P. van Oostrum, S.P.C. van Schie

Project tutor: dr.ir. H. Damveld

Coaches: ir. D. Dolkens, ir. N. Reurings

12.1 Introduction

Over the last years a persistent interest towards space exploration has developed. Several suggestions to bring humans to the surface of Mars have already been made, the first opportunity planned for as early as 2021. To this extent, the demand for a Mars entry vehicle is high. Such a vehicle should be capable to decelerate in a controlled manner through the varying and thin Martian atmosphere, while keeping the accelerations experienced by the crew limited. This is specifically a daunting task when the vehicle also has to cope with launcher constraints, namely the vehicle diameter and its launch mass. The design team was challenged to find a solution to this problem and has performed a feasibility study and a preliminary design of a controllable inflatable aeroshell to provide the hypersonic deceleration.

12.2 Mission outline and requirements

An inflatable aeroshell has high potential to deliver sufficient aerodynamic deceleration to bring human payload to the surface of extra-terrestrial locations, such as Mars. This can be done at a significantly lower mass fraction than the conventional solution: a rigid aeroshell, which may have a hypersonic decelerator mass fraction of up to 30%. The inflatable aeroshell on the other hand only has a hypersonic decelerator mass fraction of 10%. The payload-carrying capability is therefore enlarged, such that the economic feasibility of extra-terrestrial exploration and habitation missions is significantly increased. Therefore, the mission objective is defined as follows:

"Design an inflatable, controllable aeroshell for a spacecraft capable of carrying human payload to Mars."

The design of an aeroshell is primarily based on the aero capture and entry conditions. This aero capture and entry phase will be the main focus of the design. However, for proper sizing, the entire mission from Earth to Mars was taken into account, although in a low level of detail. The total mission has a duration of approximately 900 days and consists of launch, interplanetary transfer, aero capture and entry, terminal descent and lastly, return. An overview of these phases is given in figure 12.1. Requirements for the mission follow from this outline and will be stated after the mission description.

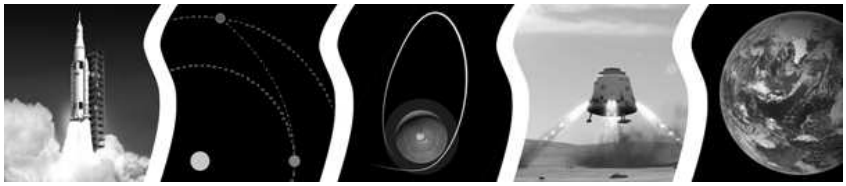

Figure 12.1: The mission overview of the launch, interplanetary transfer, aero capture and entry, terminal descent and return. The primary focus of the aeroshell design is the aero capture and entry phase. Image credit: NASA and SpaceX

Launch serves to bring the aeroshell and its payload - with a total mass of 10,000 kg for which 10% of this mass can be used for the

hypersonic decelerator - in a transfer orbit towards Mars. This is done via two velocity increments, a first one to get into a LEO parking orbit and a second one to the actual transfer orbit. The velocity increments are sized for a fast travel, namely to arrive with a velocity of 7 km/s at the edge of the Martian atmosphere. The Space Launch System is selected to deliver a ΔV of 19.6 km/s. Using this launcher, one of the biggest possible, the size of the payload is limited to 5 m.

The interplanetary transfer of 89 days has a big impact on the design. The interplanetary travelling time determines for instance the time needed to provide the crew with life support and the time the crew is exposed to radiation. Therefore it is favourable and also required to keep the transfer time low.

The third phase of the mission, the main focus of the project, starts when the vehicle reaches Mars. Instead of using retro-propulsion to get in orbit around Mars, the atmosphere is used to decelerate. This concept is called aero capture. To execute this phase of the mission the aeroshell will be deployed to its required diameter of 12 m just before arrival. In between aero capture and entry, the vehicle is placed in a parking orbit to observe the unpredictable weather conditions before descending to the Martian surface. Afterwards, the vehicle must decelerate within the hypersonic regime, ending at an altitude of 15 km with a speed of Mach 5. All this has to be done such that a final accuracy of 500 m can be attained with a control system reliability of 99.95% and within 10 days. Throughout this phase the accelerations the crew experiences are kept under 3g.

Terminal descent of the spacecraft commences as the next phase of the mission. It consists of flying through supersonic and subsonic regimes as well as landing. Retro-rockets, a parachute and struts are used to perform this phase of the mission.

The return from Mars will require several systems to already be placed by the time the crew arrives. A Mars ascent vehicle is required to lift the crew into orbit around Mars. Afterwards this vehicle will be

docked to an Earth return vehicle before returning the astronauts back to Earth.

An overview of the requirements posed on the design by the mission outline is listed:

- The entry vehicle shall decelerate from a velocity of 7 km/s at 400 km.
- The entry vehicle shall not exert an acceleration greater than 29.4 m/s^2 on any crew member during the aerocapture and entry phase.
- The entry vehicle shall attain Mach 5 at an altitude of 15,000 m.
- The entry vehicle shall reach its final position with a precision of 500 m.
- The entry vehicle shall attain its final velocity within 10 days after entering the Martian atmosphere.
- The entry vehicle shall have an undeployed diameter smaller than 5 m.
- The entry vehicle shall have a deployed diameter smaller than 12 m.
- The entry vehicle shall have a mass of 10,000 kg at the start of the entry.
- The hypersonic decelerator shall have a mass fraction no greater than 10% of the total vehicle mass.
- The entry vehicle shall have control system reliability of at least 99.95%.

12.3 Concept selection

In order to meet the stringent requirements and provide the required deceleration five different concepts were analysed. Four of these concepts featured an inflatable decelerator structure. One conventional rigid concept was analysed as well to quantify the performance benefits of inflatable concepts. Figure 12.2 shows the five preliminary design concepts. A simplified description for each of the concepts is combined with the trade-off performance.

All concepts were analysed on the basis of four trade-off criteria: hypersonic decelerator mass, deceleration performance, stability and

development risk. Trade-off performance was analysed on the basis of relative performance with representative shapes and preliminary design tools. The latter most importantly included a parametric mass model, an aerodynamic model using modified Newtonian flow and a trajectory tool based on numerical integration.

The decelerator mass is divided into structural mass, thermal protection system mass and control system mass. Deceleration performance is characterised by the lift-to-drag ratio. A higher lift-to-drag ratio allows for more control of the orbit, consequently increasing the deceleration performance. Stability was characterised using the static stability coefficients and finally the development risk was analysed on the basis of similar missions, performed tests and ongoing investigations by other parties.

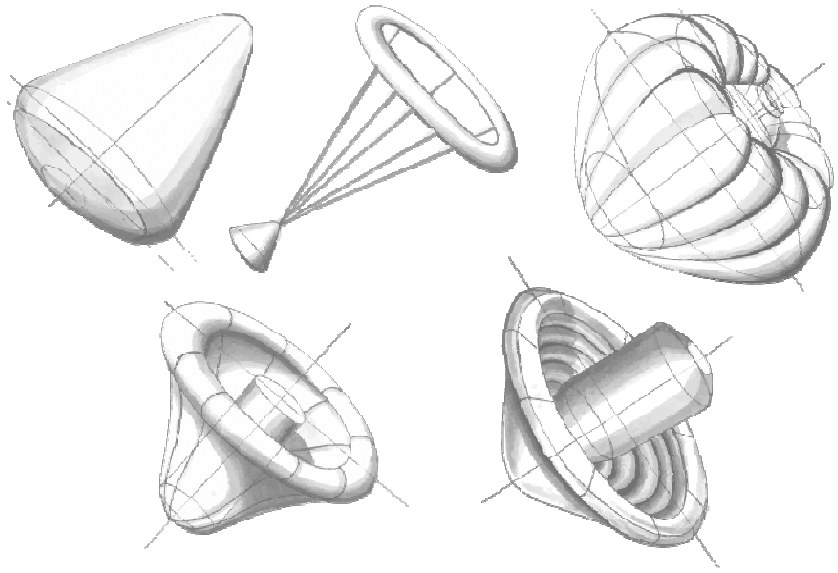

Figure 12.2: Overview of the various design concepts. From top left to bottom right: (a) rigid, (b) trailing ballute, (c) isotensoid, (d) tension cone and (e) stacked toroid

Rigid

The rigid concept is the conventional concept for (re-)entry into the atmosphere. It performs well in three of the four trade-off criteria with decelerator mass being the exception. Preliminary mass estimates

were in the order of 3,000 kg, severely exceeding the decelerator mass requirement. Prime contributors to this high mass are the inclusion of a backshell combined with increased loading due to the smaller effective surface area. The backshell serves as heat protection for the hypersonic flow impinging on the sides of the entry vehicle and may be excluded if large inflatables are placed in front of the crew module.

Trailing ballute

The trailing ballute features an inflatable ring placed behind the rigid entry vehicle. A significantly larger frontal area can be achieved, reducing the thermal loading and thus decelerator mass significantly. The aft placement of the decelerator however still requires the addition of a front- and backshell. Moreover the trailing element was found to provide difficulty in controlling the entry vehicle. Control was only found to be possible efficiently by changing the length of the individual attachment cords, something never demonstrated or even analysed in hypersonic flight before, posing a significant development risk.

Isotensoid

An isotensoid concept features a single inflatable structure inflated by using atmospheric air. This provides mass advantages, expressed in the lowest mass of all the decelerator concepts. However, performance in the hypersonic flight regime yields inadequate performance both in terms of decelerator performance and structural mass and has moreover never been demonstrated before. The shape was found to be statically unstable and provide only marginal lifting capability due to its sphere-like shape.

Tension cone

The tension cone concept consists of a single inflatable outer ring providing stiffness to the structure. The area within the ring is covered to provide additional deceleration area. Performance in the trade-off mass and deceleration performance criteria were adequate. Moreover the shape was found to be statically stable. However, only laboratory test have been performed incurring some development risk.

Stacked toroid
A stacked toroid concept consists of multiple inflatable rings stacked on top of each other to define the shape. In terms of performance the stacked toroid concept is very similar to the tension cone. It was however found to be marginally lighter and features a much lower development risk, the latter being established by a series of NASA Inflatable Re-entry Vehicle Experiments (IRVE).

Following from the trade-off ultimately the stacked toroid concept was chosen of which a design summary is given in the subsequent section. The stacked toroid concept featured no significant drawbacks and relatively outperformed the other concepts.

12.4 Final design

Following the concept trade-off the stacked toroid was chosen for further detailed design. This design is broken down into a trajectory design, inflatable structure design, control system design and crew module design. These designs were analysed with extended versions of the tools used to perform the concept trade-off. These extensions include the implementation of a 1D heat analysis and using a genetic algorithm to arrive at an optimal aerodynamic shape.

Trajectory
To comply with the aforementioned requirements the trajectory consists of an aero capture phase, a parking orbit and a final entry & descent phase. The aero capture decelerates the aeroshell through the atmosphere from 7 km/s to 4.5 km/s, reaching a minimum altitude of 50 km, such that a Mars-synchronous elliptic orbit is entered. The apocentre of this orbit is roughly 34,000 km above the Martian surface.

After the aero capture a parking orbit around Mars is entered. This is achieved by giving a small velocity increment at the apocentre of the elliptic orbit raising the pericentre to 200 km above the Martian surface. As the elliptic orbit is Mars-synchronous, the same location is viewed every time the aeroshell approaches Mars. This allows for

repeated inspection of the landing site conditions and flexibility in timing the final entry & descent.

When these conditions are acceptable, again a small velocity increment is given in the apocentre of the elliptic orbit such that the initial flight path angle at the subsequent entry is 17.2 degrees. This will initiate the entry & descent phase. In this phase the aeroshell decelerates to Mach 5 at an altitude of 15 km.

Inflatable structure

An inflatable structure has been designed that can follow the proposed trajectory while simultaneously complying with the imposed requirements. The aerodynamic shape, structure, thermal protection system, deployment system and inflation system have been designed.

The aerodynamic shape is optimised such that it can follow the trajectory with favourable aerodynamic characteristics. The inflatable will have a radius of 6 m with a half-cone angle of approximately 70 degrees. Furthermore it is important to note that the shape is asymmetric with a 0.91 m offset for the centre as shown in figure 12.3. Using a fixed 0.5 m CG-offset this allows the aeroshell to achieve a trimmed angle of attack of 22.5 degrees. Moreover a lift-to-drag ratio of 0.35, a drag coefficient of 1.3 and a static stability coefficient of -0.21 have been attained.

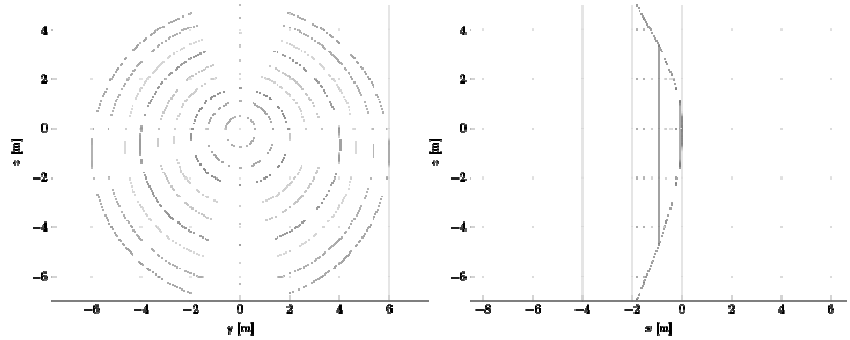

Figure 12.3 Front and side view of the aerodynamic shape displaying how the shape is constructed

To construct this shape and withstand the dynamic pressures a structure consisting of ten inflatable toroids has been designed. The asymmetric shape obtained by aerodynamic optimisation is attained by arranging the toroids at an angle with respect to one another. The result is an assembly of circular inflatables, placed at different radial distances with respect to the centre body. The rigidity is guaranteed by using radial straps that keep the toroids in their intended position. The material used for the toroids and straps is PBO Zylon®. The thickness of the Zylon® is 0.125 mm with a 0.050 mm Upilex coating to prevent the inflation gas from escaping. The total structural mass has been estimated to be 277 kg.

During the deceleration the kinetic energy is dissipated into heat. The thermal protection system is used to handle this heat and prevent it from damaging other subsystems. The aerodynamic heating is at a maximum during the aero capture phase with an incoming heat flux of 21 W/cm2. Since the aeroshell consists of an inflatable structure the materials used for thermal protection should be flexible. Furthermore they should be puncture-resistant and of course heat-resistant. For this reason Nicalon™ is used as primary thermal protector with Pyrogel® as insulator. The maximum temperature is expected to be 1,100 °C, which is well below the maximum usable temperature of Nicalon™. The thermal protection system mass is 255 kg. An overview of the material layup as used in the final design is displayed in figure 12.4.

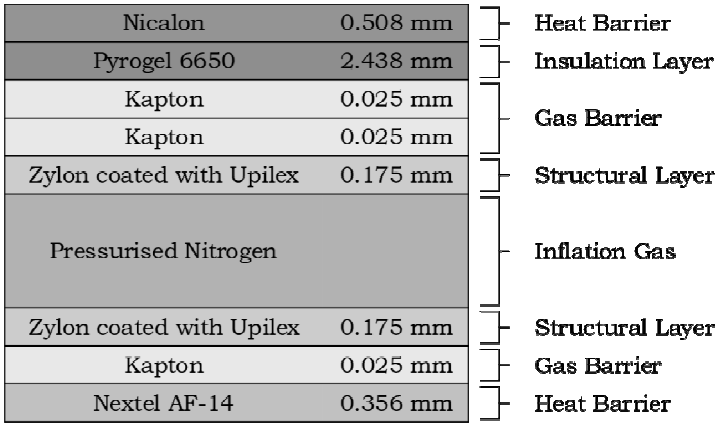

Figure 12.4 The material lay-up for the inflatable rings

During the launch the inflatable aeroshell is still folded over the crew module such that it can be stowed within the launcher from Earth. When approaching Mars the system will be deployed by releasing the inflatable aeroshell using pyrotechnic cutters. Subsequently, the system is inflated using pressurised nitrogen stored in the gas tanks.

Control system

Controlling the hypersonic deceleration requires the employment of a control system. The entry vehicle controls its trajectory via a series of rolling manoeuvres, performed by using a bank angle control system. The rolling capability is provided by a set of eight redundant thrusters. Bank control is the conventional solution for (re-)entry vehicles. More novel approaches such as an actively controlled centre of gravity offset were analysed but were outperformed by bank control in terms of control system mass and system reliability. This because a single point of failure would be introduced. An overview of the mass estimate, including the primary elements of the control system, is given in table 12.1.

For trajectory guidance a conventional set of gyroscopes and accelerometers is included. Additionally, use is made of flush atmospheric data, in which freestream atmospheric conditions are estimated using local pressures. This allows for a more accurate prediction of atmospheric conditions enhancing the control system accuracy.

Crew module

While the main focus of the design was on the aerodynamic decelerator, the crew module has been investigated to identify possible conflicts with the design of the hypersonic decelerator. The total crew module is sized to be 9,000 kg and is able to support a two man crew for the total mission duration from Earth to Mars, approximately 100 days. As the crew module was investigated primarily independent of the decelerator structure options remain open to allow for example the attachment of a habitation module, increasing the amount of astronauts that can be brought along in a single mission.

Summary of mass elements

An overview of the primary mass elements of the final design of the hypersonic decelerator is provided in table 12.1. Including a 20% contingency factor the design remains below the 1,000 kg mass requirement.

Table 12.1 Overview of hypersonic decelerator mass components

Inflatable structure		Control Actuation System	
Component	Mass [kg]	Component	Mass [kg]
Inflation gas	90	Propellant	156
Inflation system	76	Fuel tanks	12
Structural layer	110	Thrusters	44
Thermal protection layers	255		
Total	531	Total	212
Total		743	
Including contingency (20%)		927	

12.5 Conclusions and recommendations

Scientific and commercial interest in extra-terrestrial human exploration and habitation calls for a feasible and efficient solution for atmospheric entry. An inflatable aeroshell offers significantly lower mass and higher packaging efficiency than conventional, rigid solutions.

Ultimately inflatable stacked toroids are used to provide the required deceleration performance. Moreover asymmetrically stacking the toroids allows for increased lifting capabilities, improving the deceleration performance by allowing increased control capabilities. The actual trajectory control is performed by a series of bank reversals using thrusters as actuators.

The final trajectory consists of the initial aero capture, designed to perform optimal in terms of structural and thermal performance followed by a parking orbit to control the timing of the final descent.

From this parking orbit the final descent is initiated when atmospheric conditions are favourable.

However, such a novel concept poses additional risks which need to be addressed. An asymmetrically stacked toroid concept has not been considered before and requires additional investigation before such a concept can be used for manned spaceflight. The asymmetric shape may pose problems with regards to for example aeroelastic behaviour. Additionally the neighbouring mission phases require a detailed analysis which was for now outside the scope of the project. A prime region of interest would be the integration with the terminal descent phase.

13. HARV - HIGH RISK SPACE DEBRIS REMOVAL

Students: A.M.M. Biekman, L.A.B. Bolte, M.F. Döpke, T.L. Elzer, K.M. Kajak, A.E. Looijestijn, N. Rasappu, S.M. Rezvani, M.R. van Holsteijn

Project tutor: dr.ir. E.N. Doornbos

Coaches: ir. Z. Madzarevic, ir. J. Krishnasamy

13.1 Introduction

A cloud of manmade vehicles, both operational and defunct, orbits Earth. These craft intrinsically impose a collision risk on other vehicles at the same orbital altitude, especially in the crowded Lower Earth Orbit (LEO). In 2009, Iridium 33 and Kosmos-2251 collided, generating a large amount of debris. These kinds of collision events are expected to occur more frequently, due to a phenomena known as the Kessler Syndrome: colliding satellites and debris generate a debris belt, and in turn this debris initiates the forming of even more debris. Moreover, debris and defunct satellites lose altitude naturally due to atmospheric drag and solar radiation pressure. Some of these objects will re-enter the atmosphere in an uncontrolled fashion, forming a threat to human life and property on Earth.

The industry has taken upon themselves to resolve the space debris related issues. Taking action will secure the availability of important orbits and improve the reputations of space agencies like NASA and ESA.

The aim of this project is to participate in the collective debris removal efforts of the industry, by designing a technology demonstrator Active Debris Removal (ADR) system.

Seven top level requirements constrain the mission profile and physical design of this ADR system. These requirements encompass cost, mission timeframe, risk and target characteristics. From these requirements a mission statement is derived.

"This project will remove a space debris target between 4 and 12 tons from LEO before the year 2025 within a budget of € 200,000,000, in order to prevent uncontrolled re-entry of the object and mitigate the risk of collisions with other space debris and operative vehicles."

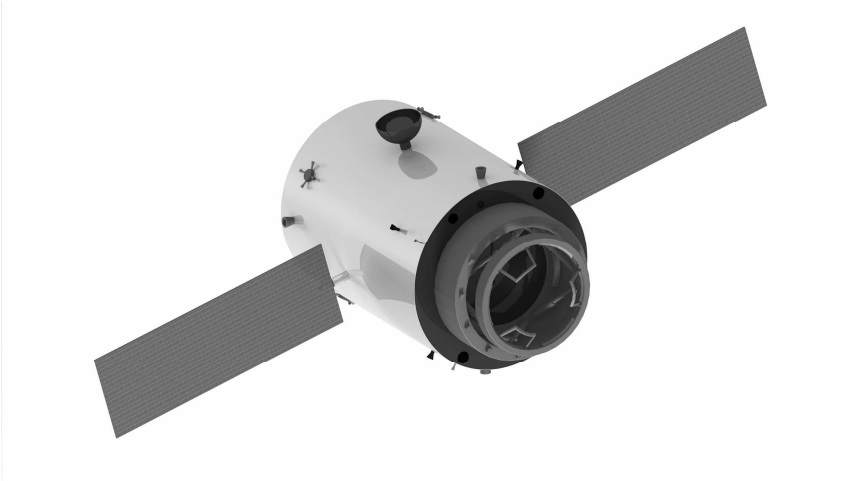

Figure 13.1: A render of the HARV spacecraft

13.2 Target selection

Before the design of an Active Debris Removal (ADR) platform could commence, a basic scope of its mission must first be envisioned. The approach was to analyse candidate targets at a range of orbital altitudes and inclinations and filter out non-applicable candidates according to top-level requirements. Then, a trade-off was performed.

In the early design phases, the possibility for multiple-removals was investigated. However, it was revealed that this would not be feasible in terms of required ΔV budgets unless all the objects are in comparable altitude and inclinations, and even then this would introduce many additionally complex facets to the mission, rendering it yet less feasible to design for with respect to the allocated project design time. Moreover as the goal of the mission is to demonstrate capability of performing debris active removal, the decision was made to opt for a single removal mission.

Furthermore, in order to systematically prioritise and narrow down the choice for a candidate debris target, a list of criteria was generated deemed most important for consideration within the selection process. The list of criteria included Feasibility, Re-entry time, Collision risks, Impact on the proprietor space agency's image, Required ΔV and Launch mass.

Subsequently a trade-off process could begin, with which to judge a list of 15 candidate debris objects. In the early trade-off phase, 8 of the targets were found to be of the SB-WASS series of US NAVY satellites, and another 2 within a similar, reconnaissance satellite category, namely the Russian Resurs DK1 and European Helios 2. The removal of these was deemed highly unfeasible due to confidentiality and lack of public access to substantial information.

Finally evaluating all criteria, accounting for a removal that is very impactful on the proprietor space agency's image, and emphasizing on near-term and unacceptable re-entry risk levels, and given the mission serves as demonstration of capability of active removal it was decided to remove a single debris object that would undergo ground-impact in the near future, The Hubble.

13.3 Space debris target: Hubble Space Telescope

The selected space debris target to be removed is the Hubble Space Telescope. Launched in 1990, this telescope has been serviced by the Space Shuttle multiple times for repairs and upgrades. One very

important aspect of the Space Shuttle servicing missions was to raise the orbital altitude of Hubble. Hubble naturally decays due to atmospheric drag and solar radiation pressure and the telescope has no thrusters on board to counteract this decay. Thruster fumes would have contaminated Hubble´s optics and science instruments and would have formed a cloud around the telescope. Due to the cancellation of the Space Shuttle program, Hubble's natural decay can however no longer be countered.

In 2015, humanity celebrates Hubble´s 25th birthday. However, humankind must look ahead. Hubble is expected to re-enter the atmosphere in 2024 at the earliest in an uncontrolled fashion.

13.4 Capture technology selection

Multiple options for the de-orbit of Hubble were considered. These methods can be categorised as follows:

- Drag augmentation by either increasing the atmospheric density (Air-burst vortex rings, tungsten dust cloud, gaseous cloud) or the ballistic coefficient of Hubble (Foam encapsulation).
- Photon momentum exchange combined with surface ablation (Earth and space-based laser).
- Ion plasma momentum exchange (Ion beam shepherd).
- Setup of a rigid connection (LIDS, robotic arm, clamper, electro-adhesion, foam capture, welding and belt capture) or flexible connection (harpoon and net) between Hubble and the removal vehicle, followed by a de-orbit burn.

A reliability analysis of the mission showed that the critical part of the mission is the capture. The main reason that the LIDS was chosen as the technology to capture the Hubble is that it is a proven technology. The other reliable and proven technology, robotic arms, is not as suitable as the LIDS for the capture of Hubble as there are no well-suited attachment points on the Hubble. The grappling fixtures that were used by the Shuttle missions are within the rotational envelope of the Hubble and are dangerous to approach in a situation where Hubble is randomly tumbling. Other technologies that were explored

were not at a suitable technology readiness level or did not provide sufficient control over the target.

13.5 Mission profile

The mission starts with the launch, which will take place from Baikonur, Kazakhstan. HARV will then be launched on a Soyuz 2.1 launcher into an orbit of 400 km altitude with an inclination of 28.5 degrees. From this point onward, the HARV needs to perform an automated rendezvous with Hubble. Rendezvous starts with absolute navigation to change its orbit to match that of Hubble and approach up to 50 km behind Hubble. From here on relative navigation starts. In this stage Hubble will be approached up to 115 m. The mating part of the mission is the next stage. This means that the LIDS is activated and approach is continued. At 10 m behind Hubble there is another hold point, where the spin around one axis is matched with Hubble. HARV stays in this point until a visual lock is made on the LIDS and when this happens, HARV will dock with Hubble. Following a successful docking, the Hubble will be despun. The last action is to make Hubble re-enter Earth's atmosphere. This re-entry takes place in the Pacific Ocean between Hawaii and the west coast of the Americas.

13.6 Cost analysis

With the USCM8 and QuickCost 4.2 cost analyses it was found that the mission is estimated to cost € 389 million, which is twice the available budget. It was concluded that the top level cost requirement is not realistic to meet.

13.7 Spacecraft design

Since a space based removal method has been chosen, a spacecraft had to be designed. The driving systems of the spacecraft are the payload, which comprises of the attachment mechanism and the attitude control system, which is responsible for approaching the target as well as getting into the pose such that the payload may be used. The different subsystem are given below.

Payload

The Low Impact Docking System (LIDS) is an androgynous closed loop feedback controlled docking system with a load sensing electromagnetic capture ring. The androgyny stands for the fact that it can also mate with its copy, instead of using a female-to-male system, such as for the Russian "probe and drogue" system used on the "Progress" automated cargo transfer spacecraft. A passive version of the LIDS is installed on the butt of the Hubble Space Telescope, making the LIDS a very good option to capture the Hubble. Because it is a feedback-controlled active system with linear actuators, it is well suited for handling relative motion that will be present during the docking of HARV and the Hubble.

Originally, the LIDS was designed for docking of the International Space Station and visiting spacecraft. Work on the version of the Low Impact Docking System started in 1996. In 2006, NASA decided that a version of the LIDS docking ring would be brought along on the last Hubble servicing mission SM4/STS-125 to be installed on the handling points on the rear of the telescope. Originally, the Orion spacecraft was planned to be used to remove the Hubble from orbit at the end of its life. By now, however, the decision has been made to continue performing science with Hubble until it is incapacitated or completely unresponsive. Because of this decision the removal mission will have to be designed for the situation where the Hubble is tumbling randomly. This complicates things and and the HARV mission has been designed to handle the unique challenges that accompany this scenario. Although the LIDS is a capable piece of hardware, it can also be modified to be more suitable for the mission, with improvements in agility for docking or energy absorption potential. In the near future of the HARV project, it will have to be studied whether the baseline performance of the LIDS is sufficient to carry out the mission or if improvements are indeed necessary.

Attitude control system

In order to conduct a rendezvous with a non-cooperative target, the attitude control system face several challenges. Firstly, the chaser needs to be manoeuvrable and should be able to detect attitude and

trajectory deviations and react quickly. For this reason the HARV is 3-axis controlled using 20 attitude control thrusters and uses an inertial measurement unit, four star trackers as well as three GPS receivers. Initial target information is obtained via radars of the Space Surveillance Network (SSN). During acquisition or in case of lost control, earth sensors and coarse sun sensors provide rough attitude knowledge.

Due to inaccuracies of the ground measurements as well as the power consumption of direct range measuring long range (50 - 2 km) sensors, an innovative navigation technology called "angle-only navigation" needs to be used: The two line-of-sight (LOS) angles (elevation and azimuth) are measured and transformed to a three dimensional range vector. However, excursions of unknown magnitude of the chaser with respect to the target cause the range vector to be ambiguous. In order to eliminate this ambiguity, a tangential impulsive transfer is calibrated from ground. This leads to a significant increase in the accuracy of the recursive Kalman-filter and provides precise position knowledge. The sensors used for this navigation technique are two visible and two infrared light cameras. During close range approach (2 - 0 km) LIDAR sensors provide direct range measurements and information about the target.

A further challenge for the HARV mission is matching the rotational rates of the target. Information about the tumbling and precession of the target is necessary to plan the docking strategy. It was not possible to pursue detailed information about this within the limited conceptual phase of the HARV project. Instead, an earlier NASA study was consulted that specified tumbling of 0.25 degrees per second and per axis. These tumbling rates may be compensated by the LIDS system even without using thrusters to alleviate relative motion. Prior to docking, the target is approached in a straight-line. Then, at a hold point at 20 m distance the chaser waits for the target to rotate into position. However, it is critical for the feasibility to simulate the tumbling rates and develop safe approach strategies. This has to be done in the next step of the design process.

Propulsion subsystem

The HARV will have a bi-propellant pressurised propulsion system, which was chosen for its high specific impulse, high reliability and adjustability of the thrust. As propellants Monomethylhydrazine (MMH) and Mixed Oxides of Nitrogen (MON-3) will be used and Helium (He) as pressurant. 3 titanium tanks of 336 L per tank for MMH, 2 titanium tanks of 293.5 L per tank for MON-3 and 2 carbon wound tanks of 44.8 L per tank for He will be used. 4 thrusters, of which each can generate 445 N thrust, will be applied for orbit control and 4 thruster clusters of 4 thrusters each for attitude control (AC). Another 4 AC thrusters will be present, which will only be used for docking. Each attitude control thruster will be able to generate 22 N.

Structure

HARV is comprised of a primary and secondary structure. The primary structure is designed to withstand quasi-static loads, sinusoidal vibrational loads and random vibrational loads in the longitudinal and lateral direction, during launch. Minimum natural frequency requirements were also taken into account. The load-bearing structure is composed of four vertical panels, with three vertices each, and five horizontal panels. These panels are enclosed in a circular cylinder. All components are made from aluminium 7075-T6. For the computation of component thicknesses, the Von Mises stress and 1st mode critical buckling loads under compression, bending and torsion were assessed for each structural member.

Communication subsystem

The visibility of the spacecraft in orbit per ground station is less than 4.5% per orbit. Tracking and Data Relay Satellite System (TDRSS) is used during the critical navigation phase. The use of a relay satellite is a necessity as continuous communication is vital during the docking phase. Potential troubleshooting that needs to be done in case of problems is also time-critical. If problems arise during docking and a physical connection is maintained between the HARV and Hubble, it will not be possible to point antennas or solar panels in a preferred way, since the Hubble might still be tumbling.

The downlink data rate required is 89.7 Mb/s for the direct ground link and 35.9 Mb/s for the crosslink. Horn and parabolic antennas will operate on the X-band and Ku-band frequency respectively. A link budget analysis has been used to determine the minimal antenna size.

Command and data handling subsystem

The provide enough dedicated processing power, the ADC and GNC have a processor separate from the main processor. The main processor handles the data and commands for the rest of the processor. A data storage device is included to store the data that is gathered during one orbit, of which the information is transmitted once every orbit in 4.24 min.

Thermal control subsystem

Active thermal control of the thruster clusters will be performed with 8 heaters with each a mass of 30 gram and a power consumption of 1.2 W. Passive control will be applied for the bus and the solar arrays with a 2 square meter quartz radiator of 5.15 kg and black surface painting on the back side, respectively. Furthermore, the LIDS and the thruster clusters will have as coating titanium oxide with potassium silicate and magnesium oxide aluminium oxide paint, respectively. For the temperature to stay within the thermal limits, the LIDS, the antennas, the thrusters, the thruster clusters and the outside layer of the bus will be made of titanium, oxidised aluminium, platinum, oxidised aluminium and vapour deposited aluminium, respectively.

Power subsystem

The power source of the HARV will consist of two 1 m by 2.93 m panel-mounted solar arrays with Triple-Junction Gallium Arsenide solar cells, which have each a mass of 8.2 kg and are each driven by a single axis solar array drive. The energy storage system will consist of 4 parallel connected series of 9 ‘SAFT VES 180’ Lithium ion battery cells each, resulting in a total battery voltage of 32.4 V, a capacity of 200 Ah and a mass of 40 kg.

Subsystem integration

Now that all the subsystems have been explained, everything is brought together. This resulted in the design of HARV as shown in figure 13.1. A more schematic overview is given in figure 13.2, which shows the biggest components inside the spacecraft. The most important design parameters of the HARV are given in table 13.1.

Table 13.1: List of the most important design parameters of the HARV

Parameter	Value	Parameter	Value
Dry mass	1,500 kg	Thrust (main thrusters)	890 N
Wet mass	3,185 kg	Power (average-peak)	392-1,118 W
Shape	Cylindrical	Cost	€389 million
Dimension (WxHxD)	2.6 x 3.9 x 2.2 m	Removal capability	±12.2 tons
Mission duration	14 days		

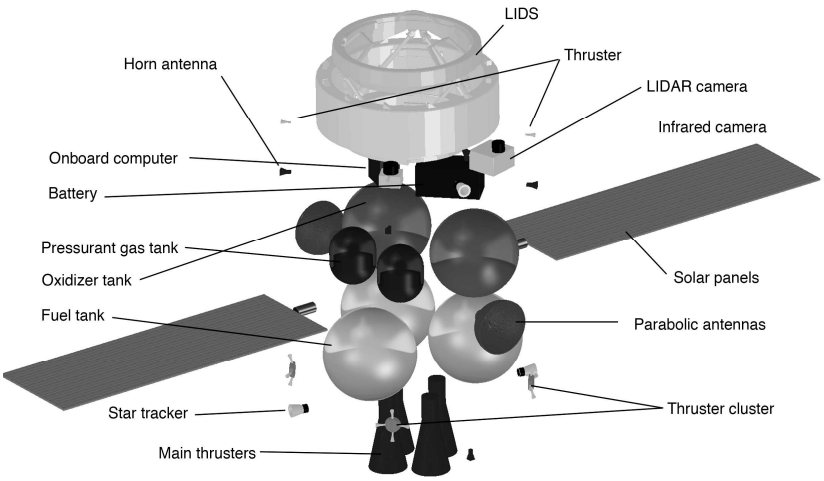

Figure 13.2: Schematic overview of the biggest components in the HARV

13.8 Conclusion and recommendations

The HARV is designed to conduct a rendezvous with the non-cooperative Hubble, dock with it and re-enter it over the Pacific in a controlled fashion. This mission as a pioneer mission within the scope of space sustainability may have an immense impact in case of successfully demonstrating a rendezvous with a non-cooperative target. However, to meet the cost top-level requirement it is necessary to use and alter an existing spacecraft such as the Progress or the Dragon.

In order to complete the mission design, an analysis of tumbling rates of the Hubble needs to be conducted. Subsequently, it is essential to come up with a strategy in order to match the target's rotational rates. This is crucial for the feasibility of the mission.

Additionally spiral approaches during the far range rendezvous should be considered in order to introduce an additional level of safety.

Furthermore, a re-design of the LIDS could reduce weight dramatically since the LIDS system is designed to allow for vacuum seal, which is not needed in this mission.

14. MOUNTAINHIGH

Students: M.M.A. Baert, E.S. Bakker, M.H.H. Kemna, H.M.J. Klijn, R.P.F. Koster, Y. Toledano, C.J.W. van Verseveld, C. Vertregt, B. Vonk, D. Willaert

Project tutor: dr. S.J. Garcia

Coaches: ir. D.S. Blom, dr. B.F. Santos

14.1 Introduction

Mountain ranges all over Earth have long been tourist attractions for their monumental size, beautiful nature, clean air and possible leisure activities. Though attractive, mountain activities may form a threat to human safety. Search and rescue (SAR) teams are constantly on stand-by and often have multiple rescue sorties per day. These missions are slow and dangerous for the involved personnel. In extremely rare cases, rescue workers use helicopters for search by pilot eyesight. These mission types on average cost 3,000 euros per hour, are dangerous for personnel, have a small endurance and have a large downtime. Therefore, there is a clear need to improve effectiveness and safety of these rescue missions. SAR teams all over the world have shown interest in the potential of unmanned aerial systems (UASs) for such improvements. However, current UASs do not live up to their expectations. In order to transcend existing UASs and to live up to the high demands, ten bachelor students have devoted ten

weeks to come up with the smart, efficient and user friendly system Nora.

The mission statement of Nora:

"Nora will provide aerial support to Search and Rescue teams while reducing the risk and the cost of the rescue operation and increasing its effectiveness."

The following text will elaborate on the details of operation and design, including the most important steps to get to this final design.

14.2 Design requirements and constraints

Nora is subjected to a number of requirements and constraints that are key to the success of the mission. The following requirements were set for Nora. Nora should:

- consist of at least one aerial device for support of ground rescue teams.
- be portable by men on foot walking on the mountain.
- have a maximum wingspan of 1.5 m.
- operate under normal weather conditions when ground support can go out with the device.
- take off and land with minimal human help.
- have detection systems to search and locate missing people.
- offer first aid help to a group of three mountaineers.
- deploy a 2 kg first aid kit with high precision at high altitudes.
- work at different altitudes, covering missions ranging from 1,500 m in Picos de Europa up to 5,000 m in the Himalayas.
- endure a mission of at least 2h and can be recharged at ground support.
- cost half of the cost of a helicopter flying during the same time.
- have a structure of at least 70 % biobased, reusable or recyclable material.

Taking these requirements along into a market research, a few constraints were derived. The total system should have a maximum

mass of 15 kg and should be separable, since it must be carried by three men. Missing persons are statistically always found within a radius of 25 km, but different types of people behave very differently. Therefore, Nora must be able to fly different search profiles. She must also be able to operate in severe weather conditions with temperatures ranging from -40 to 60 degrees Celsius and gusts up to 100 km/h.

14.3 Concept development

From the previously described requirements, the global operation could be described. Three men carry Nora into the mountains. Subsequently, she has to take off and start searching for the missing persons. When the missing person is found, Nora has to deliver a first aid kit and should then be able to continue search or return to the ground team (possibly for refuelling).

In order to find a suitable design solution to this mission profile, the design was split into three parts: the configuration of the unmanned aerial vehicle (UAV), the package delivery method and the detection method. These were first examined separately for their potential. Afterwards they were combined resulting into four options as can be seen in figure 14.1.

(a) The conventional aircraft concept is appropriate for the long endurance requirement. The main reason for this is that the wings can be optimised for efficient cruise flight. Additionally, a conventional design can achieve high flight speed which is beneficial for area coverage.

(b) The multirotor excels using its hovering capabilities. This makes it very manoeuvrable, which is certainly beneficial within mountainous and forested regions. It also provides great versatility with respect to its take-off and landing capabilities.

(c) The single rotor characteristics are similar to those of the multirotor. Its vertical rotors provide hovering capabilities which are great for manoeuvring, taking off and landing.

(d) The hybrid concept uses both rotors and wings to produce lift. This makes it have all the benefits of a multirotor combined with the benefits of a conventional aircraft. These benefits only apply to a slightly lesser extend due to some negative coupling effects.

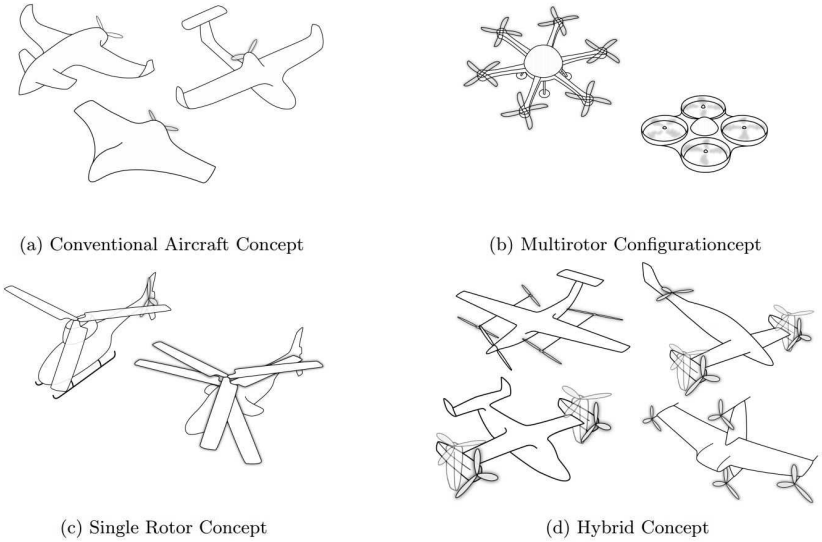

(a) Conventional Aircraft Concept (b) Multirotor Configurationcept

(c) Single Rotor Concept (d) Hybrid Concept

Figure 14.1: Conceptual configuration designs

These four concepts were traded off by a set of criteria which have a direct link with the cost and the chance of a successful mission. The hybrid configuration came out best with its combination of multiple qualities. However, within the choice for a hybrid configuration, still multiple configurations are possible, thus further narrowing down is necessary. Analysis based on conversations with experts in the UAV industry, as well as aerodynamics specialists guided the hybrid design towards a canard configuration with a push propeller, boasting quadcopter-like performance through its four vertical propellers, as can be seen in figure 14.2.

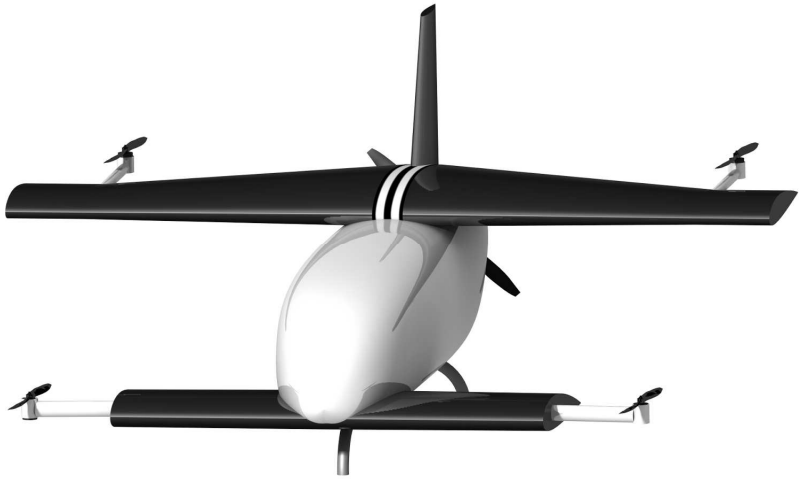

Figure 14.2: 3D View of Nora

In the following two sections the details of Nora are explained. These details are split into operational design and vehicle design, since both are extremely important for such search and rescue missions.

14.4 Operational design

The operational design consists of multiple phases. The first phase consists of the SAR team carrying Nora up the mountain. To do so Nora is designed to be separable into eight fragments. Therefore, once arrived on the mountain, Nora has to be assembled. The SAR team then has to give inputs into the system by use of a tablet interface after which the search phase commences. When the missing person has been found, the first aid kit has to be delivered, after which Nora can retire and be disassembled or continue to search for other missing persons.

Transport

To transport Nora, three backpacks have been developed to store all eight fragments. These can be carried by a team of three SAR workers. The fuselage with all subsystems excluding the first aid package will fit in the first backpack with a total mass of 8 kg. The second backpack will house the left and right wing, the left and right canard and the

tablet interface, weighing 6.5 kg. Finally the first aid kit, cruise propeller and the tail fit in the third backpack, also with a total mass of 6.5 kg. Within these masses the backpacks have space for a total of 6 kg of food, water and equipment.

Assembly

At deployment all parts can be assembled in a matter of minutes with the easy Click-Slide-Go mechanism, which can be seen in figure 14.3. This mechanism allows fast and simple attachment of the wings, canards and tail to the fuselage. The wing should simply be clicked into mount, slid to the back and then be secured using a pin. Afterwards Nora is ready to take off.

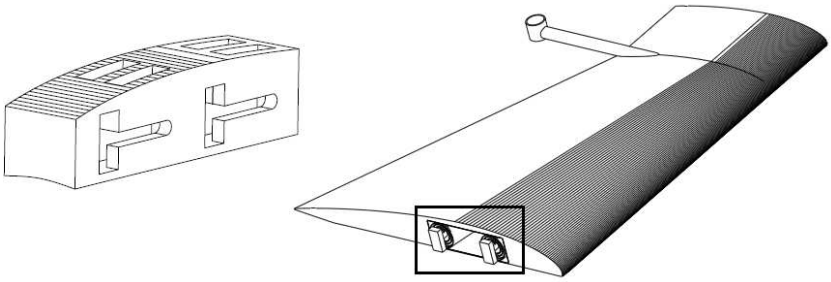

Figure 14.3: Click-Slide-Go mechanism

Interface

During search flight an intuitive tablet interface can be used to give commands to Nora. Height maps from NASA that cover the entire Earth with an accuracy of 30 m per height can be loaded on the device. These are used by Nora to fly autonomously through the mountains. Three fly modes can be selected. Firstly, the path search mode allows the operator to draw a line Nora should follow during search. A second option is area search where the operator draws an area that Nora should cover. Nora will then follow a spiral pattern to search the area. Thirdly, height line search mode can be selected where Nora will follow height lines through the mountains to stay at the same altitude.

Detection

Before Nora can start helping someone, it first has to find the missing person. In order to do this, Nora has an advanced detection system

which is capable of finding people using different detection methods, while flying one of the three flight modes. Nora can use a BAE Systems thermal camera, optical vision and radio frequencies in order to detect missing people. The use of a sound sensor is still experimental but will be added to Nora in the near future. Nora will fly at an altitude of around 240 m, which enables Nora to cover up to 21 km² per hour. Because of a smart camera pointing system and a motorized zoom lens, the camera can be used at both detection and recognition resolution, optimising the use of the camera. The required resolution and thus the required altitude was determined using Johnson's criteria for detecting people and objects. The radio frequency sensor is able to detect RECCO signals and mobile phone signals. Even when a mobile phone has no connection with the network, it can still be detected by Nora. Combining the multiple techniques improves the chance of finding the missing person.

Package

Once the person has been found, Nora will help him/her by dropping a package containing several products. The package can be dropped in two ways: Nora will either land or drop the package from an altitude depending on the situation. The package is designed to withstand a drop from 50 m above the ground. This is done using an impact attenuator, shock resistant foam and aerodynamic fins such that the package has the required attitude on impact with the ground. Once the package is on the ground, the missing person can open it and use the products inside. The products in the package can be altered depending on the mission but typically include a mobile phone, some water, water purification tablets, wind- and waterproof survival matches, an ISO thermics sleeping bag, a self-heating thermopad and high calorie bars. The mobile phone is in connection with Nora such that the missing person can communicate with the SAR team. Nora can now return and be disassembled or continue to search for other missing persons.

14.5 Vehicle design

The vehicle design can be subdivided into different subsystems. The different subsystems present in Nora are: Aerodynamics, Power & Propulsion, Structures & Materials, Control and Communications. Each subsystem will be discussed in the respective order.

Aerodynamics

Given the maximum 1.5 m span requirement, producing enough lift was a challenge for the aerodynamics. Producing enough lift is not the only design constraint, Nora also had to be stable and controllable. After several design iterations a canard configuration was chosen to be optimal for Nora. A NACA2415 wing profile will be used for both wings. Elevator control surfaces were mounted on the canard while aileron control surfaces were mounted on the main wing. A tail with rudder was added to provide more lateral stability. The fuselage was designed such that the package and all other items would fit in.

Power and propulsion

The power and propulsion system had to power 4 hover rotors and one cruise propeller for at least 2 hours. In order to design the power and propulsion system, some relevant data about Nora and her missions had to be obtained. This was done using a simulator. Next to that, engine data, a propeller model and different configurations had to be thought of. Combining this knowledge the lightest yet most efficient power and propulsion design could be found. The result was a hybrid power and propulsion system. One combustion engine which is connected to a generator, will power five electric engines attached to the rotors and propeller. The generator will also power an accumulator which powers the low power subsystems. The accumulator can also be used during extreme manoeuvring when there is more power needed than the generator can provide. The rotors have a diameter of 30 cm and the cruise propeller a diameter of 40 cm. Under normal circumstances 0.57 kg of fuel is taken along. This power and propulsion design weighs 2.7 kg and is capable of providing a continuous power of 2.2 kW.

Structures and materials

The structure is the skeleton of Nora. It connects all the subsystems. From the aerodynamics, the shape of Nora was already determined. The challenge for the structures & materials was to provide a structure which could withstand all the loads while being as light as possible. Each component (e.g. wing, tail, fuselage) was designed separately and optimised for the weight. The loads on the structure were determined using the aerodynamic data, the power & propulsion data and gust loading diagrams. By varying the structure and the chosen material the lightest option was found. In the end a carbon fibre combined with foam structure was used for Nora. In the fuselage, cut-outs had to be made such that components in the fuselage can be reached easily. The cut-outs are located on the top and the bottom of the fuselage, covering 80% of the fuselage length. The overall structural design cost, including manufacturing, has been estimated and validated by experts in the field at €3,900 with a total mass of 4.5 kg.

Controller

As Nora is an UAS, it needs a control system in order to fly. Nora has a custom designed control system which enables Nora to fly many different trajectories under various weather conditions. Nora has a hover controller, which controls the four hover engines such that she stays in the air during hovering. Nora also has a cruise controller which works completely different because now the control surfaces and the rear engine are used for control. Another controller, called the transition controller, is made to make sure that Nora is able to transition between hover and cruise safely and the other way around. The control systems mainly use a Proportional Integral Differential (PID) structured control system to control all the outputs. A simulator was made in which both the control systems was tested as tuned for Nora. In this simulator mission profiles were flown from which essential data was obtained. An example of the data obtained is the maximum power needed, the total energy needed or the required force for the control surfaces. This data was then used in the design of the other subsystems.

Communications

When Nora is on her mission, it is important for the ground team to know where Nora is and receive updates on her progress. The ground team can also give Nora new commands using the communications system. Nora is equipped with a direct Line-of-Sight data link with the ground unit. This data link has a range of 10 km. In the mountains, a direct Line-of-Sight communication is not always possible and the drone can also exceed the 10 km range from the ground unit, therefore a satellite communication system was implemented. Using this satellite communication system, Nora will always be in contact with the ground team. In order to establish these connections, Nora is equipped with a 915 MHz transceiver, a 1.6 GHz transceiver, a 2.4 GHz transmitter and a 5.8 GHz transmitter.

Combining all the different subsystems gives one final result called Nora. A 3-view drawing of Nora can be seen in figure 14.4, also some of her characteristics are shown in table 14.1.

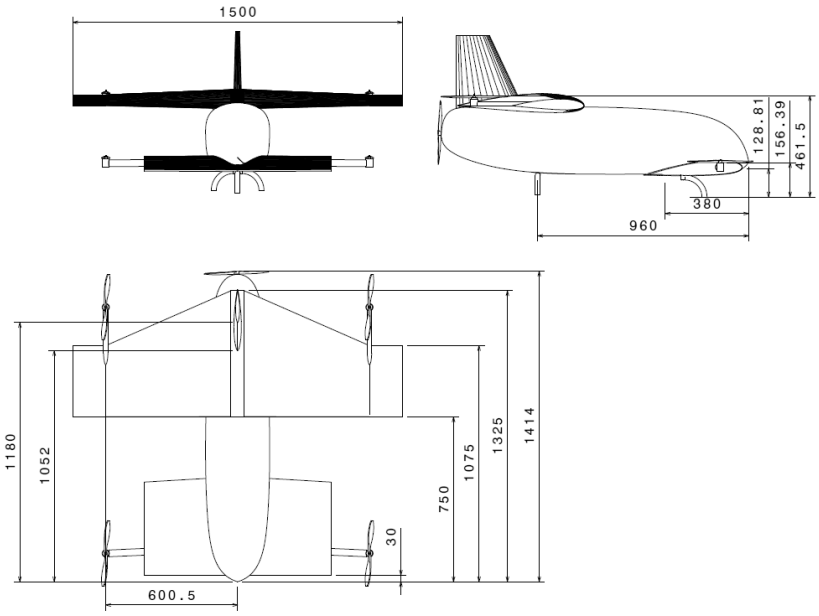

Figure 14.4: 3-view Drawing of Nora

Table 14.1: Nora's Characteristics

Endurance	2-6 hours	Vehicle Mass	11 kg
Area Coverage	21 km2h-1	System Mass	15 kg
Wing Span	1.5 m	Max. Power	5.5 kW
Purchase Cost	€25,000 unit-1	Continuous Power	2.2 kW

14.6 Conclusions and recommendations

The objective of this project was to design an aerial support drone for Search and Rescue teams. This drone should reduce the risk and the cost of the rescue operation and increase its effectiveness. As has been shown throughout this summary, Nora is the solution. Nora meets the initial requirements and even goes beyond what some of them implied. These results are an indicator for the potential success of Nora as a rescue drone as well as the potential for UASs to dominate new markets.

The innovative design solutions that were implemented in Nora can be summarised as follows:

- A hybrid design that combines endurance and efficiency characteristics of conventional aircrafts with the manoeuvrability and hovering capabilities of rotorcraft.
- A hybrid power and propulsion system that combines the endurance of an internal combustion engine with the response and power characteristics of electric motors.
- An intelligent flight controller that allows for autonomous flight in numerous weather conditions.
- An innovative separable concept that allows a group of just 3 persons to carry the system in mountainous regions.
- Application of an enlarged canard configuration to boast an increase in aerodynamic performance within a limited wingspan.
- An extremely lightweight structure that is build out of mostly recyclable and reusable materials.

- A state-of-the-art detection system that combines multiple sensors to improve detection probabilities under various conditions.

Even though Nora meets its initial requirements there are still some aspects that can be improved in the future. First of all the structure of the fuselage may be improved in such a way that it becomes separable into two parts. This would further improve the possibilities to carry Nora in mountainous regions. Secondly, the landing gear may be slightly redesigned to improve the aerodynamic performance of the vehicle. Finally some improvements should be made to the control system. This should further improve the autonomous flight performance as well as increase the safety of the design.

15. MORPHLIGHT: A MORPHING AIRCRAFT

Students: M.G. van Dijk, Y.L.M. van Dijk, J.P.P. Hemmen, J.G. Hemmes, S.J. van der Meer, E.M. de Mol, G. de Rooij, R.M. Rosenkrantz, A.M. de Windt, G.I.R. De Zutter

Project tutor: dr. A.M. Grande

Coaches: R. Merino Martinez MSc, Y. Zhang MSc

15.1 Introduction

Since its conception more than 60 years ago, the Cessna 172S Skyhawk has dominated the general aviation market. Its popularity is attributed to its versatility, safety record, cost-effectiveness and simplicity to fly and maintain. Since then advances in technology have allowed development of newer aircraft, with longer ranges, higher fuel efficiencies and higher cruise speeds. To stay ahead of the competition, the Skyhawk must be modernized with newer technologies.

Aircraft are usually designed to fly optimally at a certain flight condition, but with rising air traffic or just because of the requirements of a particular mission, aircraft often do not fly under their ideal condition. To counteract this problem, morphing concepts allow an aircraft to adapt its shape to fly faster, further, longer and

more efficient under a wide range of flight conditions, thus providing significant advantages.

The goal of this project is to design a morphing, single engine propeller aircraft with improved performance characteristics, while maintaining the same level of safety and reliability. Thus, the following mission statement can be formulated.

"To improve a Cessna 172S Skyhawk using existing morphing concepts found in literature, within a catalogue price of €375,000 per aircraft, by 10 students in 11 weeks' time."

15.2 Mission objectives and requirements

The project objective is to design a single-engine propeller aircraft for the civil market including morphing concepts. Compared to the Skyhawk, the new design shall meet more stringent top level requirements, as following.

Performance:
- Maximum range ≥ 2,000 km
- Maximum endurance ≥ 10 h
- Cruise speed ≥ 250 km/h
- Cruise altitude 2,600 m
- Take-off distance ≤ 400 m
- Landing distance ≤ 300 m

Safety and reliability:
- Same safety and reliability of the reference aircraft.
- No additional maintenance frequency for the aircraft with morphing concepts compared to the reference aircraft.

Sustainability:
- Take-off fuel consumption ≤ 2.5 L
- 80% of airplane morphing parts recyclable/reprocessable

Engineering budgets:
- Morphing concepts applied only to wings, tail plane, engine and landing gear

- Engine power and internal fuselage dimensions from the reference aircraft
- Operational empty weight ≤ 750 kg
- Maximum take-off weight ≥ 1,250 kg
- Fuel capacity ≤ 200 L

Cost:

- < € 375,000 (single standard configuration aircraft)

15.3 Design options

In order to meet the requirements, various morphing concepts are studied. These are camber, chord, dihedral, span, sweep, thickness and twist. These are explained here in further details.

Camber

This is the most common concept being considered. It is usually accomplished by using a discrete trailing edge flaps which have aerodynamic penalties. These can be avoided by continuously morphing the shape of the aerofoil, allowing the air to flow undisturbed around it.

Chord

The thickness ratio of the local aerofoil can be reduced by increasing the chord length and thus improving the aerofoil high speed performance. The wing surface is also enlarged resulting in an increase of lift and parasitic drag. When the wing surface is kept constant, the parasitic drag is reduced by increasing the chord length and thus improving high speed performance. By reducing the chord length the maximum range can be increased.

Dihedral

Changing the dihedral of the wing allows for the roll stability of the aircraft to be adjusted.

Span

Increasing the wingspan results in a higher aspect ratio, as well as a larger wing planform area. The increase in aspect ratio has a beneficial

effect on the lift over drag ratio allowing for longer loiter time and higher range. Span morphing can be achieved by two methods:
Telescopic wing extension uses one or several wing segments which can extend like a telescope.

A zero Poisson's ratio skin can change length in one direction without affecting its size in the other directions. Using this zero Poisson's ratio skin, the span can be extended, while the chord length remains the same. The skin is used in combination with a zero Poisson's ratio honeycomb structure, which provides support for out-of-plane loads.

Sweep
The advantages of sweep morphing are mostly relevant for high speed performance. It has disadvantages on the aerodynamics and structural performance and has negative effects on the stall characteristics.

Thickness
The optimum wing thickness depends on the flight speed and other requirements. A smaller thickness results in lower drag at higher speeds, but a thicker wing allows for the structure of the wing to be reduced. Thicker wings also have a higher maximum lift coefficient.

Twist
Wing twist can be used to prevent tip stall and to improve the wing lift distribution.

15.4 Trade-off

To come up with a preliminary design several consecutive trade-offs between different combinations of the previously mentioned design options is performed. These trade-offs compared performance, weight, cost and risk, where performance and weight have a higher priority than cost and risk. The combination of span morphing using zero Poisson's ratio structure, chord, and camber morphing has the highest score. Wing twist morphing can be relatively easily added to the wing tip and is thus not considered in the trade-offs.

15.5 Design process

This section covers the detailed design process followed during the project.

Performance
The performance characteristics are optimised to meet all requirements. Favourable basic planform dimensions including morphing amounts are determined. The amount of morphing is limited by the zero Poisson structure and the location and size of the Fowler flaps.

Aerodynamics
In order to optimize the aerodynamic performance of the aircraft, the aerodynamic properties of the aerofoil, wing and complete aircraft are studied. A series of aerofoils used in similar aircraft are compared and in the end a variant thereof is chosen. Several wing planform shapes are compared with each other to provide information for the final trade-off and a preliminary study on the advantages of a raked wing tip was done. Finally, CFD calculations are performed to check the accuracy of the results being calculated.

Stability and control
To ensure the aircraft is stable and controllable in all flight conditions and with all possible load cases, the tail surfaces are sized based on the requirement that they should be able to compensate for aerodynamic moments to trim the aircraft. The size of the horizontal tail area can be kept the same as the Skyhawk, or even slightly reduced if the centre of gravity range is shifted more forward. The vertical tail area should increase, as the increased wing span leads to a stronger tendency for adverse yaw.

Structures
The wing structure consists of a wing box with ribs to provide support to the skin. To allow for morphing, the wing box is split into three parts. A custom optimisation program returns the lightest wing box design and assesses whether adding a strut makes sense. It is found

that adding a strut significantly reduces the weight of the total structure.

15.6 Final design

Subsystems

The engine is replaced by a more fuel efficient, but larger, hybrid diesel engine in order to meet the take-off fuel requirement. To improve the propulsive efficiency the fixed pitch propeller is replaced by a variable pitch three blade propeller. The electrical subsystem now features fly-by-wire aileron actuation, as a cable and rod system would be overly complex on a variable span aircraft. The fixed gear is replaced by a retractable system in order to reduce drag. A speed brake is added in order to meet the landing distance requirement.

Materials

The reference aircraft is almost entirely made out of aluminium. In order to reduce structural weight while maintaining structural integrity, different materials are selected. Both thermoset and thermoplastic CFRP are used. Thermoplastic CFRP are preferred, since the matrices of thermoplastic CFRP are recyclable. The morphing parts use a zero Poisson's ratio skin, made of unidirectional carbon fibres in a polyurethane matrix. The skin is glued to a thermoplastic honeycomb structure for strength. Furthermore, parts taking large loads are made of more conventional materials, such as aluminium and steel.

Wing

The wing planform, shown in figure 15.1, consists of a tapered non-morphing section near the root. The rest of the wing is taperless and capable of span morphing. This shape is chosen to accommodate the fuel tanks, increase the cross-sectional area near the root to lighten the structure and to tune the lift distribution for better aerodynamic performance.

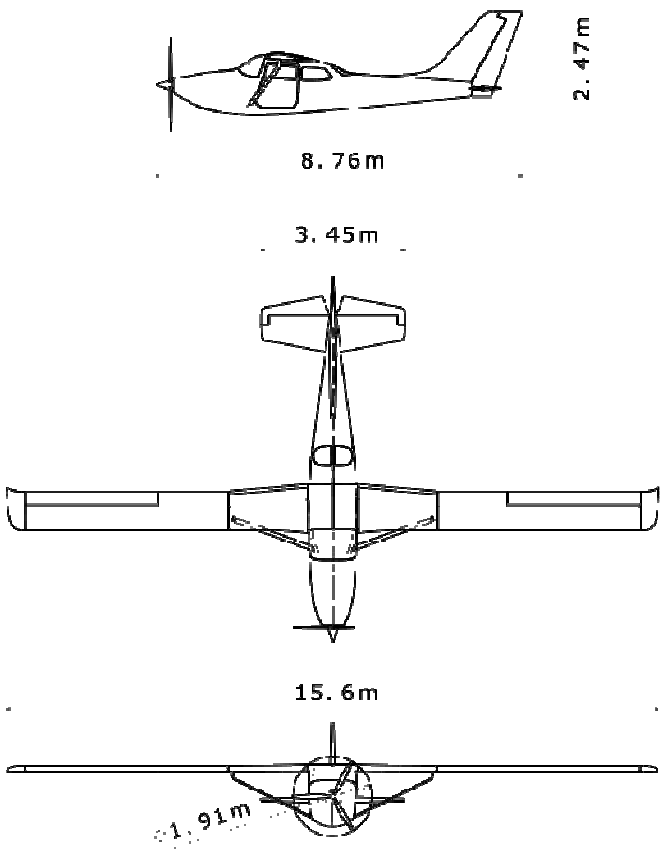

Figure 15.1: 3-view drawing of the Morphlight

To allow the wing boxes to slide, an ultra-high-molecular-weight polyethylene coating is used. The ribs are also able to slide using this same coating. Span extension is done with a rack and pinion mechanism, for which a total of four small electric motors are used. The ribs are connected to each other, through the zero Poisson's ratio honeycomb structure as shown in figure 15.2.

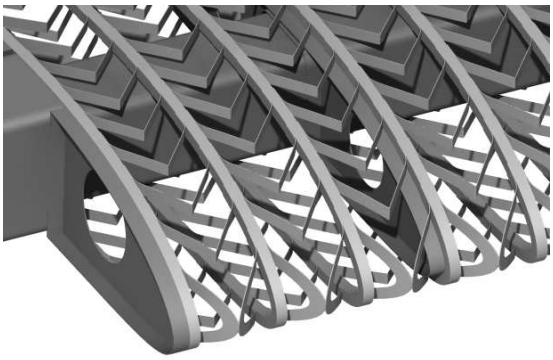

Figure 15.2: Wing zero-Poisson's ratio morphing structure

To increase the camber and chord length sufficiently and separately, a Fowler flap mechanism is used, which is shown in figure 15.3. Flap tracks, placed on the top side of the wing, first provide chord morphing after which the camber can also be adjusted.

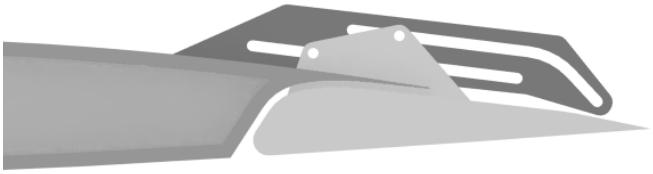

Figure 15.3: Flap sliding mechanism

The design characteristics of the Morphlight are listed in table 15.1. It can be seen that all requirements are met.

Table 15.1: Design characteristics of the Morphlight

Dimensions	Chord	1	m
	Chord (extended)	1.175	m
	Wingspan	10	m
	Wingspan (extended)	15	m
Performance	Maximum endurance	21	h
	Maximum range	2780	km
	Cruise speed	250	km/h
	Take-off distance	336	m

	Landing distance	284	m
Weights	Operating empty weight	712	kg
	Maximum take-off weight	1272	kg
Other	Catalogue price	€ 365,000	
	Take-off fuel consumption	1.93	L

15.7 Conclusion and recommendations

The Morphlight, shown in figure 15.4, meets and exceeds the given requirements. It has more flight capabilities and is more versatile than the Cessna Skyhawk. The production of morphing systems is demonstrated to be possible within reasonable cost. Through the intensive use of thermoplastic CFRP, the morphing concepts on the Morphlight are a sustainable way to increase its performance. By making use of a diesel-electric hybrid engine, the fuel consumption is reduced. The new engine is able to use either Jet A-1 or diesel, which, unlike the previously used avgas, do not produce harmful lead emissions. This results in a more sustainable aircraft. The Morphlight is statically and dynamically stable in all its configurations, and its handling characteristics are similar to Cessna Skyhawk, making it an ideal replacement.

Figure 15.4: The Morphlight in flight

It is concluded that morphing is a feasible technology to improve the performance characteristics of an aircraft. As a recommendation, more research is needed into the design and production of the zero Poisson's ratio structure. Furthermore, flying faster, by using a more powerful engine, would make morphing even more beneficial.

16. MARITIME FLYER: HERON RPAS

Students: J. Busch, R.C.A.M. van Casteren, A.E. Demir, R. Hammink, S. van der Helm, D.E. van der Hoff, K. Langemeijer, M.T. Latour, D.J. van Oorspronk, J.S. Visscher

Project tutor: dr. Ir. E. van Kampen

Coaches: J. Rohac, PhD. , S.K. Kamaludeen, Msc.

16.1 Introduction

Ports around the world are becoming busier and more difficult to oversee, making it problematic for harbour authorities and local police to control these areas. For this reason, group 6 has dedicated itself to "Increase the safety and security of maritime environments". For this purpose, a remotely piloted aircraft system (RPAS) has been designed that is able to provide surveillance in maritime environments within a 20 km radius.

A functional analysis was completed to determine a list of requirements for the RPAS, followed by possible designs using design option trees (DOT). Preliminary designs were made for four concepts, which were eventually traded off. Finally the detailed design of the maritime flyer, including all necessary subsystems for operation, was completed.

16.2 Requirements

A functional flow diagram and functional breakdown structure were constructed to provide an overview of the necessary tasks that the RPAS has to complete. A requirement discovery tree was then constructed to give an indication of the requirements that the RPAS must fulfil. Along with the self-determined requirements, the customer had set requirements for the product as well. They are as follows:

- The RPAS shall have an endurance of 4 hours
- Maximum take-off weight shall be less than 20 kg.
- Operating radius of the RPAS shall be at least 20 km.
- The RPAS shall have inherent safety aspects.
- The RPAS shall be designed to comply with certification.
- The RPAS shall have a system for detection and avoidance of static and dynamic obstacles.
- Sustainability shall be integrated in the design of the RPAS.
- Total production cost of the system shall be less than €100,000.
- The RPAS shall link video to the ground station for at least a 10 km operating radius.
- Individuals' clothes shall be identifiable by the video system.
- Ship names shall be readable.
- Objects with dimensions of 2 metres shall be visible.

These requirements form the basis for the preliminary and detailed design process as they define what design choices are plausible or not. Following this, design options could be explored.

16.3 Conceptual design

The preliminary design began with the aid of DOTs, which are hierarchical methods of finding possibilities for certain design aspects. The main DOTs used were for determining the lift configuration, propulsion system, launch method, and recovery method. The DOT for the lift configuration, which determines the design's appearance, is shown in figure 16.1.

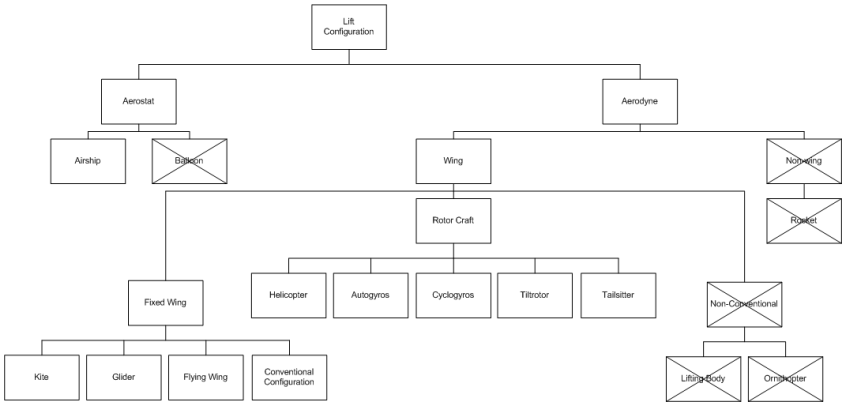

Figure 16.1: Design option tree for lift configuration

Unfeasible options were crossed out from the DOTs as they would not be able to fulfil the mission, this is shown above in figure 16.1. From these trees, it was possible to devise multiple conceptual designs for the maritime flyer. In the end, four designs were chosen to proceed to the preliminary design phase. These four designs were the airship, kite, flying wing, and conventional configuration.

As the most innovative of the four designs, the airship is a semi-aerodyne, aerofoil shaped option for the maritime flyer. Due to it being filled with helium, less propulsive power is needed to generate lift, making the airship a high-endurance option. To provide thrust and conduct imaging, three detachable quadcopters are located at the bottom of the airship. Stability is achieved for this design but due to its large surface area, controllability is difficult to achieve. Its size also brings other troubles, such as not being suitable for maritime environments due to the high wind gusts that have a large impact on its attitude.

A canard was used for the second design, namely the conventional configuration. With a high aspect ratio wing at the rear of the aircraft, and a positive lift canard, more lift is generated and aerodynamic efficiency is increased. Due to the rigidity of the structure and the materials used, it is also very suitable for the maritime environment with its high winds and humidity. On the downside, this concept is

inherently unstable due to its canard. It is also not very innovative compared to other designs.

Next is the flying wing, which is a design consisting of a single wing with a fuselage in the middle for carrying the payload. Due to its single lifting surface, aerodynamic drag is low, giving it a high efficiency and longer endurance. This low drag also allows it to have a higher cruise velocity than other designs. However, with market research it was determined that the flying wing design has a higher cost risk than other concepts.

Finally, the kite design was worked out. This concept can be compared to modern hang gliders with the flexible lifting surface in the shape of a delta wing. Using struts to connect subsystems, the kite concept can carry a relatively large amount of payload. Due to its lightweight and large lifting surface the kite is susceptible to wind gusts in the maritime environment.

16.4 Trade-off

With all preliminary designs completed it was possible to perform a trade-off so that the most suitable design can proceed into the detailed design phase. To perform a trade-off, criteria must first be determined along with their weights. Thirteen criteria were determined to be important when selecting a design, of which the most important ones were the payload capacity, suitability for maritime environment, and feasibility risk. The analytical hierarchy process (AHP) was used to determine the weights for each of these criteria. Splitting the group into two allowed for a sensitivity analysis to take place, from which it was determined that the results were too easily affected with changing weights. A second iteration was conducted for which the weights were not as sensitive to change. From this trade-off, the airship and kite were discarded due to their low scores. The conventional and flying wing did not differ very much in their scores, making it difficult to conclude the trade-off solely using this method. For this reason, qualitative reasoning was used to decide on a winner. Mainly due to the more innovative design as well as the higher aerodynamic

efficiency, the flying wing was chosen to proceed into the detailed design phase.

16.5 Detailed design

A final design was chosen and detailed design needed to be done, which includes designing all subsystems of the maritime flyer. From this detailed design phase, the final design was determined, for which the appearance can be found in figure 16.2. An overview of the steps taken for each subsystem will be given in this section.

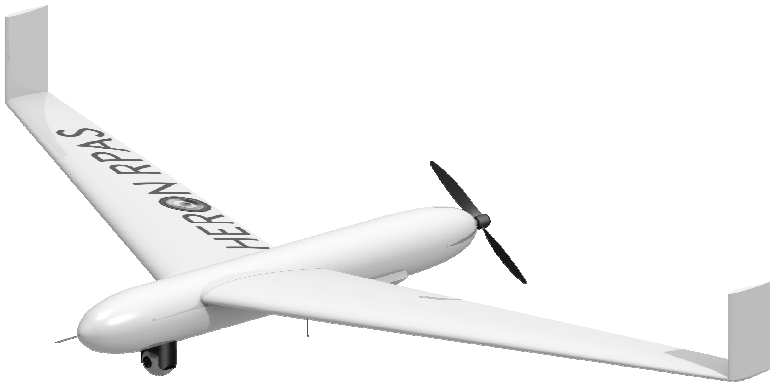

Figure 16.2: Isometric view of the HERON

Aerodynamics

The main challenge for the aerodynamics department came from the stability requirements of the RPAS. With a single wing, there is no horizontal tail surface to provide longitudinal stability. To acquire this, it is necessary to have an aerodynamic centre that is behind the centre of gravity as well as a positive pitching moment around the aerodynamic centre. The NACA 5 series was examined due to their reflex, which provides this positive pitching moment. After inspecting their characteristics, the NACA 22115 was chosen as the aerofoil due to it being cheap to produce and not prone to collection of dirt in the front cavity. It should be noted that the disadvantage of a reflex aerofoil is the lower $C_{L,max}$. Furthermore, a leading edge sweep of 25°

was applied to a wing with a span of 3.57 m and taper ratio of 0.35. The HERON flies 28 m/s at cruise and its stall speed is 15 m/s.

Stability and control

To ensure stability and controllability of the RPAS, control surfaces needed to be designed. For this purpose, elevons and rudders were decided upon. For optimal control of the RPAS, it was decided that the best flying qualities were needed, which are level 1 flying qualities. To assist in elevon and rudder sizing, models were built using MATLAB to give an indication of the responses to certain inputs. The elevons were designed to be 20% of the chord length with an area of 0.044 m^2. For lateral stability, it is important to have vertical surfaces, which are introduced by using winglets. These winglets allow for stabilizing moments in the yaw direction. For rudder sizing, a model was made to visualize the reaction of the RPAS to a 25° input of sideslip. Active yaw control led to rudders with 20% chord length of the winglet and an area of 0.009 m^2. These surfaces ensure good handling quality for the RPAS.

Structures and materials

In order ensure that the fuselage and wings are able to sustain the loads experienced during missions, it was essential that the structure of the RPAS was correctly designed. Looking at Koninklijk Nederlands Meteorologisch Instituut (KNMI) data for maximum wind gusts in the last five years, it was determined that the wings must sustain a maximum of 20 m/s wind gusts to be able to operate in 90% of the days. The ultimate load factor was determined to be 15, while maximum normal and shear stresses are 72 MPa and 50 MPa respectively. To carry these loads, a wing made of a foam core is used and reinforced by four layers of carbon fibre with a total thickness of 0.5 mm. These fibres are lain at 45° from each other to carry the bending and torsional loads. Both wings can be removed as they are attached in the middle of the fuselage. This modularity allows for easy transportability of the RPAS. A supporting structure in the fuselage will support the loads endured by the wings. To withstand the bending loads the fuselage is also made of 0.5 mm of carbon fibre, however they are lain with a 0° and 90° orientation.

Propulsion

A single propeller is used to provide thrust for the RPAS. Theoretical calculations for the power needed were first done. Using a cruise velocity of 28 m/s with an average headwind of 7 m/s, the power was determined using a velocity of 35 m/s. This gave a power required of 1346 W. Minimum efficiency of the propulsion system was assumed and a safety factor of 1.2 added to acquire a required power of 1900 W, which equals 2.55 hp. Due to the power subsystem requiring a power generator on board, engine choices were limited. This led to the decision to choose the 3W 28i engine. At 3.35 hp it provides sufficient power for the propulsion system, and its power generator is able to supply the necessary power for on-board electronic systems. Throttle is not kept at maximum for cruise velocity to minimize vibrations, therefore 6700 RPM is chosen. Applying this, the propeller pitch can be calculated, which was found to be 10 inch. A choice could be taken between a propeller diameter of 16 inch or 18 inch, from which 18 inch was chosen. This is because of the higher efficiency of the propeller at higher diameters.

Payload

For successful completion of the missions, it is necessary to have an imaging system on board. From the initial requirements and input from experts in the field of imaging systems, it was possible to determine which camera would be optimal for the mission while staying within the budget. A camera designed by Sony, the FCB-EX980SP, was chosen along with a gimbal system that is able to continuously pan and tilt the camera at a rate of 100° per second. A render of this system is shown in figure 16.3. This camera supplies live colour images up to a distance of 10 km. A video processing unit is on board to provide high quality images at lower data rates

Figure 16.3: Imaging system on the HERON

Communications

Streaming of the video feed and control of the RPAS must be done using a communications system. For this reason, two data links are used, one for streaming the video to the ground station, while the other is for command and status signals of the control system. This control system consists of microphones, transponders, and autonomous control. Microphones on the wingtips are able to detect dynamic objects during flight while transponders report the location of the RPAS to other aircraft. To provide redundancy, the payload link can be used for control in the case of a failure. The communications system is able to relay the status of all subsystems on board of the RPAS such as fuel level, battery level, and throttle value. Due to frequency restrictions, there are limitations with respect to the bandwidth that can be occupied, which means the data rate had to be set to the 2.4 GHz link for video streaming and 424 MHz for control inputs and outputs. Furthermore, the RPAS contains an autopilot.

Operations

Other than the design of the RPAS itself, the launch and recovery systems had to be designed and certification, maintenance, and safety had to be taken into account. A catapult is used as the launch system for the HERON, as it is a transportable and fast way to launch. The rail is modular and can be disassembled into parts of 1 meter. Using a pneumatic system, the RPAS is attached to the launch carriage using two pairs of prongs that connect at the wing-fuselage connection

point. It is launched at 20 m/s making it relatively easy to accelerate to cruise velocity. Once the mission is completed the HERON is recovered using a net. It can fly into the net at 17 m/s, just above stall speed, and be decelerated to a stop in about 2 meters using an elastic meshing. The launch and recovery systems are shown in figures 16.4 and 16.5 respectively.

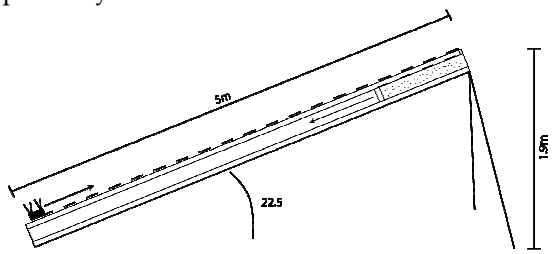

Figure 16.4: Catapult launch system

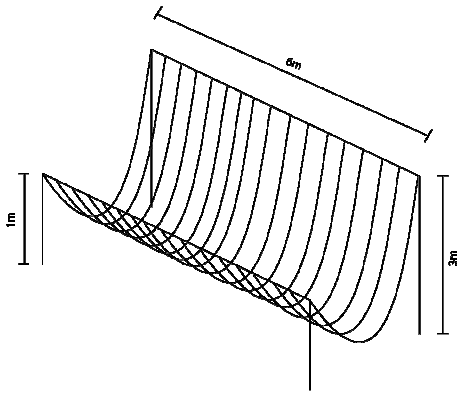

Figure 16.5: Net recovery system

Furthermore, to ensure safety and reliability of all subsystems, maintenance will be done periodically using visual inspections and checks during the HERONs lifetime. Check 'A' is a light check that includes inspecting batteries for efficiency, engine effectiveness, and visual inspections for defects. Heavy maintenance is done in check 'B', this takes apart the whole RPAS for thorough inspection of all subsystems. If errors or defects are found they must be repaired as quickly as possible.

Other than production costs of about €80,000, there are operational costs involved when using the HERON. These include fuel, salaries,

insurance, and maintenance. From the density of a gasoline/oil mixture and the fuel needed for one mission, 4.5 litre, the price of fuel per mission is equal to € 6.77. Next, the salaries for operators of the RPAS were taken as the average first year salary in the Netherlands, which is € 34,500. Salary costs per mission then equate to € 240 per mission. Insurance costs need to be paid annually and are € 4,500. This covers up to 20 UAVs and € 1,000,000 in damages to other and the RPAS. Finally, maintenance costs per year were calculated using replacement asset value for each subsystem. Per year this costs almost € 5,000. In total the operational costs are € 259 for every mission of four hours, for the entire 5-year lifetime of the RPAS.

Safety and sustainability

Throughout the design process, safety and sustainability were integrated in every design choice. Safety is difficult to assess quantatively, but was ensured through inspection, maintenance, and checking reliability of subsystems. Safety factors were applied to the subsystems structures, propulsion, power, aerodynamics, communications, and navigation. A factor of safety for structures means that the structure will still be able to support 1.5 times the maximum expected loading. In case the propulsion system reduces supplied power, the safety factor ensures that it will still be sufficient for cruise velocity. Additionally, redundancies were incorporated during design such as multiple actuators for the control surfaces so that the RPAS can be controlled if one happens to fail.

Sustainability is a large part of the design process nowadays, and it was during this design process as well. Sustainability was defined to be environmentally friendly as well as durable. These two aspects were achieved in material choice, production methods, and operations. Materials such as aluminium are chosen so that recycling is possible after the lifetime of the HERON. This is identical with carbon fibre, which can be re-used in for example the automotive industry. When looking at production methods, it is important to be able to produce the RPAS using existing methods instead of spending resources on creating new techniques. Furthermore, during operations, eco-friendliness was a very important factor. For a 4 hour

mission, the fuel consumption of the HERON is almost 500 times lower than if a harbour patrol boat were to be used. An efficient engine was chosen to make sure that fuel consumption and emissions were as low as possible. Durability during operations is ensured by periodic inspection and maintenance.

16.6 Recommendations and conclusion

Further activities that can be done after the completion of DSE include scale model testing, validation, full scale model testing, and finally production. For further improvements in the design process, some recommendations can be made. More iterations of the design, such as for the structures and propulsions subsystems will be beneficial to the weight of the RPAS. Iterations will optimise the design to its fullest extent. Further investigation into the reliability of a single engine could be done to further increase safety of this design. More detailed models of the aerodynamic efficiency of the fuselage could also be done. Optimisation of the fuselage may also reduce total size of the RPAS. Finally, paid frequencies may be an option to increase the effectiveness of the communications link.

At this moment, the HERON RPAS has been designed to fly at 28 m/s, have an endurance of at least 4 hours, be suitable for maritime environments, and stream live video. All design aspects of the detailed design phase have been covered, and group 6 is confident in saying that they have “Designed an RPAS to increase safety and security of a maritime environment”.

17. PLASMA ACTUATED UAV

Students: E.G. Algera, Y. Bauer, A.E. van Hauwermeiren, V.C. van 't Laar, E.J. Pronk, T. Roos, K. Saß, V.C. Sonneveld, N.D. Waars, S. Wang

Poject Tutors: dr. M. Kotsonis, dr. A. Sciacchitano

Coaches: dr.ir. J. Ellerbroek, W. Yu MSc

17.1 Introduction

Imagine looking out of your window while flying at night. Instead of complicated moving flaps, slats, ailerons and other control surfaces, you see a pattern of glowing plasma dancing over the wing. This could very well become reality in the near future! The one problem is that plasma only works well at low speeds for now, and therefore it can only be applied to small UAVs. As a first step in the right direction and to prove the concept of plasma control, the Plasma Actuated UAV was realised.

The question then remains: How to control an aircraft with plasma? The answer is plasma actuators. In short, a plasma actuator is made up of two electrodes, separated by a layer of dielectric material. It is attached to the wing or tail, so that when a high voltage is applied over the electrodes, plasma is generated. This cloud of plasma accelerates the air, and a change in lift is realized. Recent research has shown promise for the application of plasma actuators in control of

UAVs. The actuators have no moving parts, are easier to maintain and are less complex than servos and hinges. Next to that, the response of plasma actuators is remarkably fast.

The realisation of the Plasma UAV proved the concept works at low speeds. And who knows? In a few years, you might look out of an airplane window and notice they successfully applied this new technology to larger, manned aircraft!

17.2 Requirements and constraints

At the beginning of the project, a set of requirements was set by the customer. These requirements drive the design of the plasma controlled UAV and are listed below.

Functionality
- The UAV shall have no moving control surfaces.
- The UAV shall be controllable using plasma actuators.
- The UAV shall have at least equal maximum pitch, roll and yaw rates as similar UAVs.

Performance
- The UAV shall have a minimum range of 10 km.
- The UAV shall have a minimum endurance of 2.0 hrs.
- The UAV shall have a maximum wing span of 3.0 m.
- The UAV shall have a minimum payload of 1.0 kg.

Systems
- The UAV shall have an autopilot with pre-programmed flight modes.
- The UAV shall have a two-way telemetry compatibility

Costs
- The UAV program shall have a maximum cost of € 10,000.

Sustainability
- The UAV shall produce equal or lower noise than similar UAVs
- The UAV shall have equal or lower emissions than similar UAVs.

17.3 Conceptual design and trade-off

The mission objective for the plasma UAV is:

"to design a fully plasma controlled UAV, which can obtain control rates comparable to conventional UAVs".

A conceptual design was devised that would most effectively suit this objective, while meeting the top-level project requirements.

This resulted in a conceptual design that is comprised of a fuselage mounted underneath a wing, resembling a high-wing configuration. This serves to ensure lateral stability and impose extra robustness during landing. An engine and propeller are mounted aft of the fuselage, leading to a pusher configuration. This was done to shield the propeller during impact and give a possible optical payload a maximum field of view when installed in the nose. The tail, providing stability to the aircraft, is mounted via two booms connecting the tail to the wing. Using booms instead of an elongated fuselage would shift the centre of gravity of the aircraft forward, thereby increasing the stability of the design.

The tail itself has to provide both lateral and longitudinal stability and therefore features both a horizontal and vertical surface. An inclined surface is often used on UAVs (e.g. a V-tail), but this was regarded too complex due to the coupling of control motions. Next to that, this configuration would reduce the effective surface on which plasma actuators can be mounted. To increase the effective control surface area of the tail, an H-tail configuration was chosen. This configuration allows the UAV to profit from the benefits of a T-tail due to the partly shielded edges of the horizontal and vertical surfaces, effectively making them more efficient.

The prop-wash generated by the propeller degrades the quality of the airflow and this raised some concerns over the effectiveness of the plasma actuators on the horizontal tail. Investigation of the nominal prop-wash showed that the cylindrical shape of this disturbed flow could pass below the horizontal surface if it is mounted sufficiently

high. This resulted in a Pi-tail configuration. The concern that the Pi-tail could lead to a deep-stall during operations, as often encountered in aircraft with a high-mounted horizontal tail, was discarded. This is due to the fact that the tail has quite a long arm, and will therefore be out of the stall wake of the main wing.

The landing and take-off procedure, a rather stringent part of the design, were split up in the different possibilities. General UAV take-offs are a hand-launch, a runway take-off or a bungee assisted launch. The initial design mass of 8 kilograms already proved to be too high for a hand-launch and it was found that this weight class is usually launched with a transportable bungee as a runway take-off requires extra logistic efforts and lessens the effective flown range. Therefore the Plasma UAV is launched with the assistance of a bungee. The landing can be performed with an undercarriage, with the belly, with a parachute or with assisted landing (e.g. a net). The design weight and the comparison between reference UAVs showed that a belly landing would be the most straightforward approach. This type of landing also complies with earlier design trade-offs, such as an aft mounted propeller, a twin boom connected tail and a high wing configuration.

17.4 Design overview

The result of the trade-off was used to proceed with the actual design of the plasma UAV. This section elaborates on the configuration and layout of the designed UAV, before the detailed design of the subsystems is discussed.

The final design of the plasma UAV is shown in figure 17.1. The UAV can be divided roughly into three parts, the wing, the fuselage and the tail, respectively. As was mentioned before, a high-mounted wing is used in order to achieve enough ground clearance to perform a belly landing. The tail of the UAV is connected to the wing by two booms. The specifications of the UAV are illustrated in table 17.1.

A 3 m wingspan is used in the final design of the UAV. This is also the maximum wingspan as specified by the requirements. The aspect ratio is 7.75 and a stall speed of 10 m/s is used in the design. The total length of the UAV (from antenna tip to tail trailing edge) is 3.15 m. In order to accommodate the several subsystems, such as the engine, parachute and payload the fuselage is approximately 1 m long.

The propulsion system of the UAV is located in the back of the fuselage. An electric motor is used to drive the propeller, which is mounted between the two booms. Electric engines have several advantages over combustion engines for this UAV, for example their weight and environmental impact. The batteries, providing power to the engine, the flight controller, the plasma actuators and the parachute are placed at the centre of the fuselage. The parachute is included in the design to perform a controlled emergency landing.

Control of the UAV is achieved with the plasma actuated control system. Instead of moving control surfaces, plasma-generating electrodes are placed on the wing. How these electrodes are used to control the wing is explained in the section on the detailed design. To accommodate the experimental control system, adaptations to the flight controller had to be made, special aerofoils had to be implemented and a very lightweight UAV structure was required.

Table 17.1: Specifications of the plasma UAV

Parameter	Value
Wing span	3 m
Wing surface area	1.16 m^2
Aspect ratio	7.75
Cruise speed	13 m/s
Total mass	9.96 kg
Endurance	2.0 hr

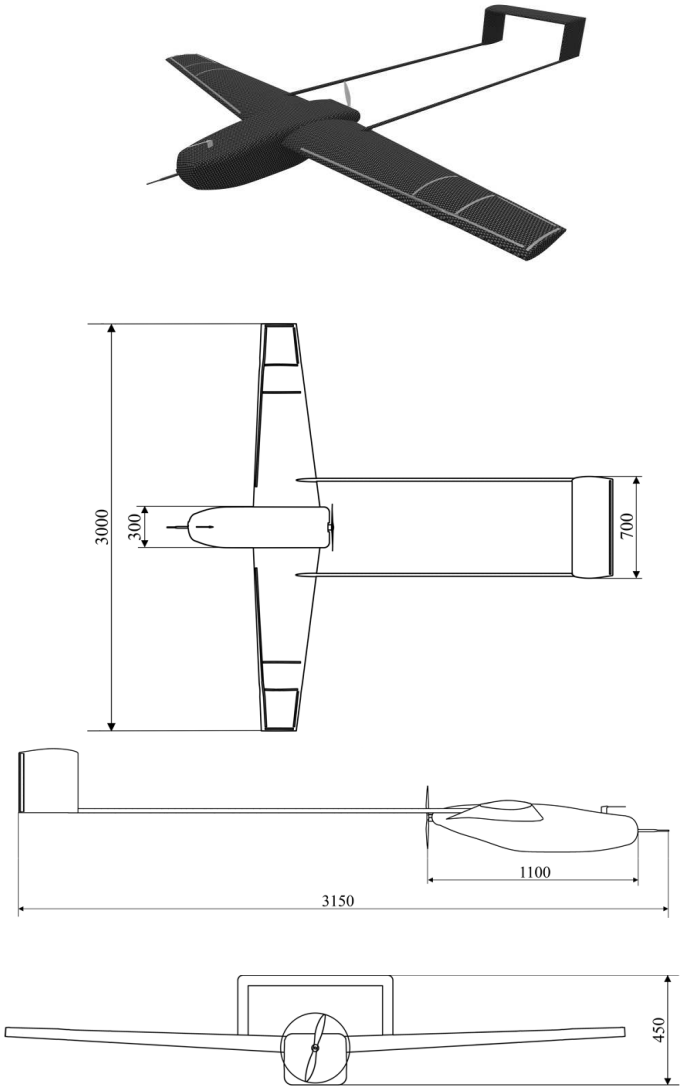

Figure 17.1: Overview of the designed plasma UAV

17.5 Detailed design

Introduction to plasma actuation

Plasma is one of the four fundamental states of matter, alongside solid, liquid and gas. It is the most energized state and although quite

unfamiliar, surrounds us all the time. Have you ever seen lighting, flames, stars or neon lights? Then you've seen plasma! The most straightforward way to produce plasma is by applying a high voltage across two electrodes, ionizing the air in between them. A dielectric layer between them makes sure that no spark can form and a cloud of plasma builds up, this is called a dielectric barrier discharge (DBD). When an alternating current (AC) is applied to this plasma actuator configuration shown in figure 17.2 the plasma can be sustained and settles on the dielectric barrier, like a glowing purple blanket.

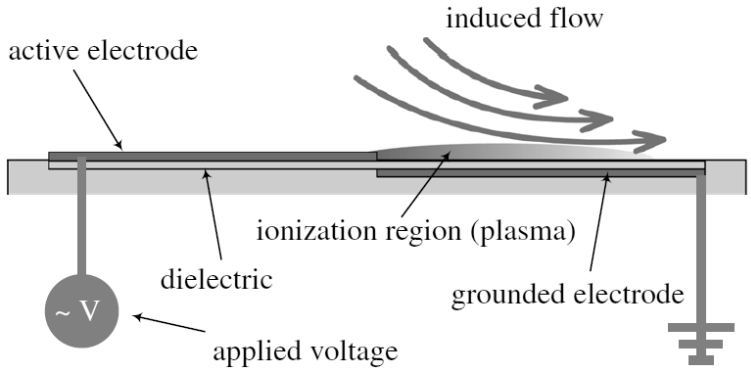

Figure 17.2: Configuration of the dielectric barrier discharge plasma actuator

But how can one steer an aircraft with plasma? The plasma cloud effectively accelerates the air in the boundary layer. This gives an on-demand control of the flow field that can be applied in various ways to change the lift produced by a wing or tail.

Plasma control mechanisms

Eight mechanisms were identified with which the plasma actuators could produce a change in lift over a wing profile (ΔCL). Conventional UAVs and other aircraft are steered by deflecting control surfaces, which produce a similar ΔCL. Eventually three of the eight mechanisms were applied to the Plasma UAV, after performing a trade-off. In the section control and stability the effect of the plasma actuators is actually quantified.

To be able to roll, pitch and yaw, the strongest mechanism was used. This 'circulation control' requires a blunt trailing edge of the wing, with the plasma actuator stuck on the back pointing downwards. When switched on, the actuator changes the whole flow and makes the wing produce a little more lift. If this lift is created asymmetrically around the centre of gravity, the UAV will start to roll, pitch or yaw.

The plasma mechanisms are not strong enough to pitch up with a plasma actuator on the tail, so a different mechanism had to be devised for this motion. The elimination of the wing tip vortices, or 'vortex control' proved to be a viable candidate for this. Plasma actuators placed in the direction of the flow, creating vortices on the wing tips. These vortices block the air that wants to flow over the wing tips from the high-pressure lower side of the wing to the low-pressure upper side. The induced ΔCL creates the desired pitch-up moment.

When performing a belly landing, the UAV has to fly as slow as possible, which requires a high angle of attack of the wing. At a certain angle, the air has such difficulty following the aerofoils' downwards curvature, that it separates and the wing stops producing lift. To guide the flow around the surface, standard high lift devices can be used like the slat systems on wings of conventional aircraft. In 'separation control', the third mechanism used on the UAV, a plasma actuator on the leading edge makes the air over the wing turbulent, increasing the resistance to separation and allowing the aircraft to fly at higher angles of attack.

Plasma control mechanism testing

In order to find out what effects plasma actuators have on the behaviour of an aerofoil, two mechanisms were tested in a wind tunnel. Separation control and circulation control were analysed, as they were most likely to succeed in controlling the UAV. The test was done in the M-tunnel at the TU Delft on a NACA63-618 cambered, sharp trailing edge aerofoil.

In the testing of the separation control mechanism, plasma actuators were proven to extend the lift production to higher angles of attack, up to about 22 degrees. This result shows the mechanism is fit to use as high lift devices, where low speeds, high angles of attack and high lift coefficients are needed. In the circulation control test, where the plasma actuator is installed on the trailing edge, a ΔCl is already achieved at an angle of attack of 2 degrees, and at rather high speeds. This makes circulation control ideal for yaw, pitch and roll control.

Control and stability

With effect of plasma actuators quantified, it is essential to assess the stability and controllability of the UAV. This is done using XFLR5. A 3D UAV model is built in XFLR5 with the fuselage modelled as a point mass. Firstly the stability is examined with static stability derivatives generated by XFLR5. When the UAV is statically stable, the dynamic stability can also be assessed with the eigenvalues. Furthermore, with the stability requirement, the tail size, tail length and the fuselage position can be determined.

For controllability, based on the geometry and weight, the software estimates the moment of inertia of the UAV, which is then used to calculate the control rates with Euler's rotation equation. The results are presented in Table 17.2.

Table 17.2: Control rates of the UAV

Control rates	Value [deg/s]
Pitch up	18
Pitch down	55
Roll	47
Yaw	36

As can be seen from the values in the table, the UAV is capable of performing normal manoeuvres, and the control rates are comparable with other UAV control rates.

To meet the stability requirements, the components in the fuselage are carefully arranged. Some component positions are fixed, e.g. the motor and propeller on the rear of the fuselage and the flight

controller near the centre of gravity of the UAV. Moreover, the payload should be placed in the rear of the fuselage. Taking these constraints into account, the components of the fuselage are arranged in a logical order.

Power

The power subsystem provides power to mainly four components: The flight controller, the electrical motor, the parachute and the plasma actuators. Because an electrical power system has to be fitted for plasma control, also an electrical propulsion system was chosen. The propulsion system consumes most of the power and therefore, to meet the endurance requirement, lithium-polymer batteries are used because of their high specific energy.

A brushless electrical motor in combination with a 16 inch carbon fibre propeller generates maximally 16.0 N thrust and 232 W of nett available power to overcome drag and to climb after take-off. The engine and propeller are mounted in the rear of the fuselage, between the booms to ensure ground clearance during landing.

The batteries have a DC signal with a voltage of 22.2 V. For plasma actuation, this DC signal has to be converted to AC, before being amplified to a high voltage of 34 kV (peak to peak). Automotive ignition coils, normally used to generate high voltage for spark plugs in internal combustion engines, are used to amplify the signal in the UAV. Switches between the DC to AC converter and the ignition coils, operated by the flight controller, are installed to activate different groups of plasma actuators. Since there are seven groups of plasma actuators, also seven switches and seven ignition coils have to be incorporated. Although these ignition coils are designed for low weight, at 175 g each they drive the mass of the high voltage system.

Regular control surfaces have variable deflection angles, whereas plasma actuators can only be turned on or off. To achieve variability in the effect of plasma actuators, the power signal to the plasma actuators is pulsed, where the flight controller controls the duty cycle of this pulsed signal.

Structures and materials

The final structural design of the UAV consists of the three main components. The largest one is the wing – tail assembly, which as the name suggests, consists of the wing and tail structures (PUR 35 kg/m^3 foam-core and TeXtreme 1027 carbon fibre skin) permanently bonded through hand-lamination to a carbon fibre tube. The other two components are fuselage components (both made with 1mm Airex C51 foam and TeXtreme 1027 carbon fibre sandwich). One large part (about three quarters of the fuselage surface) holds all the hardware. The smaller part can be removed to access this hardware. The fuselage is mounted to the wing through a rubber lined interface-fit. Structurally, the wing is the centre of the UAV since both the tail and fuselage transfer their loads to it, and the wing itself is subjected to the large aerodynamic loads.

An extreme flight condition load case was made, all the reaction forces and moments on the wing were evaluated to then compute the internal loads and determine whether the minimum amount of carbon fibre material was sufficiently strong to withstand the loads. From the analysis it was clear that the structure was capable of withstanding the flight loads with a 40% margin (composite failure is defined by an equation, and if the result is above 1, failure occurs. The maximum loading was 0.6, leaving a factor 0.4 as margin before failure).

Regarding impact, the fuselage is capable of withstanding a 2.5 g landing with a safety factor of 1.5, however due to the complexity of the UAV shape, it was not possible to assure that the booms in the wing would not shear out of the carbon skin if the tail were the first part to hit the ground.

17.6 Conclusion and recommendations

The plasma actuator controlled UAV carrying a 1.0 kg payload over a range of 10 km with an endurance of 2.0 h, is competitive in its class. By omitting moving control surfaces, the UAV responds faster and is more reliable than existing designs, reducing maintenance costs. The

UAV configuration is as follows: The fixed-wing monoplane is driven electrically by a 400 W propeller behind the fuselage, has a high wing configuration and high mounted H-tail connected by two booms. Energy is stored in 0.33 kWh lithium-ion polymer battery cells. The UAV takes off with a launcher and performs a belly landing or, in case of emergency, deploys a parachute. The UAV has a relatively large wing surface area, due to the low cruise speed necessary for effective plasma control. The resulting aircraft has a mass of 9.96 kg.

The UAV is controlled exclusively by plasma actuators, integrated on both the wing and empennage. Three flow control mechanisms are used to roll, pitch and yaw the aircraft. In order to quantify two of these control mechanisms, a wind tunnel test was conducted during the project. By combining the results of this wind tunnel test with literature on plasma actuator performance, the plasma control forces were determined and the control rates of the aircraft were calculated. These control rates were found to be comparable to those of similar UAVs with conventional control surfaces. The UAV can be flown with a remote controller or an autopilot with two-way telemetry.

All top-level requirements that were set at the start of the project were met. Nonetheless, improvement is considered in two fields: plasma actuation and structures. For example, the performance of a new dielectric layer could be investigated. This would consume slightly more power, but it is more durable. Moreover, a more extensive wind tunnel test is proposed to quantify the novel wing-tip mechanism and further examine the (electromagnetic) 3D interactions. Secondly, equal amounts of carbon fibre were used over the entire wing to ensure that the design does not fail. Employing a more advanced structural model can lead to a lower structural weight by reduction of foam and carbon fibre volume, which benefits the overall UAV performance.

18. SHAPE – Design of a CubeSat Attitude Determination and Control System for Very Low Earth Orbit Earth Observation

Students: T. de Boer, J. Brederveld, R. Diaz, R. Drost, D. Gerritzen, B. Kizavul, S. Rosanka, B. Stijnen, L. Wheeler

Project tutor: dr. ir. J. M. Kuiper

Coaches: dr. D. Gransden, ir. X. Mao

18.1 Background

Group S08 of this Design Synthesis Exercise is challenged by the customer with the following project objective.

"Design a Very Low Earth Orbit, VLEO, CubeSat to enable Earth Observation for a spatial resolution 4 m with 5 degree pointing accuracy (goal) at a maximum price of € 500,000 (goal)."

This chapter explains how this challenge was accomplished.

18.2 Introduction

In the last few years the need for low cost Earth-observation satellites has grown, providing new market opportunities for space companies. These opportunities can be divided into two main categories: high revisit time and high spatial resolution. The spatial resolution for this exercise is already pre-set, meaning a high revisit time can be a main goal.

The fact that the satellite will be positioned in a Very Low Earth Orbit presents a major challenge. VLEO present many design difficulties due to the nature of the atmosphere at this altitude. The atmosphere is affected by solar and magnetic flux ensuring that the temperature and density fluctuate significantly. In combination with the free molecular flow, the fluctuations demand a complex model to predict disturbances.

Therefore, SHAPE, a Stable and Highly Accurate Pointing Earth-imager, is an exceptionally stable satellite in a VLEO in these harsh conditions, which provides a high accuracy for high-resolution Earth imagery. In order to achieve a high level of stability, SHAPE makes use of a momentum wheel and the principle of conservation of angular momentum. The momentum wheel is integrated into the design of two conventional 3-Unit CubeSats. The rotational speed of the wheel is 7000 rpm to ensure its momentum counters the torque of the external disturbances caused by the atmosphere.

It is important to note that a single SHAPE cannot be used to compete in the market of high revisit time for a low-cost satellite. However, a constellation of SHAPEs provides an option that will allow for a higher revisit time. Another bonus to a constellation is that the more units ordered, the lower the unit cost becomes but total cost of the constellation increases.

18.3 Requirements

For this design, a few main requirements were given by the customer. These were derived from the mission objective.

Table 18.1: List of the key requirements

Requirement	Value
Spatial resolution	4 m
Pointing accuracy	5 °
Operational orbit	230-380 km
Unit cost	< € 500,000
Mission Lifetime	> 90 days

18.4 Environment

As previously mentioned, the satellite will be orbiting Earth in a low altitude range of 230 to 350 km. In such a low orbit, the thermosphere plays an important role. The thermosphere contains a low density of molecules, which affects the satellite in many ways. Firstly, the molecular temperature at the thermosphere is relatively high, with a value of 900 K to 1600 K. However, it is important to keep in mind that this represents the energy state of a single molecule, and therefore the ambient temperature is much lower due to a low density. Also, the density changes throughout the thermosphere are significant, sometimes by an order of ten. This is mainly due to solar and magnetic flux.

Furthermore, pressure is related to temperature and density, meaning any changes in density also affects the pressure in the same manner. Knowing all these changes in the thermosphere, it is possible to model the flow. The temperature and densities were calculated by means of the NRLMSISE-00 model. Combining this model with the Sentman equations, it was possible to calculate the lift and drag coefficients of

each panel of the CubeSat. Adding the normalised values results in the total lift and drag coefficients, from which the total drag was found.

18.5 Conceptual design

From the requirements that were given and derived, possible concepts were designed. Many out-of-the-box solutions were neglected due to their infeasibility. However, a list of possible solutions was made. Since the focus was on altitude determination and attitude control, these concepts were recorded in table 18.2.

Table 18.2: List of all concept choices

Attitude Determination	Attitude Control
Baseline	Spin Stabilisation
Sentinel	3-axis Control
Imaging	Gravity Gradient

Firstly, the concepts for attitude determination consisted of the baseline, the Sentinel and lastly, the image determination solution. The baseline solution comprises of using two sensors with a large separation distance in between them, which could receive GPS or Radar in order to determine the position and attitude. The Sentinel concept uses external images to determine the satellite's position when in the field of view of another satellite's camera, for instance, of the Sentinel satellites. The image determination method would compare the location of a landmark captured in an image with the desired position of this object in this image determined beforehand.

Secondly, the chosen concepts for the attitude control consisted of the spin stabilisation, 3-axis control and gravity gradient. The latter uses the gravitational field of the Earth in its favour to ensure that the satellite always has the same side pointing to the Earth. This is done by moving the centre of gravity of the spacecraft. Spin stabilisation ensures stability by initialising a spin, which uses the principle of

momentum conservation to ensure small disturbances can be counteracted. 3-axis stabilisation uses actuators, such as thrusters, reaction or momentum wheels. This assures stabilisation along all axes.

Finally, from these trade-offs, the 3-axis design suggested to be the best choice for this mission, followed by spin stabilisation. However, the power consumption of 3-axis control is significantly higher than for spin stabilisation. Therefore, spinning was the preferred choice. Nevertheless, spin stabilisation only allows control along two axes, meaning another external means of control was needed. Hence, the choice of using dual spin, which consists of a satellite using the spinning and 3-axis control simultaneously, was proposed. This was the first major step towards the final design.

At the time of the conceptual design phase, the group had to design more concepts that focused on dual spinning. The first of the iterations consisted of a 3-unit CubeSat where the last cube spins for stabilisation. This seemed as a promising concept, however, it would not have provided enough stability for imagery. A second design, consisting of a T-shape, where the horizontal part of the T turned on its axis. This seemed promising until further research proved that it was over-designed. Since the spinning would stabilise the pitch angle, extra means of changing this stabilised pitch angle was required, in order to keep the T-shape pointed towards the Earth. The third concept of having two 3-unit CubeSats placed in parallel was examined. In this case, one of the cubes would be spinning for stabilisation. However, as indicated before, this concept was not stable enough. The final design required a different method of spin stabilisation and therefore, the solution will be described in the next section.

18.6 Final design

The final design uses the spinning concept in combination with a 3-axis stabilisation system. However, there is a slight difference with the previous concepts. The spinning stabilisation is provided by a large

momentum wheel placed between two 3-unit CubeSats, as seen in figure 18.1. This wheel provides stability on two axes, namely the nadir and cross track axis by using the principle of momentum conservation. By using a large enough momentum, the disturbances of the environment can be overcome.

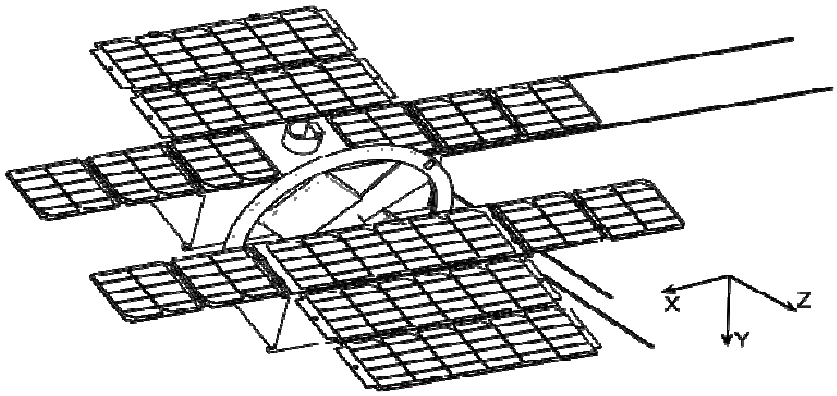

Figure 18.1: SHAPE Final Design

Payload

During the first iteration, the ANT-2A camera was chosen, since the spatial resolution of 4 m was possible at an altitude of 288 km. However, this lead to a life time of roughly ten days, which is not an attractive mission lifetime. Therefore, the ANT-2A was used as a base to get a better design that was optimised for spatial resolution. This resulted in a design offering the required resolution at an altitude of 350 km, which was designed by D. Dolkens. This increased the lifetime to approximately 200 days. This was achieved by using an off-axis modified Ritchey-Chretien Telescope in combination with two corrective lenses, which enables a compact design solution.

When considering the stability required by the satellite platform to ensure picture quality, it was calculated that a pointing accuracy of 1.3° is necessary with this payload design. Therefore, the requirement for the pointing accuracy, in consultation with the customer, was redefined from 5 to 1.3°.

Momentum wheel

Once the payload was chosen, it was important to consider how to stabilise the spacecraft. The momentum wheel plays the most important role in the control and therefore it had to be sized properly. The wheel had to provide enough momentum to counteract any disturbance torques induced by external means. Therefore, the forces from the environmental analysis were combined to calculate the required momentum. Many possible combinations of mass and rotational speed were examined. After many iterations, the optimal solution when considering the mass and size of the wheel, is shown in table 18.3.

Table 18.3: Sizing values of the momentum wheel

Variable	Value
Momentum	0.014 Nms
Mass	0.469 kg
Outer Radius	0.15 m
Inner Radius	0.13 m
Thickness	0.01 m
Spinning Speed	7,000 rpm

Attitude determination and control

There will be three main phases for this satellite, mainly the detumbling, solar and eclipse phase. For the last two, the momentum wheel will provide stability. However, the detumbling phase requires additional control, since in this phase, the wheel is stationary. Considering the conditions, 3-axis appeared to be the best solution, as the satellite will have rotation along all three axes during the detumbling. Therefore, appropriate sensors and actuators are needed. After many design iterations, the final ADCS design consists of six coarse sun sensors, used mainly during detumbling, a fine sun sensor, and a horizon sensor in order to have more accurate measurements during the mission of SHAPE. Additionally, an inertia board was

chosen for extra sensors. Actuation is provided by the four reaction wheels and three magnetic torquers. In order to determine the orbital position and velocity, a GPS sensor is used. Satellite to satellite tracking can be enabled in order to provide location data up to centimetre level accuracy.

Bearings

To allow the momentum wheel to spin freely, without vibrations, an innovative bearing design has been proposed. A magnetic bearing is incorporated, since less vibrations will be induced on the satellite. Also, the friction is negligible, no lubrication is needed and there is no wear. Magnetic bearings can be split up into passive, active and electrodynamic. For this design, an electrodynamic bearing is chosen. This bearing achieves its accuracy once the wheel is spinning at 5,000 rpm. These have the advantages of 3-axis stabilisation, compared to the conventional 2-axis magnetic bearings. Since the wheel does not have an initial spin of 5,000 rpm, ball bearings are needed to ensure smooth rotation until this angular velocity is achieved. The angular velocity, for which the satellite is designed, is 7,000 rpm. This is done to increase the stiffness and to ensure that the minimum velocity of 5,000 rpm still occurs at the end of the mission life-time.

Propulsion

Since the mission life is expected to be of 200 days, propulsion for orbital maintenance is not required. Therefore, the propulsion is only needed to spin up the momentum wheel to 7,000 rpm. For this, it was decided to use two MEMS Resistojet thrusters, designed by the TU Delft, which were incorporated into the momentum wheel. Each thruster will be connected to a tank of bio-ethanol. The two tanks are interconnected to provide redundancy in case of a single fuel line failure. By using this combination, the momentum wheel can be spun up to 7,000 rpm in less than 40 hours, which can only be done once, since the propulsion system is a blowdown system.

Command and data handling

Once the payload is stable, it will be functioning during the solar part of the orbit where a large amount of data, approximately 33.8 GB per

orbit, must be processed. The on board computer has enough storage space for 100 GB of data, which is roughly 16 orbits, or one mission day. The command and data handling system also controls the communications between subsystems, such as the ADCS and propulsion. Therefore, three main connections are used, which are the I2C, high speed and Radio Frequency connections.

Telemetry, tracking and control

Once all the data has been processed and stored, it must be sent to the ground stations for further processing. To do this, the information must be sent within a contact time of 9.4 minutes per ground station. After a few design iterations, an X-band transmitter was chosen in combination with a micro strip patch antenna. This allows a data rate of 50 Mb/s. The telemetry, tracking and control subsystem must also receive commands from the ground stations and be able to send system statuses of each subsystem. Therefore, another antenna system is needed. A transceiver was chosen that could work in both Very High Frequency and Ultra High Frequency. This was chosen in combination with four monopole antennae which allows for a download and uplink of 9,600 and 1,200 b/s, respectively.

Power

The imaging phase requires a power of 10.68 Wh whereas the eclipse needs a lower power, namely 5.5 Wh. Therefore, to provide sufficient power, 25 solar panels were used. This in combination with a main battery, provides the power requirement for one orbit multiple times. This enables the power subsystem to counteract less power generation in one orbit as well as enough power for a safe mode. While sizing the battery, a pre-mission phase was also taken into account which mainly covers the detumbling phase and the boot-up of all subsystems. Due to the fact that a slip ring could not be installed in the momentum wheel to provide power to the propulsion subsystems, an additional battery was installed in the momentum wheel. This battery provides enough power for the thrusters of the propulsion subsystem.

Structure

All of the above systems must be placed within the structure. Therefore, in terms of the structure of the satellite, it is important to take into account the loads that occur during the launch. In most space applications, the launch phase is the most critical phase. For that reason, the satellite has to be attached to the launch fairing in a certain way in order to minimise the risk of failure. For SHAPE, a configuration where one end is free and the other end is clamped is chosen. This allows the satellite to be able to withstand the loads during launch and also reduces the risk of failure during deployment, which could occur if both ends were clamped. Furthermore, a vibrational analysis was performed, from which can be concluded that the natural frequencies, where the resonance phenomenon can occur, are avoided. The calculations for the natural frequencies were done with the use of a simplified analytical model, which was then confirmed by a numerical model.

Thermal

Once the structure provides enough support for all the subsystems, it is important to ensure that the temperature of the satellite is kept within the operation range. In order to make sure every subsystems is able to function, the temperature should be kept between -10 and 30°C. The thermal properties of each part of the skin throughout the CubeSat were analysed by creating a model. This model incorporates all incoming and outgoing radiation, calculating the temperature range of the skin panels throughout the orbit. This was then used to tailor the panels with appropriate material, which were mainly control paints and coatings on the external surface of the panels. The external thermal control materials were white paint and aluminised Kapton. Additionally, MLI insulation was considered for areas surrounding critical components, such as the payload.

18.7 Conclusion

In conclusion, SHAPE is a platform designed to withstand the instabilities commonly experienced by other satellites at Very Low Earth Orbits, with a goal of improving the effectiveness of the satellite

for high-resolution Earth imagery. A momentum wheel at the centre of the design plays the main role in stabilising the platform using a simple, trusted, reliable and efficient method.

18.8 Further recommendations

Now that this project has come to an end, it is important to note some of our recommendations that future engineers could consider:

- Further investigate solar panel deployment with a risk analysis.
- Consider constellation applications.
- Further improve the aerodynamic efficiency of the CubeSat by changing the location of the momentum wheel.
- Apply a MAD-configuration for the Sun-sensors.
- Make the mirror moveable in order to increase the pointing accuracy.
- If a launch at 500 km should be used, investigate an aerobrake in order to decrease the altitude faster so the mission can begin earlier.
- If a launch at 500 km should be used, investigate the use of a more efficient battery.

19. THE HUULC: DESIGN OF A HYDROGEN-POWERED UNMANNED ULTRA LARGE CARGO AIRCRAFT

Students: T.Q.M.B. Clar, J.I.C. Dierickx, K. Eken, M. de Feber, M. Gillis, D. Korovilas, J.M. Neuman, J. Stoof, R. Suárez Millán, R.A. Viet

Project tutor: dr.ir. G. La Rocca

Coaches: dr.ir. H.G.D. Visser, prof.dr. C. Wang

19.1 Introduction

'Why compromise speed for price?' - a question often faced by the modern consumer in today's globalized market. Currently over 90% of long-distance goods are transported by sea, an inexpensive but slow solution. Air transport, on the other hand, is fast, reliable and flexible but is often prohibitively expensive. The best-of-both-worlds scenario - next-day delivery at a low price - is a concept consumers may only dream of. On top of not offering a simultaneously fast and inexpensive service, both modes of transport contribute significantly to global environmental pollution. A solution to these 21st century problems is needed, to give consumers fast, inexpensive but environmentally-friendly transportation of their goods. The authors believe this solution is embodied in the HUULC - a hydrogen-powered, unmanned, ultra-large cargo aircraft, capable of transporting 100 maritime TEU containers.

19.2 Mission objectives and requirements

The HUULC program's mission statement is formulated as follows:

"Team HUULC will design the HUULC, a freighter aircraft that will pioneer in sustainable high capacity air transport, competitive with maritime cargo shipping from 2030 onwards"

To accomplish the mission objective, multiple requirements are given by the customer. The design of the HUULC is based on the set of top level requirements provided in table 19.1.

Table 19.1: Customer top level requirements

Requirement	Value
Freight Rate	250% of container ship freight rate ($1,150 per TEU for the far-east to North-Europe maritime connection)
Payload	1,200 metric tonnes
Cargo bay capacity	100 lightweight TEUs (20ft airlift containers)
Fuel	Cryogenic hydrogen
Range	6,000 kilometres/3,250 nautical miles at max payload
Cruise altitude	5,000 - 8,000 meters (to limit contrail formation)
Configuration concepts	Only wing-lifting concepts
Crew	No crew and crew support systems
Pressurization	No pressurization
Entry into service	2030
Development technologies	Existing or currently emerging technologies

19.3 Business model

Freight transport is a global business, characterised by an enormous, fiercely competitive market. It is thus imperative to correctly pinpoint the position of the HUULC within this market in order to maximize its impact.

Air cargo's small market share of 1% by mass, resulting from its high freight rates, does not provide favourable conditions for the introduction of an ultra large cargo aircraft in the air cargo market, particularly when the market suffers from chronic overcapacity. Containership on the other hand, has a 14% market share by mass and has the highest growth rate of all transport modes, providing a window of opportunity for market capture through innovation.

By positioning the HUULC aircraft as a direct competitor to maritime containership with a freight rate comparable to shipping, it is expected that a portion of the low-value goods traditionally transported by ship will opt to pay slightly more for a service which is 30 times faster. In parallel to competing with maritime shipping, the HUULC is still a freighter aircraft with a much lower freight rate than typical air cargo services, hence demand is also expected from high-value, air cargo goods. This results in maritime container transport as the primary target market of the HUULC program, whilst air cargo being the secondary target market.

19.4 Network and airports

The network chosen for the HUULC crosses three major trade routes and serves four major trade regions, namely the Yangtze River Delta region, Western Europe, South-East United States of America and the United Arab Emirates. The maximum estimated market share in total amount of transported TEU containers is 1.16%. Two hubs are chosen, both as refuelling and distribution connections, in the region of central Russia and Alaska. An impression of the network can be found in figure 19.1. In total, 325 HUULC aircraft will be produced, with an operative availability of 85%.

Figure 19.1: The global network of the HUULC program

Due to its 200 meter wingspan, existing airports cannot accommodate the HUULC aircraft. At the same time, existing airports are congested and charge high fees, resulting in a hiked freight rate. To avoid these issues, six new dedicated global airports have been developed, near the cities of Shanghai, Terneuzen, Memphis, Dubai, Novosibirsk and Anchorage. The estimated cost of building and operating these airports is $19.2 billion US dollars, far less than the costs the program would incur from the use of existing airports. As an example, the design of the airport to be built near Terneuzen can be found in figure 19.2.

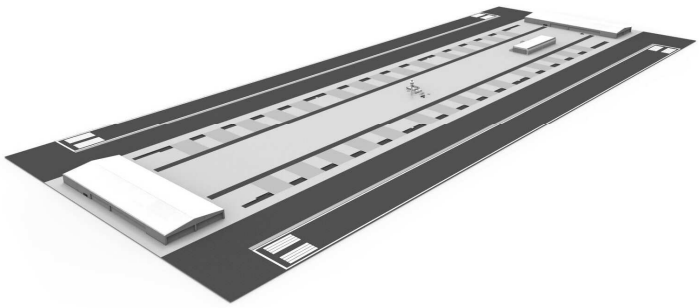

Figure 19.2: The design of the HUULC airport near Terneuzen

19.5 Configuration concepts and trade-off

A total of four different conceptual configuration concepts and one variant have been investigated. A trade-off was performed based on a list of criteria that best comply with the HUULC mission requirements and constraints. The four configurations included a conventional configuration, attractive due to its design maturity, a joined wing configuration, attractive due to its high aerodynamic efficiency, a twin boom concept, attractive due to its structural efficiency and parallel loading in both fuselages and a blended wing body (BWB), attractive due to its high aerodynamic efficiency and increased fuel efficiency. A flat-nose variant to the BWB was developed, known as the Burnelli variant, to improve payload handling and to provide a more streamlined payload bay shape. Sketches of the configuration concepts are found in figure 19.3.

To perform the conceptual design trade-off, a total of 16 design criteria most relevant to the HUULC mission were defined. The most important criteria included: development cost, operational cost, design risk, safety, payload handling, maintenance, sustainability, aerodynamic and structural efficiency. The concept configuration which won the trade-off was the BWB Burnelli variant, mainly due to its superior aerodynamic and structural efficiency, better payload handling qualities and sustainable aspect.

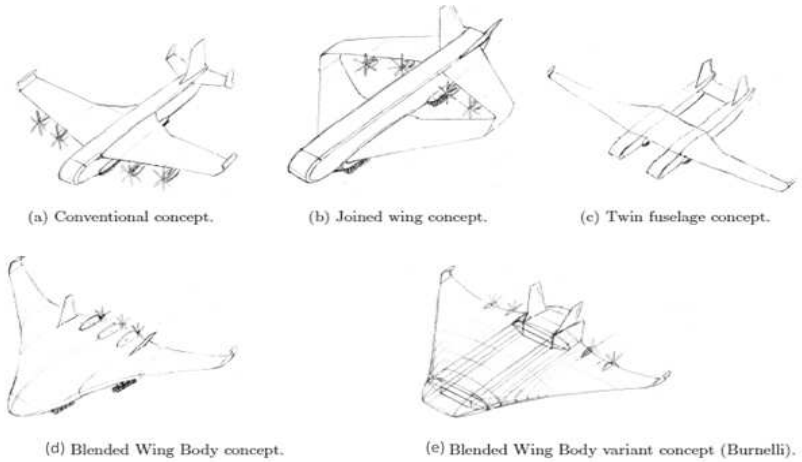

Figure 19.3: Four initial configurations and one variant

19.6 Aerodynamic planform design

The aim of the aerodynamic model is to create a planform design which complies with the maximum required lift coefficient of 1.60 during cruise and 1.75 during landing. Also, a lift-to-drag ratio of 26 is required for the fuel efficiency of the HUULC. To comply with the design of the BWB Burnelli, a flat nose in combination with a flying wing was designed. The BWB Burnelli concept shown in section 19.5 has such a large wing that the surface area is too large and the drag will increase to such a level that the lift over drag ratio would never be met. Therefore, it is chosen to increase the wingspan of the HUULC while keeping the area constant. As a result, the lift requirement was met and the lift over drag ratio increased to a value of 28.3. During cruise, a lift coefficient of 0.62 is reached at an angle of attack of three degrees. Four different NACA aerofoils are chosen in the form of the NACA 2415 for the fuselage, the NACA 2420 and NACA 2422 for the fairing and the NACA 2424 for the wing. An impression can be found in figure 19.4. The most important parameters of the aircraft are as follows:

Table 19.2: HUULC Main characteristics

Wingspan	200 m	Aspect ratio	5.58
Fuselage length	100 m	Taper ratio	10
Fuselage width	25 m	$C_{L_{cruise}}$	0.62 @ 3 deg. A.o.A
Surface area	7175 m^2	$\left(\frac{L}{D}\right)_{cruise}$	28.3

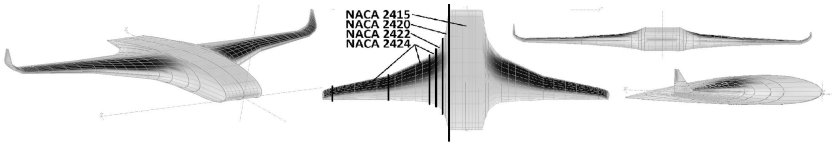

Figure 19.4 - Final aerodynamic planform

To comply with the landing requirements, a single slotted flap system was chosen. This resulted in the required increase in lift coefficient of 0.15. The wetted area for the flaps is estimated to be 1,700 m^2.

19.7 Final design

The HUULC is the largest aircraft ever designed in history. It can lift 1,200 tons of payload off the ground, dwarfing the 253 tons of payload transported by the world's current largest aircraft, the Antonov An-225. Due to its sheer size and the radical new technologies used in its development, the HUULC design has brought innovative thinking to a new level.

Propulsion system

With a total required power of 316 MW, equivalent to the power of 10 Airbus A400M aircraft, designing the propulsion system of the HUULC required innovative technologies. To meet this high power requirement without the need for an unrealistic number of engines, a propfan engine has been designed, with two contra-rotating shafts, consisting of eight blades per shaft. A total of eight engines are positioned on the leading edge of the wings, each engine having a propeller diameter of 10.05 meters and a net power output of 39,664kW.

Structural characteristics

The HUULC has a span of 200 meters and a length of 100 meters, surpassing the dimensions of any other aircraft. Furthermore, the aircraft is a blended wing body for which a small amount of preliminary sizing documentation was available. As a result of these challenges, the structural sizing of the HUULC was an important aspect of the design. The internal structure of the aircraft is subdivided into a wing box and a fuselage box structure, comprising of standard aircraft structural components including stringers, plates and ribs. By simulation, nonlinear and multivariable global optimization functions have been used to reduce the internal structure as much as possible and still comply with the loads present on the

airframe. Figure 19.5 shows the resulting internal structure of the HUULC, made of Aluminium 7075 T6.

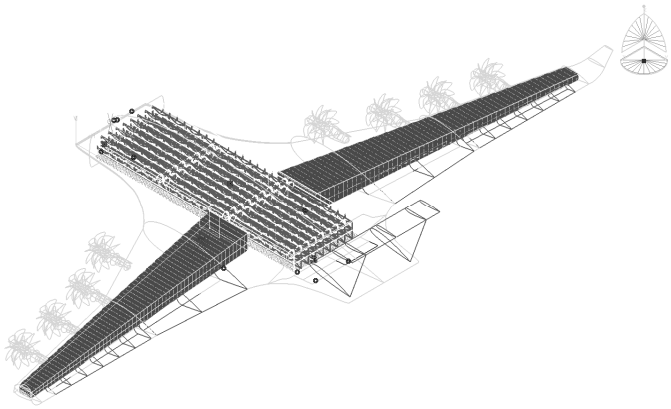

Figure 19.5: The internal structure of the HUULC

Unmanned operations

The absence of a flight crew on the HUULC has several implications on the design of the aircraft. Pressurisation systems, which generally decrease the fatigue limit of the aircraft and thus its lifetime, are no longer necessary. Control system interfaces are not present in the HUULC but rather in a specially designed Ground Control Station. This enables weight saving, but these are partially compromised by the added communication systems. The presence of cut-outs such as doors and windows is also unnecessary, which improves the structural integrity of the aircraft and allows for a weight reduction.

The unmanned operations are performed autonomously for most phases. Critical phases such as take-off will be remotely piloted. A direct C2 link is used for the critical phases, whereas a SATCOM link is used to transmit important flight state information to the Ground Control Station during cruise.

With the majority of applications being military, unmanned aircraft have yet to persuade public opinion on their safety in commercial aviation. However, the authors strongly believe that there is no better way to break this taboo, than by introducing a non-passenger aircraft

into the market, to pave the way for the automation of most or all civil aviation.

Payload (un)loading system - CargoFlo

Minimizing turnaround time is essential to maximize profit. To ensure each HUULC is on the ground for as little time as possible, a new and innovative logistics architecture called CargoFlo has been designed to load and unload aircraft as fast as possible. Automated guided vehicles will work together to load departing TEUs from the nose, whilst simultaneously unload arriving TEUs from a hatch near the tail. A schematic of the CargoFlo architecture is shown in figure 19.6. This architecture has been synergized with the roads in the purpose-built airports, to ensure cargo is transferred to and from cargo hangars as fast as possible.

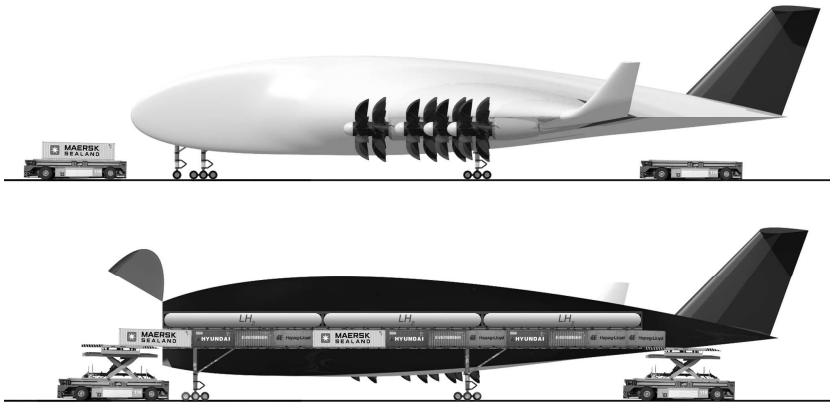

Figure 19.6: Simultaneous (un)loading using the CargoFlo architecture

19.8 Hydrogen strategy

Sustainable aviation is the future of mankind. Liquid hydrogen produced through renewable energy resources is key in reaching the goal of carbon free aerial transport. Nowadays, using hydrogen comes with higher cost than using conventional fossil fuels, which is one of the main reasons why hydrogen is not widely used in aviation yet. Due to ever diminishing fossil fuel reserves and increases in hydrogen production technology maturity, it is expected that within the next

twenty years the production price of liquid hydrogen will come down to equal the production price of kerosene, after which it will drop even further. Considering the combination of environmentally and climatically clean transport at low prices makes it the obvious choice to fuel the HUULC program.

The sustainable hydrogen production process for the HUULC program is illustrated in figure 19.7. It requires investments for the construction of renewable energy generation facilities, electrolysis & liquefaction plants and storage tanks.

During the peak years of the HUULC program (2050-2075) the six airports combined need to have the capacity to generate and store 36.6 million kilograms of liquid hydrogen every day. To ensure the HUULC fleet can be fully operational, a hydrogen strategy has been defined including the construction of four wind turbine parks, one solar pv park and the upgrade of a hydroelectric plant. The advantage of using hydrogen propellant is considerable as carbon emissions are eliminated and through a lowered cruise altitude NO_x emissions are minimal compared to current day aviation. The elimination of carbon emissions saves the planet from almost 7,700 gigatonnes of harmful greenhouse gasses, almost twice as much as the European union emitted in 2013.

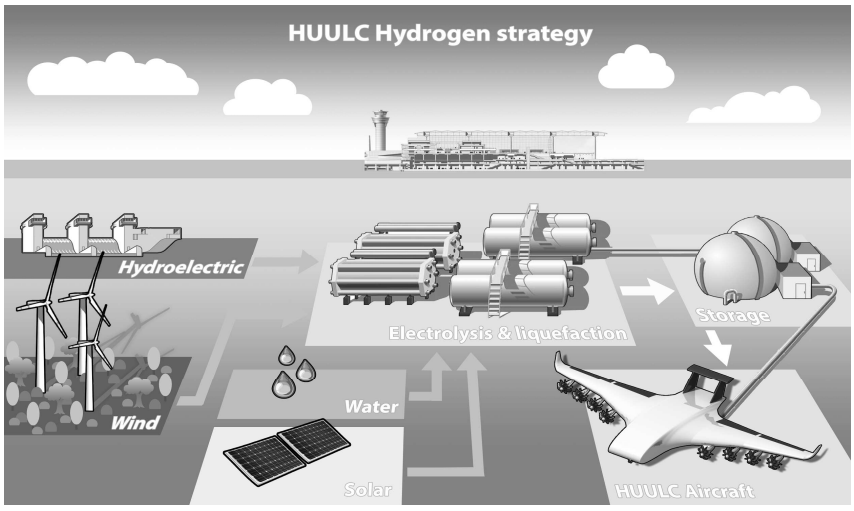

Figure 19.7: A visual overview of the HUULC hydrogen strategy

19.9 Cost analysis

The cost breakdown of each aircraft is given in table 19.3, with airport costs included in operations costs. Each HUULC costs $761.2 million to produce - twice as much as an Airbus A380 Freighter, for eight times the payload capacity. Over the entire program life of 65 years, a total program budget of $905.4 billion arises, with a total program cost of $876.3 billion, leaving a total program budget surplus of $29.1 billion.

Table 19.3: Cost breakdown per HUULC aircraft, including airport costs

Lifecycle phase	Budget [M$]	Estimated costs [M$]	Budget surplus [M$]
R&D and production	780.0	761.2	18.8
Initial spares	8.4	4.8	3.6
Operations & maintenance	1,866.5	1,861.5	5.0
System phase-out & disposal	55.7	25.5	30.2
Total per unit	2,710.6	2,653.0	57.6

19.10 Conclusions

A solution for the question 'Why compromise speed for price?' is found in the form of the HUULC, a hydrogen-powered, unmanned, ultra-large cargo aircraft, capable of transporting 100 maritime TEU containers - a payload weight of 1,200 tons respectively. An analysis in the business model turned out that maritime container transport is the primary target market of the HUULC program, whilst air cargo being the secondary target market. The network chosen for the HUULC crosses three major trade routes and serves four major trade regions, namely the Yangtze River Delta region, Western Europe, South-East United States of America and the United Arab Emirates, including two refuelling hubs in central Russia and Alaska.

The concept configuration chosen for the HUULC is the BWB Burnelli variant, mainly due to its superior aerodynamic and structural efficiency, better payload handling qualities and sustainable aspect. An aerodynamic model is built in order to achieve a lift coefficient of 0.62 at an angle of attack of three degrees and a lift over drag ratio of 28.3. For the propulsion of the HUULC, a propfan engine has been designed, with two contra-rotating shafts each. In total, eight engines will be placed on the leading edge of the wings. To ensure each HUULC is on the ground for as little time as possible, a new and innovative logistics architecture called CargoFlo has been designed to load and unload aircraft as fast as possible.

During the peak years of the HUULC program (2050-2075) the six airports combined need to have the capacity to generate and store 36.6 million kilograms of liquid hydrogen every day. To ensure the HUULC fleet can be fully operational, a hydrogen strategy has been defined including the construction of four wind turbine parks, one solar pv park and the upgrade of a hydroelectric plant. The cost analysis led to the fact that each HUULC costs $761.2 million to produce - twice as much as an Airbus A380 Freighter, for eight times the payload capacity. Over the entire program life of 65 years, a total program budget of $905.4 billion arises, with a total program cost of $876.3 billion, leaving a total program budget surplus of $29.1 billion.

19.11 Recommendations

To improve the design, a second and third class sizing has to be made. Also, for the aerodynamic model, a more professional CFD tool should be used in order to correctly predict the interacting vortices. To improve the structural sizing, a finite element method should be used in order to predict the forces, stresses and flows even better. To maintain the profitability of the HUULC project, the business model and cost analysis should constantly be updated over time in order to anticipate unexpected changes in the targeted markets and the program itself.

20. MOONRAKER-DRAX: NEXT STOP EUROPA

Students: V. van den Bercken, S. Burger, N.M. Dekkers, J.M. Hoogvliet, A.V. Kassem, R. Kok, T.A.H. Kranen, G.P. van Marrewijk, F.T. Melman, B. Mulder

Project tutor: dr.ir. E. Mooij

Coaches: ir. F. Esrail, ir. S. Woicke

20.1 Introduction

Europa, one of Jupiter's icy satellites, shows promising conditions for possible extra-terrestrial life in the Solar System. It may hide life in the ocean beneath its icy crust. This icy crust can protect organisms from Jupiter's radiation belts. Europa, discovered four hundred years ago by Galileo Galilei, is even believed to be internally active.

The first spacecraft to visit the Jovian system was the Pioneer 10 in 1973, followed by Pioneer 11 one year later. These spacecraft were the first to take close-up pictures and measurements inside the Jovian system. The Voyager was the first to discover the icy exterior of Europa in 1979. In 1995 the Galileo spacecraft was the first to enter into an orbit in the Jovian system, making close approaches to Callisto, Ganymede, Io, and Europa. It discovered possible liquid water beneath Europa's icy exterior.

20.2 Mission need and objectives

A team of 10 TU Delft students of Aerospace Engineering conducted a feasibility study for a mission to Europa. This mission needs to be capable of achieving the science objectives, which are described below. The primary requirements for this mission are the following: the measurement duration shall be 3 months, with a launch no later than September 2025 and a total mission cost of maximum 2.5B EUR. Any exposure to hazardous materials shall be avoided for all personnel involved and mission success shall be larger than 95% (excluding launch). COSPAR regulations, the regulations of exploring extra-terrestrial bodies, should be adhered to for Europa, which also requires that a clear end-of-life strategy should be included in the design.

The need statement is defined as follows:

"The scientific community wants to analyse the ice layer and the subsurface ocean on Europa to establish the conditions for possible life."

Following the need statement, the mission statement is defined as:

"A team of 10 aerospace engineering students from Delft University of Technology will conduct a feasibility study for a space mission to analyse the ice layer and the subsurface ocean on Europa to establish the conditions for possible life, which is to be launched no later than 2025 and will not exceed a total cost of 2.5B EUR."

20.3 Objectives

Investigating Europa's habitability includes investigating the presence of any water within and beneath Europa's icy shell, investigating the chemistry of the surface and ocean, and evaluating geological processes that might produce the chemical energy needed for life. Also important is to characterize the nature of the exchange of material between the ocean and the surface ice. To achieve this goal, the following objectives are established:

Composition

- Characterize surface and sub-surface (organic) chemistry, analysing both endogenic, and exogenic processes, which affect the composition.

Ocean and ice shell

- Determine the thickness and salinity of Europa's ocean
- Determine the thickness of Europa's ice layer and any water regions within it
- Locate regions of heterogeneity
- Establish seismic activity and its variation over the tidal cycle.

Geology

- Identify processes that exchange material between the surface and sub-surface
- Identify the processes and rates by which the surface forms and evolves
- Characterize the physical environment of the near-surface and sub-surface region.

Geophysics

- Determine the internal structure of Europa and its dynamics.

20.4 Concept description

After conferring with the customer the team discovered that a stand-alone mission would not be feasible for ESA in terms of launch date and financial resources. For this reason the design team opted for a piggyback mission, an addition to a NASA Europa multiple flyby mission (formerly called Europa Clipper). The main reason for designing a piggyback mission is to reduce cost. This reduction is achieved by sharing the same launcher, as well as sharing knowledge and resources.

From the midterm review onwards, three different piggyback concepts were analysed. These include a single lander, a single orbiter and a combined orbiter/lander. The customer suggested to investigate if a piggyback mission would be feasible for a mass of 350 kg, even though this was not a strict requirement from NASA.

Single lander

Firstly, the single lander was analysed. This would be a hard lander, since a soft lander would be simply too heavy. The hard lander will be a penetrator, which will impact the surface of Europa at a speed of around 300 m/s. The penetrator will then bury itself between 0.3 and 3.0 m into the ice. However, with respect to telecommunications, the single penetrator was found to be infeasible without changing Clippers trajectory. Clipper will encounter Europa only once every fourteen days. Taking into account the limited lifetime of a penetrator, which is two weeks, all data has to be sent within one flyby. This would mean that almost no scientific data could be sent back to Earth, so this would be a high-risk mission.

Orbiter and lander

To improve the communication link between the penetrator and Earth, a relay orbiter could be taken on-board Clipper. The main function of this orbiter will be gathering the data from the penetrator and relaying these data back to Earth. The orbiter will also be provided with an imaging package, which includes a laser altimeter to increase the scientific value of the orbiter. More instruments could lead to an increase in the mass, as well as the power required, which would again result in an increase of mass. The number of images is limited by the maximum data rate, which can be achieved. This combination, in each possible way, violates the mass constraint of 350 kg significantly. The orbiter/lander combination investigated in this report has a total wet mass of 750 kg.

Single orbiter

A single orbiter was also investigated, but the mass of this orbiter was in the same order of magnitude as for the combination. Furthermore, the scientific return for this concept for this mass will be lower than for an orbiter/lander combination, as no in-situ measurements can be performed. A single orbiter can therefore never fulfil the scientific requirements that drive the investigation on the conditions for life on Europa. The single orbiter mass is high, because orbiter instruments generally consume a significant amount of power and require a high

data rate, leading to heavy subsystems. Therefore, the orbiter/lander concept was designed in detail in this report.

20.5 Mission description

As mentioned above, a piggyback orbiter penetrator was decided upon after the trade-off. The mission developed is named Moonraker-Drax and will be a piggyback orbiter/lander mission attached to the Europa Clipper. The name of this piggyback mission will be related to its fellow traveller, the Clipper. Because the mission will 'sail along' with Clipper, it will be named after the topsail of a Clipper-style warship, the Moonraker. Without having a Moonraker, a Clipper warship could not be named Clipper. Together they therefore form the perfect couple. However, because not only an orbiter is designed, also the lander has to have a name assigned to it. It is chosen to relate this lander to Drax, the villain from the Bond movie "Moonraker", based on a book by Ian Fleming.

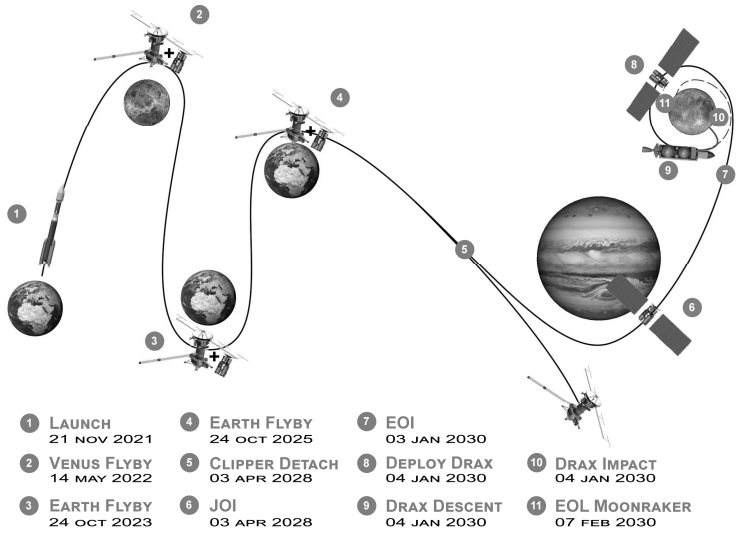

Figure 20.1: Mission timeline

The orbiter/lander combination will therefore from now on be referred to as Moonraker-Drax. The main purpose of the 'piggyback' concept is to share the same launcher, and therefore reduce the mission cost. ESA will not support large class missions having a

budget of 2.5B EUR, and the launch of a dedicated spacecraft will not be before 2030. The piggyback concept, however, can be performed within a budget of 500M to 700M EUR. Moonraker will detach from the Clipper before Jupiter's orbit insertion. This way the influence on the design of the Clipper mission is kept to a minimum. After separation from Clipper, the spacecraft will first perform a Jovian tour of a year passing by several moons to reduce the required ΔV for Jupiter orbit insertion. After the Jovian tour, Moonraker will enter into a polar orbit around Europa. This orbit is chosen to enable global ground track coverage. The orbiter will then deploy the penetrator called "Drax". Moonraker will then mainly function as a relay satellite, although it will also do some measurements.

20.6 Design Moonraker orbiter

Moonraker is a 0.8 x 0.8 x 1.6 m orbiter with a dry mass of 262 kg. Table 1 shows a summary of the design characteristics of the orbiter. Its main function is to collect data from the penetrator and relay this to Earth. In addition, altitude measurements are performed at the same time as Doppler measurements from Earth. This allows for developing a 15th-order and degree accurate spherical harmonics gravity model. Moonraker is powered by a 13.5 m^2 GaAs solar array and data transmission to Earth occurs at a maximum rate of around 3 Kbit/s. The extreme radiation environment requires a mass of 40 kg on shielding material. The main engine of Drax is used to propel the Moonraker-Drax combination before separation. After separation of Drax, the GNC thrusters are used to provide the required ΔV for Moonraker.

The total ΔV needed to land the penetrator is 4,400 m/s. This gives a total wet mass of Moonraker-Drax of 756 kg.

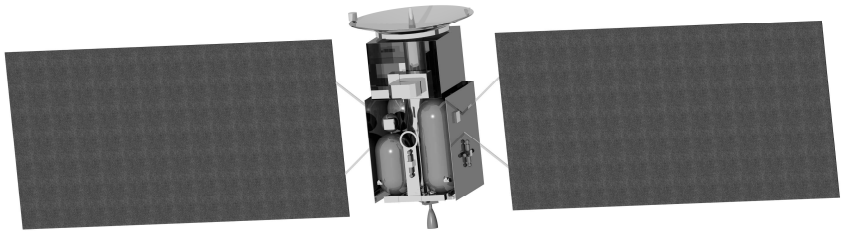

Figure 20.2: Moonraker 3D render

Table 20.1: Moonraker fact sheet

Trajectory	Interplanetary transfer	VEE-GA, Delta-V = 3852 m/s
	Jovian tour	Tour 11-O3, series of 15 flybys and 6 manoeuvres, Delta-V = 1656 m/s
	Europa orbit	h = 244.29 km, e = 0.005, I = 90 deg, RAAN = 90 deg, Argument of periapsis = 270 deg
	Groundtrack separation	5 deg at equator, 10 deg near poles
	Perturbations	Delta I = 16 deg, Delta-V to counter = 371 m/s
	TOTAL Delta-V	2127 m/s with 5% margin 2233 m/s
Shape	Rectangular	
Dimensions	1.6x0.8x0.8m	
Power	Solar arrays	2x deployable wings Solar cells: 33% IMM4J CIC GAaS Total area: 13.5 m2, 122 W (EOL Europa orbit)
	Battery	2x Lithium Ion, BoL energy: 588 Wh
	Bus	28V MPPT regulated bus
Thermal	Europa	Goldized kapton blankets, vault heaters, radiators, variable conductance heat pipes, movable structural cover
	Near Sun	Radiators, high-gain antenna heat shield, variable conductance heat pipes
Communi-cations	X-Band Earth link	1x fixed HGA, 1.3 m parabolic, 1x MGA, HGA shared boresight, 2x LGA, omnidirectional transceiving, 2x SSPA, power 21 W
	UHF-Band relay	1x LGA, helical UHF antenna
DHS	OBC	Based on 1750a processor
Propulsion	Fuel	96N Hydrazine/NTO main engine, 12x 0.5 N Hydrazine reaction control thrusters
	Thrust	96 N (main engine) / 12x0.5 N (thrusters)
	Tanks	2 cylindrical fuel tank 2 cylindrical oxidiser tanks
Structure	Central thrust structure	Honeycomb sandwich beams for support, spring loaded separation system

GNC	Sensors	2x star tracker, 6x Sun sensor, 1x SIRU
	Actuator	12x 0.5 N thruster
Instruments	SILAT	12 W / 5 kg / 0.3x0.3x0.3 m
	SI	Stereo Imager (2048x2048 & 1024x1024 pixels), 7 m/pixel resolution
	LAT	Laser altimeter
	RMS	2x IEUSD sensor, 2x SEU detector, 6x TID dosimeter, 1x surface potential monitor 4 W 4 kg
Radiation	35.9 kg	20% copper and 80% tungsten alloy
Cost	521 M EUR	
Weight	Dry	260.3 kg
	Wet	665.9 kg

20.7 Design Drax penetrator

Drax is a surface penetrator and deployment system with a total dry mass of 44.2 kg. See tables 2 and 3 for a detailed overview of the design parameters. It is deployed, powered by the deployment stage, from the central structure of Moonraker from a circular 244 km altitude orbit. After about two hours, it impacts the South Pole of Europa at 285 m/s, burying itself up to 3 m in the ice layer. This will require a ΔV of about 1100 m/s. Drax will undergo decelerations up to a g-force of 20,000 during impact. Therefore, its structure and equipment are designed and tested for this extreme condition. Once under the surface, it deploys a drill to take a surface sample of the ice. A microbiology package, including a micro spectrometer, analyses the samples. Data are transmitted from Drax to Moonraker for 37 s per orbit of 2.5 hours. After 14 days, the Drax mission ends, as sufficient data has been gathered and the batteries are expected to be empty. In this period, 13 Mbit of scientific data has been transmitted and a total of 400 Wh has been used for the descent and measurements.

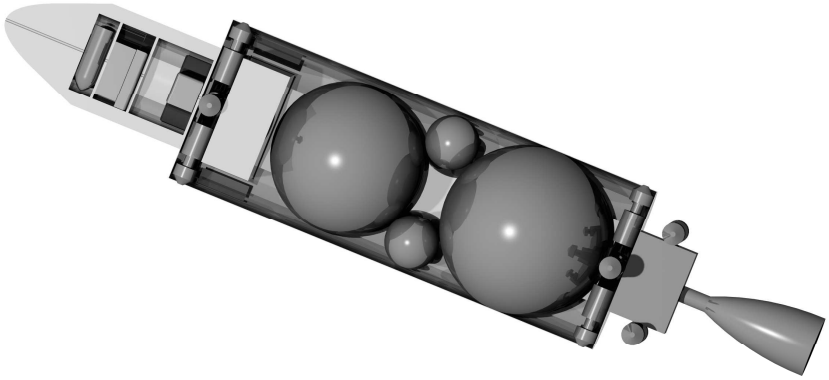

Figure 20.3: Drax and descent stage 3D render

Table 20.2: Drax fact sheet

Shape	Bullet-like	
Dimensions	Diameter	0.195 cm
	Length	0.38 m
Power	Battery	1 x Lithium/Carbon Monoflouride BoL energy: 400 Wh
	Bus	12.5 V regulated
Thermal	Warm bay	Double-walled vacuum flask, titanium low-conductance supports, heaters
	Cold bay	Drill heating
Communications	UHF-Band relay link	1x LGA
DHS	On-Board Computer	
Mechanics	Drill door	
Structure	Titanium shell	Crushable structure inside to limit impact loads
Instruments	Seismometer	Magnetometer
	Descent camera	Sampling drill
	Micro biology package	Micro imager
Weight	Dry	23 kg (incl. margin)

Table 20.3: Descent stage fact sheet

Shape	Long spherical	
Dimensions	Diameter	0.315 m
	Length	1 m
Power	Battery	1 x Lithium/Carbon Monoflouride BoL energy: 23 Wh
	Bus	5.2 V regulated
Propulsion	Fuel	Hydrazine/NTO
	Thrust	96 N main 12x0.5 N
	Tanks	1 spherical fuel tank, 1 spherical oxidizer tank
Structure	AL structure	Engine accommodation with limited heat paths to core structure
GNC	Sensors	SIRU
	Actuators	12 x 0.5 N Thrusters
Radiation	1.7 kg of 20% copper and 80% tungsten alloy	
Weight	Dry	20.9 kg (incl. margin)
	Wet	67.4 kg (incl. margin)

20.8 Conclusion

The conclusion of the detailed design of the Moonraker mission is that a `piggyback' orbiter/penetrator combination is not feasible within 350 kg. The final system wet mass is 756 kg. This large mass is mainly attributed to four factors. The low solar intensity at Jupiter and the long transmission path towards Earth make the telecommunication and power systems relatively heavy. The harsh radiation environment of Europa also requires a high mass radiation protection. Finally, the large ΔV budget requires a propellant mass, which is more than half of the mission wet mass. To reduce the mass of the system, the orbiter only functions as a relay satellite for the penetrator and cannot carry additional instruments apart from an altimeter. This reduces the telecommunications and the power subsystem mass, and therefore the propellant mass. The design can fit the 350 kg if the orbiter is dropped and the design of the trajectory of Clipper is changed such that it can transmit the data of the penetrator.

21. ELECTRIC HELICOPTER

Students: M.S.T. van den Aarssen, L.M.A. Declerck, M. Dirkzwager, R.J. Everaert, M.W. Goedhart, A.A.E. Naorniakowski, J.M.F. van Neerven, E.A. Schouten, K. Schreiber, K.F. Yip

Project tutor: dr. M.D. Bos-Pavel

Coaches: J. Carvajal Godínez M.Eng., ir. T. Visser

21.1 Introduction

The current helicopter aviation branch contributes to worldwide pollution on two fronts. First, greenhouse gases are emitted by the piston engines or turbines, used to power the majority of helicopters. Second, helicopters produce significant noise. Although the helicopter community accounts for a small part of the transportation sector, the helicopter itself is more polluting than other aerial vehicles.

Lowering the emissions by using (hybrid) electric propulsion is the main driver during the project. Hybrid electric propulsion is an option only if it can be adapted to a fully electric system in the future, when the properties of electric power sources improve. This is why the following mission need statement was set for the H2Copter:

"The emission of a typical helicopter surveillance mission should be lowered by using an electric or hybrid-electric two-seat rotorcraft by the year 2020, that should be able to fly fully electrically in the future."

The typical surveillance mission the helicopter is designed for is shown in figure 21.1. The cruise speed is 105 km/h, while the maximum speed is 130 km/h. The H2Copter will cruise for 100 km, perform a surveillance mission for 30 minutes, and return to its starting point.

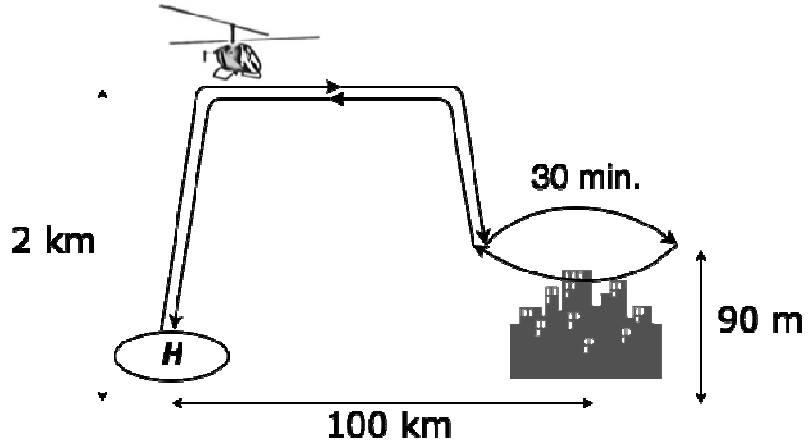

Figure 21.1: Schematic overview of the design mission

21.2 Concept selection

Although the mission is defined as a helicopter surveillance mission, a helicopter is not the only solution. Three different concepts are chosen: a coaxial helicopter, a gyrocopter and a tilt wing aircraft. The concepts are illustrated in figure 21.2.

Coaxial helicopter

The first concept is a coaxial helicopter, which has two counter-rotating main rotors. Thus no energy for the tail rotor is required. A hydrogen electric powertrain is chosen because current state-of-the-art batteries are not able to provide the necessary energy to carry their own weight over the complete mission. Additionally, the electric powertrain can solve the issue of yaw control in coaxial helicopters, by using a different motor for each rotor of which the torque can be changed.

Gyrocopter

The second concept is a gyrocopter, which has a non-powered rotor to lift the aircraft and a separate propeller to provide the necessary thrust. Gyrocopters are able to fly at low speeds, but opposed to a helicopter, it has no hovering capabilities. This means that ground assist is needed for a vertical take-off. A hydrogen electric powertrain is chosen for this concept.

Tilt wing aircraft

The last concept is a tilt wing aircraft. Six rotors can provide lift during the take-off phase, after which the complete wing can tilt. While cruising these rotors are used as propellers and provide thrust, while the wing can deliver the required lift. The energy required is then considerably less than that of the first two concepts. Because only peak power is needed for take-off, batteries are the best solution.

Concept trade off

It is found that the coaxial helicopter is the most suitable design for the mission, because of its wider range in VTOL, hover and surveillance performance. Furthermore, the certification process is well established, the ground space required is smaller and transport is more accessible. The chosen energy source is hydrogen, which leads to a fully electric design. Hydrogen has a longer lifetime, less polluting disposal and safer storage than batteries.

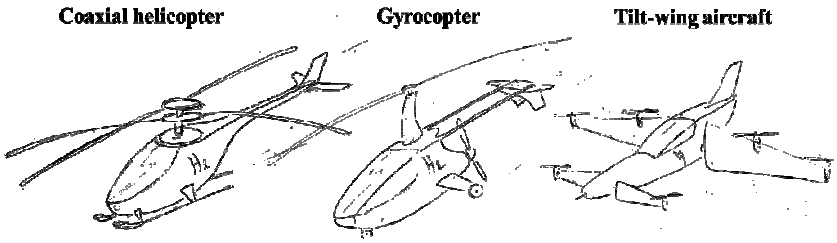

Figure 21.2: Sketches of the concepts

21.3 Design

With the chosen concept the design of the helicopter components starts with specifying weight budgets. When these budgets are not violated it will ensure good integration of the subsystems.

Rotors

All the rotor blades consist of the VR-12 aerofoil, which is chosen because of its favourable aerodynamic properties as a high stall angle, drag divergence Mach number, and lift over drag ratio. The skin and web are made of carbon fibre reinforced plastic, which is filled up with Compaxx-700-X foam.

The rotors are sized using blade element theory, but the coaxial configuration introduces an additional challenge: the interference of the wake of the upper rotor with that of the lower rotor. As a consequence, the lower rotor always operates at different aerodynamic conditions than the upper rotor. Because the wake is different during hover, climb, and cruising flight, these flight phases are analysed separately.

For the sizing of the rotor the aerodynamic coefficients are calculated, from which the final forces are found. After iterations an optimal rotor design is found, using the criterion that the torque needs to be shared between the rotors. This is necessary to leave a net torque on the fuselage. The properties of the rotor system can be found in table 21.1.

Table 21.1: Final parameters of the rotor system

Radius	4.5 m
Chord	0.23 m
Solidity	0.0323
Rotor separation	1.0 m
Rotational speed	45.2 rad/s

Propulsion

The hydrogen propulsion system consists of three major components: a storage tank for the hydrogen, a fuel cell to convert the hydrogen to electric energy, and the electric motors to drive the rotor.

Two electric motors are commercially selected, one for each of the rotors. The Enstroj EMRAX 268 is a three phase synchronous AC motor, capable to spin with a maximum power of 90 kW. Because the fuel cell can only deliver DC, an inverting motor controller is required to transform to AC with the right amplitude and frequency.

A proton exchange membrane fuel cell, typically used in transportation, is chosen because of its relative low weight and low operating temperature of 80°C. In the stack a total of 850 cells are placed in series to deliver the minimum voltage required by the motor controllers: 450 V. The maximum power produced by the fuel cell is 185 kW, but only 153 kW can be used. The difference between these values is explained by the power the balance of plant requires. To pressurize outside air to 2 atm. a 23 kW compressor is required. The fuel cell stack requires a large cooling system to control the environment, as it is only 35% efficient at max power. Four radiators are used with four fans placed on each to provide the necessary air flow. Two pumps are used to make the water flow through all components that need to be cooled, which are the fuel cell stack, the motors and the motor controllers.

A composite hydrogen pressure tank needs to be self-designed, because the available options are either the wrong size or of a too high weight. The designed tank is filament-wound, and adapted to aerospace standards, with a safety factor of 1.5 on tensile stress and an additional factor of 1.25 to account for overpressure. This results in a weight saving of 100 kg compared to the initial estimation based on existing hydrogen tanks.

Cockpit and body

Skids are used as landing gear, because of its lightweight and simple design. Because the gross weight of the H2Copter is relatively low,

skids are found to give sufficient ground control. These are sized to satisfy the regulations set by EASA CS-27. The same regulations are used to design the body structure. A steel tubular structure is used as chassis, because of its ease of maintenance and the favourable fatigue properties of steel.

The cockpit mainly consists of screens which show all the flight data. The images of a infra-red camera, which is placed underneath the H2Copter, can be shown on the screens as well to assist the pilots during surveillance. All systems are powered by the fuel cell, but DC/DC converters are used to get to the right voltage. The big canopy gives both pilots, which are in tandem configuration, a wide range of view. These visibility and the camera give an optimal cockpit to perform the surveillance mission.

Rotor hub

The electric powertrain creates possibilities for innovations in the rotor hub design. Because the electric motors are relatively small, they are placed in the rotor tower. These motors are attached to a single-stage planetary gearbox, of which the annulus is directly connected to the rotor. This results in a non rotating hub, reducing both the drag and the complexity of the system. Because the planet gears are not moving, these are used to put the drivelines and cooling tubes through. The hub is shown in figure 21.3.

A gearbox with a ratio of 7:1 is necessary between the motor and rotor. This is because electric motors typically work more efficiently at high rpm, higher than mechanically possible with the rotor blades. Because the hub is not connected to the fuselage via moving parts, it can easily be displaced. This is a useful result which can be used for stability purposes.

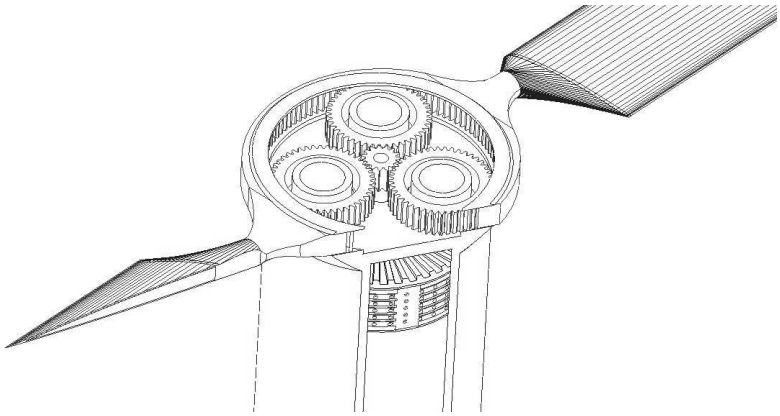

Figure 21.3: The planetary gear box above the electric motor, integrated in the rotor hub

Stability and control

The H2Copter is equipped with standard helicopter controls: cyclic stick, collective and pedals. The cyclic stick can cause the H2Copter to move forwards, backwards and sideways. The collective will cause the helicopter to ascend and descend. The pedals are used to yaw. Instead of the standard swash plate, the rotor is controlled by flaps placed on the trailing edges of the blades. Extending the flaps will create a moment on the blades, changing the pitch angle. The flaps are controlled by Piezo servos, which are not activated by a mechanical link, but by a fly-by-wire system. For the coaxial H2Copter, yawing is done by changing the thrust distribution over both rotors. If one rotor is loaded more than the other one, a moment is induced around the vertical axis and the H2Copter will yaw. This increase in rotor loading is achieved by setting a higher collective servo flap deflection on one of the rotors.

A complete flight dynamics model is prepared and analysed for the final design, taking into account a different thrust distribution over the two rotors. This allowed for a stability analysis and controller design. Furthermore, the hub is placed in such a position, that the centre of gravity is directly below it. It is found that during cruise the short period, the subsidence roll and the spiral motion are stable, that the phugoid is unstable and oscillatory, and that the Dutch roll is stable and oscillatory. A proportional-differential controller that feeds

back the pitch angle and pitch rate is implemented in order to achieve a stable linear and nonlinear system, which satisfies the regulations set by EASA CS-27.

Horizontal and vertical stabilizers are designed to provide stability and to allow for trimming. The lifting line theory is used to determine the lift coefficient and an optimization process is performed to reduce the total wetted surface area, which results in low skin drag.

Final design

To improve manoeuvrability a small mass moment of inertia is needed, meaning that the components are located as close to the centre of gravity as possible. Since the centre of gravity is preferred to lie close to the centre of the rotors, the goal is to move the components with large inertia and mass close to the axis of the rotor blades. The pilot, hydrogen tank and the fuel cell position is of great influence on the overall position. The locations of the subsystems are presented in figure 21.4.

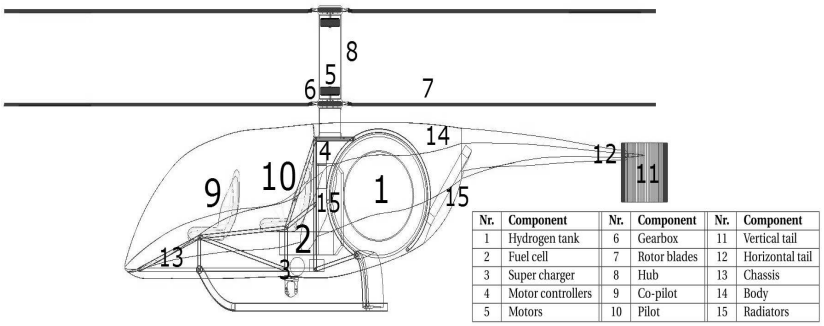

Nr.	Component	Nr.	Component	Nr.	Component
1	Hydrogen tank	6	Gearbox	11	Vertical tail
2	Fuel cell	7	Rotor blades	12	Horizontal tail
3	Super charger	8	Hub	13	Chassis
4	Motor controllers	9	Co-pilot	14	Body
5	Motors	10	Pilot	15	Radiators

Figure 21.4: Schematic side-view, showing the component packaging of the rotorcraft

The gross weight of the H2Copter is 1,065 kg. The final weight breakdown is shown in figure 21.5. It can be noted that the hydrogen propulsion system of the H2Copter is heavier than the one of a conventional helicopter. However, the rotor blades, hub and skids are all lightweight subsystem designs.

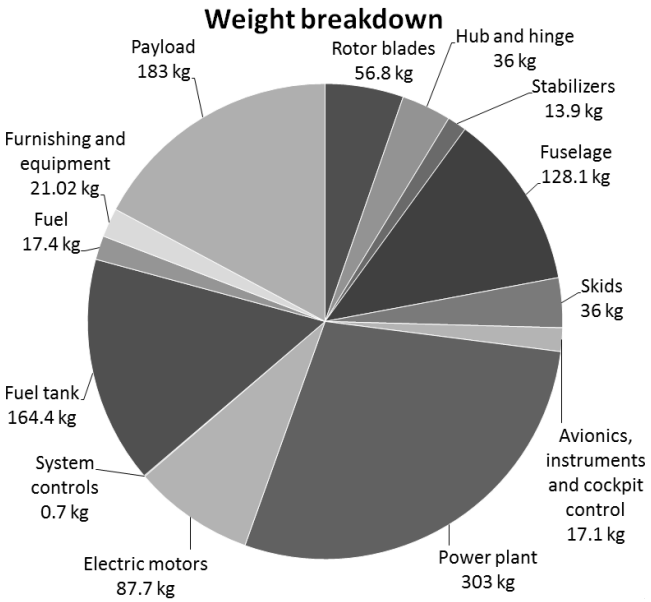

Figure 21.5: Weight breakdown of the H2Copter

21.4 Sustainability

Although the H2Copter's hydrogen propulsion has no direct emissions, during its lifetime it will damage the environment. A life cycle assessment is performed, considering all life phases, such as development, production, operation, and disposal. The ReCiPe method is used to obtain a single score for the sustainability. To make a comparison with other rotorcraft, the scores are scaled to passenger-kilometre values. The single score of the H2Copter is 0.0088 points/pkm. This indicates a 65% smaller impact on the environment than a conventional helicopter, that is conceptually sized for the same mission. From figure 21.6 it can be noted that hydrogen production and compression are the main contributors to the environmental impact.

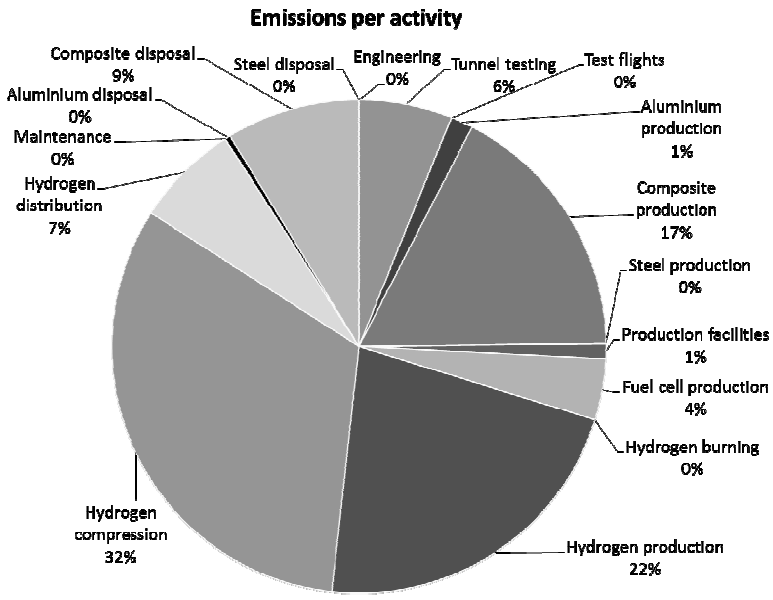

Figure 21.6: Contributions to the single score of the life cycle activities

In helicopters, two main contributors to the noise can be distinguished: the main rotor and the tail rotor. To predict the noise generation of the H2Copter, a statistical log-linear relation based on weight and rotor diameter is obtained. The noise reduction by removing the tail is quantified by looking at helicopters with ducted fan tails. Because of the interaction between the two main rotors, the blade-vortex interaction noise increases. This has an influence especially during landing approach, explaining the relatively high 88.2 EPNdB, which is 2.1 EPNdB below the certification level described by CS-36. Removing the tail leads to great noise reductions during the other flight phases, take-off and overflight: the noise levels are 7.8 EPNdB and 9.4 EPNdB below certification levels, respectively.

21.5 Market strategy, operations and logistics

The main goal of the H2Copter is to provide affordable and practical alternatives to fuel burning and polluting helicopters. This goal is achieved by selling hydrogen based helicopters, selling patented

innovative technology and providing an example to the industry. The competitive advantage of the helicopter will be its innovative, electric and silent design.

From the helicopter industry, the market price for a coaxial helicopter is estimated. The added value of the electric propulsion system is determined from the automotive industry. This results in an expected acceptable selling price of the H2Copter of $333,000 ± 26%. The total production cost of the H2Copter is $349,000, with the airframe and avionics system as main contributors. A selling price of $380,000 is needed to break even in 2050. The H2Copter will therefore aim at a market of high quality and high price. Because of the electric powertrain and the less complex drive shaft, the H2Copter is more reliable and less maintenance is required compared to a conventional helicopter.

21.6 Conclusion

It can be concluded that innovative characteristics are proposed in various subsystems of the final design. First, a hydrogen-electric powertrain is implemented with a pressure tank and a fuel cell. This is a green solution, but it is currently heavy. Second, a novel engine-hub integration is used, in which two engines can be used independently. Finally, no swashplate is used for controlling the H2Copter. It is replaced by servo flaps on the rotor blades. The final weight of the H2Copter is 1065 kg and it is able to achieve the range and endurance of the mission. The final design of the H2Copter is shown in figure 21.7.

The conclusion can be made that a hydrogen powered, electric helicopter is feasible, functional, innovative and definitely sustainable. From the life cycle assessment of the final design, it is obtained that the H2Copter is 65% more sustainable than a conventional helicopter using a fossil fuel based engine sized for the same mission. All in all, the H2Copter is on the forefront of helicopter innovation. It is a technological leap towards the sustainable future of the rotorcraft, which is also competitive, easy to fly and maintenance-friendly.

Figure 21.7: Final rendering of the H2Copter

22. UNMANNED CONTAINERIZED CARGO FREIGHTER

Students: M. Boukema, G.J. van Dam, L.K. Hassan, E. Hoogeboom, M.H. Jagtenberg, R. Janssen, U. Malik, L.G.M. Meijboom, M.K. Sakyi-Gyniae, P.A. Scholten

Project tutor: ir. P.C. Roling

Coaches: J.D. Brandsen MSc, G. Caridi MSc

22.1 Introduction

From the first cargo flight in 1911, cargo air transportation is recognized as one of the most time efficient means of transportation over long distances. However, for the past 100 years aircraft design has stagnated. New technology is already available and the markets are in need of a more time and cost efficient way to transport cargo. The project objective is therefore stated as follows:

"Design an unmanned containerized cargo freighter that can reduce the cost of shipping by air and the time required for inter-modal transfers and transport on the ground."

The market analysis shows that a market share in its segment of about 20% could be possible, which comes down to 500 aircraft to be produced.

22.2 Requirements

The final design of the unmanned cargo freighter shall meet the following requirements:

- The take-off runway required shall be less than 3,000 m.
- The landing runway required shall be less than 2,000 m.
- The maximum payload range shall be at least 3,000 nmi.
- The maximum payload weight shall be at least 20,000 kg.
- The maximum payload volume shall be at least 50 m^3.
- The aircraft shall comply with CS-25.
- The 55 dB SEL contour shall be 50% smaller compared to an Airbus A320.
- The fuel usage, CO_2 production and direct operating costs shall be less than 25% per metric tonne of payload of a Boeing 747-400F.
- The wing span shall be less than 80 m.
- The unit production cost shall be less than 50 M€.
- The total load shall be shifted from the aircraft to a road capable truck and vice versa in less than 30 minutes.

22.3 Conceptual design

To start with the design process, it is important to come up with a design which suits the mission of the project. In order to do so, a brainstorm session is held in which every group member participates and comes up with a variety of concepts which are both innovative and technically feasible. The three concepts which turn out to be best after initial trade-off are the formation flying aircraft, the flying wing aircraft and the blended wing body aircraft. The inspiration of these concepts can be seen in figure 22.1.

Formation flying

This concept is designed to fly in formation. Specific characteristics of this concept include tail mounted jet engines which minimize the wing tail drag interference, and low mounted wings. These assure undisturbed movement of the wing vortices, which are the driving principle of any formation flying concept. The remainder of the

design resembles that of a conventional aircraft. It has default wings and vertical and horizontal stabilizers. The fuselage is shaped such that it can easily be pressurized. The shape of the aircraft is beneficial in terms of cargo compatibility and the cargo can be loaded from the nose of the aircraft.

Flying wing

The flying wing concept is a low altitude propeller driven aircraft. Because it is flying at low altitudes, pressurization of the cargo is not necessary. The main advantages of flying wings are the increased aerodynamic characteristics: they have higher lift-to-drag ratios and therefore are able to take-off with a higher gross weight, at the same dimensions, and have a lower fuel consumption. The main disadvantages follow from stability properties. Due to the fact that flying wings do not have horizontal stabilizers, longitudinal stability must solely be provided by the main wing.

Blended wing body

The blended wing body design resembles the flying wing concept at the front in order to maximize aerodynamic efficiency, whereas the rear of the aircraft features a tail structure to accommodate improved operational compatibility and assure inherent stability. It features jet engines mounted on top of the wing and it is supposed to operate at high speed and at high altitudes. The pressurization will happen in a separate pressure vessel, due to the fact that the outer skin of the centre body is difficult to pressurize because of its shape.

Figure 22.1: Formation flying concept, flying wing concept and blended wing body concept

Trade-off

Each one of the three concepts is investigated to find the initial weight, aerodynamic properties and other characteristics. Also a cost

analysis is performed. A trade-off is performed to determine the best concept. The criteria chosen to use in the trade-off, in the order of importance, are:

- Operating cost
- Sustainability (fuel and emissions)
- Safety (proof of concept)
- Noise contour
- Production cost

Taking these criteria into account, the blended wing body concept was chosen, which was named ATLAS.

22.4 Final design

Now that the final concept has been chosen, the final design phase has started. In this section, the most important design decisions regarding aerodynamics, structures, operations and the unmanned part will be explained, as well as an overview of the final design of ATLAS.

Aerodynamics
The aerodynamic analysis of the aircraft is strongly influenced by it being a blended wing body. The analysis is divided between two different wing segments: the body segment and the outer wing.
The body segment needs a certain height to accommodate the cargo and the outside shape is defined by an aerofoil. This results in a compromise between aerofoil thickness and body length. The thick aerofoil shape in combination with the preferred high cruising speed steers the aerofoil selection towards a supercritical aerofoil, a type that is designed to minimize the wave drag for transonic flow regimes over the aerofoil. In contrast to the body, the outer wing has a thin aerofoil to reduce pressure and wave drag.

The zero lift drag coefficient of the aircraft is reduced by the shape of the design. In particular, the fuselage drag is significantly lower compared to conventional aircraft, since little fuselage area is in contact with airflow. The design is more aerodynamically efficient

than conventional aircraft. Aerodynamic characteristics of the design are a lower wing loading because of an increased lifting surface area and a high lift over drag ratio.

Structural design

The structural design is started with the pressurized cargo bay. Due to limits in the centre body height imposed by the blended wing body concept, the pressure vessel height must be kept small accordingly. To realize this, use is made of the multi-bubble concept, in which non-circular shapes are approximated using circular arcs, interconnected through reinforcing walls, resulting in in-plane stresses in the walls only. The cargo bay and pressure vessel dimensions are shown in figure 22.2.

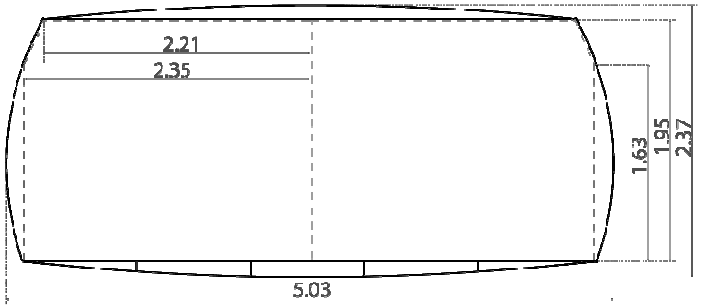

Figure 22.2: Cargo bay and pressure vessel dimensions
(front view with dimensions in metres)

Where a conventional commercial aircraft continues its wing box straight through the fuselage, ATLAS' wing box has to be diverted around the pressurized cargo bay in order to make efficient use of the space inside the cargo bay. To accommodate this, integrated bulkhead and spar configurations are designed, inspired by the General Dynamics F-16. Buckling loads encountered at the middle of the centre body are found to be critical for the sizing of the structure.

Using composite materials, the structural weight of ATLAS is kept to a minimum which, through the snowball effect, decreases the overall weight of the aircraft. This introduces sustainable solutions through decreased material usage for production and improved fuel usage during operative life.

Operations

Efficient ground operations are imperative to the Turn-Around Time (TAT) of an aircraft where economic benefits and efficient use of airliner's fleet can be achieved. In regards to this, the TAT of ATLAS is crucial. Decreasing the TAT enables ATLAS to perform more flights per day compared to conventional air cargo freighters. This results in an increase in revenue for airliners.

The cargo bay of ATLAS is designed in such a way that four 20 feet truck-compatible containers or multiple different Unit Load Devices (ULDs) can be accommodated. It is even possible to carry two 40 feet containers in the aircraft. The use of ULDs also ensures that ATLAS is competitive within the current air cargo market and the design of the intermodal containers offers consumers flexible and efficient packaging means. These intermodal containers are integrated with intelligent technologies, improving the cargo transport chain. The control over the entire cargo chain is accomplished by implementing smart sensors and container tracking via GPS.

Moreover, ATLAS is designed to have simultaneous loading and unloading, which is implemented using the cargo-slide concept. Loading is performed via a nose door that splits in the middle and opens to the sides, while unloading happens via doors in the back. The containers are safely moved horizontally inside the aircraft by using ball transfer units, which are implemented in the floor of the cargo bay. The usage of these transfer units ensures that different types of cargo can also be transported. The containers are secured to the aircraft by using fasteners in the floor. Furthermore, refueling can be performed simultaneously with the cargo loading, which decreases the turnaround time significantly.

As a result of these design choices, a TAT of 24.4 minutes is possible for ATLAS. This is a substantial improvement compared to current freighters with an average TAT of 30-50 minutes. When simultaneous loading and unloading is performed by trained ground cargo handlers, a TAT of 12.6 minutes can be achieved.

Unmanned

The European Aviation and Safety Agency (EASA) have written a policy for airworthiness certification of un-manned aircraft systems (UAS). Until a type-certificate especially for UAS is created, the policy is used as a guideline in the certification process. The policy statement contains the following two main objectives:

Airworthiness objective: With no persons on-board the aircraft, the airworthiness objective is primarily targeted at the protection of people and property on the ground. A civil UAS must not increase the risk to people or property on the ground compared with manned aircraft of equivalent categories.

Environmental protection objective: Where applicable, a UAS must comply with the essential requirements for environmental protection as stipulated in basic regulations. The top level requirements for ATLAS already comply with these environmental regulations.

To meet the objectives of this policy, three different communication types are developed: 'flight preparation', 'flight operation' and 'ATC, control room and aircraft'. The unmanned cruise flight is performed by flying over pre-programmed way-points. To make sure all other phases of the unmanned flight can be performed safely as well, different kind of sensors and subsystems are implemented in the aircraft.

To ensure safety, several system modes have been identified. The failure modes are split in aviation, navigation, communication and mitigation failures. Depending on the kind of failure, a failure mitigation mode is activated. Detecting failures can be done by simulating the response of the aircraft to different inputs to its subsystems. If the response does not match the response of the simulation, the aircraft 'detects' the undetected failure. In this case the aircraft should assess if it can 'learn' to control itself again by monitoring its response to inputs it is giving to its subsystems. If this is possible, the aircraft should perform a forced landing on either an

airport or a selected site that ensures that there are no casualties on the ground. If the aircraft becomes uncontrollable it should perform an emergency landing.

Since ATLAS is unmanned, it has been designed such that all eigen motions are stable. Doing so, ATLAS can keep flying without diverging from its stable position, which is important when for example in case of failure the computer needs some time to reboot.

ATLAS design

The 3-view drawing of ATLAS can be seen in figure 22.3. A 3D view can be seen in figure 22.4, and the opened nose doors can be seen in figure 22.5. Finally, the most important design parameters of ATLAS can be seen in table 22.1.

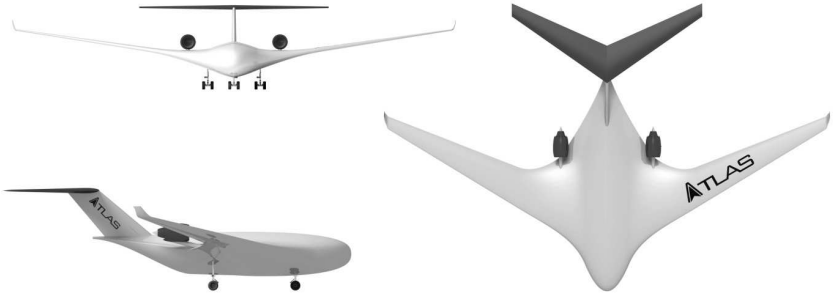

Figure 22.3: Side view, front view and top view of ATLAS

Figure 22.4: 3D view of ATLAS

Figure 22.5: Opened nose doors during front loading of ATLAS

Table 22.1: Most important design parameters of ATLAS

Parameter	Value	Unit
MTOW	579,250	N
Max. payload mass	30,000	kg
Max. range @ typical payload	3,000	nmi
Mach number @ cruise	0.72	-
L/D	19.6	-
Aircraft unit cost	30.2M	€
Direct operating cost	0.1364	USD/tkm
Turnaround time	12.6	minutes
Cargo bay volume	102	m^3
Container height	1.95	m
Container width	2.35	m
Container length	5.7 / 11.4	m

22.5 Conclusion

The preliminary design is based on a market analysis with multiple concepts. Based on different criteria, the blended wing body concept is chosen. The high aerodynamic efficiency and inherent stability due to the tail result in an exceptional combination for the operating cost and sustainability. The design is profitable and has a relatively small environmental footprint.

The subsystems of the aircraft were then designed in more detail. The subsystem design is performed using an iterative process, where new

information provides more accurate results than previous estimates. The internal subsystems of the aircraft focus on the environmental control of the cargo bay, which has to function without direct human intervention. Several computer controllable protection systems are designed to ensure the safety and preservation of the cargo. The operational design of ATLAS concentrates on the aircraft being unmanned, considering primarily safety for people on ground. Different failure modes are considered along with appropriate responses.

Several important requirements are driving this design. These requirements steer the design to a high level of performance for multiple categories. The direct operation cost, fuel consumption and produced emissions, when compared to a Boeing 747-400F (per tonne of payload per kilometre), are reduced with 75%, 50% and 46% respectively. Also, the noise production is reduced by 78.5%, when compared to an Airbus A320. Even though the fuel and emissions requirements are not fulfilled, it does push the design towards a significantly lower fuel consumption.

In summary, ATLAS performs significantly better than any cargo aircraft flying today. In the context of increasing fuel prices and high consideration for the environment, ATLAS is a sustainable choice due to its low fuel use and low noise contour. The compatibility with other transport modes makes delivery times shorter and the low operating cost makes it profitable.

22.6 Recommendations

For the propulsion system it is highly recommended to work closely with the manufacturer of the engine and other related systems. This enables the designers to get more accurate values for the inlet design. Also, using CFD is recommended for calculating the flows in and around the engines. Moreover, more accurate models for scaling the engines are recommended to be used. In that way internal systems can be scaled as well, and more accurate values can be obtained of the actual engine used.

To investigate the aerodynamic properties of the aircraft more accurately, it is recommended to do wind tunnel tests and use CFD. This will model the viscous flow effects better, which results in more accurate and realistic aerodynamic values. Next to that, it is recommended to investigate the usage of a morphing wing. A morphing wing can show great advantages in terms of fuel efficiency during different mission segments. For the aerodynamic properties, it is recommended to perform experimental and field tests, for example a wind tunnel test, of ATLAS.

For the structural analysis of the aircraft, most of the assumptions that are taken into account can be incorporated in the program with additional resources. For example, by not neglecting deformations, stress can be computed more accurately. This makes it possible to perform a vibrational analysis. The major drawback of the current analysis is that it only considers the pressure vessel, and the spars and skins in the wing. Any other structural members, for example the tail, engine reinforcements, wing ribs, fuselage longerons, stiffeners and rivets, have not been taken into account. If one wants to fully analyse the aircraft's structure, a detailed FEM analysis should be performed. For the structural analysis it is also recommended to perform laboratory tests, for example a wing bending test.

For the unmanned part, it is recommended to design the actual software program that will be used to link for example the sensors to the actuators. Also it is highly recommended to talk with the regulators, to make sure regulations allow unmanned flying, and that changes are being made on CS-25 for unmanned aircraft. For the unmanned part it is also recommended to evaluate a combination of failures. For now, only single failures have been evaluated, and not two failures at the same time.

It is also recommended that more research is carried out to establish how airports and people will adapt to this new design. For example, whether a large portion of airport staff will require specialist training, or how airport operations will be affected by the introduction of unmanned aircraft, need to be investigated before unmanned aircraft

can be commercialized. It is also recommended to do more research about whether unmanned flying will be accepted by the public, and whether this acceptance will improve if unmanned aircraft only transport cargo.

Finally, it is recommended to investigate the possibility of flying even higher than the current cruising altitude of 12,500 m. This would be beneficial for the fuel consumption and operating cost, but would make it harder to have stable eigen motions.

23. SKYFI

Students: S. Angelovski, Y.A. Antonio, T. Bussink, A. Carrera, Y. Chen, J.K. El Sioufy, J.H. Freiherr von der Goltz, G.R.W. ten Hove, G. de Jong, K. Rado

Project tutor: dr.ir. E.J.O. Schrama

Coaches: M. Schmelzer MSc, Z.X. Zheng MSc

23.1 Introduction

In modern days, it is very crucial for people to be available and able to stay connected with everyone at any time in both private and professional life. Especially with the internet becoming increasingly important in every aspect of peoples life. It is hard to imagine that large areas of the world do not have the infrastructure to provide such services. This is why companies like Iridium and Inmarsat have developed satellite systems which can provide global or nearly global communication networks. However the downside of these existing systems is that they are expensive to use.

Even though some of these systems can be used for search and rescue missions, the tendency is that they usually depend on GPS and would be unable to locate their users in case the network is out of service. More than anything, in case of emergency, global communication networks are especially useful in remote areas with little to no

infrastructure currently existing. In such area, more time is needed for the rescue team to arrive, thus the time it takes to communicate the information should be kept lowest possible. It is also worth considering the solution for a scenario when an incident occurs which leaves the person in question unable to send an emergency signal himself. A passive location service will then be needed. In the case of MH370, none of the existing systems were able to pick up a signal and track it with sufficient accuracy.

Hence a system is needed which can provide at least basic communication and search and rescue services on a global scale.
This leads to the following mission need statement:

"Provide satellite-based voice, text, image transfer, basic internet and tracking functionality to affordable, low-power, portable devices anywhere on the planet for a ten year period"

23.2 Requirements

From the mission needs, several requirements can be derived which will drive the system design:

- The system shall be able to connect users to Internet.
- The system shall provide full coverage of the earth at any time with success rate of 90%.
- The system shall be able to transceive text messages at a data rate of 1 kilobit per minute.
- The system shall be able to connect a phone call or send a picture at a data rate of 10 kilobit per second.
- The whole system's operation time shall be 10 years.
- A portable device with an omnidirectional antenna shall be able to establish communication to the space segment when there is a non-obstructed field of view.
- The system shall be realized within an initial (virtual) budget of 500 M€.
- At the end of its life, the spacecraft shall have a minimal impact on the space debris density.

- The spacecraft shall comply with the International Traffic in Arms Regulations (ITAR) regulations.
- The spacecraft shall comply with the International Telecommunication Union (ITU) regulations.
- The system shall be able to locate the user within a 2 km radius within 1 hour.
- The user shall be able to successfully connect to the system within a period of 15 minutes

23.3 Concept selection.

Several concepts were developed which were expected to be able to fulfil all of the above requirements. These concepts were first categorized as:

- "Stand-alone" concepts which are fully and autonomously developed.
- Concepts which use an existing communication system and add to it.

The three "stand-alone" concepts were further categorized by the altitude at which they operate:
- Many CubeSats in VLEO.
- Several micro satellites in LEO.
- A few larger satellites in MEO.

The two other concepts were:
- Add Doppler tracking to Iridium.
- Add one polar VLEO orbit constellation to INMARSAT.

The trade-off criteria for these concepts were the budget, SAR capabilities, sustainability, communication subsystem and system complexity. Using a large number of CubeSats in VLEO was the most promising concept due to its low cost and advantages when it comes to the communications subsystem design. It also promised good sustainability and SAR capabilities.

23.4 Final design

The satellite design which was found to fulfil the requirements most efficiently and effectively is visualized in figure 23.1. Table 23.1 presents the key specs of each system subcomponent.

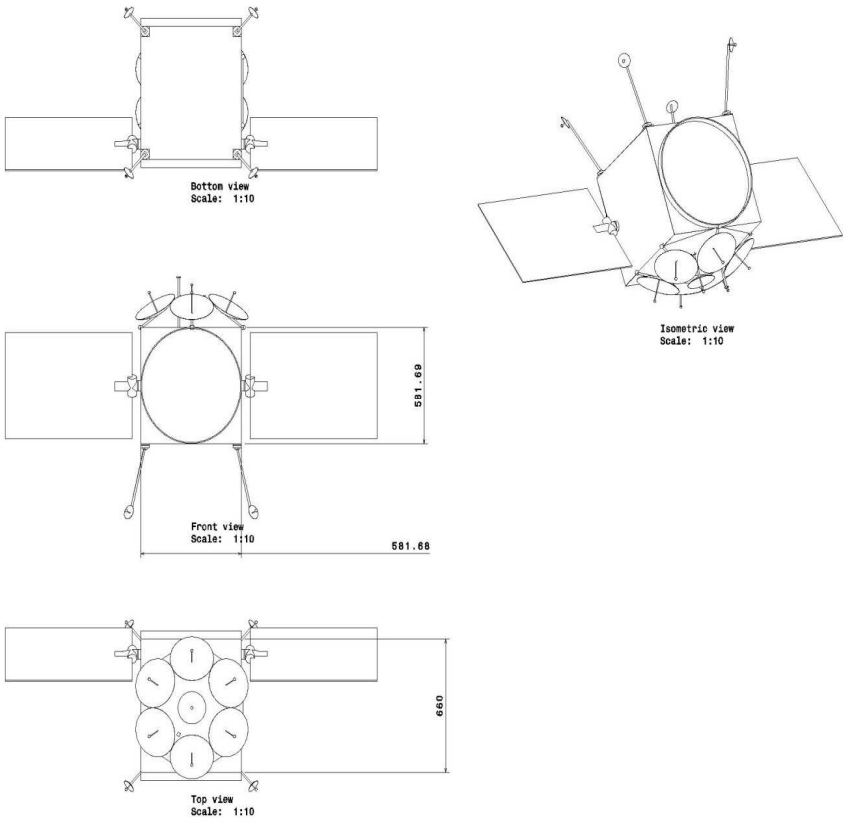

Figure 23.1: 3-view drawing and isometric view of one satellite

Table 23.1: Main design parameters of the communication system

Subsystem	Key properties
Astrodynamics	19 orbital planes 11 satellites per orbit (+ 1 redundant) Inclination of 82° Initial altitude of 550 km, minimum operational altitude of 500 km
Communications	1 patch antenna (ground station) 4 parabolic antennas (crosslink) 7 parabolic antennas (user communications) Total mass of 41.1 kg Total power consumption of 89.2 W Data rate per satellite of 700 kBps
SAR	Doppler Tracking Accuracy of 8.3 m Tracking time of 8.2 minutes (2 passes)
Power	Battery mass of 11 kg Solar array mass of 12.75 kg, 2 panels Solar array size of 0.72*0.6 m^2 each Total provided power of 104 W
ADCS	Magnetorquers, Magnetometers, Sun sensors, Gyroscope Maximum manoeuvre duration of 727 s Total mass of 2.5 kg Total power of 4 W 3-axis control with a pointing accuracy of 5°
Thermal Control	2 patch heaters Total power of 0.4 W Total mass of insulation material 5 kg
Structural design	Total mass of 21.2 kg Aluminium, Titanium, Kevlar and Graphite epoxy Satellite volume of 0.6x0.6x0.65 m^3
Sustainability and Decay	Total time in space of 14 years 500 km reached after 8 years without Orbital lifetime extended by 2 years
Propulsion	Mono-propellant: Hydrazine Propellant mass of 0.565 kg One thruster with a thrust of 1 N

Even though the initial concept was using CubeSats in VLEO, multiple design iterations lead to a LEO concept using much bigger satellites. The altitude was required to ensure the satellites remain in orbit long enough; however, the high altitude caused the mass and power consumption of the communication subsystem to become

significantly higher than initially planned. So while designing to comply with all the requirements, there was a change of concept.

Astrodynamics

The main goal of the orbital design was to achieve a constellation which would cover every part of the earth at least 94% of the time. Only 90% were required, however a safety margin was applied to account for coverage losses due to i.e. pointing inaccuracy. A Walker star constellation with a slight offset (inclination of 82°) was found to be most efficient in terms of coverage vs. number of satellites used.

Communications

The ground user antenna design was driven by the omnidirectional antenna of the user device and its low power. This had to be compensated for by using high gain parabolic antennas. Similarly, due to the high space loss, the cross link antennas are also parabolic but with a much smaller half power beamwidth, due to the fact that the position of the other satellites is known and the antennas can be steered accordingly. The relatively small patch antenna could only be designed this small because the ground stations can provide a high power signal which is a lot easier to pick up for the satellite than the user device signal. Size, weight and power consumption of the communications payload are the reason why the CubeSat structure was no longer viable and larger satellites had to be considered.

SAR

As one of the main features of this mission, the tracking capability of the SkyFi mission was supposed to be independent of other systems like GPS. For that reason, Doppler tracking became the method of choice, as it only requires the user device to be connected to track it. The users are tracked by the satellites and the satellites are tracked by the ground stations, from which the location of each user can be determined.

Power

The power subsystem design was strongly dictated by the communication subsystem. Almost 90% of the total power is allocated

towards it. Battery and solar panel mass became the second factor which strongly increased the total satellite mass. Due to the lack of surfaces to mount solar panels on, deployable and rotatable solar panels were chosen. Together with a yaw motion of the satellite, the rotation from a motor means it can point towards the sun at all times except during eclipse time.

ADCS

This subsystem was designed with multiple mission components depending on it. First of all, the coverage needs to be maintained, which means the satellite needs to be nadir pointing at all times. At the same time, the satellite needs the correct yaw to allow sun pointing solar panels over the entire day time of the orbit. The pointing accuracy was also kept low in order to minimize communication signal losses.

Thermal control

To prevent the satellite from both overheating and freezing, the temperature limit of each subcomponent was determined. According to the resulting temperature requirements, coatings, paint and insulation was applied. Only little power is needed by this subsystem to keep the propellant warm enough using the patch heaters as all the other subsystems use their own operational heat to keep themselves sufficiently warm during the eclipse.

Structure design

Both the launch loads and the natural frequency of the launcher were obtained from the launcher user guide. The structural components were designed to carry these loads or increase the natural frequency of the satellite to be at least twice as high as the one from the launcher. The satellite structure consists of 5 different materials: 2 aluminium alloys, a titanium alloy, graphite epoxy sheets and Kevlar. The structure design is strongly correlated with the thermal control and designed to fit the needs of both.

Sustainability and decay

The orbital decay was important in 2 ways: firstly, the satellite needs to remain at a certain operational altitude range in order to provide sufficient coverage. Secondly, adding space debris to the already considerably littered orbits around earth was to be avoided in order to comply with the United Nations Office for Outer Space Affairs (UNOOSA) regulations. These regulations demand that no satellite shall remain in orbit for longer than 25 years after its mission has ended. Additionally, space debris avoidance needed to be accounted for, which was done by increasing the amount of fuel on each satellite so it can fly an evasive manoeuvre.

Propulsion

Three manoeuvres needed to be accounted for in this mission: debris avoidance, orbit maintenance and constellation maintenance. As mentioned before, a part of the delta V budget is used to evade uncontrollable space objects about (or threatening to) to collide with the satellite. Because the mission itself doesn't require any manoeuvre, delta V budget is only needed to maintain the constellation and to increase the time spent in the operational altitude range by 2 years.

23.5 Conclusion and recommendations

The chosen design is capable of fulfilling all connectivity and data rate requirements as well as provide Doppler tracking of any user any time. The system can maintain its operational altitude for 10 years and does not require re-launches. It is capable of accurately determining and controlling its attitude to be constantly nadir pointing. Power is provided using 2 movable solar arrays which will point towards the sun at all times. The propulsion system provides the satellite with the capability to evade space debris and keeps the satellite at a sufficient altitude. With using 468.6M€, SkyFi stays within the budget of 500M€ while complying with all top level requirements. The system is designed for 1,000,000 users out of which 5% are expected to be using the system simultaneously.

In order to provide higher data rates, better connectivity or to host more users at the same time, the system could be expanded by either launching more satellites or by increasing each satellites communication system capacity, hence making it both heavier and more power consuming, which would require a higher budget.

24. E-SPARC: AN AEROBATIC RACING AIRCRAFT

Students: J. Hoogendoorn, P. Hulsman, D.A.J. Peschier, O.F. Pfeifle, W. Plaetinck, H.C. Prins, B. Roëll, L.N. de Ruiter, E.T.B. Smeets, N. Weber

Project tutor: dr.ir. S. Shroff

Coaches: dr ir. A.C. in't Veld, ir. M.F.M. Hoogreef

24.1 Introduction

Following in the footsteps of the automotive industry with the successful implementation of Formula E, the E-SPARC design is the world's first all-electric racing aircraft. E-SPARC stands for "Electrically, Sustainably Propelled Aerobatic Racing aircraft". The objective of E-SPARC is to prove the feasibility of a sustainable and high performance alternative for the current aircraft in aerobatic racing. Thereby, the aim is to present a design worthy of competing in the popular Red Bull Air Race. Given the combination of being the world's fastest growing international motorsport with the commitment towards reducing the carbon footprint, the Red Bull Air Race provides the optimal platform for the E-SPARC design.

These objectives are summarized in the mission need statement of the E-SPARC design:

"To design an electrically propelled aerobatic racing aircraft with a group of 10 Aerospace Engineering students of Delft University of Technology and have its first flight in 2025 costing no more than 300,000 Euro, in order to test and show the feasibility of electrically propelled, high performance, sustainable aircraft."

24.2 Design requirements

To achieve the aforementioned objectives, a series of top level requirements has been defined for E-SPARC.

Performance

- Minimum climb rate: 7 m/s
- Minimum design cruise speed: 120 km/h
- Service ceiling 5,000 m
- Safety and reliability
- Ultimate load factor: 18g

Endurance

- Race time: 3 minutes at full throttle
- Take-off and landing: 30 minutes at half throttle
- Sustainability
- Electric power supply

Other

- Manufacturing cost: € 300,000 (first prototype)
- Experimental category aircraft
- 1 pilot
- First flight before 2025

24.3 Conceptual designs and trade-off

Having identified the objectives and design requirements, next to determine was which aircraft configuration satisfies the requirements and yields an optimal performance. Several basic, yet feasible, aircraft configurations were defined with varying positions for the wings, empennage and propulsion system. An initial trade-off resulted in the following three conceptual aircraft configurations: a conventional

design, a canard aircraft and a bi-plane. A schematic representation of these configuration is given in figure 24.1.

Conventional configuration

The current Red Bull Air Race aircraft all have this type of configuration, which is proven to be successful. The electric motor and power supply would be positioned between the nose and cockpit of the aircraft, with a puller propeller located in front. The straight wing is positioned just behind the aircraft's center of gravity and the empennage is located at the rear of the fuselage. Although a proven concept, this design is not optimized for efficiency, as the horizontal tail has to produce negative lift to enable longitudinal moment equilibrium.

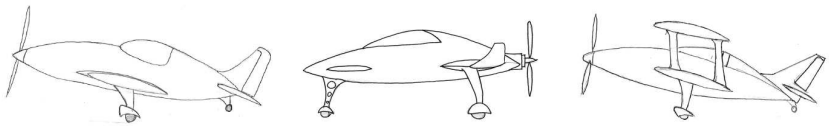

Figure 24.1: From left to right, Conventional, canard and bi-plane conceptual aircraft configuration

Canard configuration

With a canard configuration, the horizontal stabilizer is located near the nose of the aircraft. Thus, it is positioned in front of the aircraft's centre of gravity and therefore produces positive lift to provide the required longitudinal equilibrium. As such, the required lift is produced by both the wing and canard in contrary to just the wing for a conventional aircraft. This enables a smaller wing, which in turn reduces the overall aircraft weight, drag, power required, and rolling inertia, making it more sustainable and competitive. However, a canard configuration requires careful aerodynamic analysis to obtain proper stall characteristics. Furthermore, the pusher propeller adds another constraint to the design in terms of propeller clearance.

Bi-plane configuration

The bi-plane has been a favourite among aerobatic aircraft because of its low roll inertia resulting from the relatively short wing span required for the two stacked wings. This attribute is also favourable in

races. The configuration features a puller propeller and conventional empennage. However, despite the improved manoeuvrability, the second wing adds more weight and drag to the overall aircraft design when using composites relative to other designs, which negatively influences the aircraft performance.

To determine which configuration would be best, a trade-off was performed using the analytical hierarchy process. This trade-off combined different criteria including: aerodynamic efficiency, manoeuvrability, design complexity, safety and power loading. This trade-off resulted in the choice for a canard configuration.

The next phase consisted of the preliminary design phase in which the aircraft's main subsystems were designed in greater detail. An overview of the work performed by each department throughout this design phase is given in the following sections. The complete design can be seen in figure 24.2.

Figure 24.2: Final design of E-SPARC

24.4 Aerodynamic analysis

Aerodynamically, the design aimed for optimal performance characteristics in the Red Bull Air Race. The configuration therefore required the simultaneous optimization of the main wing and the canard design in terms of aerodynamic efficiency, low drag during different flight situations and a maximum lift coefficient of 1.78 during high-g turns. Using DATCOM methods for 3D corrections leads to a required 2D aerofoil lift coefficient of 2.1. Using a genetic algorithm and XFoil the optimal combination of aerofoils was found

for both lifting surfaces. The main wing features a NACA 9216-42, modified NACA four series aerofoil and the canard has a NACA 12311-62 aerofoil, see figure 24.3.

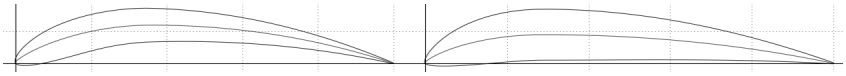

Figure 24.3: On the left: canard aerofoil, on the right: main wing aerofoil

The canard aerofoil was designed with a lower thickness to chord ratio than the main wing. A thinner aerofoil results in a sudden stall, which is desirable for the canard since the sudden loss of lift drops the nose of the aircraft, enforcing stall recovery before the main wing stalls. Furthermore, the canard has been designed with a relatively high cambered aerofoil and a larger aspect ratio than the main wing. This implies that the canard has a higher lift coefficient for a given angle of attack than the main wing, which promotes stall of the canard prior to the main wing.

In addition to the 2D aerofoil analysis, a 3D analysis was performed to study the effects that are introduced by the wing planform. Because the canard is located upstream of the main wing, it produces downwash and thus affects the flow over the main wing. The 2D aerofoil was implemented in XFRL5 and an analysis tool from ESDU (93015). The results were then compared to the required values for turning and landing performance. If the 3D results were found not to satisfy these requirements, the aerofoil design was modified and iterated until a solution was found. As can be seen from figure 24.4, the downwash from the canard reduces the lift at the inboard sections of the main wing. This analysis supported the sizing of the wing planform to ensure that the lift production of the wing and canard combined would be sufficient.

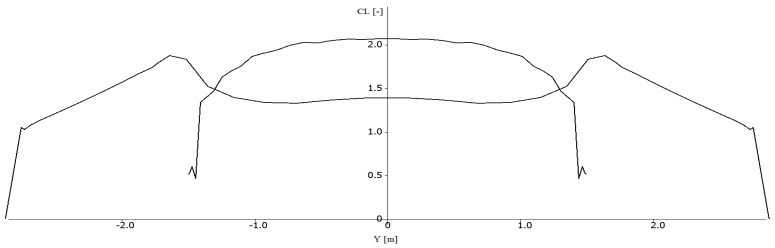

Figure 24.4: The interference of the canard on the lift distribution of the wing.

Finally, a drag estimation was performed using statistical analysis tools, which resulted in a zero-lift drag coefficient estimate of 0.034. The resulting preliminary wing design has an Oswald efficiency factor of 0.78. With an aspect ratio of 6 and a wing area of 5.2 square metres, the wing span is only 5.6 metres. The canard design features a maximum lift coefficient of 2.0 with an aspect ratio of 8 and area of 1.1 square metres. The relatively low velocities further imply that sweep angles are not required for either lifting surfaces, but more important was that zero leading edge sweep would minimize the flow propagation from root to tip, reducing the risk of tip stall. A taper ratio of 0.45 was found to be preferable for the main wing as it allows for a more elliptical lift distribution.

24.5 Structural analysis

The structural analysis includes the layout and material choices for the wing, canard, landing gear and fuselage design. Every subsystem in the structures group was designed to withstand the 18g ultimate load factor.

Fuselage

As a starting point for the structural fuselage design a monocoque structure was assumed in order to achieve a lightweight design. The different failure modes for a monocoque structure are strength failure and plate buckling of the skin. During the analysis of these failure modes it was discovered that stiffeners are required to prevent skin buckling, therefore resulting in a semi-monocoque design with two additional failure modes: column buckling and crippling of the stiffeners.

Accounting for all these failure modes, the design resulted in a simplified shape and 10 evenly spaced stringers with an area of 47.5 mm^2 and a skin thickness of 1.7 mm, which is also sufficient for impact resistance.

Wing and canard

Since no fuel tanks are required in the wings a foam sandwich structure was used for the wing and canard. For sandwich panels there are a lot of different failure modes of which face sheet strength failure or face sheet wrinkling were assumed the most critical for the design. The thickness is calculated based on the requirement that all the stresses in the face sheets would not exceed the ultimate shear or normal stress. For the normal stress the symmetric wrinkling stress was more critical than the material yield stress. Asymmetric wrinkling was deemed not critical because the core is thicker than 5 mm.

This resulted in a face sheet thickness for the wing that decreases continuously from 1.56 mm until the minimum thickness for impact resistance of 0.5 mm is reached. For the canard the face sheet thickness decreases from 3.9 mm to the minimum value of 0.5 mm.

Landing gear

For the main landing gear, it was decided to choose an off-the-shelf leaf spring design that meets the required height of 0.72 m to provide propeller clearance and to achieve the desired weight fraction on the nose wheel. The Lazer/Stephens-Acro gear of Grove Aircraft Landing Gear Systems Inc. was chosen.

24.6 Stability and control analysis

The stability analysis of a canard configuration shows that achieving stability and controllability is more difficult than for a conventional configuration. The possible range for the longitudinal centre of gravity position is very limited for a small canard area. However, due to the electric powertrain, the centre of gravity position remains fixed during flight. Furthermore the battery can be split into modules to set

the centre of gravity position where it is needed by distributing the modules accordingly.

By creating scissor plots using the relation between the area fraction of canard and main wing (S_c/S) and the longitudinal centre of gravity position (x_{cg}), as shown in figure 24.5, the requirements for stability and controllability can be determined. It is found that the furthest aft position of the centre of gravity is at 2.35 m from the nose of the aircraft. Moving the centre of gravity forward would require increasing the canard area.

The same analytical approach was taken for the vertical stabilizers, this time considering the stabilizer area with respect to the fuselage side area (S_{vt}/S_f). This fraction is again plotted over x_{cg}, shown in figure 24.5. Since the moment arm of the vertical stabilizer decreases with moving the centre of gravity (CG) back, smaller areas can be realized with a more forward CG, contradicting the findings for the canard size. Also, to keep the CG between the aerodynamic centre of the fuselage and the vertical stabilizers, the most forward position for the CG is at 2.28 m from the nose of the aircraft. Thus, a very limited CG-range is found. It is determined that x_{cg} should lie at 2.34 m from the nose. The results can be seen in table 24.1.

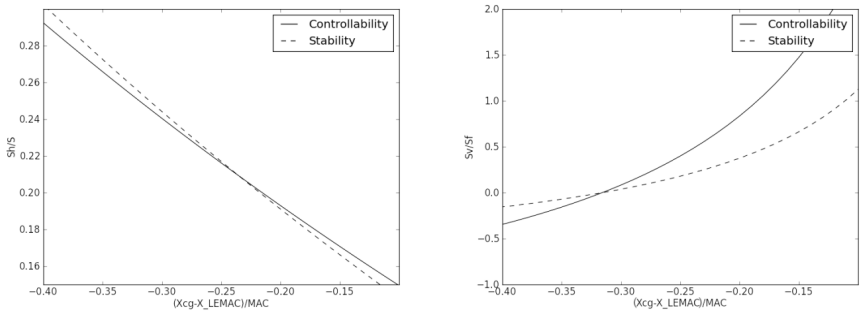

Figure 24.5: Longitudinal and directional stability/controllability curves on the left for the horizontal tail, on the right for the vertical tail.

Table 24.1: Required centre of gravity location and stabilizer area

c.g.	S_c	S_{vt}
2.34 m	1.14 m^2	0.3 m^2

In order to avoid that the vertical stabilizer disturbs the airflow through the propeller, a classical tail was replaced by two winglets. This has the advantage of not introducing asymmetrical airflow through the rotor.

The control surfaces sizes were estimated using a Torenbeek method based on reference aircraft and scaled to E-SPARC. Then the performance achieved was checked and the control surface were up- or downsized accordingly, to meet the requirements.

Typical for the Red Bull Air Race are the high roll rates that are required. Thus an aileron analysis was performed by setting up the equation of motion for rolling. Two aerodynamic coefficients needed to be estimated using a DATCOM method: the aileron effectiveness and roll damping coefficient. By simulating the response to a full aileron deflection a steady roll rate of 460 deg/s was obtained. In figure 24.6 the roll acceleration $\dot{p}$ and roll rate p are shown as function of time. As can be seen the steady state is achieved after only 0.5 seconds.

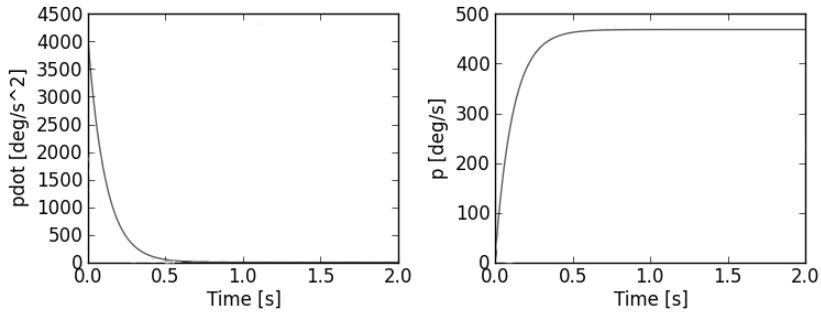

Figure 24.6: Roll behaviour at full aileron deflection and maximum velocity of E-SPARC.

24.7 Powertrain analysis

The powertrain is the subsystem where the differences between an EV and a conventional aircraft are extremely well visible. The overall powertrain efficiency is improved due to the high efficiency of the electric motor and the battery. Components that were sized and/or designed are the propeller, drive shaft, electric motor and the battery pack.

Propeller design

The propeller design has been conducted with the methodology from McCormick (1979) and XRotor, of which the latter uses an extension of the classical blade-element/vortex formulation. The aim of the propeller design was to reach high power and thrust at a high efficiency. The result was a custom designed, 3-bladed, composite, single propeller with a diameter of 1.62m, which still allows for sufficient ground clearance. A contra-rotating propeller design was considered but resulted in a higher system weight despite the slightly improved efficiency and ground clearance. It would also increase cost and complexity.

Motor design

The electric motor was sized in parallel with the propeller. The main reasons are torque matching of the propeller and electric motor, as well as an efficient operating range of the electric motor at certain rotational speeds. Matching the torque avoids the need for a gearbox and only a direct driveshaft is required. For these reasons a rotational speed of 2750 revolutions per minute was chosen. This rotational speed of 2750 revolutions per minute in combination with the required diameter of the propeller (for the thrust) resulted in blade tip velocities below Mach 0.7 at sea level altitude. The chosen electric motor has a power density of 5.2 kW/kg, based on the newly developed electric motor by Siemens. It was assumed that before 2019 a motor can be manufactured with the same characteristics as the YASA 750, but with a much higher rated power output of 136.4 kW.

Battery pack

A major component within the powertrain is the battery pack, which amounts to approximately a fourth of the maximum take-off weight. The battery pack design was based on Lithium-Sulfur Ultra Light Pouch Cells by Oxis Energy, with an expected specific energy of 500 Wh/kg and a cycle life of 1500 cycles in 2019. The battery pack was optimized for low weight, resulting in a mass of 100.7 kg, corresponding to a capacity of 50.37 kWh. It has 273 cells in series and 12 cells in parallel. Due to a confined fuselage volume and very restrictive stability and controllability requirements, the battery pack was split into 12 modules, also increasing the reliability of the battery pack. These modules allowed for enough flexibility regarding the volume and CG limitations. A feasibility study proved that air cooling would be very well possible by applying a so-called parallel cooling strategy for the modules. Figure 24.7 gives an overview of the electrical power flow in the powertrain.

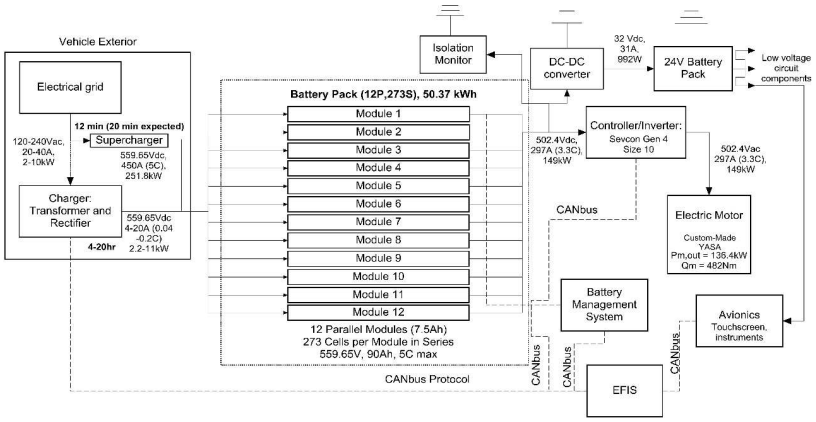

Figure 24.7: Electrical power flow diagram

24.8 Final preliminary design

E-SPARC's preliminary design lay-out is presented in figure 24.8. This preliminary design is the result of the accumulation of the aforementioned design decisions. A systems engineering design approach ensured consistency of design values, despite the constant need to update parameters. An overview of the significant geometric parameters for this preliminary design is given in table 24.2.

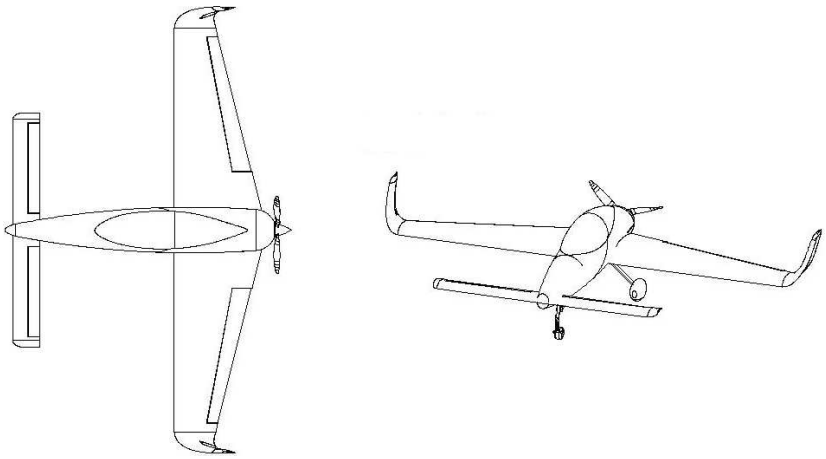

Figure 24.8: Exterior lay-out of E-SPARCs preliminary design

More importantly, the performance characteristics of E-SPARC are also given in table 24.2. In addition to the performance characteristics listed in table 24.2, a track analysis was performed to simulate E-SPARCs performance around the 2008 San Diego, Red Bull Air Race track.

The track analysis was a simulated race against the EXTRA-300S which raced the actual track in 2008. The EXTRA-300S flew the simulated track in 93 s while E-SPARC took 2 s longer with 95 s. Even though E-SPARC is slower, this does not mean the E-SPARC concept is not feasible, it still shows the feasibility of an electric racer. Even with the current track time E-SPARC would provide an exciting race and would show feasibility of a high performance electrically propelled aircraft, which is its main objective.

Table 24.2: Geometric parameters and performance characteristics of E-SPARC

Geometric Parameters			Performance Characteristics		
Parameter	Value	Unit	Parameter	Value	Unit
Wing span	5.56	[m]	Maximum speed	101.6	[m/s]
Wing aspect ratio	6	[-]	Stall speed	29.3	[m/s]
Wing taper ratio	0.45	[-]	Maximum rate of climb	15.3	[m/s]
Wing sweep quarter chord	-3.6	[deg]	Maximum roll rate	460	[deg/s]
Canard span	3.02	[m]	Ultimate load factor	18g	[-]
Canard aspect ratio	8	[-]			
Canard taper ratio	1.0	[-]			
Canard sweep quarter chord	0.0	[deg]			
Vertical fin area	0.3	[m2]			
Fuselage length	4.0	[m]			
Propeller diameter	1.62	[m]			
Energy stored	50.37	[kWh]			
Power output	115.5	[kW]			
Take-off mass	417	[kg]			

24.9 Recommendations

The most important part is to increase the power to weight ratio and decrease the drag, this will result in a higher thrust and thus a higher speed and faster accelerations. From the track analysis it was found that the thrust of E-SPARC is not sufficient at this point to provide the needed accelerations to win the Red Bull Air Race. Several iterations should still be done to increase the performance of E-SPARC. In further design steps the aircraft and its subsystems have to be further refined and optimized, using for example CFD analyses and wind tunnel tests to further optimize the aerodynamic design. While these activities will influence the current design parameters it can be concluded that E-SPARC, as presented now, has proven the feasibility of an electrically propelled high performance aircraft.

25. ADVANCED REGIONAL AIRCRAFT

Students: M.P. Bobeldijk, M. Blom, A.M.R.M. Bruggeman, D.J.H. Cederløf, M. Haddaoui, F.S. Heeres, K.J.M. Mattheus, U. Mehmood, P.C.L. Mestrom, M. Miedema

Project tutor: ir. J. Sinke

Coaches: prof. dr. R. Curran, dr. M. Hernandez

25.1 Introduction

Regional aircraft are used on short routes to transport passengers between smaller airfields as well as hub airports. Market forecasts predict that the regional aircraft market will grow significantly in the coming 20 years. Therefore, a regional aircraft capable of dominating the regional aircraft market is designed. The mission statement is as follows:

"Design a competitive regional aircraft that implements the latest technologies and is market-ready in 2025."

25.2 Requirements

The Advanced Regional Aircraft (ARA) should comply with several requirements that are listed below.

- The production of the aircraft shall have a high degree of automation.

- The new aircraft shall be designed with the latest technology, implementable within 5-10 years.
- The production of aircraft shall comprise 25 aircraft per month with an option to increase to 40 per month.
- The maximum runway length at sea level shall be 1,500 m at MTOW.
- The minimum range of the aircraft shall be 1,500 km.
- The number of passenger shall be in the range of 75-90 passengers.
- The aircraft shall comply with the latest regulations (2015).
- The aircraft shall have a 10% lower fuel burn on a 1,000 km trip when compared to a direct competitor that is in operation today.

25.3 Conceptual designs and trade-off

The configuration of the ARA is based on the aircraft type, wing position, engine type and engine location. The considered options are given below.

- Aircraft type: three-surface, canard or conventional aircraft.
- Wing position: low wing, mid wing and high wing.
- Engine type: turbofan, turboprop, Geared TurboFan (GTF) and the Open-Rotor Engine (ORE).
- Engine location: wing, fuselage or tail.

First of all, the concepts were checked for feasibility with respect to the client and airworthiness requirements. Secondly, a trade-off was performed for all of the remaining options with the following criteria: structural weight, aerodynamic efficiency, fuel efficiency, noise emission, development risk and maintenance cost. In figure 25.1 the four concepts with the highest trade-off scores are shown. From the trade-off it was found that the three-surface aircraft with ORE mounted at the tail configuration (bottom-left in figure 25.1) was the best choice for the ARA.

However, after consulting the client and external sources it was decided that this configuration is not realisable within 10 years. Therefore, the second best option was chosen which is the conventional aircraft with GTFs mounted underneath the wing (top-

left in figure 25.1). The engines are housed in chevron nacelles to reduce the noise emissions. From a trade-off it was determined that jet-A1 fuel is the best fuel choice for the ARA, fuel types such as LNG and hydrogen were deemed unfeasible in the coming 10 years. The option for bio-fuel is reserved for the aircraft operator and can be implemented in the ARA. By using GTFs instead of conventional turbofans it is possible to achieve a reduction of 27 million euros (jet fuel A1 spot price at May 2015) over the ARA's lifetime (30 years).

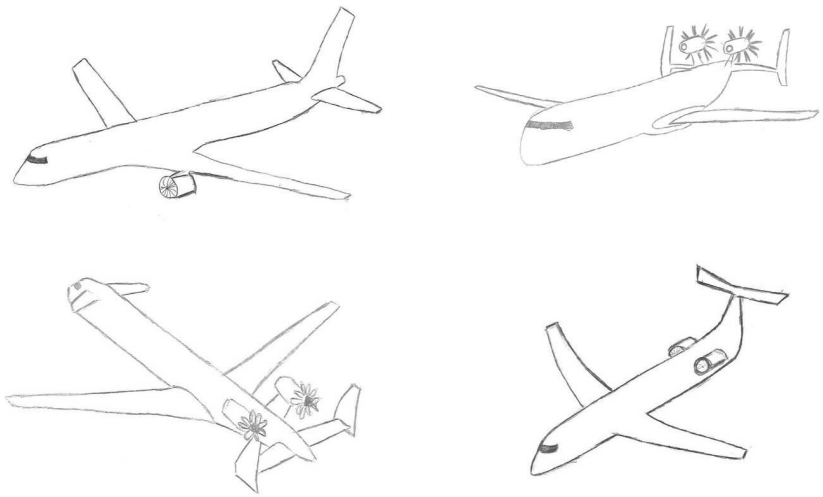

Figure 25.1: Conceptual design configurations

25.4 Details of final design

Main wing

The ARA has a low mounted wing and throughout the wing a single aerofoil is used, namely the NACA-1408. At a wing sweep angle of 27° this aerofoil scored the highest in a trade-off based on 70 aerofoils. In order to achieve the required lift during take-off and landing at an acceptable angle of attack double-slotted Fowler flaps are used. The flaps are located at the leading edge span from the root to 70% of the wing span. In table 25.1 the characteristic wing dimensions and parameters are given.

Spoilerons are implemented to allow for roll control at high speeds. For low speed roll control outboard ailerons are used. For the ARA, it was decided to specifically investigate morphing ailerons. In a later phase the theory used and knowledge obtained could be implemented on other control surfaces to optimise the aircraft further. In a trade-off, four concepts were evaluated. The criteria on which the selection took place were weight, maintenance, morph-ability, development risk, reliability and noise. The concept with the most potential is the Fishbone. This concept is shown in figure 25.2.

The Fishbone is a compliant mechanism; this greatly reduces the amount of separate parts used. As a result, this increases the reliability of the ailerons. The Fishbone is designed in such a way that it allows for a maximum deflection of 25° and by having several individual actuators in the span-wise direction the aileron can also twist. This results in an aileron that can delay flow separation to a great extent in each flight phase and as such achieve improved aerodynamic performance throughout the flight.

The Fishbone can be visualised as a central beam connected to a very elastic skin via a number of stringers and ribs; all spaced in an structurally optimised way. The most aft 6% of the aileron is solid and has tendons connected to it, which are connected to a pulley in front of the aileron. By pulling the tendon on the upper or lower side of the aileron, the aileron deflects towards that side. The aileron itself is integrated in the main wing through transition regions. These ailerons need to be very flexible and able to withstand many load cycles. They are made out of Ultra High Molecular Weight PolyEthylene (PE-UHMW), as is the skin, which is very durable in all weather conditions. The beam, stringers, ribs and trailing edge, are an integral part with different mechanical needs. They are constructed out of an unidirectional epoxy reinforced glass fibre composite.

The FLOTIN winglet of the ARA comprises of an optimised Whitcomb configuration with raked tips. Combining the aerodynamic and structural analysis, the winglet has an aerodynamic efficiency of 10% when compared to a wing without winglet, but has an added

structural weight of 3%. The total fuel reduction due to the winglet is approximately 6%.

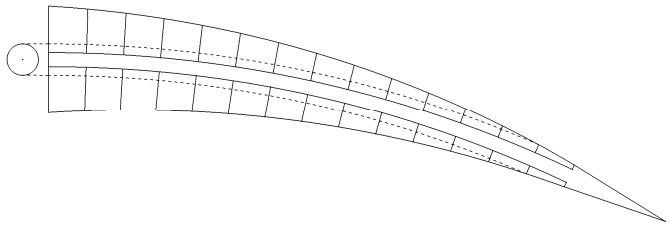

Figure 25.2: The Fishbone aileron concept

Landing gear

The ARA has a tricycle landing gear configuration due to superior ground steering capabilities and allows the pilots to take-off, land and taxi with more ease. Furthermore, the tricycle landing gear configuration levels the aircraft resulting in more comfort for the passengers when on the ground.

The operational efficiency of an aircraft operator can significantly be improved by taxiing using an Electrical Green Taxiing System (EGTS). Each wheel of the main landing gear is equipped with an electric motor to propel the aircraft. The APU generator is used to power these motors. This way, the aircraft can taxi without the use of the main engines. EGTS results in savings up to 4% of total block fuel. Furthermore, green taxiing reduces exhaust and noise emissions significantly. The aircraft is also able to perform its own pushback without the assistance of a tug leading to faster turnaround times.

Empennage

For the boundary layer control of the empennage, sweeping jet actuators and micro vortex generators were investigated. The jet nozzles eject air that flows over the tail to energise the boundary layer and thus delaying flow separation. The possibility of having sweeping jet actuators to control the flow over the rudder was discarded, since the disadvantages such as the weight of the actuation system, complexity, reliability and power consumption outweigh the advantages of jet actuators. Vortex generators are small vanes

mounted upwards that are used to influence the airflow over the aircraft by delaying separation. Besides applying them on the empennage, they will also be used on the nacelles and the wing. This is a relatively cheap and convenient approach to boundary layer control.

The horizontal tail area was sized in order to comply with the stability and controllability requirements. The vertical tail area was determined from reference aircraft. The horizontal and vertical tail area can be found in table 25.1. Based on the airworthiness regulations, the elevator was sized. On an aircraft with a tricycle landing gear, the elevator must be able to rotate the aircraft about the main gear and lift the nose with specified angular pitch acceleration. For the dimensions of the ARA, this results in a required pitch angular acceleration of $4.00^{\circ}/s^2$. After the required angle of attack at take-off was determined to be 14.3°, moments were taken around the main landing gear to determine the required lift of the horizontal tail surface. By using the maximum deflection of the elevator for the ARA of 25°, the required elevator surface area was determined to be 7.28 m^2.

The rudder was sized for the one engine inoperative condition. By keeping the rudder deflection with the maximum of 30°, a rudder area was determined of 5.10 m^2. The rudder does not take up the entire vertical tail span, which results in additional structural support. The final empennage sizing parameters are shown in table 25.1.

Fuselage

In figure 25.3 the 4 abreast single class cabin layout is presented. A two class configuration is possible as well. All cargo is stored in a separate section behind the cabin allowing faster ground operations. Following detailed structural analysis of metal and composite fuselage structures, a custom high strength carbon fibre reinforced PEEK (HSCF-APC2) composite with optimised ply orientation was found to be the lightest. A life cycle analysis showed that this material choice lowers the fuel consumption by 5% over the life of the ARA.

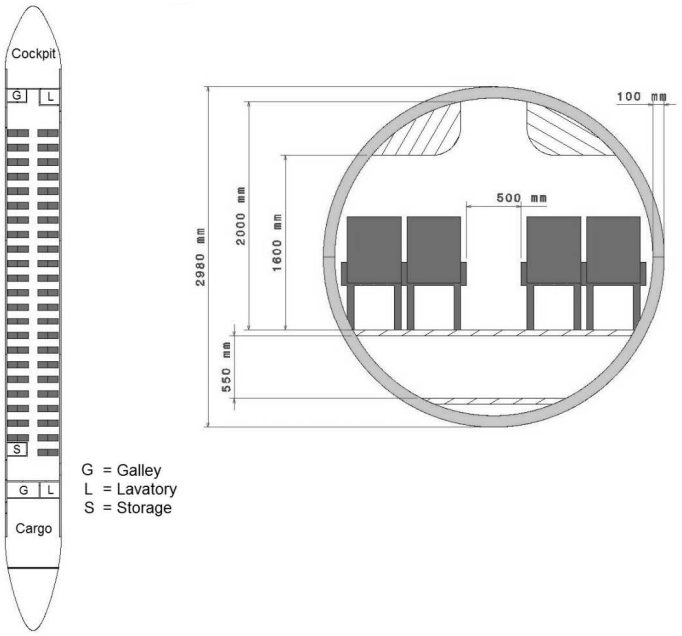

Figure 25.3: Fuselage lay-out for a one-class configuration

25.5 Performance

In figure 25.4 the payload versus range diagram of the ARA can be found. Point A indicates the harmonic range of the aircraft of 1,500 km, point B indicates the design mission range of the ARA of 2,000 km, point C indicates the maximum range of 2,250 km that can be obtained when the ARA takes off at MTOW with full fuel tanks and reduced payload and point D indicates the ferry range of 4136km. Performance parameters such as maximum thrust, take-off distance, stall speed, etc. can be found in table 25.1.

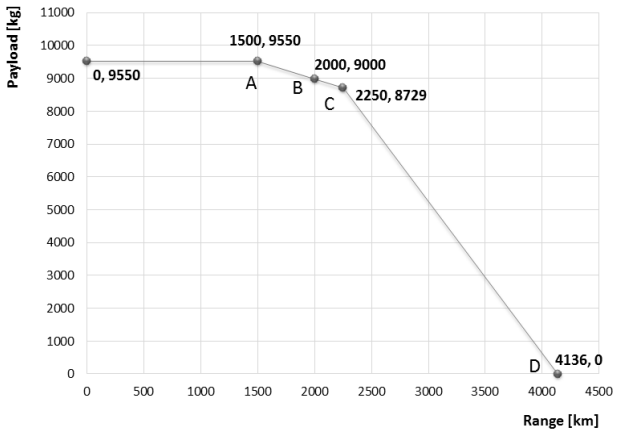

Figure 25.4: Payload versus range diagram of the ARA

25.6 Conclusions and recommendations

From trade-offs it was found that the best configuration for the ARA is a conventional configuration with GTFs mounted underneath the wing and a conventional tail. Morphing ailerons are used in order to increase the aerodynamic efficiency and reliability, and to reduce the maintenance costs. Furthermore, by adding the custom FLOTIN winglet the fuel efficiency of the ARA is increased significantly. Using micro vortex generators for the empennage the stall speed and runway length is reduced. By using the HSCF-APC2 composite for the fuselage a significant reduction in weight is obtained and the frequency of scheduled maintenance checks can be reduced due to outstanding environmental resistance properties, as has already been demonstrated on other composite aircraft. Lastly, by implementing an EGTS the turnaround times and the level of required infrastructure are reduced, resulting in lower operational costs.

The main design parameters of the ARA are shown in table 25.1 and the final design is presented in figure 25.5. It is recommended to refine the ARA structurally and aerodynamically using CFD and FEM analysis techniques. Furthermore, it is recommended to initiate prototyping, testing and certification processes for novel technologies (such as the morphing control surfaces) as soon as possible to ensure full compliance with airworthiness regulations.

Table 25.1: Main design parameters of the ARA

Parameter	Symbol	Value	Unit
Aspect ratio (including winglets)	A	10.8	[-]
Aerofoil	-	NACA-1408	[-]
Cruise altitude	h_{cruise}	11,000	[m]
Cruise Mach number	M_{cruise}	0.8	[-]
Design range	R_{design}	2000	[km]
Dihedral angle	Γ	3	[°]
Fuselage diameter	d_{fus}	2.98	[m]
Fuselage length	l_{fus}	35.8	[m]
Horizontal tail area	S_h	27.3	[m2]
Horizontal tail span	b_{ht}	11.7	[m]
Incidence angle	i	1.84	[°]
Landing distance	x_{land}	1,400	[m]
Landing stall speed	$V_{s,land}$	48.9	[m/s]
Maximum fuel weight	$m_{fuel,\ max}$	5,800	[kg]
Maximum Take-Off Weight	MTOW	34,465	[kg]
Maximum thrust	T_{max}	152	[kN]
Number of crew	#crew	2+2	[-]
Number of passengers	#pax	90/81 (1-class/2-class)	[-]
Operational Empty Weight	OEW	19,945	[kg]
Quarter-chord sweep angle	$\Lambda 0_{.25c}$	27	[°]
Root chord	c_r	5.77	[m]
Seat pitch	x_{pitch}	31	[inch]
Take-off distance	$x_{take\text{-}off}$	1,400	[m]
Take-off stall speed	$V_{s,take\text{-}off}$	48.9	[m/s]
Taper ratio	λ	0.3	[-]
Tip chord	c_t	1.73	[m]
Unit cost	-	42,000,000	[EUR]
Vertical tail area	S_v	21.0	[m2]
Vertical tail span	b_vt	6.31	[m]
Wing area	S	104.8	[m2]
Wing span	b	31.9	[m]

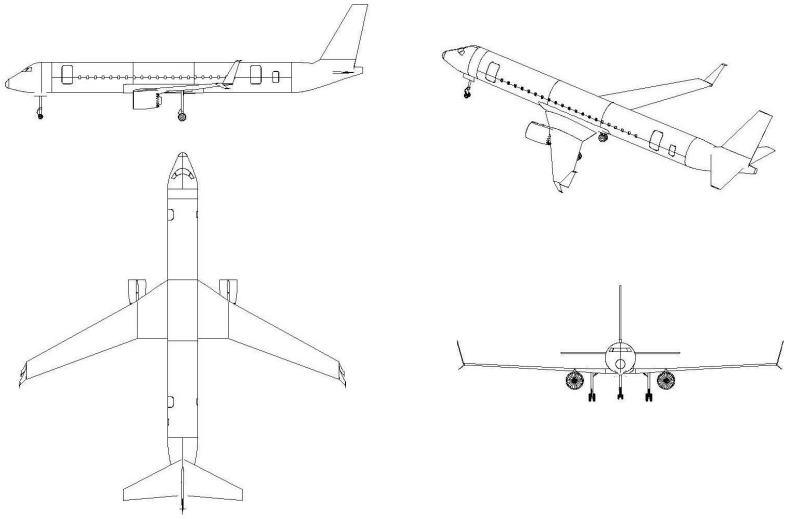

Figure 25.5: Four views of the final design of the ARA

The final design of the ARA meets all of the requirements stipulated in section 25.2 except the requirement that the production of the aircraft shall produce 25 aircraft per month with an option to increase to 40 per month. After an extensive market analysis it was found that if this requirement was satisfied, the total demand of regional aircraft would be satisfied in 4 years. This requirement was not met as the high production rate for a relative small amount of products is not cost effective. Furthermore, the orders range from 2020 until 2035 and therefore the orders are spread over 15 years instead of 4 years.

26. A QUIET, ADVANCED, LOW-EMISSION REGIONAL JET, THE QLEAR Q-50

Students: D.K. Arnell, T.E. Boogaart, S.C.D. Hellemans, A. Ion, R. Nederlof, N. Nuus, M.U. Oudkerk, G.N. Pappie, T.F. Spaan

Project tutor: dr.ir. W.J.C. Verhagen

Coaches: G. Correale MSc, dr. A. Cooperman

26.1 Introduction

With sustainability becoming an important aspect of our lives, gaseous and acoustic emissions need to be continuously reduced significantly. QLEAR Q-50 is a revolutionary 50-seat, low emission regional jet, which will serve as a stepping stone towards sustainability, meeting the strict emission reduction requirements set by the European Commission for 2050.

26.2 Objective and requirements

The objective for this project was

"to design a regional jet aircraft, comparable to the Bombardier CRJ200 or Embraer ERJ145, however with improved emission characteristics."

The design should comply with the following requirements:

- 50 seat capacity.
- Maximum range of 2,000 km.
- Minimum cruise speed of Mach 0.75.
- Service ceiling of 10,278 m.
- 50 % reduction in CO_2 emission.
- 25 % reduction in NO_x emission.
- 50% reduction in acoustic emission.
- MTOW should not exceed 23,000 kg.
- Unit cost should not exceed USD 35 million (2014 level).
- Return on investment should be 5% after 5 years.
- Scheduled entry into service in 2035.

26.3 Market analysis

Urbanization is a phenomenon that has been present for centuries, and is expected to continue. Urbanization will further boost the demand for air transportation, as today's market concentrates on connecting larger cities. Therefore it is expected that the low and mid-density markets will experience a boom, making regional aircraft an essential element for the future of the aircraft industry.

The next step is to take a look at the stakeholders of the regional jet market at this moment and identify the potential position of the Q-50. In the 50 seat market at this moment, the main competitors would be CRJ200, ERJ145, and ATR42. However, the CRJ200 is no longer produced and will therefore slowly fade out of the market, creating a niche which can be filled by the Q-50. The market share that will be captured is expected to be around 35%, allowing slight growth for ERJ and ATR and leading to a production of 805 Q-50 aircraft.

26.4 Concepts studied

In the preliminary design phase, 16 concepts were considered. The concepts included several wing configurations and propulsion

systems. Among others, a Prandtl wing was considered, as well as distributed propulsion and a hybrid design. After a trade-off, eliminating for concepts that included too many novelties to be feasible (for example Prandtl wing combined with hybrid propulsion), only three concepts were left and they were compared to each other in more detail. The three concepts that were studied in order to come up with the best configuration to meet the requirements can be seen in figure 26.1.

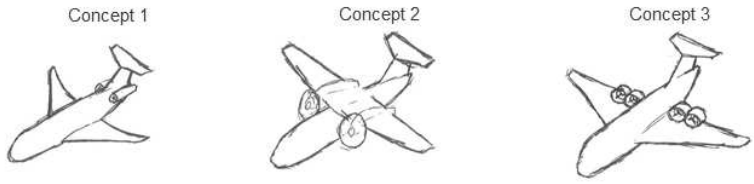

Figure 26.1: Concept drawings

Concept 1 is a conventional design, very comparable to the competition, with a low wing configuration, a T-tail, and two turbofan engines positioned on the rear fuselage. The second concept is a high wing configuration with wing mounted turboprop engines and the third concept is a hybrid design with ducted fan engines. In table 26.1 the most important properties of the three concepts are shown.

Table 26.1: Concept characteristics

	Concept 1	Concept 2	Concept 3
MTOW [kg]	20,860	21,932	26,444
OEW [kg]	11,000	14,000	14,500
Unit price [million USD]	19.11	26.93	25.59
Power required [kW]	1,617	1,250	2,000
Cruise speed [Mach]	0.75	0.55	0.55
CO_2 [kg/min]	40.4	29.7	29.7
NO_x [kg/min]	38.3	19.6	15
Noise [EPNdb margin from stage IV]	20	16	22

26.5 Trade-off process

During the trade-off process a lot of specifics became clear, and therefore the need for a more analytical trade-off method arose. As a solution, the Analytical Hierarchy Process (AHP) was applied, where all criteria are compared with each other, one by one. After comparing the criteria, a matrix is set-up of which the eigenvector determines the criteria weights. The criteria and corresponding weights, that were compared in order to perform the trade-off are presented in table 26.2.

Table 26.2: Concept trade-off criteria and weights

Criterion	Weight
Emissions	46.2 %
Performance	17.8 %
Cost	27.4 %
Risk	8.6

Emissions are considered to be a killer requirement, therefore this criterion gets the highest weight. Cost is considered the second most important criterion, as an expensive, non-profitable aircraft will not be sold and therefore continuing the design would be a waste of time. Performance comes third as all three concepts will be able to fly at reasonable speeds and altitudes, with a reasonable weight. The idea behind this is that whenever the aircraft is able to perform, have low emissions and have reasonable costs, it does not matter how much the aircraft weighs or if it flies at Mach 0.7 or 0.8. The least important in this case is the risk criterion. Of course low risk is beneficial, however all design choices are made with the safety regulations in mind. Besides that, one should be aware of the fact that whenever new ideas and novel technologies are implemented, risks have to be taken. These risks will not endanger the safety of the passengers.

Afterwards, a grading method was set-up, to grade each concept on each criterion fairly. When a concept performed really bad, a 1 was given and when a concept performed outstandingly a 9 was given. A grade of 5 meant that the concept performs as the competition (CRJ200, ERJ145). Using this trade-off method, concept 1 was the winner and was used in the final design phase.

26.6 The QLEAR Q-50

As was explained in the previous section, concept 1 was selected to enter the final design phase, what would end up as the QLEAR Q-50. Where QLEAR is an acronym of the characteristics that define our design philosophy: Quiet, Low Emission, Advanced, Regional. Q-50 indicates the 50-seater type. In figure 26.2 the final design is shown. In the following sections the most advanced systems of the aircraft, which cause the Q-50 to be a revolutionary design, are presented and discussed.

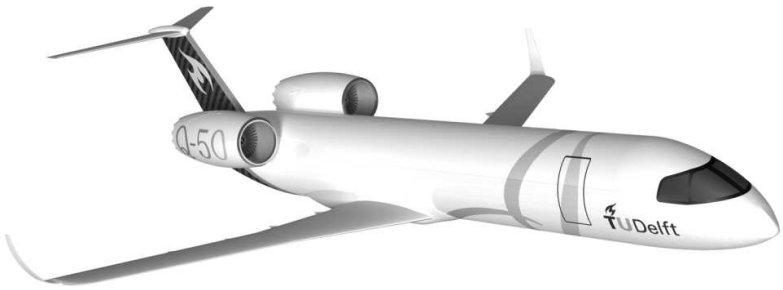

Figure 26.2: The QLEAR Q-50 design

Wing design

From the first class weight estimation, the required wing surface was determined and this was the start of the wing design. Keeping in mind that elliptical lift distribution is most favourable, the taper ratio and the sweep angles were determined and the planform design was finalized. Another important aspect of the wing design was the aerofoil selection. For the aerofoil selection also the analytical hierarchy process was applied, yielding the criteria weights shown in table 26.3.

Table 26.3: Aerofoil trade-off criteria and weights

Criterion	Weight
Critical Mach number	53.3 %
Lift over drag	27.7 %
Maximum lift coefficient	11.4 %
Moment coefficient	7.6 %

Where the critical Mach number was considered the most important criterion, as shock waves lead to separation and a huge increase in drag which is highly unfavourable. After this trade-off, the EQ 1030/3070 aerofoil was determined to be the most suitable. However, from a structural point of view it became clear that inserting and designing a wing box in such a curvy aerofoil was going to be a very lengthy process. Therefore the second best option, the NACA 07-411, was eventually chosen as the wing profile, having a very straight lay-out. The geometry of the NACA 07-411 wing profile can be seen in figure 26.3.

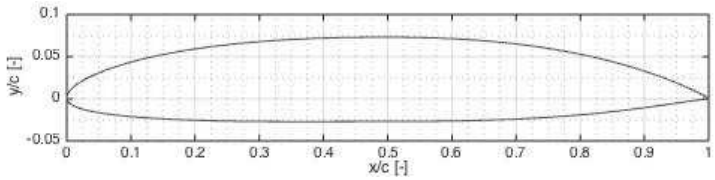

Figure 26.3: NACA 07-411 geometry

The NACA 07-411 has a maximum thickness to chord ratio of 11% which is very thin, as thicknesses between 12 and 15% are commonly found. This very thin aerofoil leads to a lighter wing and high aerodynamic performance.

Another aspect of wing design is the design of the high lift devices, spoilers and ailerons. The sizing criterion for the high lift devices is that they should be able to provide the lift coefficient increment necessary to land. This criterion leads to double slotted flaps at the trailing edge, and full span slats at the leading edge. The outboard section of the trailing edge that is not occupied by flaps is occupied by the aileron. The spoilers were designed such that the landing distance requirement of 1,500 m can be met. In figure 26.4 the final lay-out of the wing can be seen. Table 26.4 also shows the values of the wing geometry.

Another feature of the wings is the addition of blended winglets, that reduce the vortices produced at the wing tips and therefore reduce the drag, hence reduce the fuel consumed and the emissions.

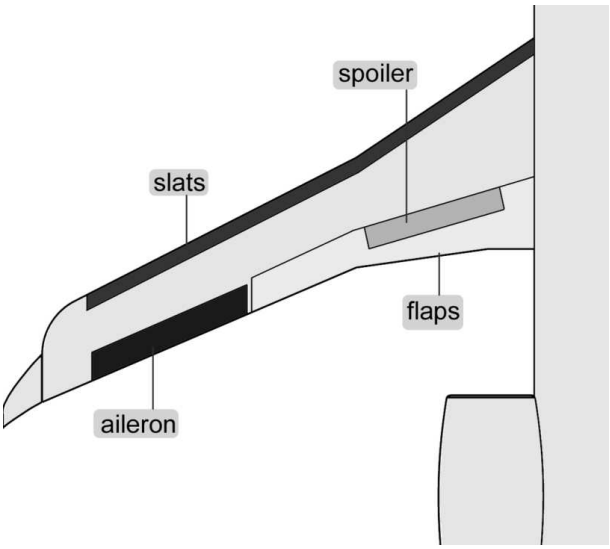

Figure 26.4: Wing planform

Tail design

Having designed the wing and its subsystems, the next step was to design the tail with T configuration. A distinction is made between the horizontal and vertical tail design. One of the differences appears for example in the choice of aerofoil. For both segments a symmetric aerofoil is needed, as the surfaces need to be able to provide both positive and negative forces. However the vertical tail needs a slightly thicker aerofoil, as it needs to be strong enough to support the horizontal tail. On the other hand a symmetrical aerofoil means a lower critical Mach number and therefore needs a higher sweep angle.

Another important part that comes into play when designing the tail is the design of the control surfaces, elevator and rudder, the main stability providers. In order to size the elevator, the take-off configuration was considered as the most critical phase, since the horizontal stabilizer is required to provide enough negative lift to assure a certain rotation angle during take-off. For the rudder design the cruise phase was determined to be the most critical. In figure 26.5 the outcome of the tail analysis is shown.

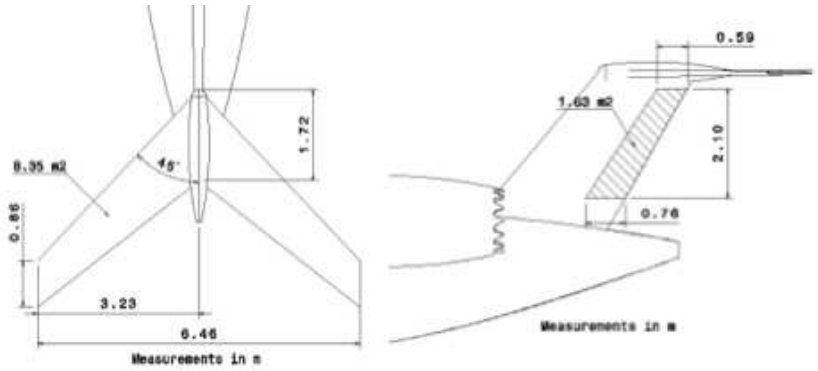

Figure 26.5: Horizontal and vertical tail geometry

Materials

The design philosophy during the design was to keep everything as light as possible, which was possible due to the high unit cost requirement of 35 million dollars. This opened doors for more advanced materials such as composites over ordinary aluminium. With the use of composite materials, the weight can be significantly reduced which gives a lower required thrust and therefore a lower required fuel consumption. 50% of the Boeing 787 Dreamliner has been made out of advanced composite materials.

This use of composites in the airliner saved 20% in the total aircraft weight. This weight reduction comes at a cost however. As explained the price of composites is significantly higher than metals, and also the operating costs are higher.

The QLEAR Q-50's structural parts such as the wing box, tail structure, and fuselage will be made of Carbon Fibre Reinforced Plastic (CFRP). The stiffening elements will also be made out of CFRP and they will be bonded to the skins. The CFRP used will be Hexcel M91. CFRPs are expensive and therefore Glass Fibre Reinforced Plastics (GFRP) will be used for less structurally demanding components, for instance the cockpit panels, overhead bins, and the inner walls of the fuselage. Honeycomb structure will be utilized in the control surfaces because they allow for very light and strong structures however they have a large volume, but this is not a problem

for the control surfaces. The floor in the cabin is another component made of a honeycomb structure.

Lastly the engine utilizes a large range of materials. Most of which are metal alloys. Ceramics such as Ceramic Matrix Composites (CMC) are used for turbine blades because of their high temperature tolerance. Ti-6Al-4V, A titanium alloy, is used for engine parts that operates under less high temperatures, think of compressor blades. Another advantage of titanium alloys is their high strength to weight ratio. It does come at a higher price. Finally the engine cowling and fan are made of Aramid Fibre Reinforced Plastics (AFRP) in order to achieve a weight reduction.

Propulsion system

With both noise and gaseous emissions being part of the most important requirement, it was decided that a new turbofan should be designed by the team. The design will be made by the QLEAR Q-50 team themselves. Multiple new technologies will be used on the new engine, all of which will be explained next. First of all the fan will be geared to allow for different rotational speeds for the fan and for the low pressure compressor. This allows for a more optimal design for both the fan and the compressor, since both can be operated at their respective optimal rotational speeds.

Since the fan is large, the tips can reach supersonic speeds. Therefore, in a normal twin spool engine the low pressure compressor speed is limited by the fan maximum rotational speed. When a gearbox is used, the compressor speed can be increased, which will improve the pressure ratio without creating shockwaves at the fan tips. The gearbox does add weight to the engine but the increase is compensated by a lighter engine cowling.

The engine cowling, fan casing and fan itself will be made from composites which will compensate the weight increase. General electric has used composites on their latest engines which in their case saved 160 kg. This engine is a bit more than twice as small and the weight saving will therefore be around 60 to 70 kg. This will suffice

for the increase in weight from the gearbox. But the gearbox is not the only weight increase. The engine will use an intercooler to reduce NO_x emissions.

An intercooler cools down the temperature of the airflow after the compressor. In this design the intercooler will be placed behind the low pressure compressor and instead of using a cooling fluid the bypass airflow is used for cooling the flow. This gives a lower core flow temperature which reduces the NO_x emissions. It also increases the bypass airflow which gives a better gas mixing at the nozzle and a slightly increase in thrust from the bypass flow. Downsides are the increased weight and the complexity of an intercooler. In order to get the desired temperature drop the intercooler must work very efficient.

In order to see what the required pressure ratios and efficiencies for the components are a model was made using Gas Turbine Simulator 11 by NLR. GSP allows for intercooler simulation and gives estimations for emissions. Using the software, the effectiveness of the intercooler can be checked. It can be seen that the performance decreased due to the pressure loss introduced by the intercooler, but the CO emissions halved and the NO_x emissions dropped 25 %. The CO_2 emissions where lowered because of the higher pressure ratios which meant a lower required fuel consumption than the competition. Furthermore the maximum thrust at sea level is 34 kN and the specific fuel consumption at sea level is 0.32 lb/lb/hr.

Fuselage

One system that makes the Q-50 revolutionary by its looks and design, is the windowless fuselage, which is currently not present on the regional jet market. The reason for not choosing windowless is the fact that windows need to be replaced by screens in order to maintain passenger comfort by showing the surroundings. Screens are heavy and expensive and therefore it nullifies the benefit of a lighter fuselage structure due to the lack of cut-outs. However, as technology keeps on improving and innovating, new opportunities present themselves. With paper thin OLED screens being produced at the moment, and assuming a price evolution comparable to the LED screens, a

windowless fuselage actually becomes a great advantage and would be feasible in 2035. The structural analysis during the design phase is greatly simplified, the operational empty weight is reduced, and savings in operational costs of at least 400,000 dollars per life span are achieved. The interior of the cockpit and fuselage will be up to standards, using NextGen navigation systems and providing the passengers with Wi-Fi and power ports on board.

Apart from the technical advantages, the unique image of the Q-50 and the high tech screens that are present in the cabin will appeal to the whole target market.

26.7 Conclusions and recommendations

The main characteristics of the Q-50 have been discussed and a factsheet is presented in table 26.4

Table 26.4: Q-50 factsheet

Scheduled entry into service	2035
Crew	2 + 1
Seating capacity	50
Length	26.4 m
Wing span	19.2 m
Height	6.25 m
Wing area	43 m2
Fuselage diameter	2.6 m
Turn radius	22.8 m
Take-off thrust	55 kN
Max. payload weight	5,000 kg
Empty weight	9,755 kg
Max. take-off weight	17,420 kg
Range	2,000 km
Cruise speed	867 km/hr
Flight ceiling	10,278 m
Time to climb	7.2 min
Maximum climb angle	11 degrees

It can be concluded that a quiet, advanced, low-emission, regional jet, in other words the QLEAR Q-50 is ready for the next step. The next step for the Q-50 will be to enhance the design, by performing more extensive calculations and real-life tests. For example the wing should undergo several wind tunnel tests in order to increase its performance and to identify the right implementation of the winglets. Another aspect of this design that cannot do without real-life tests is the determination of the noise-level. After the design is complete and all tests have been performed, the production of the Q-50 aircraft can start.

27. DISTRIBUTED PROPULSION FOR COMMERCIAL TRANSPORT AIRCRAFT

Students: A. Bhowal, L.E. van den Ende, M.P. van Hoorn, M.J.C. Kolff, V. Margos, R.F.H. van Maris, J.I. Nijsse, T.E.H. Noortman, J. Peeters Salazar, F.T.H. Wong

Project tutor: dr.ir. M. Voskuijl

Coaches: Ir. D. Peeters, Ir. O. Stroosma

27.1 Introduction

Currently, many industries focus on becoming more environmental friendly. This is due to the depletion of natural resources, but it also offers benefits in terms of marketing, public relations and cost. One of the industries which is inspired in becoming greener is the aerospace industry. Aircraft have become more and more efficient and less polluting over the past years and this trend will likely continue. However, to sustain this trend new aircraft concepts which offer better performance have to be researched and developed. One of the ways to lower the fuel consumption and reduce the emissions is by making use of a distributed propulsion system. The designed aircraft features such a propulsion concept and is called Vimana.

Distributed propulsion is the discipline of spreading the airflow and propulsive forces across the aircraft, by installing more but less powerful engines. The goal of this technology is to improve the

aircraft performance, such as the fuel efficiency and the noise emissions. Due to these smaller engines, it is easier to integrate them into the airframe. This leads to drag and mass reductions. Other benefits that are made possible by distributed propulsion are making use of boundary layer ingestion to reduce drag, a reduction in tail size due to the reduced criticality of a one engine inoperative scenario and reducing the mass of the landing gear due to engine clearance.

27.2 Mission objective and statement

The objective of this project is:

"to design a single aisle, commercial transport aircraft with a distributed propulsion system."

Subsystems other than the propulsion subsystem should be proven technology to the largest extent. In this manner, the potential reduced emissions and noise levels can only be caused by the distributed propulsion system. To quantify these reductions, a comparison will be made by designing a reference aircraft based on the Airbus A321. Our mission statement is therefore as follows:

"design a medium range commercial transport aircraft with a distributed propulsion system and to quantify the potential performance benefits by comparison with an existing reference aircraft."

The design philosophy behind Vimana is to start off with a conventional design and to allow deviations only if they supported the distributed propulsion technology.

27.3 Design requirements and constraints

As with every project there are top level requirements, these are listed below.

- REQ-TL1: The aircraft shall accommodate 180 passengers in a single class configuration.

- REQ-TL2: The aircraft shall be able to transport 18,500 kg payload.
- REQ-TL3: The aircraft shall have a maximum payload range of 6,100 km.
- REQ-TL4: The aircraft shall have a cruise speed of Mach 0.78 at 11,000 m.
- REQ-TL5: The aircraft shall have a maximum speed of Mach 0.82 at 11,000 m.
- REQ-TL6: The aircraft shall require a take-off field length of no more than 2,100 m at ISA sea level and maximum take-off weight (MTOW) condition.
- REQ-TL7: The aircraft shall require a landing field length of no more than 1,600 m at ISA sea level and maximum landing weight (MLW) condition.
- REQ-TL8: The aircraft shall have a service ceiling of at least 12,000 m.

The inclusion of a distributed propulsion system opens a wide array of new design possibilities. However, the final design must be able to efficiently operate within the actual established air traffic network. This is particularly applicable for airports: Vimana should not require major modifications in their infrastructure.

Vimana should adhere to international regulations (EASA and FAA standards). Special attention should be paid to the one engine inoperative condition (OEI), as it is assumed that a distributed propulsion system will relieve this otherwise driving requirement.

In order for this project to be successful, quality standards must be met in terms of reliability, availability, maintainability and safety. Finally, the designed aircraft with a distributed propulsion system should be able to compete with current standard configuration aircraft such as the Airbus A321 in terms of reduced emissions, direct operating cost and noise. The target of the design mission is to reduce both CO_2 and NO_x emissions by 25% per passenger kilometre. Furthermore the noise, compared to an Airbus A321, should be reduced. These top level requirements and constraints function as a starting point for sizing the aircraft, to perform initial estimates.

27.4 Concepts

Once the key requirements and constraints for the distributed propulsion aircraft have been defined, five concepts were generated.

Concept 1: Geared turbofan
This concept deviates the least from existing aircraft. It features a conventional tube-and-wing configuration with 9 geared turbofan engines which are downscaled versions of existing engines featured in state-of-the-art aircraft such as the Airbus A321. Taking weight, specific fuel consumption and propulsive efficiency into account, the optimal number of engines was estimated to lie between 9 and 12 elements. The propulsive configuration envisions 3 engines located below each wings. A total of 3 additional engines are located at the back of the fuselage; this design choice was made due to the potential benefits of fuselage boundary layer ingestion.

Concept 2: Geared transfer
The second concept delves into mechanical systems by means of energy transfer. This concept separates the power generating turboshaft unit from the thrust producing fans and connects them with a shaft and gear system. From initial power estimates it was determined that 14 fans with a 1.2 m diameter located spanwise should be sufficient to fulfil the thrust and power requirements. For every fan, 2 gearboxes are present for power transmission. In terms of redundancy, 3 engine clutches evenly distribute the power in case of a one engine inoperative condition. From the initial calculations it was found that a small cooling system was required for the gear and shaft system.

Concept 3: Hybrid non-superconductive design option
The next concept features a hybrid system: it consists of conventional mechanical engine cores with electrically driven fans. The primary architecture of the non-superconductive hybrid design option consists of 3 gas turbines for turboshaft applications located aft of the fuselage. These are connected to generators which then distribute the power to the individual propulsion units located on the entire wing span.

Additionally, a battery is installed on board the aircraft for auxiliary usage during power intensive phases such as take-off and climb.

Concept 4: Hybrid superconductive design option

Using superconducting materials enables weight savings compared to the non-superconductive hybrid system, while delivering the required power. The fourth concept takes the projected improvements in engine technologies as well as in specific superconductive materials into consideration. The big advantage of using superconductive motors, generators and cabling is that it has almost no power losses. The introduction of superconductive technologies requires the implementation of a cryocooling system in order to enable the superconductivity of the individual components. This concept makes use of Neon as a coolant and liquid methane as a heat sink. After cooling, the liquid methane can be mixed with conventional jet fuel in specific fractions to be burnt as propellant. The architecture of the hybrid superconductive design features 2 embedded engine cores also located at the back of the aircraft; 10 fans of 0.78 m diameters provide the required propulsive power.

Concept 5: Liquid natural gas blended wing body

The final concept aims to include distributed propulsion technologies into an unconventional configuration: the blended wing body. The inherent increase in available volume opened the opportunity to investigate alternative fuel sources: liquid natural gas was chosen as the primary energy source. Adaptations on the propulsion system include the incorporation of heat exchangers and cross-flow valves in order to ensure redundancy. The final architecture features 10 engines located on top of the centre section of the blended wing body so the system benefits from boundary layer ingestion.

27.5 Trade-off

From these five concepts, one is finally selected and worked out in detail. This is done with a trade-off procedure. In this manner, the concept that is the most promising to fulfil the requirements is

selected. Most trade-off criteria are based on top level requirements and are given a large weight. To obtain a good comparison, it is necessary to quantify as many criteria as possible. The trade-off criteria with corresponding weights can be found in table 27.1. The criteria are also subdivided into smaller components but these are not listed.

As the Airbus A321 is used as a benchmark, an improvement of a criterion is graded with +1, +2 or +3 depending on how large the improvement is. The same logic holds if something is worse than the Airbus A321, hence negative grades are given.

As can be seen from table 27.1, the superconductive hybrid concept is selected from the trade-off. The main trade-off criteria which resulted in the hybrid superconductive aircraft, are the sustainability and noise emissions. This was expected, as the main focus of the distributed propulsion aircraft is reducing its harmful emissions and noise. Although it seems from this trade-off that all concepts are worse than the Airbus A321 as they have all negative scores, this is not the case. The technological readiness level is obviously not as good as the Airbus A321 and therefore reduces the final score.

Table 27.1: Concept trade-off

Trade-off Criteria	Weight	Concept 1	Concept 2	Concept 3	Concept 4	Concept 5
Technological Readiness Level	20%	-0.25	-1.00	-0.75	-1.50	-2.5
Operability	15%	-1.35	-2.35	-0.30	-1.10	-1.30
Stability	5%	-1.0	0.00	1.00	1.00	-3.00
Sustainability	40%	0.34	0.13	-1.47	0.23	-0.02
Noise Emissions	20%	-0.25	0.25	0.75	0.75	0.00
Final	100%	-0.2157	-0.4521	-0.5824	-0.1724	-0.8532

27.6 Final design

Besides the propulsion system being different, it can be seen in figure 27.1 that the most notable feature of Vimana is the lack of a vertical tail. A more elaborate discussion on these two subsystem will be given further on.

Figure 27.1: Final design of the distributed propulsion aircraft Vimana

As also can be seen, Vimana features a conventional tube-and-wing configuration, with an aft swept wing. The SKF 1.1 supercritical airfoil is used, with double slotted fowler flaps and slats to achieve the required lift requirements. A lower noise level is achieved by means of fan shielding, less drag noise due to a smaller landing gear and empennage, and lower exhaust jet velocity. The final design of Vimana is presented in a 3-view drawing, depicted in figure 27.2.

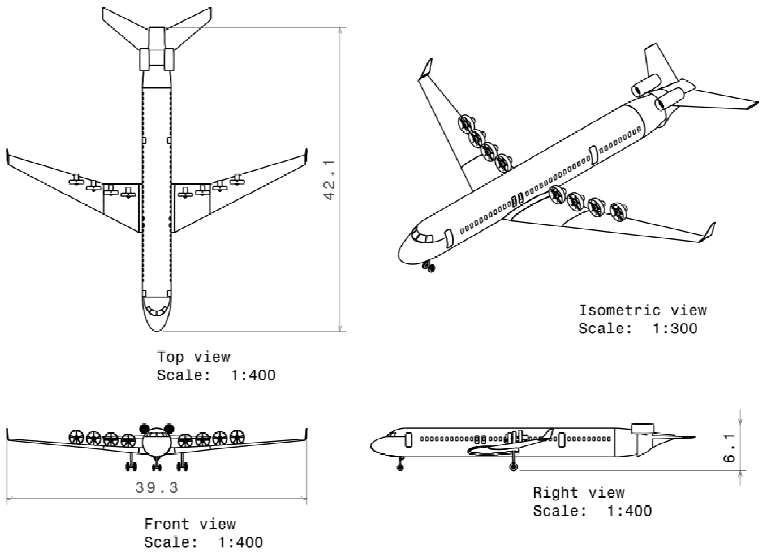

Figure 27.2: 3-view drawing Vimana aircraft

Propulsion system

One of the main focuses while designing Vimana, is the propulsion system. More details will therefore be given on this aspect. As mentioned before, Vimana has a High Temperature Superconducting (HTS) hybrid propulsion system, allowing for high efficiencies (99.5%) and compact sizes in the electric motors and generators.

Three turboshafts are placed at the back, enabling fuselage boundary layer ingestion, thereby reducing drag. These turboshafts, power three HTS generators, which in turn drive eight HTS motors. The electric motors power the eight fans, which can achieve a large effective by-pass-ratio due to the significant volume of air being blown by the fans resulting in a high propulsive efficiency.

The aforementioned HTS motors and generators have to be cooled, in order to achieve the HTS properties. This cooling is achieved by cryocoolers attached to the generators and motors, keeping them at cryogenic temperatures. The cables that transfer the power are HTS cables, which are immersed in Neon in order to keep them at cryogenic temperatures as well. The motivation for using such cabling

as opposed to regular electricity conducting copper wiring is that HTS cables have an efficiency of 100%, which means that they have no electrical resistance.

This propulsion system then allows for a maximum power output of 48.48 MW for the turboshafts and 36.94 MW for the motors. Both turboshafts and motors are sized for one engine and one motor inoperative scenarios respectively. This architecture is visualised in figure 27.3.

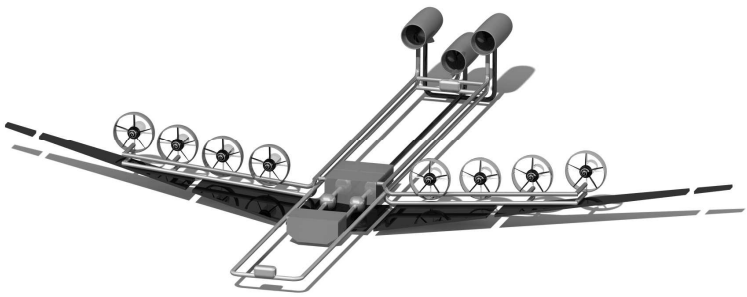

Figure 27.3: Propulsion architecture of Vimana

Empennage

One of the most notable features of Vimana regarding the empennage is that it does not have a vertical tail, allowing for weight savings and drag reduction. The propulsion system of Vimana allowed for this design choice, by using an advanced differential thrust system which enables directional and lateral control. Of course, lateral stability will still have to be provided, even when a vertical tail is not present.

The solution for this is to have an active stability system. By using split ailerons lateral stability can be provided. These split ailerons can also be used to provide control in combination with the differential thrust system, if necessary.

Performance

After the design processes that were conducted for the individual aspects, the performance characteristics following from the design were analysed. The top-level requirements were all met by Vimana,

with a service ceiling that was exceeding the requirement (13,000 m). The most important parameters of Vimana are presented in table 27.2.

Table 27.2: Design parameters of Vimana

Parameter	Value	Unit
Wing Span	39.27	[m]
Wing Surface Area	148.04	[m^2]
Mean Aerodynamic Chord Length	4.33	[m]
Operational Empty Weight	46,523.78	[kg]
Maximum Take-off Weight	88,393.88	[kg]
Thrust Loading (T/W)	0.157	[-]
Wing Loading (W/S)	5,778	[N/m^2]

Next to Vimana, a reference aircraft was designed, which was based on the Airbus A321. Performance parameters of Vimana are compared to this reference aircraft and are presented in table 27.3.

Table 27.3: Performance parameters

Parameter	Reference Aircraft	Vimana	Unit
Maximum L/D	18	20.3	[-]
Cruise L/D (begin-end)	17.5-15.92	19.06-17.29	[-]
Specific fuel consumption	1.3471E-05	1.1675E-05	[kg/Ns]
Climb rate at sea level	25	9	[m/s]
CO_2 emissions	4.691E-02	3.75E-02	[kg/km/pax]
NO_x emissions	1.823E-04	1.447E-04	[kg/km/pax]

Cost

Next to the comparison made between the reference aircraft and Vimana on performance aspects, a comparison on cost was also made.

This comparison was done with respect to the Airbus A321 instead of the reference aircraft as current data could be obtained.

Table 27.4: Cost parameters

Cost Category	Airbus A321	Vimana	Unit
RDTE	1,865	4,694	[million $]
Manufacturing	43.67	71.78	[million $/aircraft]
Acquisition	864,838	1,421,946	[million $]
Direct Operating	20.11	28.5	[$/nm/aircraft]
Indirect Operating	10.05	14.2	[$/nm/aircraft]

From table 27.4, it can be observed that large discrepancies are present between the Vimana and the Airbus A321 in terms of costs. These discrepancies however, are explainable and even logical to some extent. It is hard or even impossible to design a new, more efficient aircraft which is also cheaper than existing aircraft.

The discrepancy in the Research, Development, Test and Evaluation cost (RDTE) is mainly due to the fact that Vimana uses novel technologies. Also facilities need to be constructed, whereas these are already present for the Airbus A321.

The discrepancies in manufacturing and acquisition costs are due to the fact that these costs are associated to the same parameters used to determine the RDTE cost. Thus, the same explanation is applicable for this discrepancy.

The operating costs discrepancies are expected to reduce, as oil prices tend to increase. This is due to the fact that Vimana is less susceptible to oil prices compared to the Airbus A321 as it consumes less fuel. Finally, the total profit of Vimana is expected to be higher than the Airbus A321.

27.7 Conclusion and recommendations

The distributed propulsion system of Vimana is based on a hybrid concept containing three turboshaft engines, electrically powering eight fans distributed over the span of the wing. Various novel design choices, enabled by the distributed propulsion concept, were implemented.

Superconducting motors, generators and cabling are used to minimize electrical losses. In order to ensure superconductivity, these rotating machines are cryocooled using liquid Neon as a coolant. Furthermore, methane is used as a heat sink for the generators and motors after they have been cryocooled. Due to the placement of the fans on top of the wing, there is a less stringent requirement on ground clearance. Therefore, shorter landing gears are present resulting in a lower mass. Other mass savings have been achieved by omitting the vertical tail. Vimana will perform yaw control by using differential thrust settings, combined with the use of split ailerons. Boundary layer ingestion and wake filling are effects that the aircraft has been specifically designed for. This is observed at the aft of the fuselage with the body integrated turbine intake and the trailing edge of the wing, where fans ingest the wake. This results in fuel reduction and lower greenhouse emissions. Besides, the methane used as heat sink will be mixed with jet fuel and used as a propellant.

Implementing the aforementioned design choices results in benefits in terms of noise and emissions. The former is expected by virtue of fan shielding, a low fan outflow velocity, and engine placement within the fuselage. Despite the omission of the vertical tail plane and shortening of the landing gear, the empty weight of the aircraft is higher than that of the reference due to added components within the propulsion system. However, there is a marked reduction in the MTOW due to a lighter fuel load. Significant performance benefits are attained through the use of BLI and high electrical and propulsive efficiencies. This, in conjunction with the use of methane as an additional propellant, contributes to the aforementioned lighter fuel load. Most importantly, this also results in more than 20% decrease in CO_2 and NO_x emissions. A preliminary cost estimation results in an

operating cost of $0.085 per available seat kilometre for Vimana, as opposed to $0.060 for the reference aircraft. Vimana is noticeably more expensive to operate, but it is certainly more eco-friendly.

Recommendations for future activities are linked to CFD analyses and wind tunnel tests that will have to be done to confirm the expected performance benefits. This research relates to the noise and aerodynamic performance gains due to boundary layer ingestion and wake filling. Besides, the combination of differential thrust and split ailerons that will be used for lateral control should be designed in more detail. For each major design decision that will be made, an extensive trade-off should be made. This should be followed by an iteration that will confirm whether the design performs as good as expected.

28. SCOUTDROID: INSPECTION POCKET DRONE

Students: H.N. Basien, D.S.A. ten Brink, R. Cirera Rocosa, G.I. Földes, S.C. Hungs, E.J. Kroon, V.A. Pereboom, N.D. Potdar, C.H.C. Vlemmix, S.E.C. Voorhoeve

Project tutor: ir. C. de Wagter

Coaches: J. Rohac PhD., Z. Hong, MSc

28.1 Introduction

Emergency services often encounter situations in buildings where it is dangerous to go inside to inspect, assess the situation and check if there are still people waiting to be rescued. Examples are fires in high rise buildings and unstable or collapsed structures after explosions or earthquakes. In many cases rescue teams enter the area, risking their lives; sometimes with lethal consequences.

For use in this type of situations, the scoutDROID is designed, aimed at complying with the following mission need statement: "Emergency services are in need of a portable, quickly-deployable, user friendly, innocuous, unmanned outdoor and indoor inspection system for danger zones."

Based on this, the project objective statement for the Inspection Pocket Drone project is:

"Design a backpack-sized UAV (and its corresponding ground station) equipped with a visual inspection system, enabling users to identify objects of interest, that is operational within one minute for safe use outdoors and indoor confined places for a duration of at least 10 minutes."

28.2 Requirements

The most important requirements as set by the stakeholders are as follows:

- The total system shall be deployable and operational in less than 60 seconds.
- The vehicle shall be able to enter through a 50x50 cm opening during operational conditions.
- The payload shall be able to provide image quality sufficient to recognise persons at 5 m distance.
- The vehicle shall be safe to fly around people and not cause trauma upon collision.
- The vehicle shall withstand impact loads caused by its collision with its surroundings.
- The system shall be able to operate in 90% of Dutch weather conditions.
- The vehicle shall be able to communicate with the ground control station with a minimum range of 100 m through 2 brick walls.
- The system shall be operational for at least 10 minutes.

28.3 Concept selection and trade-off

In the preliminary design phase the top level concepts were divided in flight concepts and casing concepts. Seven flight concepts and four casing concepts were considered. Combining the compatible flight concepts with the casing concepts resulted in twenty high-level concepts. After a first preliminary trade-off this number was brought down to four:

- Quadcopter with meshed protective ring.
- Coaxial contra-rotating rotor with two swashplates and protective hull.

- Coaxial rotor with swashplate and protective hull but with an added protective cap.
- Coaxial contra-rotating rotor with two swashplates and meshed protective ring.

In order to do a proper trade-off between the four concepts some top level calculations have been performed to have values for the parameters needed to make a comparison of all concepts.

The final concept is the coaxial contra-rotating rotor with two swashplates, protective hull and protective cap. In this concept the translational movement is controlled by a double swashplate mechanism, while yaw control is provided by differential thrust. The hull around the rotors serves as protection for the blades, space to store payload and systems and as a duct to improve the rotor efficiency.

28.4 Subsystem design

To show the results of the scoutDROID, this section elaborates on the details of the subsystem design.

Propulsion and power

For both indoor and outdoor flight the scoutDROID relies on two contra-rotating three blade rotors inside a duct. Because of the duct, the radius of the propellers can be smaller than a non-ducted design, for the same values of thrust. The three blades per rotor increase the thrust while keeping the radius the same at a minimal cost of weight increase. Contra-rotating rotors have increased efficiency as the lower rotor experiences part of the wake of the upper rotor which increases the thrust generated by the lower rotor. These rotors are actuated via two swashplates, one for each rotor.

By tilting the swashplates differential pitch is generated over the blades which induces a moment allowing for pitch and roll control. Both swashplates are actuated by the same three servos, allowing them to tilt to any angle that is required for pitch and roll control.

Yaw is controlled by differential thrust between the two rotors. The blade aerofoil used is specifically developed for use in helicopters and the blade twist distribution is optimised for the interaction between the two rotors. The blade twist is such that the blades do not experience negative lift or stall during full thrust flight and hovering. The rotors are driven by lightweight brushless motors, that take their energy from two compact lithium polymer battery packs. These packs also power the rest of the payload through battery eliminator circuits integrated in the electronic speed controllers.

Payload and on board computer

A large part of the performance and reliability of the UAV system depends on the configuration of the payload components, on-board computer and software inside the drone.
The payload of the UAV consists of the following main components:

- Camera module for video recording and 5MP stills
- Thermal camera module
- Sonar ranging sensors
- GPS receiver and antenna
- High brightness LEDs and blinking awareness LEDs

The most important elements of the payload are the camera modules included in the design. The choice is made to include first-person view functionality which means that the UAV has a direct video stream from the front camera to the operator in order to control the drone outside the direct line of sight. This will enable the user to fly and manoeuvre the system without requiring full autonomous behaviour and navigation.

Two camera modules are included. One visible light camera board capable of recording VGA quality (640 x 480 pixels) video at 30 fps, which is sufficient to recognize persons at 5 m distance. Furthermore, the camera also has the option to record high resolution 5 MP stills which can be stored on-board to assess in further detail at a later stage of the mission.

In case the mission conditions become more demanding, for instance with smoke attenuation, the operator can switch to the thermal camera module. This small FLIR Lepton long wave infrared camera is as well included in the design to provide the functionality to detect fire hotspots and detect the presence of persons in low visibility conditions.

In order to increase the level of in-flight autonomy, sonar sensors are included as ranging devices as an aid for the operator to manoeuvre the UAV, for instance in confined spaces. A total of six sonar sensors are mounted on the drone to measure the distances to the UAV surroundings in all six possible directions of movement. Sonar sensors are robust and low-power devices that also work properly in low visibility conditions and in presence of smoke and dust.

The lightweight GPS receiver integrated on the flight controller board adds additional navigation capabilities for the UAV. High brightness LEDs make it possible to use the visible light camera as well in very low-lighting conditions.

The on-board computer system is designed to be lightweight and have a low power consumption while providing sufficient computational power and speed. To make the implementation and future use of the chosen on-board computer system efficient, the hardware also provides a suitable development platform for the internal software and is compatible with all attached hardware components, making use of off-the-shelf components as it largely decreases development time and costs and has proven reliability and performance.

The on-board computer consists of two parts. A NavStik flight controller board is used combined with an additional Gumstix Overo Earthstorm computer with a 1GHz Cortex-A8 processor used for video compression and additional data processing. The on-board computing platform is based on Paparazzi. Paparazzi is a system of open source hardware and software designed for use with many types of unmanned aerial systems like fixed-wing craft, helicopters and multicopters. Because of the open-source character of the platform,

the Paparazzi software can be tailored and expanded according to the needs of the user. The payload and on-board computer architecture have a combined weight of 93.3 grams excluding wiring and a power consumption in full operation of 3.8 Watts.

Communications

Indoor situations imply the signal will most likely be obstructed by obstacles such as brick or (reinforced) concrete walls. This has a large negative effect on the received signal power as it is greatly attenuated. First it was investigated how significant the impact is of a concrete wall and the atmosphere at blocking the signal, the signal properties that are affected and the consequences to the link quality. Also the effects of physical wave behaviour, including reflection, refraction and interference were accounted for by modelling signal propagation based on empirical models.

After establishing the sources of signal attenuation, and defining the signal propagation model, a simulation was performed to compute the minimum transmitter power required to communicate at a variable frequency, for fixed range, or vice versa. Once the minimum transmitter power was known for different frequencies and ranges, the design was chosen such that the requirement on a 150 m communication range through reinforced concrete wall and the legal restrictions were complied with. The simulation results showed that the only frequencies capable of transmitting according to requirement and within legally acceptable transmitting power levels (less than 1 Watt) are the sub-GHz frequencies. Regarding the legal aspect, the 868MHz band is the unlicensed transmitting frequency for The Netherlands which is also the region of the UAV's operation.

Knowing the required minimum transmitting power and frequency, a market research was conducted to find off-the-shelf transceiver modules that would fit within this design space. The best solution was selected to be the SiFlEX02-R2-HP transceiver module which delivered in terms of performance and complied with legal restrictions. The module uses asynchronous serial communication and is capable of transmitting at 750 mW over a maximum range of 278 m

with a directional data rate of 1 Mbps. Another benefit of this module is its ability to be customised to operate on the 900MHz band which is unlicensed in several countries including the United States of America. After the module selection, antennae are required to be able to transmit and receive signals, and for this a set of two quarter-wave wire antennae were chosen to be placed on opposite sides of the UAV. The module's antenna diversity feature allows it to switch between the antennae to establish the best link quality between the ground station and UAV. The antennae are placed on an inclined downward edge of the UAV for optimal signal coverage of the ground.

Given that the signal can be transmitted across a sufficient range, it is necessary to design the receiving end. For simplicity, the same transceiver module is used on the ground control station. In this case, two large (1.25 wavelength) dipole antennae were chosen to have maximum gain and coverage.

With this system, it is possible to transmit a live video feed at 24 frames per second, at a resolution of 576 by 324 pixels. For safety and to avoid signal snooping, the signals to and from the UAV are encrypted with AES-128 so that no unauthorised people can hack into the data feed and possibly access sensitive information or gain control of the UAV.

Structures

The structure of the scoutDROID is comprised of two main load carrying parts, the hull and the struts. The hull is the circular element that encloses the rotors and houses inside of it all the components of the payload, OBC, communications and power subsystems. The hull is made out of PA 640-GSL, a low density polymer. Its dimensions are such that the hull's structural integrity is assured under all the loading conditions the UAV will encounter during its mission. The most demanding loading condition is encountered when the UAV collides against its surroundings. In order to reduce the load on the structure upon impact, the hull is surrounded by a thermoplastic closed cell foam, called Plastazote MP15FR. The top and bottom of the hull are completely covered by the foam while the external side of the hull has

10 stripes of foam evenly spread around it. This distribution allows the cameras and sensors placed in the hull to have the required field of view for their operation. The foam acts as a spring, increasing the impact time, and thus reducing the maximum load. In addition, due to its damping properties, it reduces the rebound velocity.

The second load carrying part of the structure is comprised of three struts that connect the hull to the propulsion elements located in the centre of the scoutDROID. The struts have a circular cross section and are made of high density polyethylene, a low density material with a high tensile strength. While the length of the struts is set by the propulsion subsystem design, the inner diameter and thickness was chosen to minimise the weight of the struts, while preventing structural failure under any of the loading conditions. As with the hull, the impact loads were the critical loads that drove the design, but another type of loads was very important as well: vibrations. The propulsion subsystem can induce vibrations in the UAV. These vibrations have a negative impact in the performance of certain payload and navigation instruments. Since the struts connect the source of the vibrations to the hull that houses these instruments, the struts were also designed to reduce the vibrations they transmit.

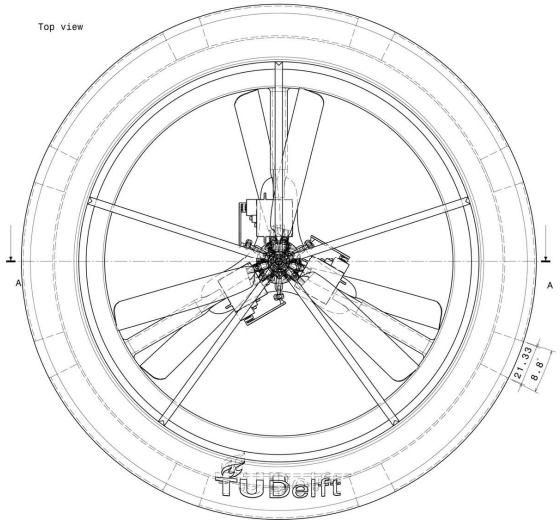

Figure 28.1: Top view drawing of the scoutDROID, dimensions in mm

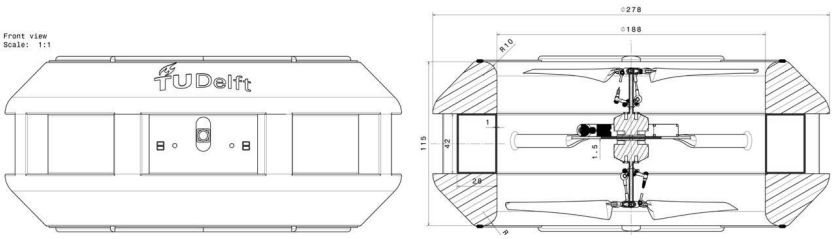

Figure 28.2: Side view drawings of the scoutDROID, dimensions in mm

28.5 Sustainable solutions

The sustainability of the UAV design is assessed from a social, economic and environmental perspective.

To make the design socially sustainable, it was outfitted with identification lights and custom paint jobs which can be chosen by the user. This enables any user to clearly identify the UAV's purpose and goals when using the device. To comfort the general public on the safety of the UAV, operators are required to obtain an RPAS license to be able to operate this device to show he or she fully understands and has mastered the UAV's controls and capabilities. And lastly, the UAV is outfitted with a foam layer to protect the environment and the UAV on impact, and the top and bottom of the duct are covered with a spoked cap to prevent injury when operated near persons.

Considering economic sustainability, lowering system costs was achieved by using mainly off-the-shelf components, reducing production costs. When selecting the components, special attention was paid to durability to make sure the UAV can perform multiple missions before parts need replacing, which makes the product as a whole more attractive.

The hull, the protective foam structure and the rotor blades are custom designed, and made out of different materials each. These materials, along with according manufacturing method proves all to be a good choice in terms of environmental sustainability. All components passed the sustainability assessment, even the batteries. New processes for recycling batteries are continuously developed and

employed by companies like Tesla, enabling us to recycle more than 80 percent of the LiPo batteries, and this made it possible to reach the goal of 80 percent recyclability of the UAV as a whole.

28.6 Conclusion

Returning to the project mission statement: "Design a backpack-sized UAV (and its corresponding ground station) equipped with a visual inspection system, enabling users to identify objects of interest, that is operational within one minute for safe use outdoors and indoor confined places for a duration of at least 10 minutes." This goal is successfully achieved in this project.

The design process began with an elaboration on the top-level requirements. Several concepts were generated using combinations of several flight and casing concepts, which fulfilled the requirements. After several trade-offs, based on preliminary calculations and qualitative comparison, the most feasible concept was selected. This concept was worked out in detail, it consists of a circular hull housing the payload and a coaxial contra-rotating propulsion system.

Table 28.1: Main characteristics of the scoutDROID

Vehicle Mass	533 grams
Mission Duration	>10 minutes
Range	>250 meters
Diameter	27.8 cm
Height	11.5 cm
Power	81 Watts
Costs (Development, man hours, certification)	€ 242.000

The hull houses six sonar sensors, a thermal camera and a visual light camera capable of streaming video to the ground station and taking 5 megapixel pictures. The main characteristics of the scoutDROID can be found in table 28.1.

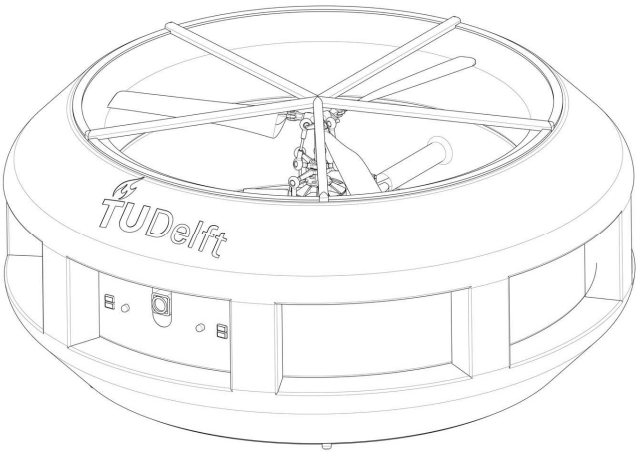

Figure 28.3: 3D view drawing of the scoutDROID

28.7 Recommendations

At this point the detailed design phase of the scoutDROID is completed. Next development and design phases will mainly consider software development and prototyping.

Improvements are expected to be made in the drag estimation of the UAV by using wind tunnel tests and in the control system of the UAV.
As for the on-board computer and payload, currently off-the-shelf components are used to ensure rapid development, compatibility and modularity. However, customizing the hardware parts increases efficiency and can reduce weight which is suggested to consider in future development phases.

Furthermore it is recommended to start the certification process as soon as possible. The certification process is expected to be lengthy and time consuming, taking at least 3 months. This however has to be completed before any sales can be made.

As the UAV market is developing and innovating rapidly, quick prototyping and customer feedback is required to ensure a short time-to-market and make sure that the product meets the expectations.

29. LEOPARDSAT CONSTELLATION

Students: T. Benedicto Rinaudo, T. Boerdijk, D.L. Coolen, S. al Jaberi, R. Jacobse, J. Klapwijk, M.P. Nieuwenhuijsen, D.J.P. Schroyen, W. de Zeeuw

Project tutor: T. Watts

Coaches: dr. P. Liu, ir. J. Geul

29.1 Introduction

In collaboration with the Space Office of the Royal Netherlands Air Force (RNLAF) an assignment for the DSE was formulated. The assignment is to make a conceptual design of a constellation of spacecraft for an Electronic Intelligence (ELINT) mission to detect and locate radars and Global Positioning System (GPS) jammers.

Mission statement

A mission statement was formulated for the project. The mission statement describes the assignment in one sentence and is as follows:

"This ELINT smallsat constellation project will, over the course of eleven weeks, study the feasibility of and generate a conceptual design for a space asset capable of detecting, recognizing, and locating target signal sources (L-, S- and, X-band radar, and GPS jammers) and providing the RNLAF with this data from 2019 onward at a total constellation cost of less than € 25 million (excluding launch and operating costs)."

In this study, a conceptual design is made for the space segment consisting of the spacecraft and the constellation geometry. Other aspects, such as production, ground segment and support segment are discussed briefly. The objective is to produce a design down to a subsystem level. This conceptual design assists the RNLAF in the development of a space asset.

Importance of intelligence

Detailed knowledge about a particular area is essential for military decision makers and can be the difference between mission success or failure. Classical sources of intelligence are human, optical, and electronic.

With the advent of spaceflight, spaceborne Earth Observation missions became possible. Imaging from space is a well-known type of intelligence and is mostly associated with 'spy satellites' and offers worldwide access. ELINT is the process of monitoring the radiofrequency spectrum to intercept signals of interest that can provide information about certain systems. Radars, jammers, and Identification, Friend or Foe (IFF) systems are examples of such systems of interest.

Detection of GPS jammers is a relatively new need, because of the increasing dependency of civil and military systems on the GPS system for geolocation and time synchronisation. The need is also driven by the observed effectiveness of simple and cheap GPS jammers, many of which are handheld or easily transported.

29.2 Requirements

At the start of the project the RNLAF formulated top level requirements for the design. These requirements served as boundary conditions and constrained the design space of the project. The initial requirements were further specified to lower level requirements during the project. The most driving initial requirements are listed below:

- The mission shall have a lifetime of five years.
- The constellation shall cost no more than € 25 million (excluding launch and operation costs).
- Each spacecraft shall have a maximum mass of 200 kg.
- The launch window of the mission shall be between 2017 and 2019.
- The constellation shall have a maximum orbital altitude of 650 km.
- The constellation shall only make use of ground stations on Dutch soil.
- The constellation shall be capable of intercepting radar emissions within the 1-4 GHz and 8-12 GHz frequency bands.
- The constellation shall be capable of localising radar systems with an accuracy of 1,200 m.
- The constellation shall be able to locate GPS jammers with an accuracy of 200 m.

Some of the initial requirements were relaxed after a technical feasibility study and due to budget constraint. The initial budget was increased to € 45 million after an initial cost estimate. The localisation accuracy of radar systems was increased to 5000 m. These changes were made in agreement with the RNLAF.

29.3 Electronic intelligence methods

The basic function of the constellation is the interception, identification, and localisation of radars and GPS jammers. Firstly, the constellation must be capable of intercepting the signals, meaning that the constellation must be capable of distinguishing the signals of interest from space. Secondly, the constellation must analyse signals of interest to identify radars and jammers. Finally, the localisation process is initiated for emitters of interest. All these tasks are performed by the Electronic Support Measures (ESM) module, the general name for such a type of instrument.

Signal characteristics

Identification of signal sources is done by analysing signals of interest and comparing parameters detected signal with a signal library. Modern military radars have the capability to emit a large, but finite

number of different signals. This is achieved by varying signal parameters within a certain range. These parameters and their range are the building blocks of a signal library and are thus of great interest to adversaries. This information is obtained by manned ELINT missions and is not a task for the constellation. GPS jammers emit a fixed, continuous signal and are easily identified. The main difficulty is distinguishing signals originating from two identical jammers.

Localisation methods

Jammers and radars exhibit different emission behaviour and require different techniques for localisation. Radars emit series of short pulses with high power in a narrow main beam and much lower power in unwanted side lobes. Interception of a single emission at different locations is thus not guaranteed and localisation is performed using only a single interception of each emission. GPS jammers emit a continuous signal using omnidirectional antennas, allowing interception of the same signal at different locations.

Effective methods for localisation are Time Difference Of Arrival (TDOA) and Frequency Difference Of Arrival (FDOA). They can be combined to obtain a high accuracy. TDOA is performed by using several intercept receivers with a known separation. By measuring the time of arrival of a signal at the different intercept receivers, the time difference is used to triangulate the emitter's location. FDOA works in a similar way and uses the Doppler-shift of the incoming signal. TDOA and FDOA require a large separation between at least three intercept receivers and an accurate, synchronized, time measurement. The required accuracy of the time of interception was found to be 2.5 μs and the required accuracy of the frequency measurement was found to be 0.25 Hz. When these requirements are met and four intercept receivers are used, GPS jammers can be located with an accuracy of 60 to 200 m between latitudes of 0° to 70°.

Radars are located by using the Angle of Arrival (AOA) method as only a single interception is required. Using an antenna array, the direction of the signal can be determined. When two angles with respect to the spacecraft are measured, a line can be drawn from the

spacecraft to the radar. The accuracy of the AOA method is driven by the accuracy of the AOA measurement made by the antenna array, the error in the attitude determination of the spacecraft, the distance between the intercept receiver and the radar, and the elevation of the spacecraft with respect to the radar. It was found that with an overall AOA determination error of 0.5° a localisation accuracy between 1.85 km and 6 km can be achieved, depending on the frequency of the signal and elevation for an orbital altitude of 500 km.

29.4 Concepts

During the concept generation phase of the project many design options were listed to meet the various requirements. This was followed by an analysis of the different options to select the most promising ones. The different design options were first listed in a morphological chart, describing all the possible concepts. After a critical analysis the morphological chart was reduced in size and four concepts were selected for a detailed trade-off.

The main trade-offs were between on-ground or on-board processing and between identical or non-identical spacecraft. The signal processing equipment is the most complex and energy consuming of the spacecraft. The use of non-identical spacecraft would allow a more optimised design for certain functionalities, such as GPS jammer localisation or radar localisation. In the final trade-off a calculation of the required data rate for on-ground processing was made and resulted in a very high data rate. Further investigation in distributed payload options showed that this would not provide a significant advantage and would only add to the overall cost of the constellation. The concept with on-board processing and identical spacecraft was finally selected. The constellation will consist of four spacecraft flying in a square formation. The spacecraft can be seen in figure 29.1.

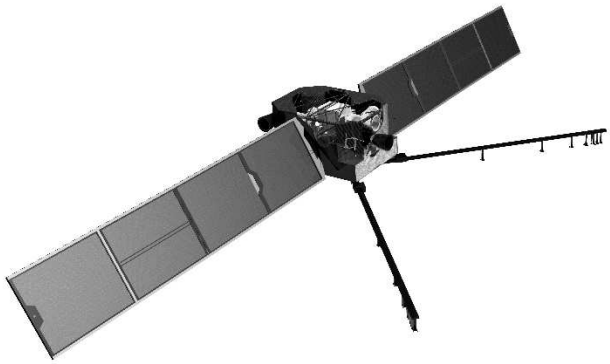

Figure 29.1: Drawing of the final concept with open view of the internal components

29.5 Final design

After the final concept selection the detailed design of the constellation was performed. The project assignment was to design the spacecraft down to subsystem level. For all components the higher level requirements were listed and an analysis of the interaction between different subsystems was made. For each subsystem the inputs and outputs were listed to enable effective interface management. The driving subsystems for the design are discussed in this chapter. An overview of the subsystems can be seen in figure 29.2.

The spacecraft main bus structure is designed as a hybrid sandwich panel bottom and truss upper structure. The trusses and antenna array booms are made out of filament wound carbon fibre. The sandwich panel is made out of carbon fibre face sheets and an aluminium honeycomb core. This design was selected for its high stiffness and low thermal expansion. Both are required to meet the AOA measurement accuracy of the antenna array.

During the final design the electrical harness, command and data handling, and thermal management were analysed to list specifications and requirements. Operational aspects such as

production, testing, verification and validation, and in orbit commissioning were also discussed.

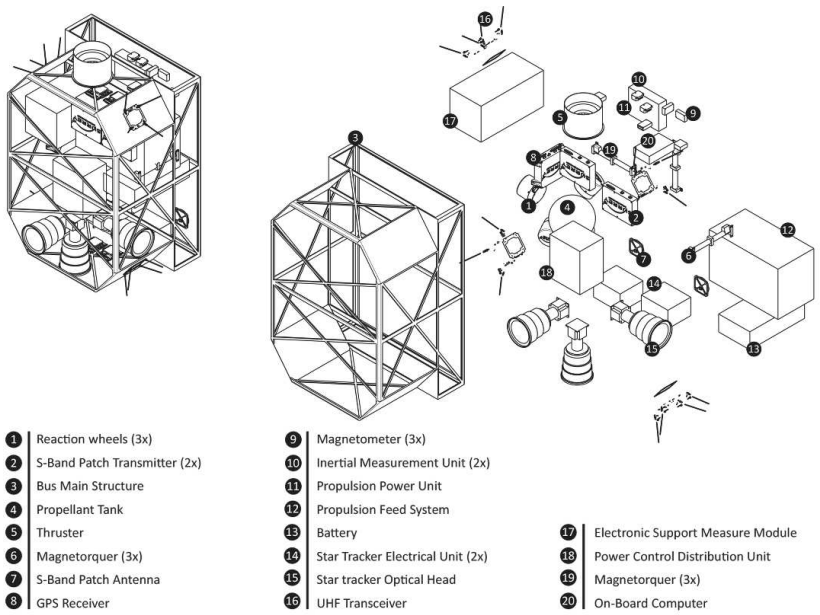

Figure 29.2: Exploded view of the spacecraft bus with all subsystems without the antenna array

Payload

Signals are intercepted by the antenna array and are fed into one central module to perform all the ELINT operations. Radar emissions are detected and characteristics like the number of pulses, the pulse length, and the frequency range are measured. These are a few examples of signal parameters used for radar type identification. During the design process, specifications and functionalities were set up for the ESM module to enable identification and localisation. Determination of the AOA from the raw antenna input is a function for the ESM module.

The antenna design is primarily driven by the localisation of radars as the AOA of the signal needs to be computed in three dimensional space. This is done using phase comparison of the incoming signals at multiple antenna elements placed in an array. To achieve the required accuracy in the angle of arrival, the array for the L- and S-band needs

to be at least 2.4 m long, and the array for the X-band is 1.6 m long. Using a binary spacing scheme this results in a seven-element linear array for the L- and S-band and a nine-element linear array for the X-band. Two linear arrays are used to compute the two angles. The arrays for the L- and S-band and for the X-band are placed on the same boom, but every array needs an orthogonal counterpart to provide the bearing information in the orthogonal direction. For the antenna elements, Vivaldi antennas are chosen for the L- and S-band, since they are ultra-wideband antennas, covering the whole 1-4 GHz frequency range. Patch antennas, which are very small, are used for detection in the X-band. For the GPS jammer localisation, no angle of arrival information is needed. Two redundant patch antennas, which provide at least 5 dBi of gain for the whole area of interest are used.

Orbit and launch

The constellation geometry for the mission consists of four spacecraft orbiting in two orbital planes. The orbits are circular at an altitude of 500 km and have an inclination of 100°. For optimum performance in geolocation the two orbital planes are separated by 700 km at the equator, which is 6° of difference between the right ascension of ascending node of the two planes. The distance between two spacecraft in the same plane is 500 km, and to prevent collisions an along-track phase shift of 100 km between the two orbital planes is used. The distance at the equator is larger than the minimum required by the geolocation method, because the distance between the spacecraft in the two planes decreases with latitude. Using this geometry the separation requirements for the localisation method are met.

The launch is performed by a Vega launcher operated by Arianespace from the Guiana Space Centre in Kourou, French Guiana. The Vega launcher is capable of launching all four spacecraft in one launch, and is able to perform the required plane-change to insert the spacecraft into their respective orbits. The Vega launcher was selected because it can fully meet the orbit geometry requirements and is operated by NATO countries.

Propulsion

To prevent orbital decay as a result of aerodynamic drag, and to de-orbit the spacecraft at the end of the mission, a propulsion system is needed. The total amount of ΔV required for the mission was calculated to be 502 ms-1. For the hardware selection many different types of propulsion systems were considered and eventually it was decided that an electrical system would be best suited for the mission, because of its high specific impulse. The xenon fuelled Astrium RIT 10 EVO ion thruster was selected. This thruster provides a thrust of 5 mN, a specific impulse of 1900 s, and a power consumption of 145 W.

The rest of the propulsion system was sized based on the specifications of this thruster. The propellant mass needed to meet the ΔV requirements for the mission was calculated to be 5.4 kg. At the mission altitude the aerodynamic drag is low, such that continuous propulsion is not required. The thruster shall only be activated when the spacecraft is over the poles, when the payload can be switched off in some cases. This reduces the required peak power output of the system.

AOCS

The Attitude and Orbital Control System (AOCS) is designed to provide the required pointing accuracy and control as well as the orbital position knowledge. The localisation method requires a high pointing accuracy, which is achieved using four reaction wheels. These reaction wheels have a torque authority of 11 mN and a momentum capacity 0.46 Nms to provide the main attitude control of the spacecraft. For control during de-tumbling and for momentum dumping, three 10 Am^2 magnetorquers are used. These magne-torquers are aligned with the three spacecraft body axes to allow more effective attitude control and to provide a course attitude determination for the star trackers. The star trackers provide attitude knowledge with an accuracy up to 0.004°. To account for possible blinding or other types of loss of attitude information, two inertial measurement units were incorporated in the design.

The orbital position is determined using GPS. The advantage of using an on-board GPS receiver for position knowledge is that it provides a 500 ns accurate time signal as well. Consequently there is no need for an on-board atomic clock to provide the constellation with an accurate time.

Power

To supply the various subsystems with electrical power an Electrical Power System (EPS) was designed. It consists of three main parts; solar array, batteries and a power conditioning and distribution unit (PCDU). The total mass of the EPS is 33 kg. The system has an average power output of 345 W and a peak power output 673 W. The electrical power is supplied to the system from two solar arrays, consisting of triple junction solar cells. Two solar arrays with a total area of 3.7 m2 provide 800 W (at end of life) to the system. With this power output of the solar arrays, sufficient power is supplied to the system for a complete cycle (sunlight and eclipse).

After the power enters the system it is conditioned and distributed by the PCDU. This PCDU consists of four array power regulation modules, two battery charge/discharge regulation modules, two equipment power distribution modules and two interface modules. The latter interpreting command data for the EPS. The number for modules in the PCDU is such that the power throughput is sufficient to supply enough power to the loads including redundancy in case one of the modules fails.

The batteries consist of Li-ion cells. Li-ion cells were selected due to their high energy density with respect to other types of cells. The batteries have an energy storage capacity of 562 Wh to be able to supply sufficient power to the subsystems during eclipse.

Communication

The Telemetry, Tracking, and Command (TT&C) subsystem is responsible for handling all incoming and outgoing communications of the spacecraft. This means communication with the ground stations for the uplink and downlink, and communication with the other

spacecraft within the constellation to exchange signal information and commands. Due to the sensitive nature of the transmitted data, all communications will be encrypted using an encryption module.

To maximise the amount of downlink opportunities, ground stations in Breda and Bonaire are proposed, since these locations are both on Dutch soil. This results in a maximum time between downlink opportunities of 6.5 hours and an average time of 2.4 hours. The downlink will be performed in the S-band with a maximum data rate of 115 kbps. The uplink will be performed on the UHF-band, due to the low required data rates for the telecommands.

To perform the geolocation of the GPS jammers, the spacecraft must exchange track data of detected jammers. This is achieved by UHF-band transceivers in combination with near-omnidirectional antennas. This enables the spacecraft to transmit data to all other spacecraft in the constellation at the same time without having to change the attitude.

29.6 Conclusion

The final design meets all but three requirements. The largest non-compliance is the cost, which is estimated to be € 88 million. Localisation of radars with an accuracy of 5000 m is achieved for elevation angles greater than 34° and is thus partially compliant. GPS jammer localisation is only possible up to 70° latitude. All other requirements are met and it has been shown that all proposed solutions are technically feasible. An overview of the constellation specifications can be seen in table 29.1.

Further improvements can be made by researching certain subsystems. It is advised to research alternative localisation methods to improve the accuracy. The antenna array design was performed with limited expertise and more research should be done to reduce the size and increase the AOA measurement accuracy. The ESM module represents a large portion of the estimated constellation costs, because it has to be developed and qualified for use in space. If

existing technology can be modified or an existing payload that meets the specifications is found, the payload costs can be reduced significantly.

Table 29.1: Overview of the spacecraft performance

Launch	
Launch date	Mid 2018
Launch vehicle	Vega
Launch site	Guiana Space Centre, Kourou
Orbit	
Orbit altitude	500 km
Orbit type	Circular, 100° inclination
Mission lifetime	Five years
End-of-life strategy	Active de-orbiting
Physical properties	
Dimensions (without solar array)	550 mm x 700 mm x 900 mm
Mass	Wet: 130 kg, dry: 124 kg
Payload	
Instruments	L-, S-, and X-band signal analysis
Coverage	Global coverage for radars
Minimum geolocation accuracy	5.0 km for radars 200 m for GPS jammers
Attitude Determination and Control	
ADCS method	3-axis stabilised
Pointing accuracy	0.04°
Position accuracy	10 m
Power	
Solar array	3.7 m² triple junction solar cells
Battery capacity	562 Wh
Power consumption	Peak: 673 W, average: 346 W
Telemetry, Tracking, and Command	
Downlink	115 kbps, S-band
Uplink	1200 bps, UHF-band
Inter-satellite crosslink	4800 bps, UHF-band
Ground stations	Breda and Bonaire
Propulsion	
Thrust	5.0 mN
ΔV budget	502 m/s